Regioselective Synthesis of Bicyclic Nucleosides and Unsymmetric Tetrasubstituted Pyrene Derivatives with a Strategy for Primary C-2 Alkylation

by

Ana Maria Dmytrejchuk

A dissertation submitted to the Graduate Faculty of

Auburn University

in partial fulfillment of the

requirements for the Degree of

Doctor of Philosophy

Auburn, Alabama

December 15, 2018

Keywords: Antisense oligonucleotides, bicyclic nucleoside, bridged macrocyclic ring, tetrasubstituted pyrene, unsymmetric pyrene substitution

Copyright 2018 by Ana Maria Dmytrejchuk

Approved by

Bradley L. Merner, Chair, Assistant Professor of Chemistry and Biochemistry

Stewart W. Schneller, Professor of Chemistry and Biochemistry

Eduardus C. Duin, Professor of Chemistry and Biochemistry

Anne E. V. Gorden, Associate Professor of Chemistry and Biochemistry

Ming Chen, Assistant Professor of Chemistry and Biochemistry

Abstract

CHAPTER 1

The incorporation of synthetic, tricyclic nucleic acid (TriNA) modifications into antisense oligonucleotides (ASOs) with therapeutic applications has been demonstrated to provide increased thermal stability relative to DNA and RNA, as well as leading nucleic acid modifications, such as locked nucleic acid (LNA). One of the major obstacles facing the development of complex nucleic acid modifications into viable ASO candidates is lengthy synthetic sequences. This work describes new synthetic strategies that involve the preparation of advanced nucleoside intermediates, which could obviate the use of inefficient glycosylation reactions (3 steps). Furthermore, using commercially available nucleosides as starting materials we envisioned a short synthetic approach to a bicyclo[*n*.2.1]undecane nucleoside intermediate, which takes advantage of regio- and chemoselective reactions. These intermediates could serve as molecular scaffolds from which multiple TriNA analogues can be prepared.

CHAPTER 2

Pyrene is a well-known chromophore frequently used in organic fluorescent materials. Its unique properties such as long-lived excited (singlet) states and its ability to form excimers have been widely exploited in many scientific fields, making pyrene and its derivatives an important fluorophore in both fundamental and applied photochemical research. To tailor the specific electronic properties of pyrene and its applications in materials science, strategies to introduce substituents about the pyrene core have been developed. However, still a major limitation for the use of pyrene in general is the lack of synthetic protocols for non-symmetric, selective functionalization of the pyrene nucleus. This work describes the synthesis of 1,2,4,5-, 1,2,9,10-tetrasubstituted and 1,2,4,5,8-pentasubsutituted pyrenes, which has been achieved by initially functionalizing the K-region of pyrene. Bromination, acylation, and formylation reactions afford high to moderate levels of regioselectivity, which facilitate the controlled introduction of other functional groups about 4,5-dimethoxypyrene. Access to 4,5-dimethoxypyren-1-ol and 9,10-dimethoxypyren-1-ol enabled a rare, C-2 primary alkylation of pyrene.

Acknowledgments

I would like to grateful acknowledge the people who have been part of my academic journey, without their help the completion of this dissertation would not have been possible. First, and foremost, I would like to thank Dr. Bradley L. Merner for his support, encouragement and academic advice. It was a pleasure to be part of his group guided by his expertise and patient assistance. I would like to thank my committee members, Dr. Stewart W. Schneller, Dr. Eduardus C. Duin, Dr. Anne E. V. Gorden, Dr. Ming Chen and Dr. Allan David for their support and suggestions.

I would like to extend my sincere gratitude to the Auburn University Chemistry and Biochemistry Department for their support, specially to Dr. Melissa Boerman and Dr. Michael Meadows for providing me with their assistance necessary in obtaining and mass spectrometric and nuclear magnetic resonance spectroscopic data. To Dr. John Gorden for his expertise in obtaining the X-ray crystal structure presented in this work. Also, I would like to thank my friends and colleagues Manuel Diaz and Dr. Hector H. Corzo for their help in the calculation of strain energies, and for providing me with different perspectives and new ideas that were very far from my way of thinking. Special thanks to the Auburn University Research Initiative in Cancer (AURIC) for their financial support on the nucleoside project, and the National Science Foundation (NSF) for supporting the pyrene project.

I am extremely thankful for the experience graduate school has left on my career and on my personal life. Developing time management strategies, an optimal working pace, realistic expectations and tactics to contain the perfectionist, as well as to keep a critical approach, were some of my greatest achievements in graduate school. However, remaining motivated during the course of a PhD is challenging. Frequent encounters with failure is the daily bread of a scientist and learning the beauty of failure was not an easy task. I would like to thank my lab mates Nirmal, Nirob, Caroline, Sydney and Kara for being an endless source of support in this journey.

I would like to thank my parents who worked hard to provide me and my four siblings with opportunities that were not afforded to them, encouraging us to be successful. Thanks to my sisters and brother for their camaraderie, and my nieces and nephews for reminding me that we only grow old when we stop playing. Finally, I would like to thank my soul mate Erol for his kindness, patience and unconditional love.

List of Abbreviations

Ac	Acetyl
Ac_2O	Acetic anhydride
APEX	Annulative π-extension
Ar	Aryl
ASO	Antisense oligonucleotide
B3LYP	Becke 3-Parameter (Exchange), Lee, Yang, Parr
Bn	Benzyl
BOC	*tert*-butyloxycarbonyl
BOM	Benzyloxymethyl
BOR	Based on recovered
Bpin	Boronic acid pinacol ester
$B_2(pin)_2$	Bis(pinacolato)diborane
bpy	2,2'-bipyridyl
CNTs	Carbon nanotubes
cod	1,5-cyclooctadiene
CPP	Cycloparaphenylene
d.r.	Diastereomeric ratio
Da	Dalton
DBU	1,8-Diazabicyclo[5.4.0]undec-7-ene
DDQ	2,3-Dichloro-5,6-dicyano-1,4-benzoquinone
DIBAL-H	Diisobutylaluminium hydride

DFT	Density functional theory
DMA	Dimethylacetamide
DMAP	4-dimethylaminopyridine
DMF	*N*,*N*-Dimethylformamide
DMP	Dess-Martin periodinane
DMSO	Dimethyl sulfoxide
DNA	Deoxyribonucleic acid
dtbyp	4,4′-Di-*tert*-butyl-2,2′-dipyridyl
equiv	Equivalent
Et	Ethyl
EtOAc	Ethyl acetate
EtOH	Ethanol
FC	Friedel-Crafts
FDA	Food and Drug Administration
Grubbs I	Grubbs first-generation
Grubbs II	Grubbs second-generation
GNR	Graphene nanoribbon
H-G II	Hoveyda-Grubbs second-generation
HRMS	High resolution mass spectrometry
i-Pr	Isopropyl
KHMDS	potassium hexamethyldisilazide
LDA	Lithium diisopropylamide
LiHMDS	Lithium hexamethyldisilazide

LNA	Locked nucleic acid
Me	Methyl
MeCN	Acetonitrile
MeOH	Methanol
mRNA	Messenger ribonucleic acid
MOE	2'-*O*-methoxyethyl
MOM	Chloromethyl methyl ether
Ms	Methanesulfonyl
MsOH	Methanesulfonic acid
Nap	Napthalenide (or naphtyl)
NBS	*N*-bromosuccinimide
NMR	Nuclear magnetic resonance
p-TsOH	*para*-toluenesulfonic acid
PAH	Polycyclic aromatic hydrocarbon
PhH	Benzene
PhMe	Toluene
PivCl	Pivaloyl chloride
PPh_3	Triphenylphosphine
PS	Phosphorothioate
pyr	Pyridine
r.t.	Room temperature
RCM	Ring-closing metathesis
R_f	Retention factor

RNA	Ribonucleic acid
SE	Strain energy
TA	Transannular
TBAB	Tetrabutylammonium bromide
TBAF	Tetrabutylammonium fluoride
TBAI	Tetrabutylammonium iodide
TBDPS	*tert*-butyldiphenylsilyl
TBS	*tert*-butyldimethylsilyl
t-Bu	*tert*-butyl
TES	Triethylsilyl
Tf	Triflyl (or trifluoromethanesulfonyl)
Tf_2O	Trifluoromethanesulfonic anhydride
TFA	Trifluoroacetic acid
THF	Tetrahydrofuran
TLC	Thin layer chromatography
TMS	Trimethylsilyl
T_m	Melting temperature
TriNA	Tricyclic nucleic acid
TsCl	Toluenesulfonyl chloride
TsOH	*p*-Toluenesulfonic acid
UV	Ultraviolet
UV/vis	Ultraviolet/visible
9-BBN	9-Borabicyclo[3.3.1]nonane

Table of Contents

List of Figures

CHAPTER 1 Strategies to Access Bicyclic Nucleoside Modifications Containing *cis* and *trans* Furanose-Bridged Macrocyclic Ring Systems for the Construction of Tricyclic Nucleic Acids with Applications to Antisense Technology

1.1 Antisense Technology

Traditional small-molecule therapeutics target biomolecules, most commonly proteins associated with human pathologies with the goal of modulating their function in a disease process and treat the targeted condition.[1] However, not all proteins are suitable for drug interactions, meaning that they not possesses folds that favor interactions with small drug-like molecules, and even fewer are appropriate pharmacological targets.[2] Antisense-based therapeutics is a relatively new drug discovery platform that offers an alternative for diseases treatment where pharmacological targets are inaccessible with traditional approaches.[3]

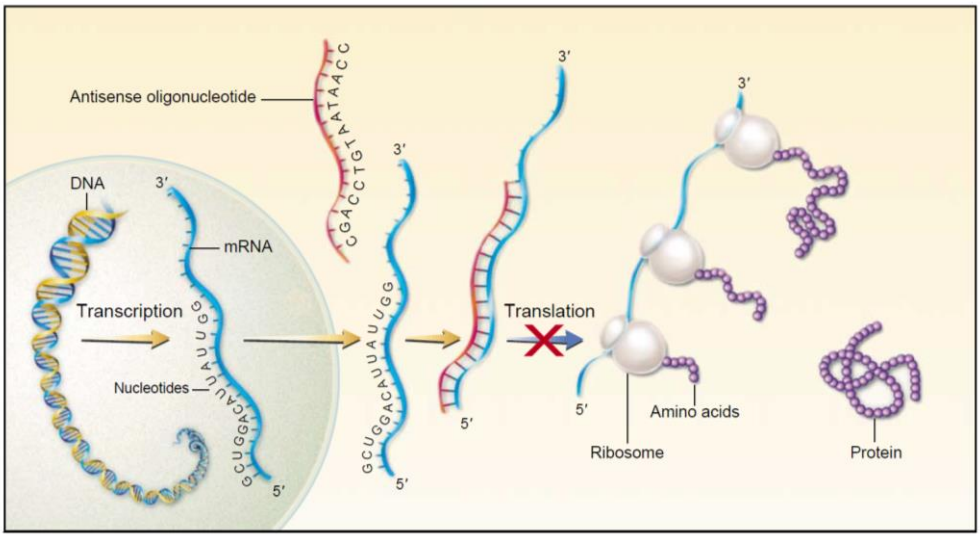

Figure 1. Overview of antisense-based therapeutic approach: ASO binds to a specific mRNA and prevents it from being translated into protein[4]

Antisense drugs are one step back in the protein modulation process, instead of directly targeting proteins associated with a disease, the antisense approach targets messenger ribonucleic acid (mRNA) to stop the production of a pathogenic protein (Figure 1). The principle behind the antisense technology mechanism is simple: during the production of any protein, mRNA (the sense strand) must remain as a single stranded molecule in order to be converted (translated) into protein. Antisense-based drugs are short (12-25 nucleotides)

synthetically-modified oligonucleotides containing a complementary sequence (*i.e.,* an antisense sequence) to the target mRNA transcript. They are designed to bind to a specific sequence of the mRNA, creating a short double-stranded region that through different post-binding mechanism, prevents or modulates the production of the protein encoded by the targeted mRNA. Therefore, genes involved in the pathogenesis of various diseases can be effectively silenced (hence, antisense-based therapeutics are also known as *gene silencing* therapeutics).[5]

Antisense oligonucleotides (ASOs) have DNA- (deoxyribonucleic acid) or RNA-like properties and bind to the target mRNA through Watson-Crick base pairing – hydrogen bonding between nucleobases and related base stacking (Figure 2). The clear (potential) advantage in this method of drug design over traditional small molecule-based therapeutics, is that the only required structural information about the target RNA is its base sequence. This makes the antisense drug design process more rational and efficient than the classic small molecules drugs design, because it targets a less structurally diverse macromolecule, containing building blocks that come from a four-letter alphabet code.

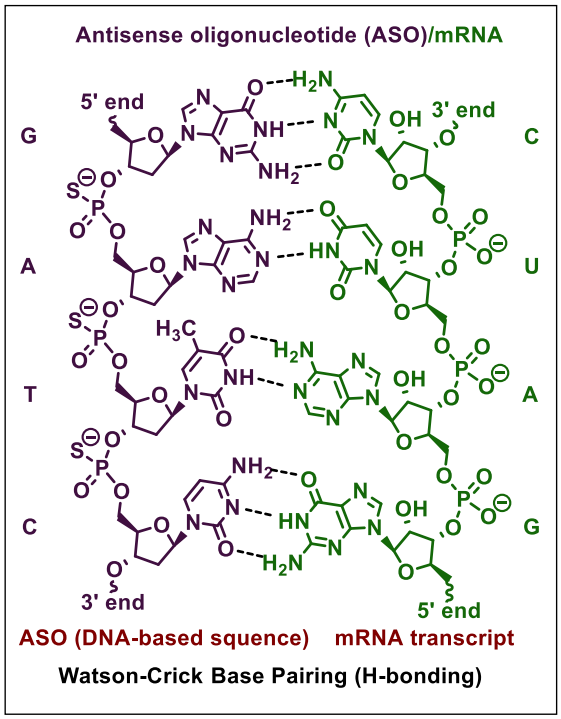

Figure 2. ASOs/Target mRNA binding interactions

There are different mechanisms by which ASOs regulate gene expression, and these are classified based on post-binding events as mentioned earlier. The two most common mechanisms include direct regulation of the RNA function by binding the designed ASOs.[6,7] In the translational or hybridization arrest mechanism (Figure 3A), the hybridization of the ASO/targeted mRNA sterically blocks the ribosomal translation process preventing the expression of the encoded protein. The antisense-mediated cleavage mechanism takes advantage of enzymes that after duplex formation are activated and rapidly degrade the target mRNA (Figure 3B).

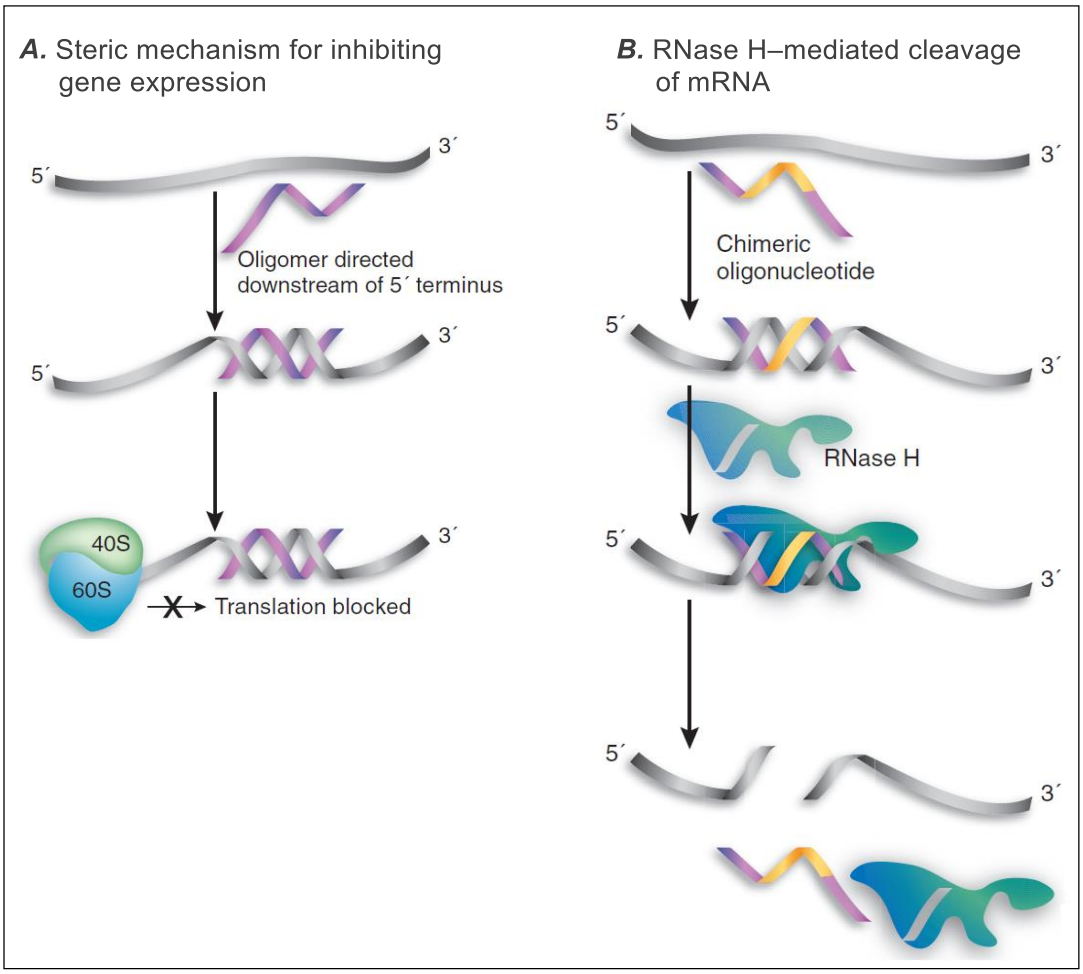

Figure 3. Antisense Mechanisms. a) Steric mechanism for inhibiting gene expression. b) RNase H–mediated cleavage of mRNA[8]

Despite numerous research and drug development efforts over the past thirty years, only six ASOs have been approved by the Food and Drug Administration (FDA) for clinical use.[9] In August of 1998, Formivirsen (trade name Vitravene®), a first generation 21-base phosphorothioate oligodeoxynucleotide, debuted in the pharmaceutical market as an antiviral drug used in the treatment of cytomegalovirus retinitis, a condition that occurs predominantly in immunocompromised patients. Fifteen years later, Mipomersen, a second generation 20-base 2'-*O*-(2-methoxyethyl)-modified ASO construct, with phosphorothioate-containing 2'-deoxynucleotides located in the center of the drug molecule, was commercialized under the name of Kynamro® as a cholesterol reducing agent in patients with genetic

hypercholesterolemia. Since then, many obstacles for the of ASOs as safe drugs have been overcome, resulting in four recent FDA approvals. Pegaptanib (trade name Macugen®) is an aptamer that was approved by the FDA in 2004 for the treatment of neovascular age-related macular degeneration, and Eteplirsen (trade name Exondys 51™) was approved for treatment of Duchenne muscular dystrophy in 2016 is a morpholino phosphorodiamidate antisense oligomer, and Nusinersen (trade name Spinraza®), an 18-base 2'-*O*-(2-methoxyethyl)-modified ASO was also approved in 2016 to treat, for the first-time, spinal muscular atrophy, a rare and often fatal genetic disease. In October of this year, Tegsedi™ a 20-base 2'-*O*-(2-methoxyethyl)-modified ASO construct, was approved for the treatment of the polyneuropathy of hereditary transthyretin-mediated amyloidosis.[10]

1.2 ASOs as therapeutic tools

As therapeutic tools ASOs must survive (*in vivo*) and function as single-stranded molecules. Unmodified single-stranded oligonucleotides are extremely sensitive to nuclease attack and thus susceptible to rapid degradation before reaching their target, limiting their use as drugs. To enhance their drug-like properties, structural modifications have been introduced into the nucleoside monomer building blocks. Since nucleases degrade oligonucleotides by cleaving the phosphodiester linkage, first-generation ASOs addressed this limitation by chemically modifying the internucleotide backbone through incorporation of a phosphorothioate (PS) linkage, which replaced one of the non-bridging oxygen atoms with a sulfur atom (Figure 4). The PS linkage significantly increases stability to enzymatic degradation making this one of the most widely used backbone modifications in antisense-based therapeutics.[11] Second and third-generation conformational ASO monomer modifications involved structural variations in the ribose sugar portion of the nucleotide monomer units, which would alter the capacity of ASOs to hybridize with RNA. These include modifications at the 2'-postion, as well as annulation of the furanose ring to afford bicyclic and tricyclic nucleoside modifications.

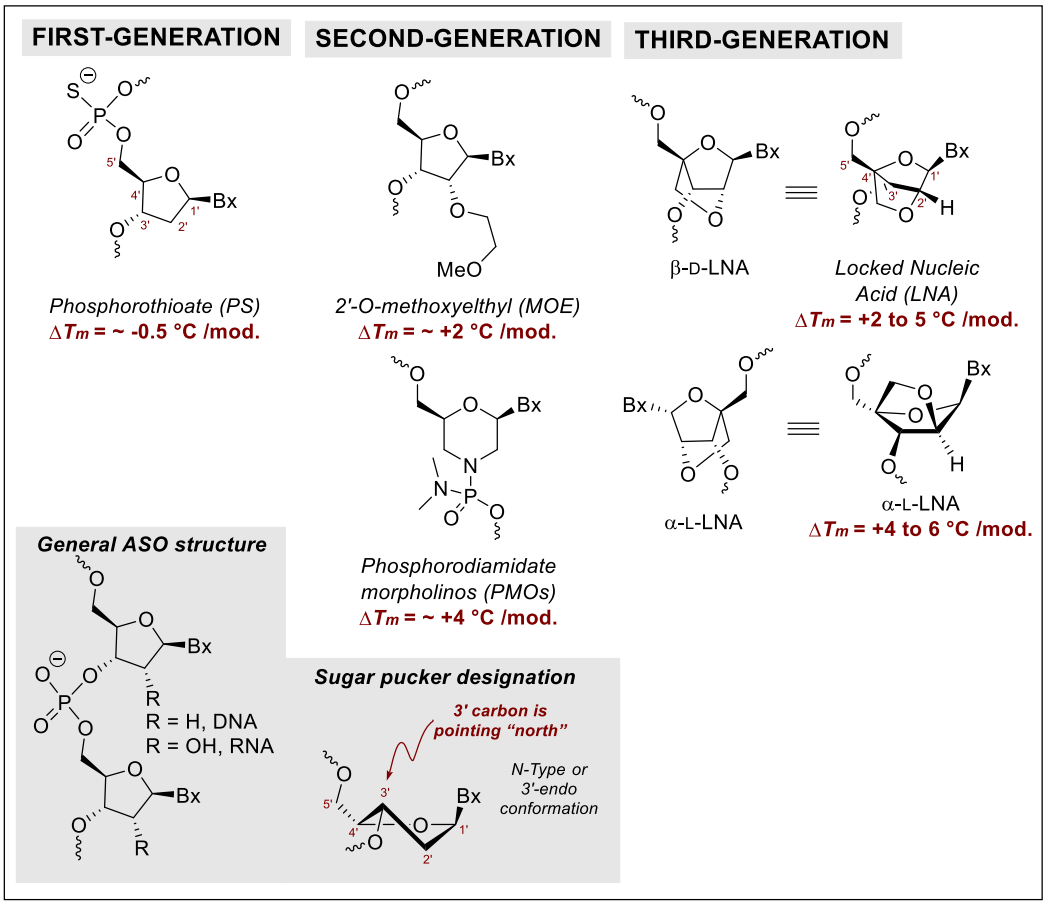

Figure 4. First, second and third-generation ASO monomer modifications

ASO potency is measured by binding affinity, which is in turn measured by melting temperature (T_m). An increase in T_m indicates an increase in binding affinity, and this is experimentally measured by slow heating of the ASO/mRNA double-stranded molecule causing separation of the duplex structure through disruption of the Watson-Crick base pairing interactions (Figure 4). The temperature at which 50 percent of the base pairs are dissociated in the ASO/mRNA duplex is T_m. Generally, ΔT_m values are reported relative to unmodified nucleosides that have the same nucleobase as the modification under investigation (Table in Figure 5).[12]

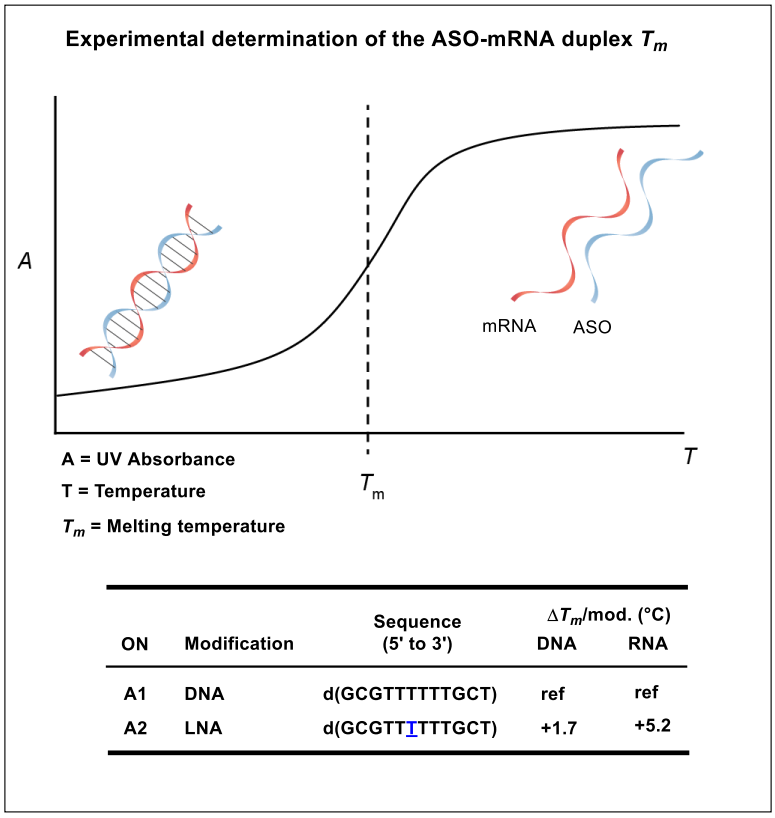

ON	Modification	Sequence (5' to 3')	ΔT_m/mod. (°C) DNA	RNA
A1	DNA	d(GCGTTTTTTGCT)	ref	ref
A2	LNA	d(GCGTTTTTTGCT)	+1.7	+5.2

Figure 5. ASOs melting temperature determination

Second-generation ASO modifications incorporate an *O*-alkyl group at the 2'-position of the sugar moiety. Arguably the most important structural modification of this class is the 2'-*O*-(2-methoxyethyl) (MOE) modification. It is known that RNA displays higher binding affinity to RNA than to DNA. The incorporation of the C2'-MOE modification into oligonucleotide sequences facilitates the 3'-*endo* or northern (N-type) conformation, which is naturally found in nucleotides when forming RNA-RNA duplexes. This pre-organization of the ASO and individual monomer units increases ΔT_m values (0.5 °C to 2 °C/modification) by minimizing the entropic energy penalty associated with the free energy of stabilization for the duplex formation with RNA. Biostability towards nuclease cleavage is also increased with the incorporation of this modification due to the ability of the MOE group to (hydrogen) bind a molecule of water and sterically hinder nuclease digestion at the C3'-position.[13]

One of the leading synthetic modifications that has been developed over the past 30+ years is locked nucleic acid (β-D-LNA) or simply LNA. LNA is a third-generation nucleic acid

modification that was reported, almost simultaneously, by the groups of Wengel[14] and Imanishi[15] in 1998. In LNA, the ribose sugar is conformationally restricted by a methylene bridge that connects the 2'-oxygen to the 4'-carbon. This bridging unit of locks the ribose sugar into 3'-*endo* or N-type conformation (sugar pucker), which in turn, confers LNA-like conformations onto the entire oligonucleotide sequences of the ASO construct. This results in a significant increase in ΔT_m (2 °C to 5 °C per modification). α-L-LNA, the C-1 epimer of the enantiomer of LNA, has also been investigated and has shown improved thermal stability of ASO constructs containing this modification with higher ΔT_m values (4 °C to 6 °C per modification) compared to its diastereomeric form (LNA).[16] Due to the improved duplex stabilizing properties of these bicyclic modifications, this area of constrained nucleic acid synthesis has emerged as important field in antisense-based drug discovery. These investigations have led to numerous bicyclic and, more recently, tricyclic nucleic acid modifications, which are discussed below.

1.2.1 Bi- and tricyclic nucleic acid modifications

Earlier efforts to introduce conformational constrain into oligonucleotide analogs were first reported by Leumann and co-workers in 1994[17] and 1997[18]. Their study was focused on the impact of more rigid sugar-phosphate backbone structures on binding affinity. For this, they synthesized nucleosides containing an "ethylene bridge" connecting 3'- and 4'-carbons, which amounts to cyclopenta-annulation of the ribose ring, affording a 1-oxa-bicyclo[3.3.0]octane unit (**6.1**, Figure 6). This bicyclic structure introduces rotational restriction around torsional angle γ. Furthermore, the 3',4'-annulation conferred conformational preorganization by mimicking the sugar pucker geometry of natural nucleotide units in DNA duplexes. The tricyclic modification later reported (**6.2**, Figure 6) was designed to provide further rigidity of the sugar-phosphate backbone. In this case, the introduction of a cyclopropane unit connecting the 5'- and 6'-centers showed an increase in ΔT_m of 1 °C to 3 °C/mod, restriction of the mobility of torsional angle γ mimics the corresponding orientation of γ in natural nucleotides units in DNA duplexes, increasing binding affinity.

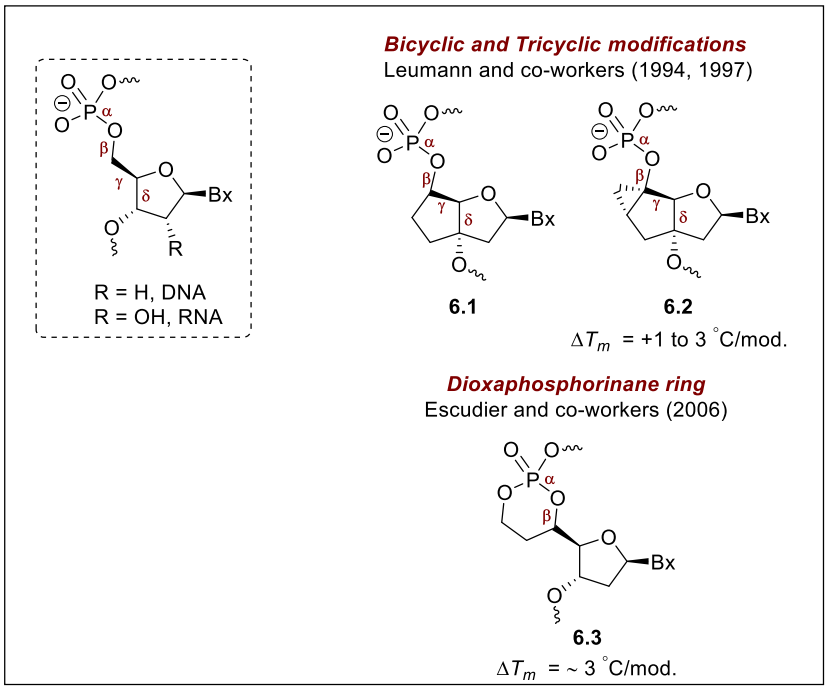

Figure 6. Strategies to introduce conformational restrictions into AOSs

In 2006, Escudier and co-workers investigated the contribution of conformationally restriction of the phosphate backbone. This was achieved by the introduction of a dioxaphosphorinane ring structure that locked the backbone torsional angles α and β of the nucleic acids. The dimeric unit synthesized in this study showed a promising increase in duplex thermal stability, with ΔT_m values of +3 °C/modification (**6.3**, Figure 6).[19]

Until 2012, the idea of introducing dual modes of conformational restriction into the ribose backbone of a nucleic acid modification was unknown. In that year, Hanessian and co-workers reported the synthesis of a tricyclic nucleic acid (TriNA) modification that showed unprecedented duplex thermal stability (ΔT_m values of +4 °C to +8 °C/modification).[20] In TriNA **6.4**, which as an α-L-LNA-like unit restricting the ribose sugar pucker into the N-type sugar pucker, conformational mobility around the torsional angle γ is restricted via spiroannulation at the C4'-position (**6.4**, Figure 6). In 2013, Hanessian and co-workers reported the synthesis of another class of TriNAs, which featured linear annulation of the ribose backbone with a six-membered ring and the incorporation of the familiar oxamethylene bridge found in the LNAs (**6.5**, Figure 6). It was found that this mode of dual conformational

restriction did not afford the same increase of thermal stability of the investigated ASO constructs.[21] Thus, it would seem that future development of spiroannulated analogs of LNAs would be a worthwhile endeavor for improving the (limited) library TriNAs and nucleoside monomers for antisense-based drug discovery.

α-L-configured tricyclic nucleic acid (TriNA)
Hannesian and co-workers (2012)

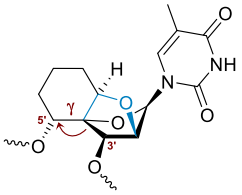

7.1

ΔT_m = +4 to 8 °C/mod.

bis-constrained nucleic acids
Spiroannulation C4′

α-L-configured tricyclic nucleic acid 2 (TriNA 2)
Hannesian and co-workers (2016)

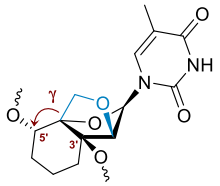

7.2

ΔT_m = ?

bis-constrained nucleic acids
Linear annulation

ON	Modification	Sequence (5' to 3')	ΔT_m/mod. (°C) DNA	RNA
A1	DNA	d(GCGTTTTTTGCT)	ref	ref
A2	LNA	d(GCGTTITTTGCT)	+1.7	+5.2
A3	α-L-LNA	d(GCGTTITTTGCT)	+1.4	+5.7
A4	α-L-TriNA 1	d(GCGTTITTTGCT)	+2.6	+7.1
B1	DNA	d(CCAGTGATATGC)	ref	ref
B2	α-L-LNA	d(CCAGTGAIATGC)	+6.5	+6.3
B3	α-L-TriNA 1	d(CCAGTGAIATGC)	+7.4	+8.3
B4	α-L-LNA	d(CCAGTGATAIGC)	+4.4	+4.5
B5	α-L-TriNA 1	d(CCAGTGATAIGC)	+4.4	+4.7

Duplex thermal-stability measurements of LNA-, α-L-LNA-, and spiroannulated-TriNA-modified oligonucleotides versus DNA and RNA complements

Figure 7. Hanessian and co-workers Tricyclic nucleoside modifications and ΔT_m values of spiroannulated- TriNA-modified oligonucleotides

While TriNAs possess outstanding stabilization of RNA duplexes (ΔT_m Table, Figure 7), their application as drug candidates in antisense technology has been limited. This is due the lengthy synthetic sequences that are required for their preparation, which points to a weakness in nucleoside-based chemical synthesis. In the Hanessian syntheses of TriNAs **7.1** and **7.2** (Figure 7), over 28 steps were necessary to synthesize the target nucleosides. All of their syntheses took advantage of well-established carbohydrate chemistry to selectively functionalize the ribose sugar ring, which ultimately required the application of a three-step synthetic protocol for the introduction of the nucleobase. The nucleobase being

installed after 18 chemical reactions were performed on a commercially available carbohydrate precursor, diacetone-D-glucose (**8.1**). In the context of the application of TriNAs to antisense-based drug discovery, the length of the synthetic sequences required for their preparation translates into high production cost, making TriNAs less attractive to the pharmaceutical companies for future development. This puts academic laboratories in a position to develop new synthetic technology that will lead to streamlined synthetic approaches to these complex targets, without the competition from pharmaceutical companies.

Researchers continue to advance the chemistry and design of the antisense drugs, so there is an increasing number of ASOs at different stages of clinical trials for the treatment of severe and rare diseases, cardiovascular and metabolic conditions, inflammations and several types of cancers.[22] Since most antisense drug candidates, that have been either FDA approved or are currently in late-phase clinical trials, have an average of 20 nucleic acid monomers incorporated into their structures (an average molecular weight of 7000 Da), more efficient synthetic protocols for the preparation of important nucleoside modifications is vital to their marketability. With this in mind, a chemical synthesis project centered on the development of regioselective reactions of nucleoside bases starting materials was pursued (see below).

1.3 Synthesis of complex nucleic acid modifications

To date, the synthesis of bi- and tricycle core structures of challenging nucleosides targets has relied on the use of carbohydrate starting materials, which requires the use of multiple protecting groups, repeated redox reactions, and the obligatory use of a three-step synthetic sequence to introduce the nucleobase into the carbohydrate backbone, making these approaches non-ideal from a step-economical point of view.

The TriNA reported by Hanessian and co-workers mentioned earlier, required 25 steps to assemble the desired tricyclic core, where only 5 steps involved skeletal building reactions (Figure 8).

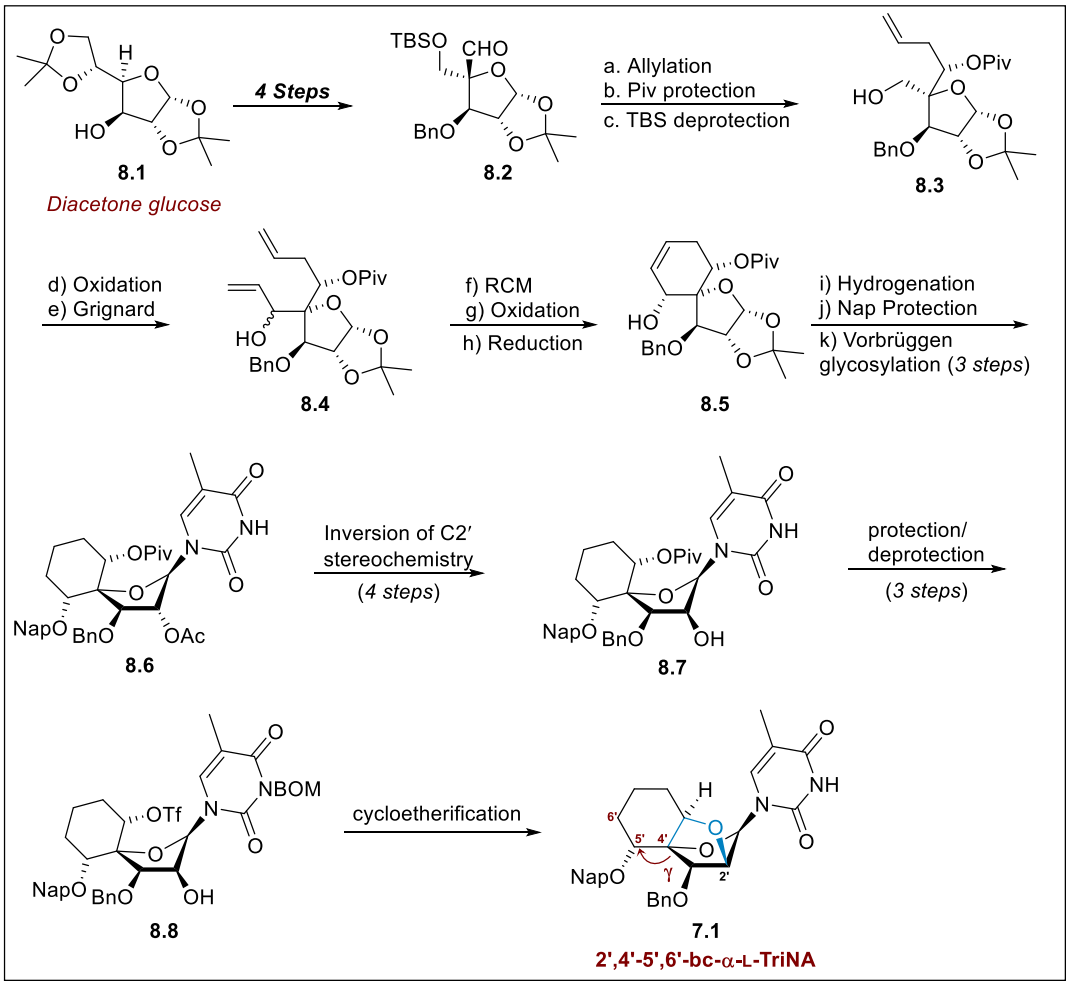

Figure 8. Hanessian and co-workers synthesis of α-L-tricyclic nucleic acid **7.1**

Using a carbohydrate starting material, diacetone-D-glucose (**8.1**), is the primary reason for the use of so many concession steps to arrive at spiro-diene **8.4** (Figure 8). Synthesis of the spirocyclic cyclohexene was achieved by ring-closing metathesis, followed by a series of redox reactions to introduce the desired carbinol stereochemistry and diastereomerically pure spirocycle **8.5** (Figure 7). Three synthetic steps were the used for the incorporation of the nucleobase into the carbohydrate to afford thymidyl nucleoside **8.6**. Finally, the 2',4'-anhydro bridge required first inversion of the stereochemistry at the 2'-position, followed by a challenging cycloetherification reaction onto the sterically hindered triflate **8.8** to afford nucleoside **7.1**.

1.3.1 The development of a streamlined synthetic protocol for complex nucleoside synthesis

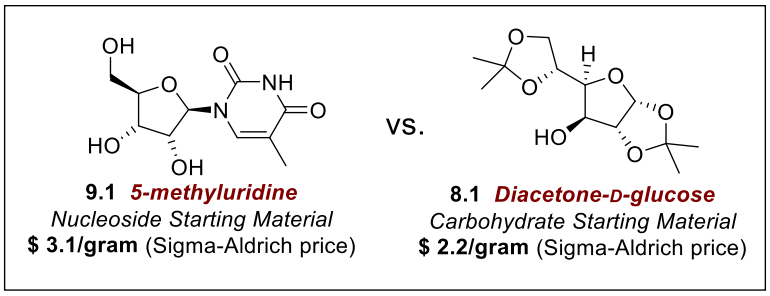

Figure 9. Nucleoside vs. carbohydrate starting material

The nucleic acid modifications that have been reported over the past 30+ years have primarily involved structural manipulations about the ribose sugar unit, with very little emphasis being placed on modification of the nucleobase due to the strong fidelity of Watson-Crick base pairing. Thus, the design of new synthetic methods or strategies for accessing complex, bi- and tricyclic nucleosides should commence with readily available nucleoside building blocks. By comparison, nucleosides are essentially equivalent in price to carbohydrates, however, structural modifications and redox reactions of nucleosides are far less prevalent when compared to carbohydrates. The latter is quite striking in view of the plethora of work that has been done in bioorganic organic and chemical biology-based research programs focused on antisense technology.[23] Nonetheless, this presents an opportunity for synthetic chemists to develop new strategies for complex molecule synthesis. The main advantages of using nucleosides as starting materials include: 1) the removal of a three-step protocol for nucleobase introduction; 2) less hydroxyl groups to protect or modify during the synthesis of more complex scaffolds; and 3) the potential for investigating synthetic intermediates (or starting materials) as new nucleic acid modifications, since the nucleobase will already be intact. The latter will also allow for direct comparisons of the effects of conformational rigidity imposed on the targets to be investigated here.

Assembly of the tricyclic core of the targeted nucleic acids was planned to be accomplished via transannular ring closure (**10.1**, Figure 10) from an appropriately functionalized bicyclic nucleoside intermediate (**10.2**, Figure 10). This novel strategy would shorten the overall reaction sequence giving rapid access to complex nucleoside cores, which makes this approach highly attractive for the development of oligonucleotide drugs. In this sense, the present study focuses on strategies for the formation of macrocycle rings *cis*-fused

(**10.3**, Figure 10) or *trans*-fused (**10.5**, Figure 10) to the furanose portion of the nucleoside at the C2' and C4' carbon atoms to yield bicyclo[*n*.2.1] scaffolds that can serve for subsequent construction of diverse tricyclic nucleoside modifications.

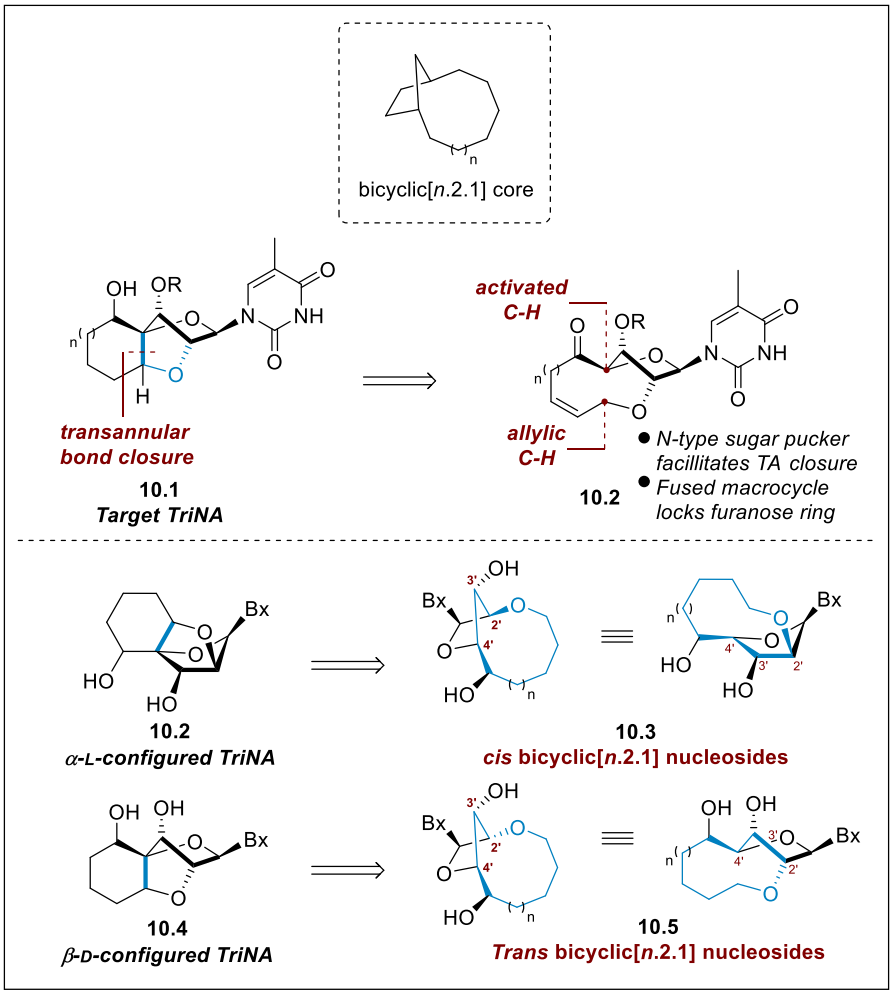

Figure 10. Structures of proposed bicyclic nucleoside modifications and strategy to assemble the tricyclic core

This type of bridging and macrocyclic constrain represents a new motif in nucleoside modifications that were predicted to restrict the rotation of the torsional angle γ and additionally set the ribose sugar portion into an *N*-type conformation, potentially favoring hybridization with RNA when incorporated into oligonucleotide sequences, therefore the bicyclic nucleoside modification itself could be tested for antisense technology.

1.4 Examples of bicyclo[6.2.1] frameworks

Bicyclo[6.2.1]undecane and related bridged macrocyclic ring structures have been of considerable interest due to their presence in bioactive natural products and their applicability as important precursors in the synthesis of other natural products such as the taxanes and their derivatives (Figure 11A).[24] These unusual and strained bicyclic structures present what Westman and Kober in 1970 called an “abnormal bonding situation at the bridgehead”.[25]

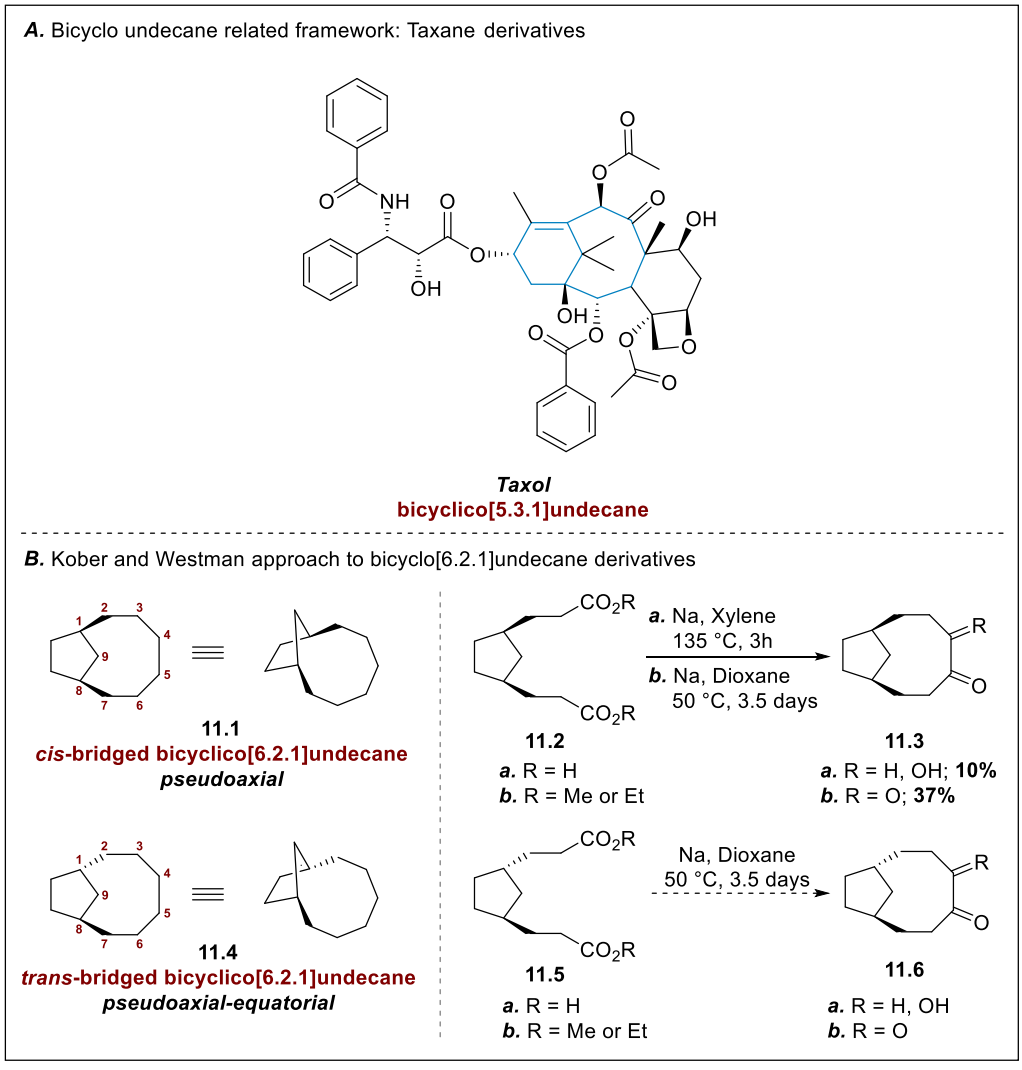

Figure 11. a) Bicyclo undecane related framework. b) Kober and Westman approach to bicyclo[6.2.1]undecane derivatives

In their study Westman and Kober proposed that the six-carbon bridge could be bonded to the cyclopentane ring in a *cis* or *trans* fashion, and due to the constrain imposed by the bridged system the bonding would be pseudoaxial in the case of the *cis*-configured bicyclic structure (**11.1**, Figure 11B) and pseudoaxial-equatorial in the *trans*-configured bicyclic structure (**11.4**, Figure 11B). They attempted the synthesis of *cis*- and *trans*-bicyclo[6.2.1]undecane derivatives through an acyloin reaction of diester ring precursors observing only the formation of the *cis*-bicyclic acyloin in low yields (Figure 11). They concluded that the failed construction of the desired bicyclic[6.2.1]undecane structures or low yielding reactions can be explained by the relatively high strain energy of the products, which is in turn, caused by transannular and torsional steric interactions, and the large entropy of activation to be overcome in bringing the two ends of the long chain in close proximity during the cyclization process.

The bicyclo[6.2.1] framework is present in several biologically active sesquiterpene lactones natural products (Figure 12). This unique class of natural products have been isolated from the leaves of plants traditionally used in rural areas of developing countries for the treatment of infections. Tagitinin A and Tirotundin isolated from *Tithonia Diversifolia*,[26] a plant native to Central America contains this peculiar oxygen bridged bicyclic core. A closely related sesquiterpene isolated from the Brazilian plant *Eremanthus elaegnus*, Eremantholide A[27] with cytotoxic properties, contains a similar bicyclic framework, with the main difference due to the presence of two conjugated endocyclic double bonds in the bicyclic core (Figure 12).

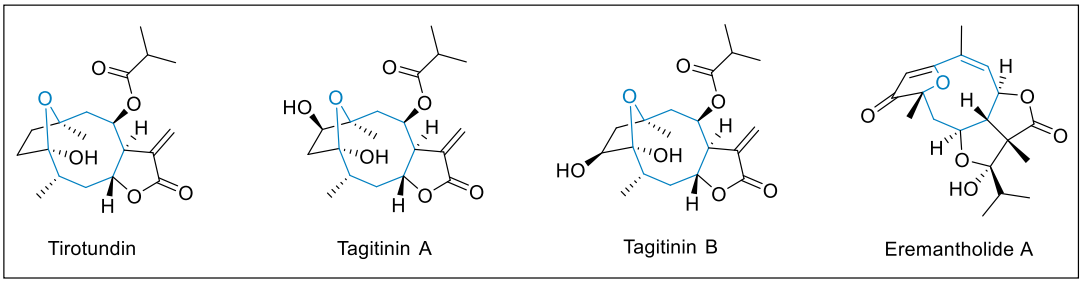

Figure 12. Bioactive sesquiterpene lactones natural products

Although numerous studies on the biological properties of Tagitinins and Tirotundin have shown they could be considered as lead compounds for the development of new drugs, the total synthesis of such compounds has not been reported. On the other hand, several reports

on the synthesis of analogous Eremantholide A are found in the literature. The reported studies explore different strategies for the construction of the complex framework that exist in these natural product, with special emphasis on accessing the 11-oxabicyclo[6.2.1]undecane core structure.

In 1989, McDougal and co-workers reported their efforts to access the 11-oxabicyclo[6.2.1]undecane framework of Eremantholide A.[28] The key step in their approach involved an ozonolysis reaction of a functionalized oxa-bridged octalin unit, to furnish **13.2**, which was then used to assemble the desired bicyclic structure by expanding of the bridging system (Figure 13A).

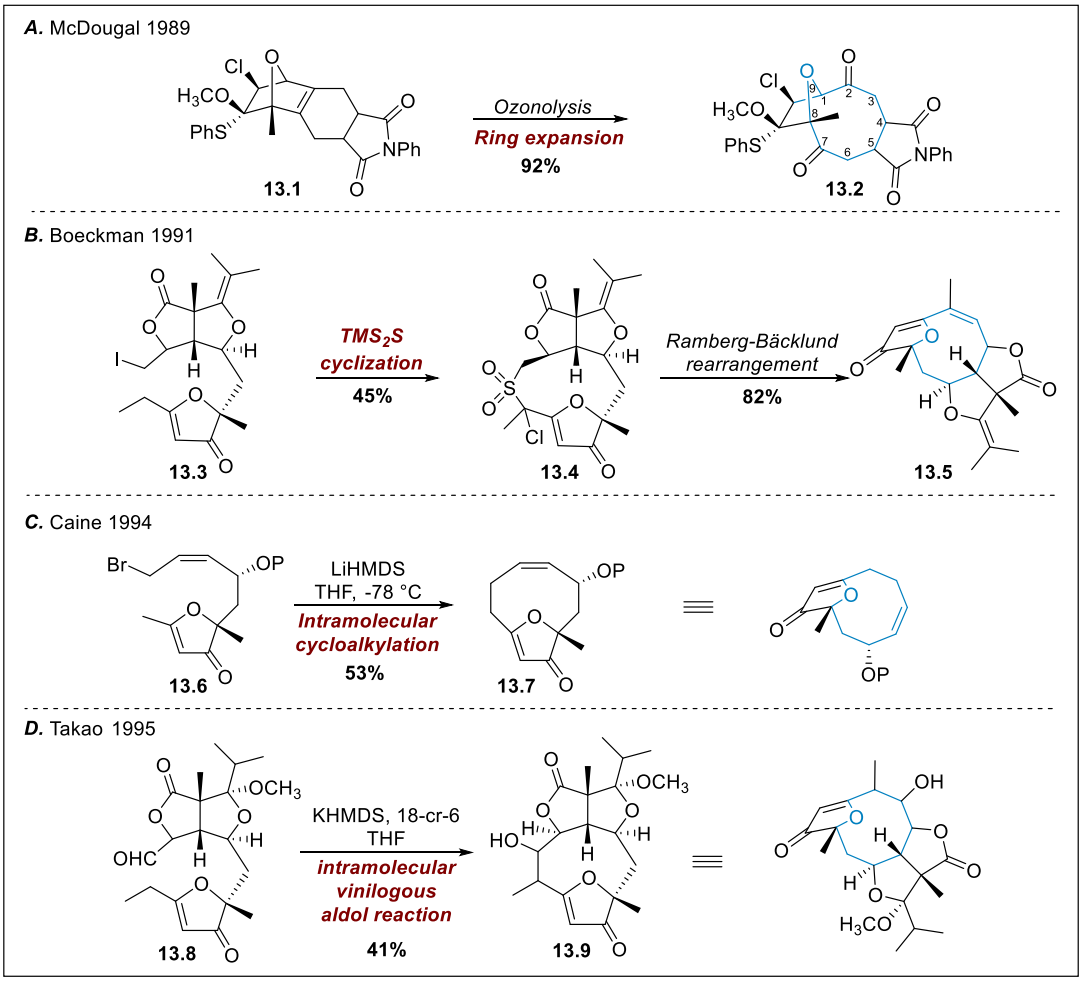

Figure 13. Selected synthetic approaches to the bicyclic core of Eremantholide A

The first total synthesis of Eremantholide A was completed in 1991 by Boeckman and co-workers (Figure 13B).[29] In their approach synthesis of the bicyclic framework was achieved by reacting bromo lactone **13.3** with a nucleophilic sulfur reagent to yield the 10-membered thiacycle **13.4**. After oxidation to the sulfone, followed by ring contraction using a Ramberg-Bäcklund reaction sequence, the desired 9-membered macrocycle was isolated in 82% yield. This also led to the formation of the intended bicyclic core structure of the natural product.

Later, in 1994, an intramolecular (cyclo)alkylation was employed by Caine and Arant in their reported approach to racemic 11-oxabicyclo[6.2.1]undec-10-en-9-one **13.7** (Figure 13C).[30] The key intramolecular cycloaddition using the appropriately substituted monocyclic 3(*2H*)-furanone derivatives yielded the desired ring structure. A year later, Takao and co-workers reported a completely different approach from that of the Boeckman group for their total synthesis of Eremantholide A.[31] In this approach, coupling of two building blocks by first, α-alkylation followed by intramolecular vinylogous aldol reaction successfully assembled the complete molecular framework and the desired bicyclic system (Figure 13D).

1.5 Ring-closing metathesis for the construction of large rings

Ring-closing metathesis (RCM) of alkenes is widely used as key step in the construction of small, medium and large rings in organic synthesis.[32] The popularity of this reaction is due to the Ru-catalyst ability to tolerate a wide variety of functional groups, as well as the possibility of further transformation of the unsaturated ring products. Thus, it is not surprising to find that recent attempts to synthesize the 9-membered ring present in the bicyclic core of Eremantholide A employed the RCM as the key reaction. In 2007, Hale and Li[33] completed the total synthesis of Eremantholide A, using a RCM reaction that employed the Hoveyda-Grubbs II catalyst to construct the bicyclic core of the natural product. In their approach, similar to that of Takao and co-workers, two building blocks were coupled by, first enolate *C*-alkylation and then the RCM. At high dilution, in toluene, elevated temperatures and 14 hours of reaction time was required to afford the strained nine-membered macrocycle in 54% yield. Due to the success of RCM to construct large rings that comprise a bicycloalkane core structure structure, our first attempts to synthesize bicyclic nucleoside intermediates was done so using a RCM-based approach (Figure 14).

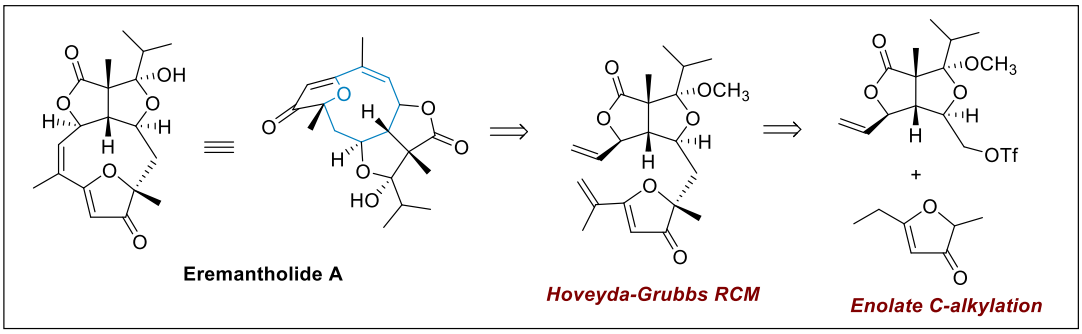

Figure 14. Li and Haley's RCM-based approach to the bicyclic core of Eremantholide A

1.6 RCM-based approach to macrocyclic precursors of β-D-TriNA analogs: synthesis of a *trans*-bicyclo[6.2.1] nucleoside intermediate

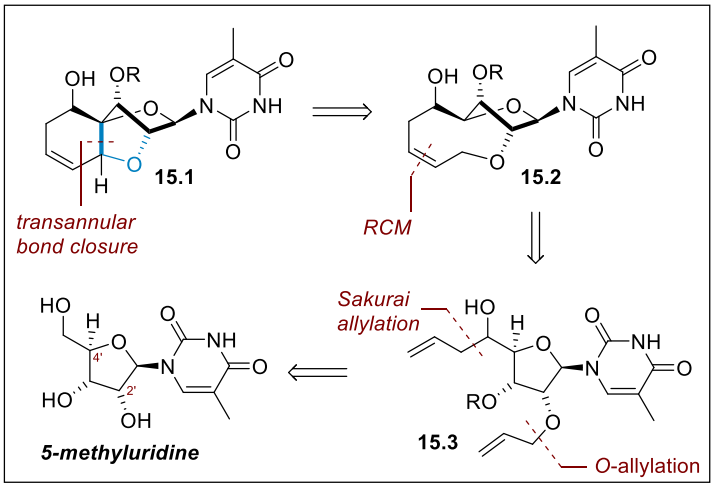

Figure 15. RCM approach to access *trans*-bicyclic[6.2.1] nucleoside modifications: β-D-TriNA analogs

The desired bicyclic nucleoside was anticipated to be assembled from a RCM reaction of diene 15.3 (Figure 15). A Sakurai allylation was planned for extension of the 5'-carbon, while direct *O*-allylation on 2'-oxygen atom would install the second alkene unit required for the planned macrocyclization.

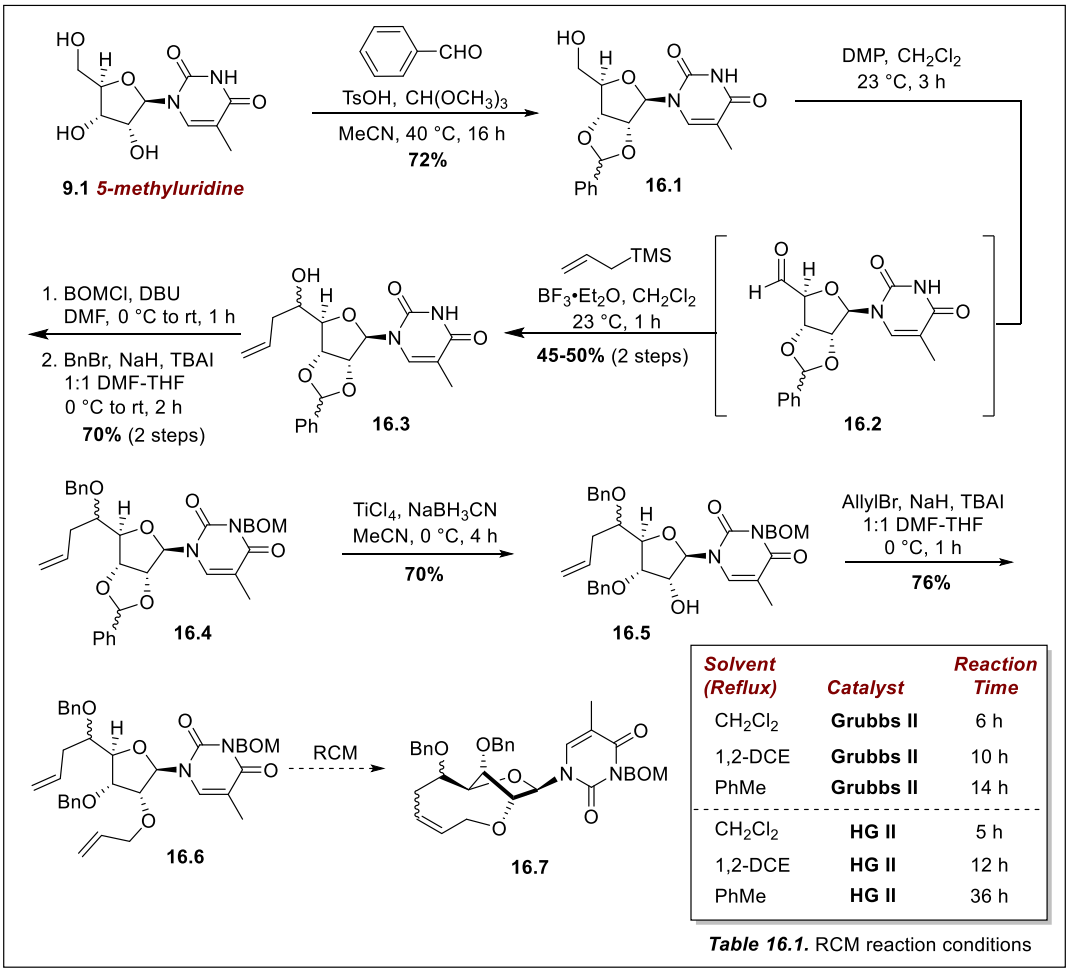

Figure 16. Synthesis of bis-allylated nucleoside ring precursor **14.6** and attempted RCM reactions to furnish bicyclic[6.2.1] nucleoside **14.7**

Commercially available and inexpensive nucleoside 5-methyluridine (**9.1**) was converted into benzylidene acetal **16.1** as a mixture of diastereomers (2:1 *d.r.*) in 72% yield (Figure 16). This transformation left the primary hydroxyl group at the 5' position unprotected and susceptible to oxidation. Treatment of **16.1** with Dess-Martin Periodinane (DMP) afforded the corresponding aldehyde **16.2**, which was directly subjected to Sakurai allylation conditions to give homoallylic alcohol **16.3** in 45-50% overall yield. Compound **16.3**, which contains one of the olefin units present in the targeted diene **16.6** could be easily synthesized on a gram scale. The regioselective synthesize diene **16.6** required the protection of both the free nitrogen atom of the nucleobase and the homoallylic alcohol to avoid unwanted side

reactions. Selective nitrogen alkylation was achieved using BOMCl and DBU in DMF, followed by direct benzylation of the 5'-OH to yield intermediate **16.4** in 70% yield over two steps. The N-BOM and O-Bn protecting groups were selected at this due the prospects of a global deprotection at a late stage in the synthesis. A regioselective opening/cleavage of the benzylidene acetal present in **16.4** was accomplished by a Ti-mediated sodium cyanoborohydride reduction to furnish only the 3'-OBn ether **16.5**, leaving the 2'-OH available for further manipulation. Allylation of the 2'-OH group under standard conditions furnished diene **16.6** in 53% overall yield. With diene **16.6** in hand we tested the RCM-based approach to **16.7** using several sets of conditions (Table 16.1, Figure 16).

All attempts to promote cyclization of diene **16.6** resulted in the formation of complex mixture. HRMS analysis of the crude reaction mixtures evidenced the presence of the expected product, however, all efforts to isolate the desired product failed.

It is well known that selection of the appropriate reaction conditions for the key ring-closing step is critical for the efficiency of the planned macrocyclization. However, the success of the methodology used to obtain macrocyclic structures is also associated with the presence of preorganizational characteristics of the open-chain precursor. Conformations and configurations can be vital to successful cyclization reactions, with the former being related to folded conformations the shorten the end-to-end distance, and the latter associated with stereochemistry that effect preorganization of the substrate. With this in mind, we set our sights on a different macrocyclization precursor – *i.e*., a diastereomer of **16.6**.

1.6.1 Synthesis of a *syn*-configured diene for an RCM-based macrocyclization

In our first attempt to synthesize the bicyclico[6.2.1]undecane framework of **16.7**, the two allyl subunits of diene **16.6**, the macrocyclization precursor, were on opposite sides of the ribose ring unit. Initially, we had envisaged that the *anti*-2',4'-diastereomer would require a more challenging RCM reaction; however, we reasoned that the same synthetic approach to this macrocyclization precursor would be amenable to *syn*-2',4'-diastereomer. Ultimately, we wanted to investigate the synthesis of both of these analogs. The six-carbon bridging unit of the bicyclic system, which comprises a nine-membered ring when the 2', 3', and 4' carbon atoms of the ribose unit are included in the macrocyclic ring count, to be formed with *trans*-relative stereochemistry (C2' and C4') causes more deformation in the ribose unit of the

nucleoside. Thus, the conformation that needs to be attained for successful RCM is more strained. We concluded that the failure to produce significant yields of the expected bicyclico[6.2.1]undecane nucleoside β-D-analog was possibly due to the relative stereochemistry at the 2' and 4'-positions and the distance between the alkene units was just too great for cyclization to occur. In that sense, our next approach was directed towards the synthesis of 2',4'-*syn*-bicyclic nucleoside analogs. In this instance the diene precursor would contain two allyl subunits on the same side of the ribose sugar unit, resulting in a lower energy conformation for the anticipated macrocyclic RCM reaction.

1.7 RCM strategy to α-L-TriNA analogs: Synthesis of a 2',4'-*syn*-bicyclo[6.2.1] nucleoside intermediate

Our synthesis plan for the 2',4'-*syn* bicyclo[6.2.1] nucleoside analog **17.1** (Figure 17), called for a RCM reaction on diallylated compound **17.3**. To this end, the same allylation protocols that were employed for the 2'-OH and 5'-C extensions of **8.1** would be applied to the synthesis of **15.2**. The major change in the synthetic plan of **15.3**, was the inversion of the C-2' stereochemistry. This would be achieved upon formation of the 2,2'-anhydronucleoside **15.5**, followed by hydrolysis.

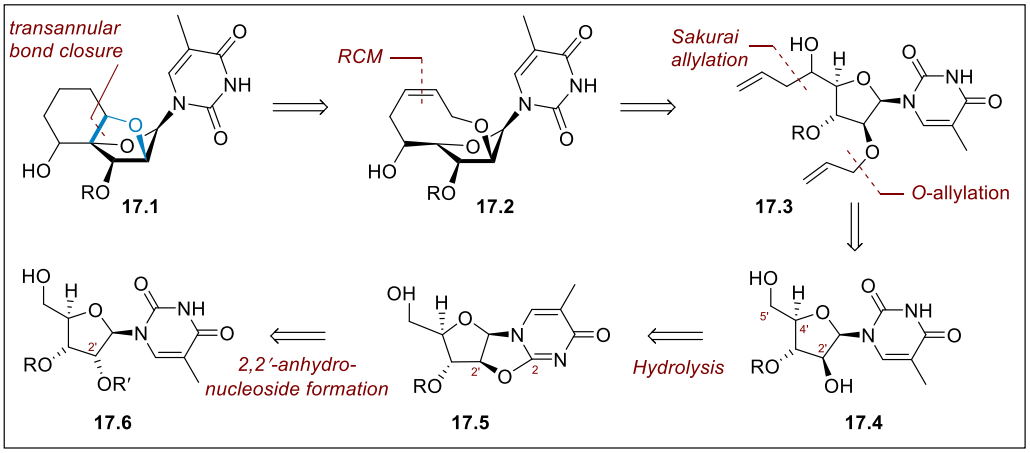

Figure 17. RCM approach to access *cis*-bicyclic[6.2.1] nucleoside modifications: α-L-TriNA analogs

5-methyluridine was converted into benzylidene acetal **14.1** (Figure 16) using a modified procedure that increased the yield of this reaction to 90% (72%, **8.1** to **16.1**, Figure 16). After

protection of the primary hydroxyl group as the TBDPS ether, regioselective cleavage of the benzylidene acetal afforded alcohol **18.1** in a 41% overall yield on a gram scale. In order to invert the stereochemistry of the C2' carbon atom, the 2'-OH was sulfonylated with MsCl in pyridine to afford **18.2** in 98% yield, followed by 2,2'-anhydronucleoside formation upon treatment of the mesylate with DBU in MeCN.

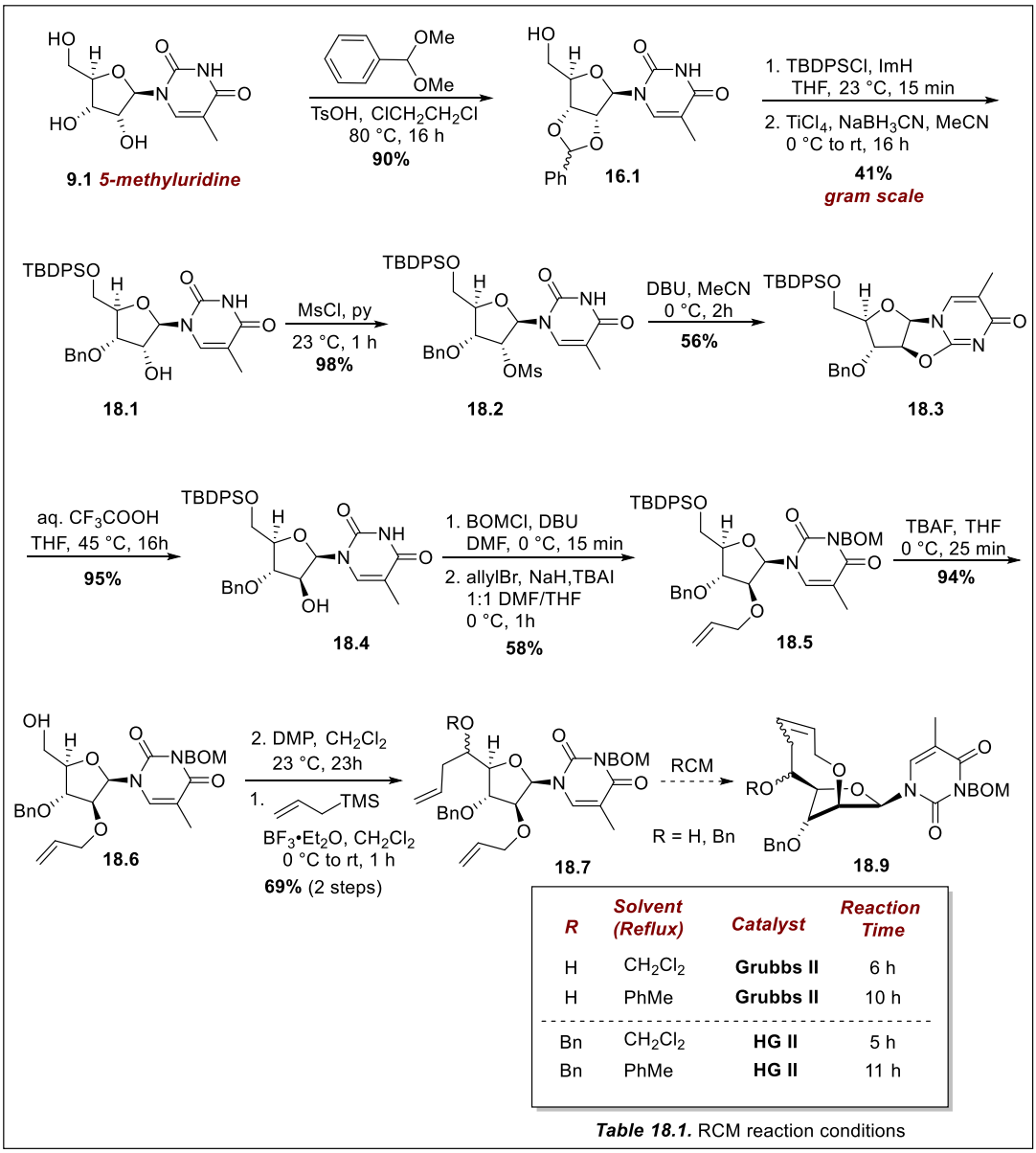

Table 18.1. RCM reaction conditions

Figure 18. Synthesis of bis-allylated nucleoside ring precursor to access *cis*-bicyclic[6.2.1] nucleoside modifications

Several attempts to open the 2,2'-anhydronucleoside **18.3** using literature procedures that employed basic conditions, resulted in the recovery of starting material, *i.e.*, **18.3** was resistant to basic hydrolysis. However, it was discovered that treatment of **18.3** with aqueous trifluoroacetic acid enabled the desired opening to yield the inverted C2'-OH in 95% yield. When **18.4** was treated BOMCl followed by allylation under basic conditions, **18.5** was obtained in 58% overall yield. After deprotection, 5'-OH in the presence of TBAF, the primary alcohol was oxidized to the corresponding aldehyde and directly subjected to Sakurai allylation conditions to afford diene **18.7** in 65% overall yield. Diene **18.7** was then subjected to RCM conditions using the conditions summarized in Table 18.1 (Figure 18).

In all the cases, the conditions used were ineffective in performing the desired cyclization. As in the previous case, RCM attempts on diene **18.7** resulted in the formation of a complex mixture from the product observed in HRMS couldn't be isolated.

It is known that medium sized ring (8 to 11-membered) formation can be difficult, and in the same way the ring precursor selection is crucial for macrocyclization, undoubtedly the structure of the ring to be formed has also a great influence on the cyclization process. Added to the previously mentioned Baeyer strain caused by bond angle deformation, ring strain due to the possible imperfect staggering factors (Pitzer strain) and transannular strain due to steric interaction between atoms across the ring being forced to be in close proximity, makes the cyclization process quite challenging in terms of the energy barrier to overcome during the ring formation. In particular, the formation of nine-membered rings using RCM or other cyclization strategies are quite limited. With not much literature guidance on the preparation of such rings, we began to consider alternative cyclization strategies that relies on the use of different cyclization precursors.

Reductive coupling methods have proven to be useful in the preparation of strained macrocycles. Specifically, the McMurry reaction, a reductive coupling of carbonyl compounds in the presence of low valent titanium reagents,[34] has served as the key step for macrocyclization in natural product total syntheses.[24]

1.8 Reductive coupling approach to β-D-TriNA analogs: Synthesis of 2',4'-*anti*-bicyclo[7.2.1] and 2',4'-*anti* -bicyclo[8.2.1] nucleoside intermediates

Since intramolecular RCM was found to be ineffective for the desired macrocyclization reaction in the synthesis of 2',4'-*syn*- and 2',4'-*anti*-bicyclo[6.2.1] nucleoside intermediates, we explored a second-generation strategy that relied on the use of the McMurry reaction to form the macrocyclic ring present in these targets, on route to assembling the desired bicyclic core structures.

Our initial approach was to use the diene ring precursors that had been synthesized in the RCM-based approach to test the viability of this reductive coupling reaction for macrocyclization of nucleoside intermediates, for which there was little precedent. In this regard, selective olefin oxidation reactions could furnish an 11-membered (dialdehyde **19.5**, Figure 19), 10-membered (ketoaldehydes **19.6** and **19.7**, Figure 19) and 9-membered (diketone **19.8**, Figure 19) annulation precursors.

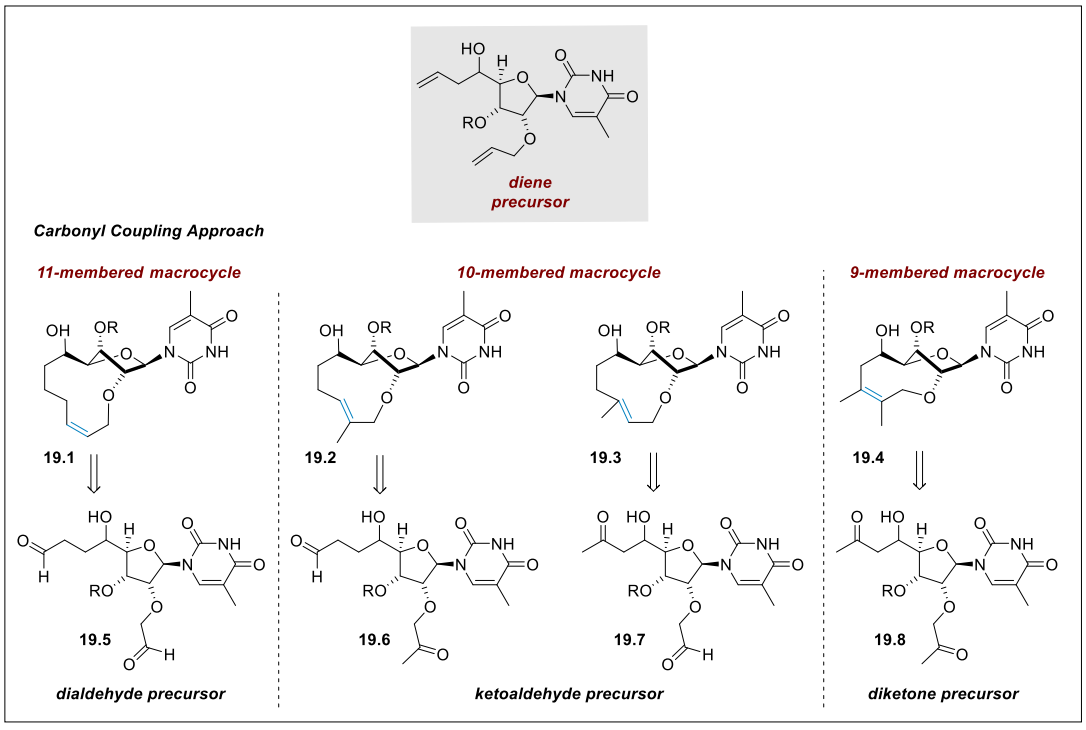

Figure 19. Carbonyl coupling approach to access bicyclo[7.2.1] and bicyclo[8.2.1] nucleoside modifications

In an initial study directed towards the introduction of the needed carbonyl subunits for the McMurry-based macrocyclization strategy, diene **16.6** was subjected to Wacker oxidation conditions in an attempt to obtain diketone precursor **19.8**, this approach didn't yield the expected diketone product and instead a complex mixture was obtained. In a second approach, alcohol **20.1** was prepared in three steps from 5-methyluridine. Protection of the nucleobase nitrogen as the N-BOM derivative was necessary in preparation for allylation of the 2'-OH of **20.2** (Figure 20). Under the same conditions that were reported above, **20.2** was prepared in near quantitative yield. Direct allylation with allyl bromide in the presence of sodium hydride and TBAI afforded **20.3** in 80%. The O-allylated nucleoside **20.3** was then subjected to cross metathesis with methyl acrylate using the Hoveyda-Grubbs II catalyst. The resulting α,β-unsaturated ester was not isolated, but rather subjected to direct transfer hydrogenation conditions, which produced methyl ester derivative **20.5** in 70% overall yield. A Dibal-H reduction of the ester at -78 °C in toluene afforded the aldehyde **20.6** in 46% yield. The synthesis of **20.6**, established a synthetic approach that would enable the introduction of a butyraldehyde unit in a nucleoside precursor for future reductive coupling.

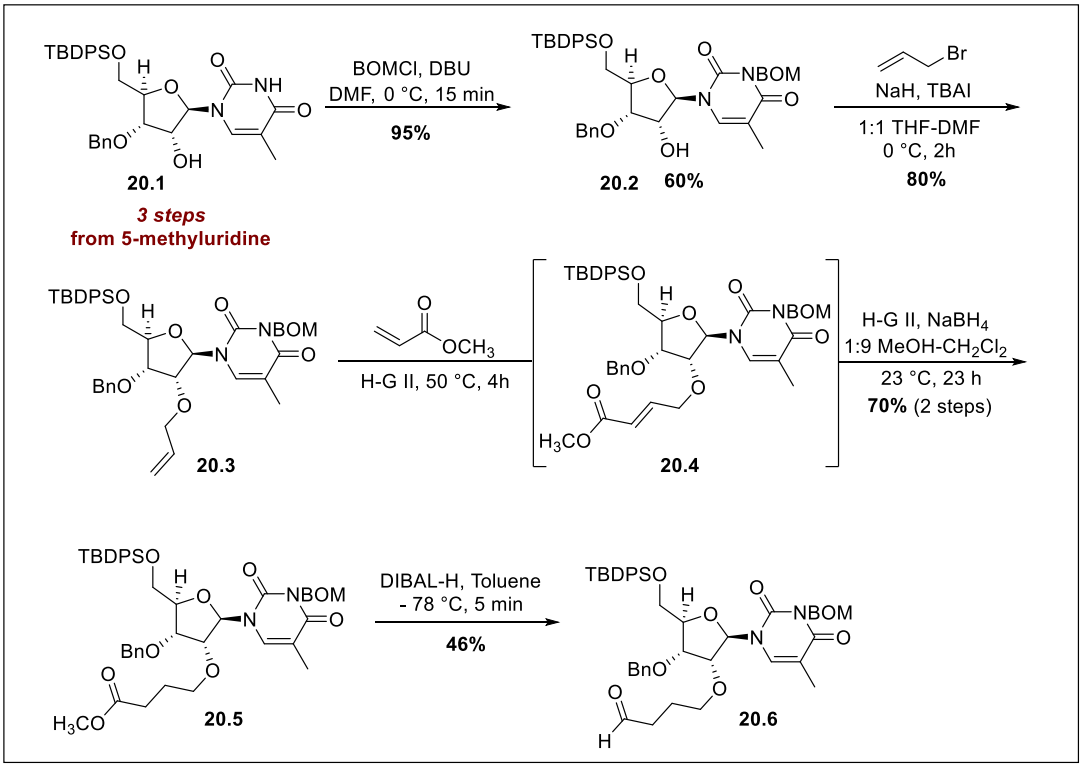

Figure 20. Installation of a butyraldehyde unit at the 2'-OH of nucleoside **20.6**

The preparation of the ketoaldehyde and dialdehyde derivatives **19.7** and **19.5**, respectively commenced with allylated nucleoside **20.3**, which was prepared in four steps from 5-methyluridine (Figure 20).

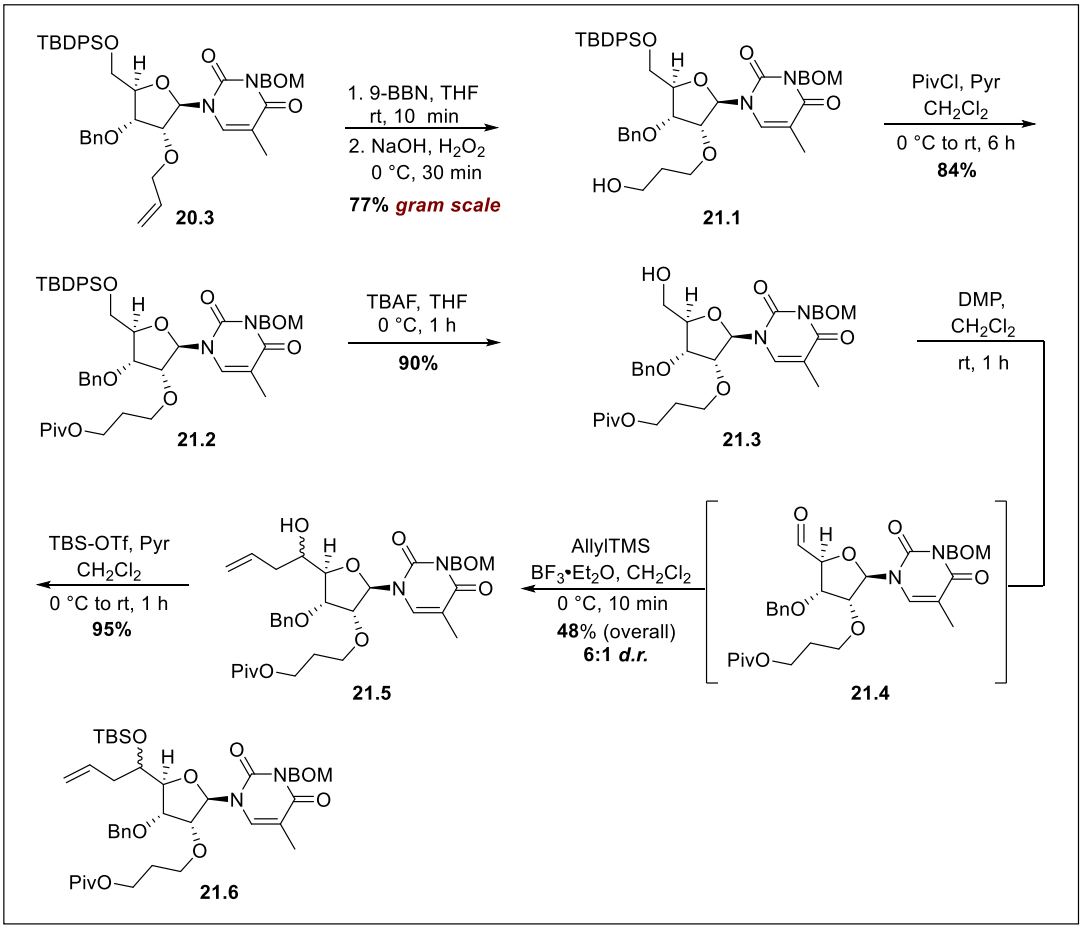

Figure 21. Installation of 2'-OH extended chain

Hydroboration/oxidation using 9-BBN afforded primary alcohol **21.1**, which was subsequently protected as the pivaloyl (piv) ester **21.2**. Removal of the TBDPS group furnished alcohol **21.3** in 90% yield, which was oxidized to the corresponding aldehyde and directly subjected to Sakurai allylation furnishing homoallylic alcohol **21.5** in 48% over two steps. It should be noted that oxidation of 5'-OH to the corresponding aldehyde should be done under Dess-Martin conditions and that the resulting aldehyde should be used immediately. All other oxidation protocols led to the formation of intractable material, and

storing the aldehyde for extended periods of time leads to decomposition, and lower yields in subsequent allylation reactions. Protection of the homoallylic alcohol as the TBS ether was done so to avoid secondary alcohol oxidation and complications during the proposed Wacker oxidation reactions. Furthermore, conversion of **21.5** to **21.6** furnished a mixture of diastereomers that could be separated by chromatography.

To convert the olefin subunit of **21.6** to the desired ketone **19.7**, Wacker oxidation using $PdCl_2$ and $Cu(OAc)_2$ in DMA/H_2O (7:1) was performed (Figure 22A).

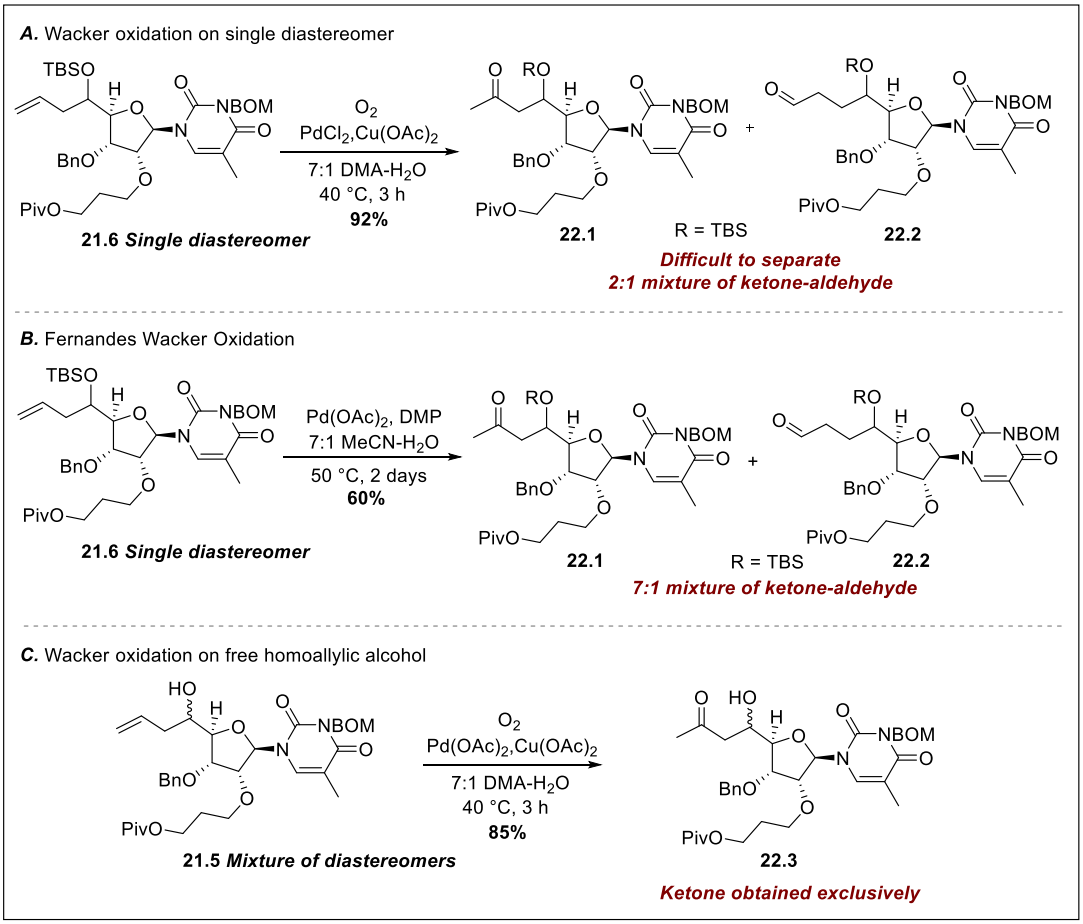

Figure 22. Wacker oxidations of 5' olefin subunit

Our expectation was that only the ketone product would be formed exclusively, however, an inseparable mixture of ketone **22.1** and aldehyde **22.2** was produced in 2:1 ratio. Fernandes and co-workers reported an alternative Wacker-type oxidation that uses DMP as

oxidizing agent to afford exclusively the Markovnikov-based Wacker products.[35] These conditions were employed on compound **21.6** to obtain a 7:1 mixture of ketone **22.1** and aldehyde **22.2** products (Figure 22B). Interestingly, when standard Wacker conditions using oxygen gas were employed on the unprotected diastereomeric mixture of homoallylic alcohols **21.5**, only the ketone oxidation product is observed (**22.3**, Figure 22C).

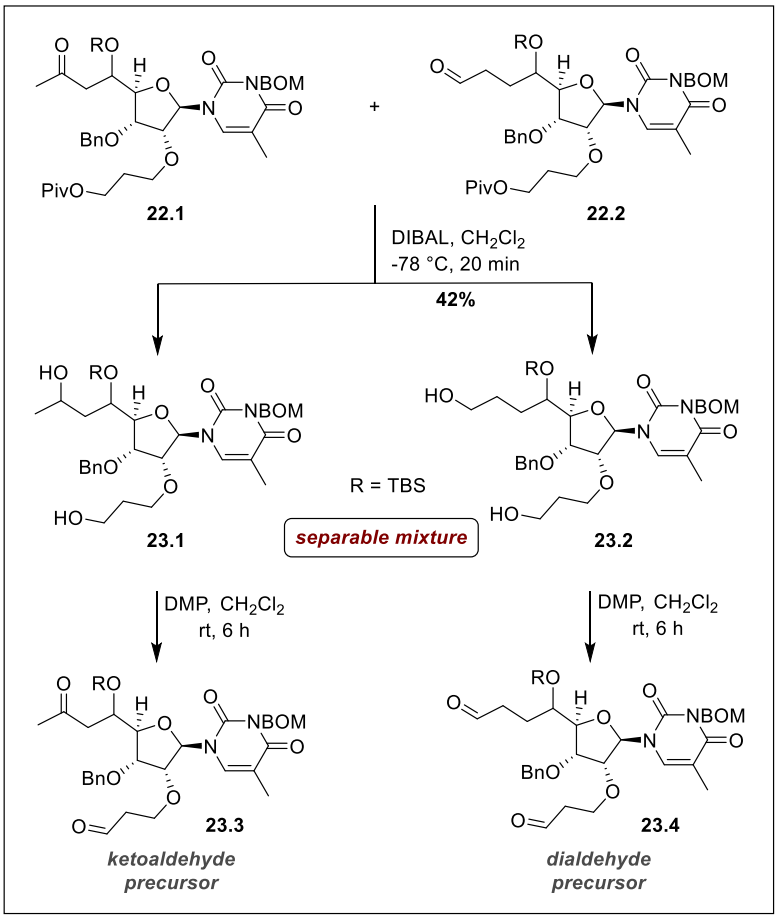

Figure 23. Final steps in the synthesis of ketoaldehyde **23.3** and dialdehyde **23.4** ring precursors

Selective removal of the pivaloyl protecting group using DIBAL also reduced the ketone and aldehyde to the secondary and primary corresponding alcohols **23.1** and **23.2** in 42% yield (Figure 23). At this point we were able to separate the alcohols and individually oxidize them to the ketoaldehyde and dialdehyde ring precursor **23.3** and **23.4**.

McMurry reaction using low-valent titanium was tested to promote intramolecular reductive coupling of ketoaldehyde **23.3** and dialdehyde **23.4** and to construct the ten- and eleven-membered macrocycles and assemble the bicyclic[7.2.1] (**24.1**) and bicyclic[8.2.1] (**24.2**) framework of the key bicyclic nucleoside intermediates.

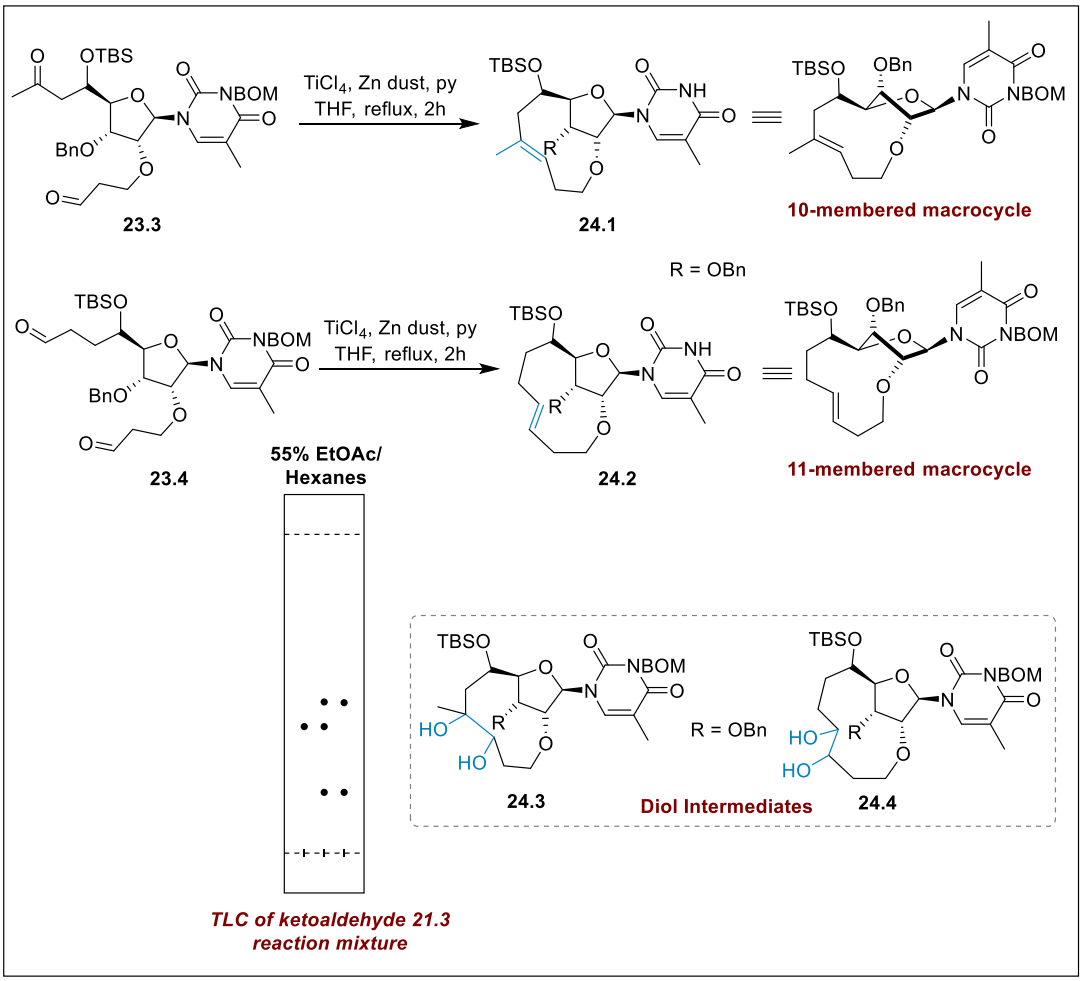

Figure 24. McMurry macrocyclizations to assemble the desired bicyclic structures

TLC experiments of the reaction mixture of the ketoaldehyde **23.3** and dialdehyde **23.4** precursors macrocyclization showed, in both cases, the formation of a less polar spot that presumably corresponded to the expected macrocycle products and a more polar spot that would correspond to the diol intermediates. The yields of the isolated material were low, and the NMR spectra were inconclusive in stablishing the structure of the isolated material.

HRMS experiments evidenced the formation of the diol intermediate **24.3** and **24.4** but not alkene macrocycle peak was observed. Attempts to improve the yields by decreasing the concentration of the reaction mixture and extending the reaction times were fruitless.

1.9 Computational studies on strain energy of *cis* and *trans* bicyclic[6.2.1] frameworks

The failure of RCM and McMurry coupling reactions to produce the macrocyclic ring contained in the targeted bicyclic nucleosides in acceptable yields seemed to be less dependent on the macrocyclization strategy used and more dependent on the strain energy (SE) of the macrocycle to be formed. The pre-organization of the ring precursor is expected to have greater influence on the success of this macrocyclization processes. The formation of the 9, 10 or 11-membered ring bridging the furanose portion of the nucleoside apparently had a large activation energy due to ring strain effects.

In this regard, the strain energy of the simplified *cis* and *trans* bicyclic[6.2.1] frameworks, where all protecting groups were removed (Figure 25) were computed using density functional theory with the B3LYP functional and 6-31G* basis set.

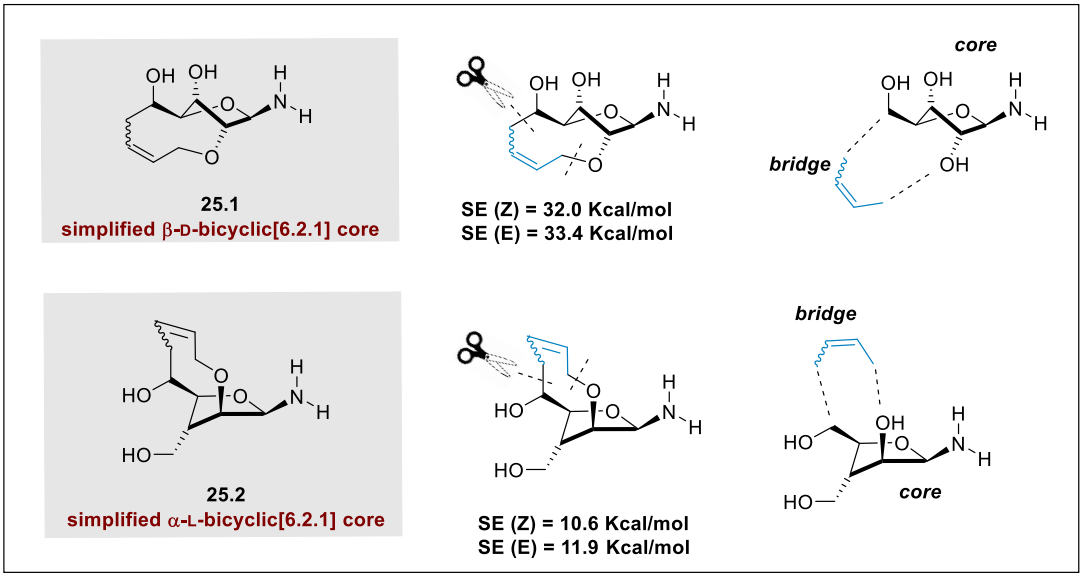

Figure 25. Simplified bicyclic structures for computational investigations

The SE was calculated as the difference in energy between the optimized bridge and core pieces of the *cis* and *trans* bicyclic[6.2.1] simplified frameworks directly separated from the lowest energy conformation of the bicyclic system, and the energy of the two components when they are allowed to "relax" (Figure 25). The largest SE values were obtained for the *trans*-bicyclic[6.2.1] framework with a 3'-exo conformation, 43.4 kcal/mol for the *Z*-configured olefin in comparison to 44.8 kcal/mol for the *E*-configured olefin. Lower SE values were obtained for the *trans*-bicyclic[6.2.1] framework with a 3'-endo conformation (**25.1**, Figure 25) (32.0 kcal/mol *Z*-configured olefin and 33.4 kcal/mol *E*-configured olefin). A dramatic decrease in SE was observed for the *cis*-bicyclic[6.2.1] framework (**25.2**, Figure 25) with values of 10.6 kcal/mol *Z*-configured olefin and 11.9 kcal/mol *E*-configured olefin.

These computed SE values are in good agreement with our initial expectations that the *cis*-bridged macrocyclic nucleoside would be more readily formed using RCM. However, the SE values reference the stability of the ring to be formed which is independent of the reaction conditions or reagents. Reactivity of the ring precursor is a determinant factor in the cyclization reaction, since precursors with an unfavorable conformation may not cyclize at all. It is possible in the cases here present that the reacting termini are not in close enough proximity for the cyclization to occur. This could be due to the bulky -OBn protecting group at the 3'-hydroxyl group, which provides steric hindrance and the need to pass through a high energy conformation.

1.10 FUTURE OUTLOOK CHAPTER 1

It was speculated that the -OBn protecting group at the 3'-hydroxyl group raises the energy barrier necessary for end-to-end cyclization. Thus, the use of an alternative protecting group that can be selectively removed before the macrocyclization process is expected to help the formation of the desired bicyclic core. The -OBn ester cannot be cleaved in **16.6** and **18.7** due to the presence of olefin subunits. The 2' and 3' hydroxyl groups of 5-methyluridine can be protected as the *p*-methoxybenzylidene acetal using PMBCl, after Ti-mediated cleavage the -OPMB group at the 3' position can be selectively remove under mild oxidizing conditions using DDQ (Figure 26A). This will allow for an investigation of the steric influence of the Bn group on the RCM reaction.

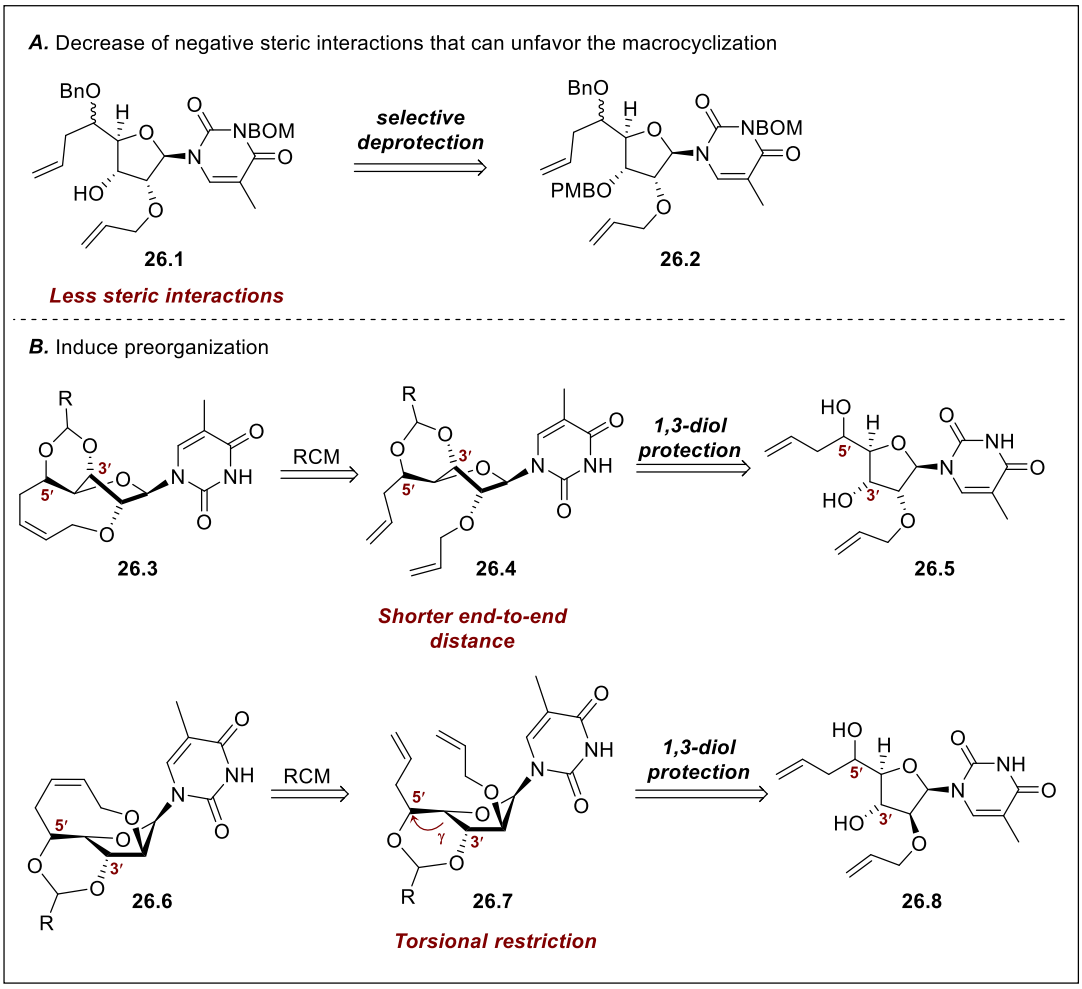

Figure 26. Future outlook: a) Selective deprotection to a less hindered ring precursor. b) Protecting group induced preorganization

To introduce preorganization into the ring precursor with the aim of promoting the cyclization, the 3',5'-1,3-diol can be protected also as a cyclic acetal (Figure 26B). It is expected that the six-membered ring formed after acetal formation would pre-organized the molecule into a more productive conformation by bringing the olefins in close proximity in the case of the *trans*-configured diene nucleoside ring precursor (**26.4,** Figure 26B).[36] In addition to the pre-organizing effect of the six-membered acetal, rotational restriction about the torsional angle γ is introduced (**26.7**, Figure 26), which is expected to lower the entropic barrier to cyclization for the *syn*-configured diene nucleoside ring precursor also.

1.11 CONCLUDING REMARKS CHAPTER 1

A short synthetic protocol for the synthesis of bis-allylated nucleosides has been developed starting from commercially available 5-methyluiridine. Macrocyclization strategies were explored for the construction of bicyclic nucleosides modifications containing *cis* and *trans* furanose-bridged macrocyclic ring structures, with the ultimate goal of constructing tricyclic nucleoside modification with potential applications in antisense technology. Ring-closing metathesis and McMurry coupling reactions were employed as macrocyclization reactions for the construction of bicyclic[*n*.2.1] frameworks (*n* = 6, 7 and 8). A different configuration of the diallylated nucleoside ring precursor was examined to test the impact of preorganization on the macrocyclization reaction. In all the cases the yield of the macrocyclization was low.

REFERENCES CHAPTER 1

(1) Bull, S. C.; Doig, A. J. Properties of Protein Drug Target Classes. *PLoS One* **2015**, *10* (3), 1–44.

(2) Bull, S. C.; Doig, A. J. Properties of Protein Drug Target Classes. *PLoS One* **2015**, *10* (3), e0117955.

(3) Watts, J. K.; Corey, D. R. Silencing Disease Genes in the Laboratory and the Clinic. *J. Pathol.* **2012**, *226* (2), 365–379.

(4) Robinson, R. RNAi Therapeutics: How Likely, How Soon? *PLoS Biol.* **2004**, *2* (1), e28.

(5) Bennett, C. F.; Swayze, E. E. RNA Targeting Therapeutics: Molecular Mechanisms of Antisense Oligonucleotides as a Therapeutic Platform. *Annu. Rev. Pharmacol. Toxicol.* **2010**, *50* (1), 259–293.

(6) Kool, E. T. Preorganization of DNA: Design Principles for Improving Nucleic Acid Recognition by Synthetic Oligonucleotides. *Chem. Rev.* **1997**, *97* (5), 1473–1488.

(7) Crooke, S. T. Molecular Mechanisms of Action of Antisense Drugs. *Biochim. Biophys. Acta - Gene Struct. Expr.* **1999**, *1489* (1), 31–43.

(8) Corey, D. R. RNA Learns from Antisense. *Nat. Chem. Biol.* **2007**, *3* (1), 8–11.

(9) Stein, C. A.; Castanotto, D. FDA-Approved Oligonucleotide Therapies in 2017. *Mol. Ther.* **2017**, *25* (5), 1069–1075.

(10) Keam, S. J. Inotersen: First Global Approval. *Drugs* **2018**, *78* (13), 1371–1376.

(11) Juliano, R. L. The Delivery of Therapeutic Oligonucleotides. *Nucleic Acids Res.* **2016**, *44* (14), 6518–6548.

(12) Chavali, S.; Mahajan, A.; Tabassum, R.; Maiti, S.; Bharadwaj, D. Oligonucleotide Properties Determination and Primer Designing: A Critical Examination of Predictions. *Bioinformatics* **2005**, *21* (20), 3918–3925.

(13) Shen, X.; Corey, D. R. Chemistry, Mechanism and Clinical Status of Antisense Oligonucleotides and Duplex RNAs. *Nucleic Acids Res.* **2018**, *46* (4), 1584–1600.

(14) Koshkin, A. A.; Singh, S. K.; Nielsen, P.; Rajwanshi, V. K.; Kumar, R.; Meldgaard, M.; Olsen, C. E.; Wengel, J. LNA (Locked Nucleic Acids): Synthesis of the Adenine, Cytosine, Guanine, 5-Methylcytosine, Thymine and Uracil Bicyclonucleoside Monomers, Oligomerisation, and Unprecedented Nucleic Acid Recognition. *Tetrahedron* **1998**, *54* (14), 3607–3630.

(15) Obika, S.; Nanbu, D.; Hari, Y.; Andoh, J. I.; Morio, K. I.; Doi, T.; Imanishi, T. Stability and Structural Features of the Duplexes Containing Nucleoside Analogues with a Fixed N-Type Conformation, 2'-O,4'-C- Methyleneribonucleosides. *Tetrahedron Lett.* **1998**, *39* (30), 5401–5404.

(16) Sørensen, M. D.; Kvaernø, L.; Bryld, T.; Håkansson, A. E.; Verbeure, B.; Gaubert, G.; Herdewijn, P.; Wengel, J. Alpha-L-Ribo-Configured Locked Nucleic Acid (Alpha-L-LNA): Synthesis and Properties. *J. Am. Chem. Soc.* **2002**, *124* (10), 2164–2176.

(17) Tarköy, M.; Bolli, M.; Leumann, C. Nucleic-Acid Analogues with Restricted Conformational Flexibility in the Sugar-Phosphate Backbone ('Bicyclo-DNA'). Part 3. *Helv. Chim. Acta* **1994**, *77* (3), 716–744.

(18) Steffans, R.; Leumann, C. Nucleic Acid Analogs with Constraint Conformational Flexibility in the Sugar-Phosphate Backbone "Tricyclo-DNA". Part 1. Preparation of [(5'R,6'R)-2'-Deoxy-3',5'-Ethano-5',6'-Methano-b-D-Ribofuranosyl]Thymine and -Adenine, and the Corresponding Phosphorami. *Helv. Chim. Acta* **1997**, *80* (8), 2426–2439.

(19) Dupouy, C.; Iché-Tarrat, N.; Durrieu, M. P.; Rodriguez, F.; Escudier, J. M.; Vigroux, A. Watson-Crick Base-Pairing Properties of Nucleic Acid Analogues with Stereocontrolled α and β Torsion Angles (α,β-D-CNAs). *Angew. Chemie - Int. Ed.* **2006**, *45* (22), 3623–3627.

(20) Hanessian, S.; Schroeder, B. R.; Giacometti, R. D.; Merner, B. L.; Ostergaard, M.; Swayze, E. E.; Seth, P. P. Structure-Based Design of a Highly Constrained Nucleic Acid Analogue: Improved Duplex Stabilization by Restricting Sugar Pucker and Torsion Angle γ. *Angew. Chemie - Int. Ed.* **2012**, *51* (45), 11242–11245.

(21) Hanessian, S.; Wagger, J.; Merner, B. L.; Giacometti, R. D.; Østergaard, M. E.; Swayze, E. E.; Seth, P. P. A Constrained Tricyclic Nucleic Acid Analogue of α -. *J. Org. Chem.* **2013**, *78*, 9064–9075.

(22) Khvorova, A.; Watts, J. K. The Chemical Evolution of Oligonucleotide Therapies of Clinical Utility. *Nat. Biotechnol.* **2017**, *35* (3), 238–248.

(23) Crooke, S. T. *Antisense Drug Technology : Principles, Strategies, and Applications*; CRC Press, 2008.

(24) Nicolaou, K. C.; Yang, Z.; Liu, J. J.; Ueno, H.; Nantermet, P. G.; Guy, R. K.; Claiborne, C. F.; Renaud, J.; Couladouros, E. A.; Paulvannan, K.; et al. Total Synthesis of Taxol. *Nature* **1994**, *367* (6464), 630–634.

(25) Kober, A.; Westman, T. Synthesis and Stereochemistry of Bicyclo[6.2.1]Undecane Derivatives. Acyloin Reactions of Esters of 1,3-Cyclopentanedipropionic Acids. *J. Org. Chem.* **1970**, *35* (12), 4161–4167.

(26) Sut, S.; Dall'Acqua, S.; Baldan, V.; Ngahang Kamte, S. L.; Ranjbarian, F.; Biapa Nya, P. C.; Vittori, S.; Benelli, G.; Maggi, F.; Cappellacci, L.; et al. Identification of Tagitinin C from Tithonia Diversifolia as Antitrypanosomal Compound Using Bioactivity-Guided Fractionation. *Fitoterapia* **2018**, *124* (September 2017), 145–151.

(27) Bhlmann, F. Sesquiterpene Lactones From Eremanthus Species. **1980**, *19*.

(28) McDougal, P. G.; Oh, Y. I.; VanDerveer, D. Synthesis of the Furanoheliangolide Ring Skeleton. *J. Org. Chem.* **1989**, *54* (1), 91–97.

(29) Boeckman, R. K.; Yoon, S. K.; Heckendorn, D. K. Synthetic Studies Directed toward the Eremantholides. 2. A Novel Application of the Ramberg-Baecklund

Rearrangement to a Highly Stereoselective Synthesis of (+)-Eremantholide A. *J. Am. Chem. Soc.* **1991**, *113* (25), 9682–9684.

(30) Caine, D.; Arant, M. E. The Synthesis of 11-Oxabicyclo[6.2.1]Undecenone Derivatives. *Tetrahedron Lett.* **1994**, *35* (37), 6795–6798.

(31) Takao, K. I.; Ochiai, H.; Yoshida, K. I.; Hashizuka, T.; Koshimura, H.; Tadano, K. I.; Ogawa, S. Novel Total Synthesis of (+)-Eremantholide A. *J. Org. Chem.* **1995**, *60* (25), 8179–8193.

(32) Gradillas, A.; Pérez-Castells, J. Macrocyclization by Ring-Closing Metathesis in the Total Synthesis of Natural Products: Reaction Conditions and Limitations. *Angew. Chemie - Int. Ed.* **2006**, *45* (37), 6086–6101.

(33) Li, Y.; Hale, K. J. Asymmetric Total Synthesis and Formal Total Synthesis of the Antitumor Sesquiterpenoid (+)-Eremantholide A. *Org. Lett.* **2007**, *9* (7), 1267–1270.

(34) Duan, X. F.; Zeng, J.; Lü, J. W.; Zhang, Z. Bin. Insights into the General and Efficient Cross McMurry Reactions between Ketones. *J. Org. Chem.* **2006**, *71* (26), 9873–9876.

(35) Chaudhari, D. A.; Fernandes, R. A. Hypervalent Iodine as a Terminal Oxidant in Wacker-Type Oxidation of Terminal Olefins to Methyl Ketones. *J. Org. Chem.* **2016**, *81* (5), 2113–2121.

(36) Blankenstein, J.; Zhu, J. Conformation-Directed Macrocyclization Reactions. *European J. Org. Chem.* **2005**, *2005* (10), 1949–1964.

CHAPTER 2 Regioselective Synthesis of Unsymmetric Tetra- and Pentasubstituted Pyrenes with a Strategy for Primary C-Alkylation and the 2-Position

2.1 Substitution Chemistry of Pyrene

Pyrene is the smallest *peri*-fused polycyclic aromatic hydrocarbon (PAH) containing four fused benzene rings (Figure 27). Pyrene is cyclic, planar and all of its carbon atoms are sp^2 hybridized, however, it has 16 π electrons, which would make pyrene non-aromatic according to the Hückel's rule. While the Hückel 4n+2 rule helps to predict aromaticity for monocyclic ring systems, it is an oversimplification for fused aromatic systems containing "individual" aromatic rings.

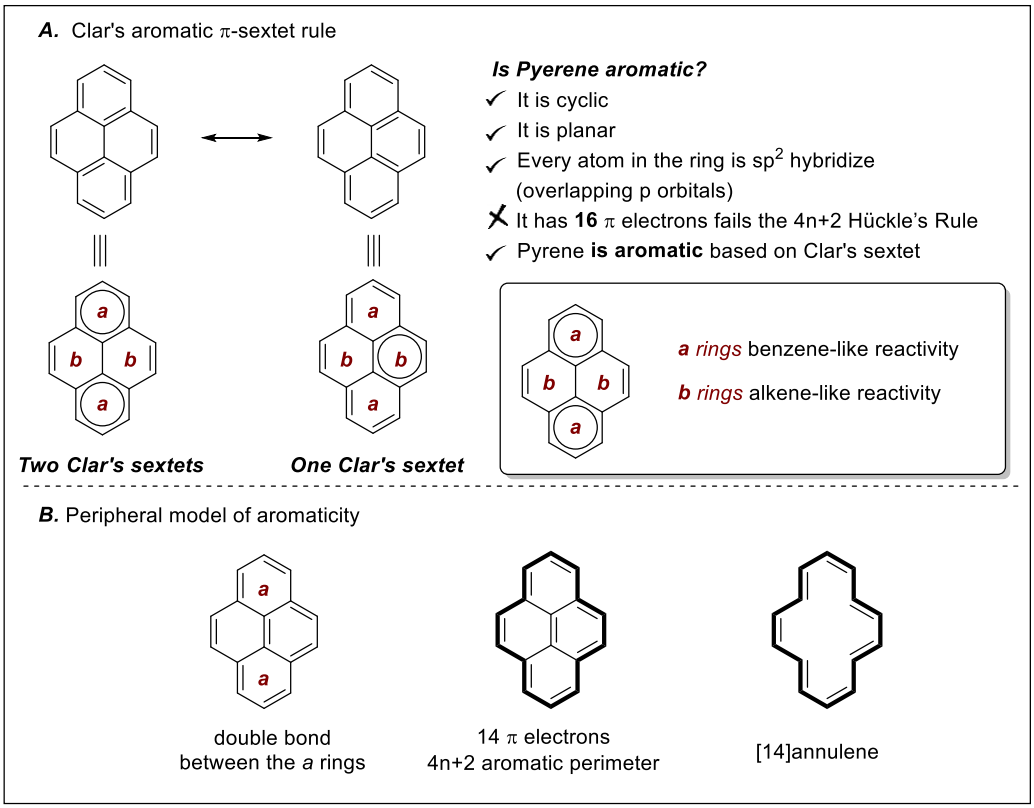

Figure 27. Clar sextets of pyrene, aromaticity and general reactivity

Pyrene is aromatic according to Clar's aromatic (or π) sextet rule,[1] which states that aromaticity can be different for each ring segment, so the Kekulé resonance structure with the largest disjoint π-sextet rings is the major contributing structure, and such rings are considered to be the most aromatic centers in a PAH (Figure 27A). Therefore, the ***a*** rings of pyrene are the most aromatic and display benzene-like reactivity, while the ***b*** rings display alkene-like reactivity. Also, the peripheral model of aromaticity can be applied to pyrene. When a double bond is placed between the two *a* rings, a [14]annulene (which is aromatic), *peri*-fused PAH is afforded (Figure 27B).[2] Due to the arrangement of π-sextets in pyrene, which affords the "best" aromatic structure for PAH, its substitution chemistry is quite different than that of benzene (see below).

Pyrene is a well-known chromophore that is frequently used in organic fluorescent materials. Its unique properties such as long-lived excited (singlet) states and its ability to form excimers have been widely exploited in many scientific fields, making pyrene and its derivatives important fluorophores in both fundamental and applied photochemical research.[3] To tailor the specific electronic properties of pyrene and its applications in materials science, strategies to introduce substituents about the pyrene core have been developed.[4] However, a major limitation for the use of pyrene in general is the lack of synthetic protocols for non-symmetric, selective functionalization of the pyrene nucleus.

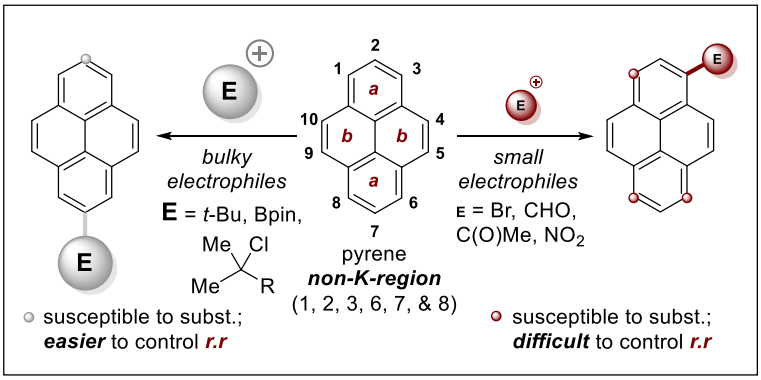

Figure 28. Electrophilic aromatic substitution (EAS) of pyrene

Following the fused ring peripheral numbering nomenclature, pyrene numbering starts from the uppermost left, non-quaternary carbon atom (ring ***a***) and moves clockwise around the PAH. The quaternary carbon atoms are not included in this numbering (Figure 28). As mentioned earlier, the ***a*** rings of pyrene are the most aromatic centers, as such they are susceptible to electrophilic aromatic substitution (EAS), with the most (activated) electron-rich positions being at the 1, 3, 6 and 8 carbon atoms. The 2 and 7 positions are essential nodes, with little electron density at these positions, and, as such, they are less reactive towards EAS. Since the ***b*** rings present in

pyrene are represented as non-π-sextets, under the Clar classification, the 4, 5, 9 and 10 positions, known as the K-region, typically display alkene-like reactivity.[5] However, it should be noted that in some instances EAS can take place at the K-region, when the apical rings (***a*** rings) are fully substituted, or too sterically hindered to undergo further substitution. Such is the case for 2,7-di-*tert*-butylpyrene.[6]

Direct non-symmetric functionalization of pyrene under EAS conditions has been a challenge for chemical synthesis. Generally, the substitution pattern can be predicted based on the nature of the electrophilic reagents (Figure 28). The use of non-bulky electrophiles produces substitution at the more reactive 1, 3, 6 and 8 positions, however, selectivity is difficult to control, yielding mono- di- and tetra-substituted pyrenes. Surprisingly, tri-substituted pyrenes are difficult to obtain under EAS conditions. Substitutions at these positions also blocks further reactions at the 2 and 7 positions. Bromination of pyrene is an example of such type of functionalization (Figure 29).

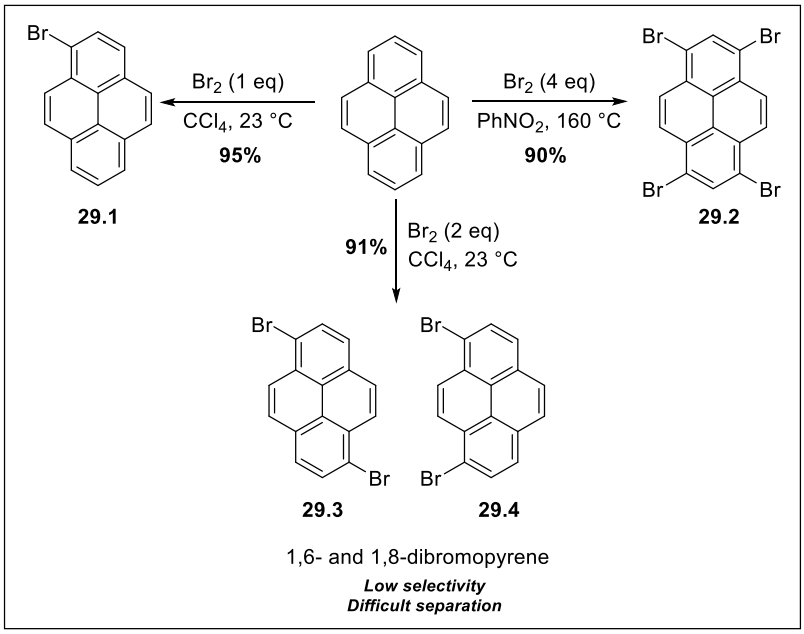

Figure 29. Bromination of pyrene

When pyrene is reacted with one equivalent of bromine in carbon tetrachloride 1-bromopyrene **29.1** is afforded in 95% yield;[7] however when pyrene is treated with two equivalents of bromine, a mixture of the 1,6- and 1,8-dibromopyrene isomers **29.3** and **29.4**

that are difficult to separate is obtained. Attempts to obtain 1,3,6-tribromopyrene results in complex mixtures of di-, tri- and tetra-brominated pyrenes.[8] The use four equivalents of bromine produce to 1,3,6,8-tetrabromopyrene **29.2** in 90% yield. Due to their capacity of participate in Pd-catalyzed cross-coupling reactions bromopyrenes have been key precursors in the development of new materials.[7]

The use of bulky electrophilic reagents has facilitated mono- and di-substitution at the 2 and 7 positions (Figure 28), due to steric interactions that would result from the *peri*-protons of the K-region and the incoming electrophile. Substitution at the 2 or 2 and 7 positions of pyrene blocks further substitution at the 1, 3, 6 and 8 positions. Particularly, *tert*-butyl substitution at one of the ***a*** rings of pyrene will block or attenuate further substitution at the neighbor 1 and 3 positions, allowing for selective functionalization of nucleophilic carbons at the unsubstituted apical ring (6, 7, and 8 positions).[5]

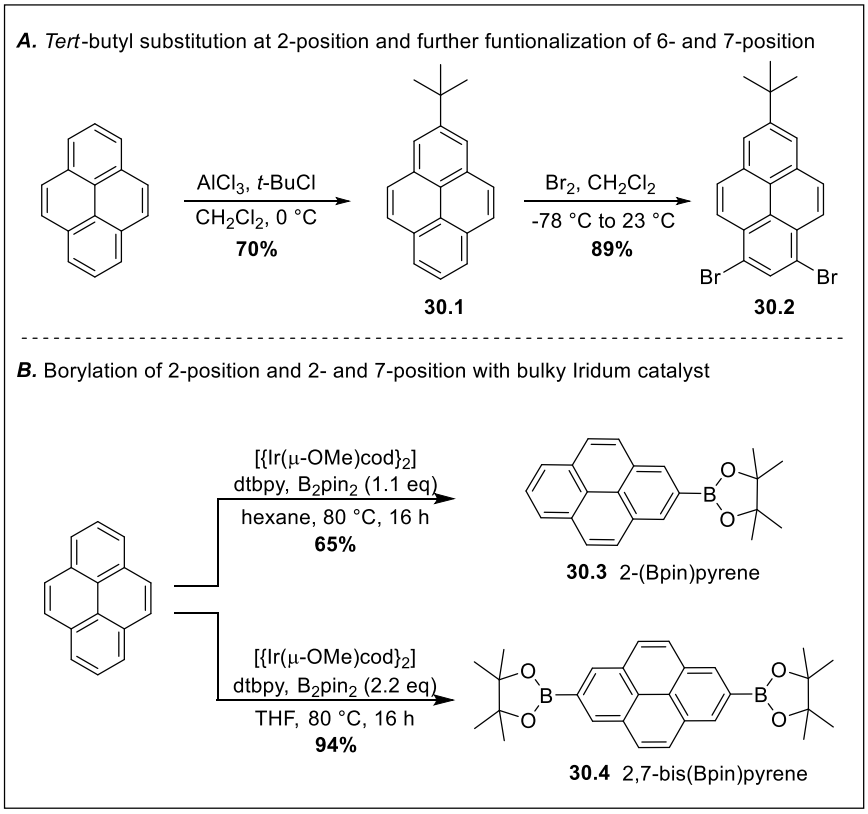

Figure 30. Mono and disubstitution at the 2 and 7-positions with bulky electrophiles

Müllen and co-workers reported the use of mono *tert*-butylation of pyrene with the aim of later functionalization of the 1 and 3 positions (Figure 30A). In their report, pyrene was converted into 2-*tert*-butylpyrene **30.1** in 70% yield after treatment with *tert*-butyl chloride in the presence of $AlCl_3$, which was then treated with two equivalents of bromine at -78 °C to obtain 1,3-dibromo-7-*tert*-butylpyrene **30.2** in 89%.[9]

Reaction of pyrene with bulky iridium-boryl complexes provides a method for the preparation of 2 and 2,7-borylated pyrenes. Such a borylation strategy is useful for Suzuki-Miyaura coupling reactions for subsequent C-C bond formation that does not require quaternization of the alkyl electrophile. The work of Marder and co-workers reported in 2012 provided a one-step synthesis to 2-(Bpin)pyrene **30.3** and 2,7-bis(Bpin)pyrene **30.4** (Figure 30B). The iridium-based catalyst used for this transformation is prepared *in situ* by the reaction of $[\{Ir(m\text{-}OMe)cod]_2]$ (cod = cyclooctadiene) with 4,4'-di-*tert*-butyl-2,2'-bipyridine, when one equivalent of bis(pinacolato)diboron is employed monosubstitution at the 2 position is achieved affording **30.3** in 65% yield, the use of two equivalents of bis(pinacolato)diboron yielded **30.4** in 94% yield.[10]

2.2 Synthesis of unsymmetrically substituted pyrene derivatives

To date, selective di- and tri-substitution of pyrene has been only achieved using indirect synthetic methods, which requires the use of multistep synthetic sequences. Such indirect methods for forming selectively functionalized pyrenes has required, first partial reduction of pyrene by hydrogenation of the ***b*** rings, followed by EAS of the resulting 4,5,9,10-tetrahydropyrene, and finally re-aromatization by dehydrogenation (Figure 31A). In this instance the ***a*** rings behave like isolated benzene rings and undergo substitution at the most accessible (least sterically hindered), *para*-carbon atom. For instance, nitration of 4,5,9,10-tetrahydropyrene affords **31.2** in 52% yield, which after reduction affords amine **31.3** (Figure 31B). Subsequent substitution after *N*-acetyl protection of the amine, in the presence of bromine, affords **31.4**, where the site of bromination is directed by the protected amine, much like that of an EAS reaction with benzene. However, subsequent substitution of **31.4**, under Friedel-Crafts acylation conditions takes place at the other π-sextet or aromatic ring to afford **31.5**. Completing the synthesis of 2-acetyl-6-bromopyrene (**31.6**) involves diazotization, followed by dehydrogenation.[11] Thus, the selective introduction of two substituents at the 2 and 6-posiitons of pyrene requires 9 synthetic operations. Bis-acetylation and the synthesis

of 2,7-diacetylpyrene (symmetric substitution) can be achieved in just 3 steps from pyrene (*e.g.*, **31.1**, Figure 31B).[12]

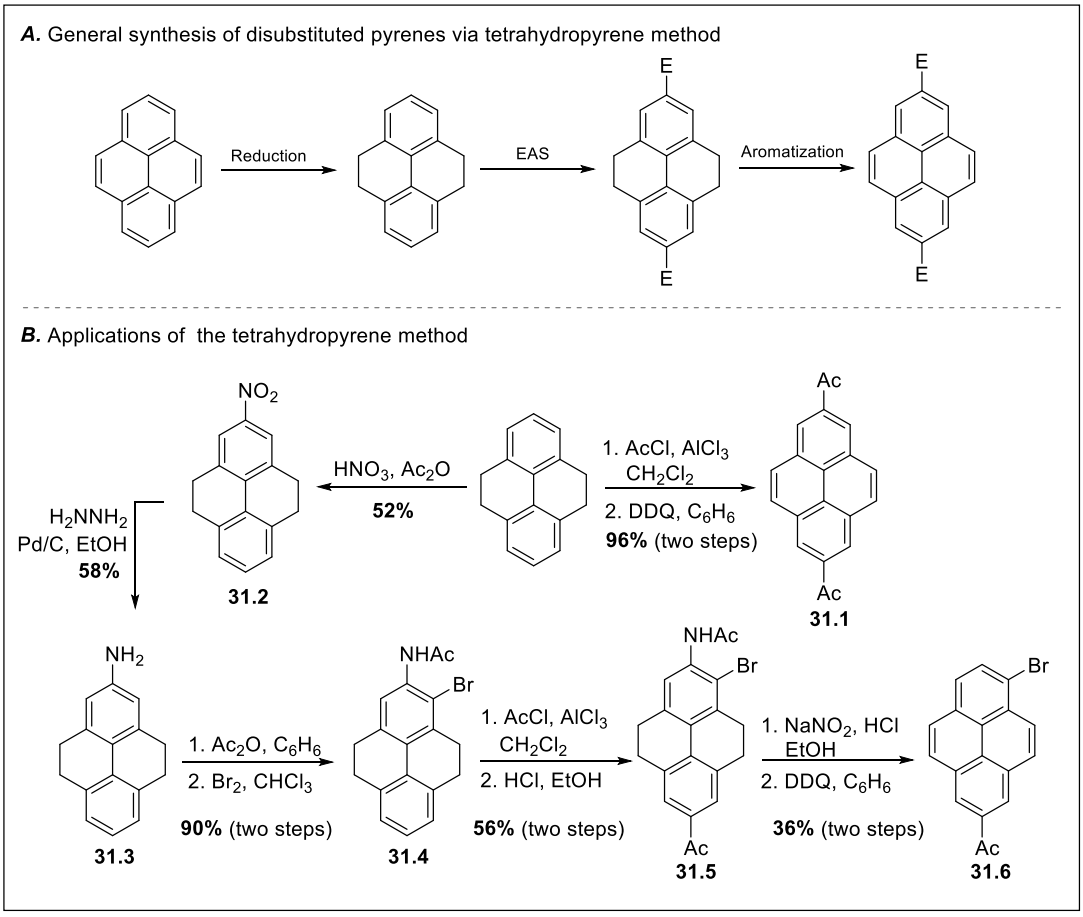

Figure 31. Selective substitution of pyrene using the tetrahydropyrene functionalization strategy

The synthesis of selectively substituted pyrene derivatives has also been achieved by converting appropriately functionalized [2.2]metacyclophanes into pyrene, upon transannular bond formation across the two benzene rings of the macrocycles such as **32.1**, followed by oxidation of the resulting tetrahydropyrenes (Figure 32A).[13,14] Cyclization reactions of substituted biphenyl derivatives, such as 2,6-dialkynylbiphenyls has also yielded unsymmetric pyrene derivatives via alkyne annulation reactions (Figure 32B).[15,16]

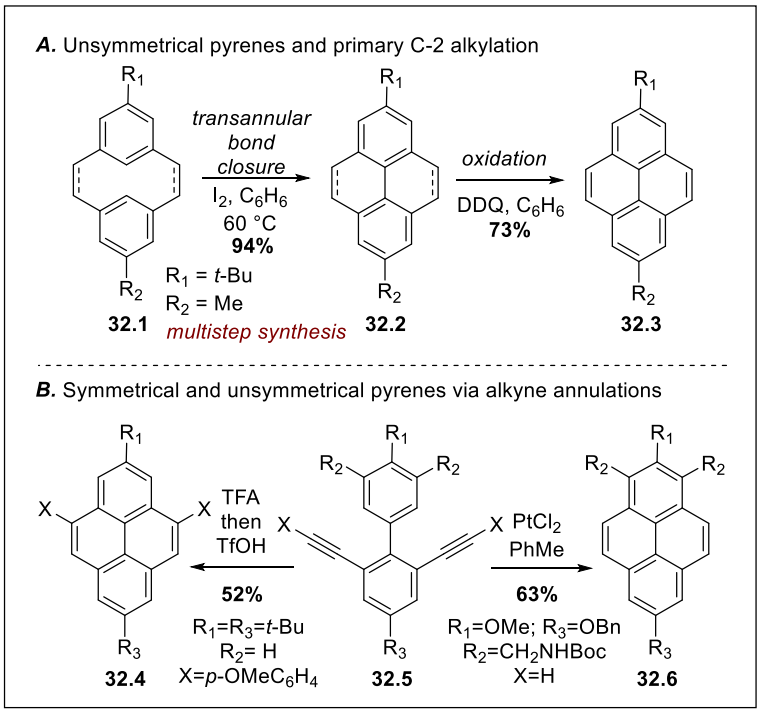

Figure 32. Indirect methods for pyrene functionalization: a) [2.2]meta-cyclophane approach; b) alkyne annulation approach

2.2.1 Primary alkyl substitution of pyrene: C-2 alkylation

The introduction of alkyl groups about the pyrene core structure is usually done so to enhance solubility of the PAH and to suppress π-π stacking of pyrene units in order to exploit the vast photophysical and electronic properties of pyrene in the field of organic materials chemistry. While mono-, di-, tri- and tetra-substituted pyrenes containing alkyl groups at 1, 3, 6 and 8 positions have been synthesize,[17,18,19] direct primary *C*-alkylation at the 2-position has been a longstanding challenge for pyrene-based chemical synthesis. When viewed as a π-extended building block of benzene, substitution of the 2 and 7 positions of pyrene, can be thought of as the analogous 1,4 or *para* carbons of benzene (Figure 33). In the context of developing new strategies for the synthesis of π-extended materials, particularly, strained macrocyclic systems such as carbon nanohoops and carbon nanobelts (CNBs), access to 2,7-di-substituted pyrene derivatives is an important starting point in the chemical synthesis of these complex (macrocyclic) systems. Merner and co-workers have recently reported on

the application of macrocyclic 1,4-diketones for the synthesis of highly strained benzenoid macrocyclic systems.[20] The development of selective functionalization reactions of the pyrene nucleus with focus on primary *C*-alkylation of the 2-position was identified as in important area for synthetic methodology development, and the main focus of the body of work discussed in this chapter.

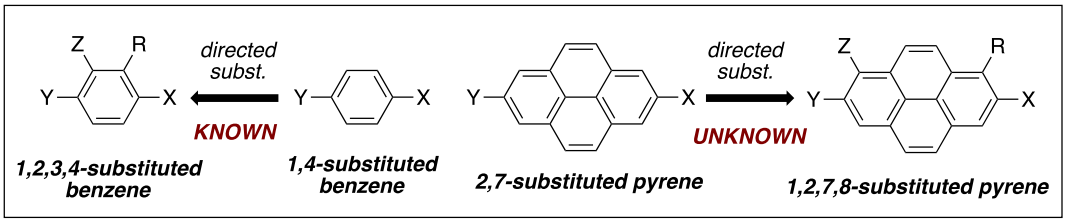

Figure 33. Pyrene as a π-extended building block of benzene

2.2.2 Substitution of pyrenes K-region and further directed substitution reactions

Substitution of the K-region of pyrene (4, 5, 9, and 10 positions) is not accessible via EAS, unless the ***a*** rings of pyrene are completely blocked from further reaction. Thus, 2,7-di-*tert*-butylpyrene (**34.1**, Figure 34) can be used to reach the K-region of pyrene. Reaction of **34.1** with six equivalents of bromine in the presence of iron has shown to produce 4,5,9,10-tetrabromo-2,7-di-*tert*-butylpyrene **34.2** in 90% yield.[20]

Itami and co-workers has reported selective annulative π-extension (APEX) of the K-region of pyrene as a part of their efforts towards the synthesis and functionalization of nanographene (Figure 34B). A double APEX reaction on 2,7-di-*tert*-butylpyrene **34.1** with three equivalents of dibenzosilole **34.3** in the presence of a Pd(II) catalyst yielded di-*tert*-butylhex-abenzotetracene **34.4** in 83% yield.[21]

Direct functionalization of the K-region of pyrene has been achieved by the formation of pyrene-4,5,9,10-tetraone **35.4** and pyrene-4,5-dione **34.7**, upon treatment of pyrene with a ruthenium catalyst.[22]

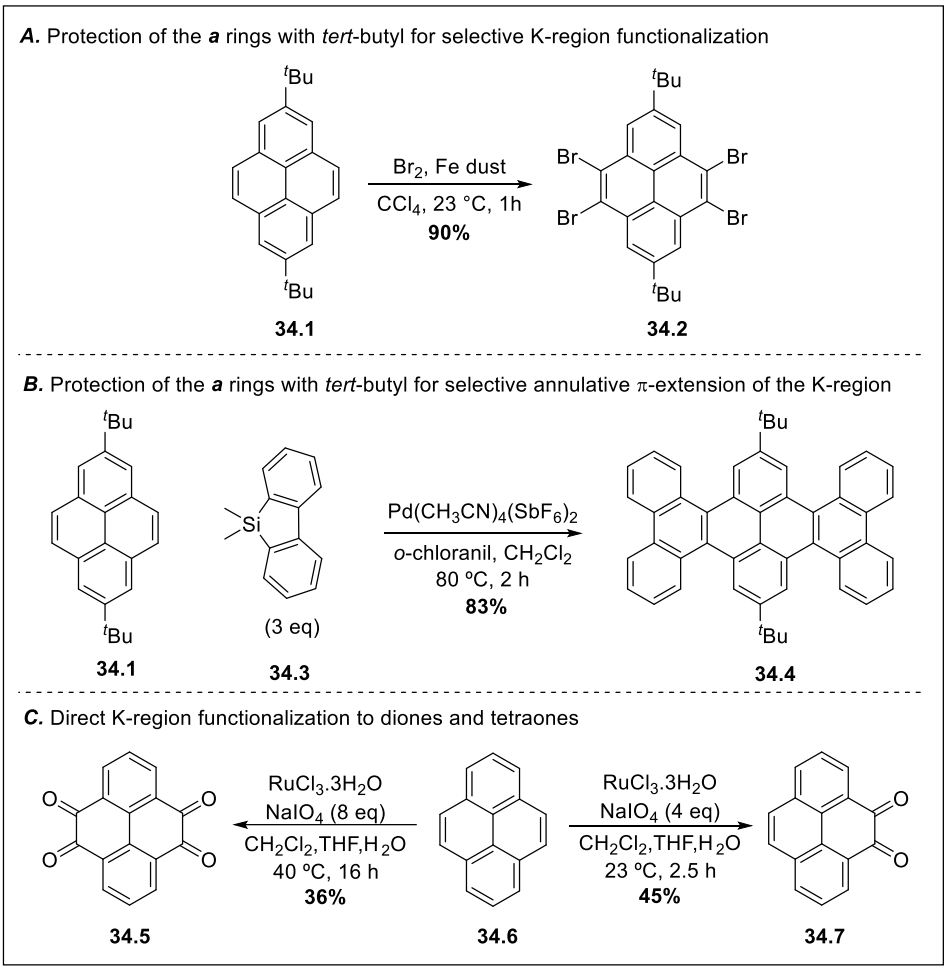

Figure 34. Selective pyrene K-region functionalization

The placement of functional groups at K-region of pyrene has been shown to be useful for controlling the regioselectivity of further functionalization reactions. The high level of regiochemistry that has been observed for such systems can be attributed to steric hindrance imposed at the 3 and 6 positions, upon K-region functionalization. For example, the introduction of methoxy groups (OMe) at the 4 and 5 positions of pyrene, after reduction of **34.7** in the presence of sodium dithionite and alkylation of the bis-enol with dimethyl sulfate, allows for regioselective substitution at the 1 and 8 positions. This strategy has enabled the synthesis of 1,4,5,8-tetrasubstutited pyrene derivatives, which was used by Bodwell and co-workers in the in the synthesis of pyrenylalkynyl macrocycles (Figure 35A).[22]

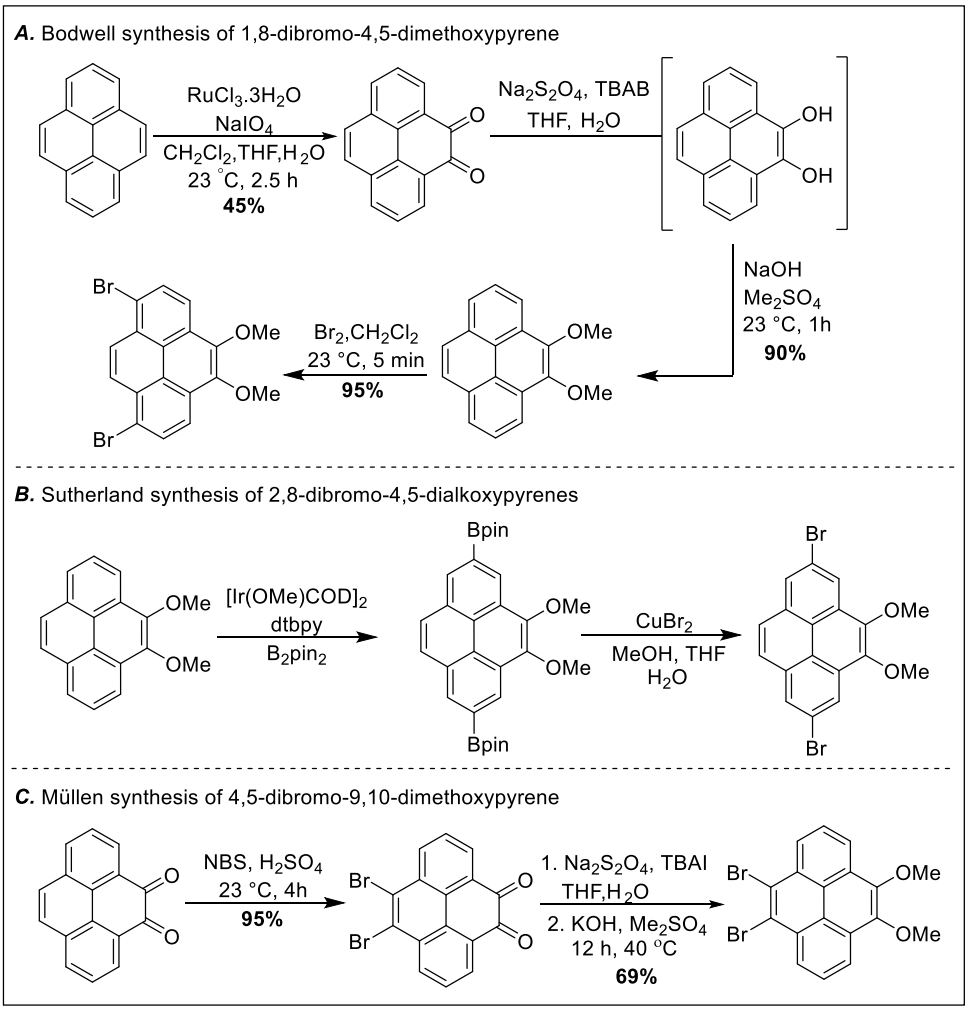

Figure 35. Synthesis of tetrasubstituted pyrenes by initial functionalization of the K-region

A similar approach was employed by Sutherland and co-workers[23] for the synthesis of 2,7-dibromo-4,5-dialkoxypyrenes (Figure 35B). Borylation of the 2 and 7-positions of 4,5-dimethoxypyrene was achieved using the aforementioned borylation procedure developed by Marder and co-workers, followed by a copper(II) bromide-mediated bromination to give **35.4** in 40% yield (Figure 35B). 4,5-Alkoxypyrene derivatives have also been used for selective unsymmetric functionalization of the K-region, as exemplified by Müllen and co-workers synthesis of 4,5-dibromo-9,10-dialkoxypyrene **35.6** for use in organic field-effect transistors (Figure 35C).[24]

2.3 Synthesis of trisubstituted pyrene derivatives with primary alkylation at C-2

With the target of developing strategies for selective functionalization reactions of the pyrene nucleus, and a focus on primary *C*-alkylation of the 2-position, our group originally tried to take advantage of a the monobromination of pyrene to afford **29.1** (Figure 36).

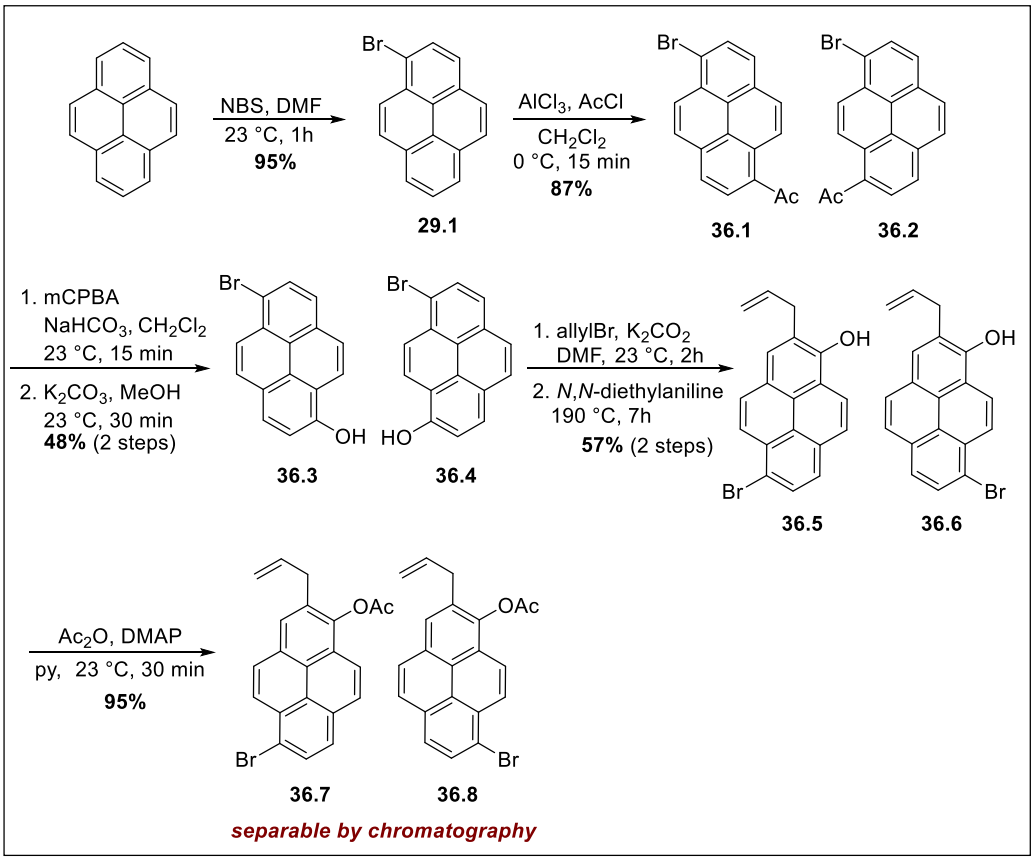

Figure 36. Initial synthesis of tetrasubstituted pyrene derivatives with primary C2-allylation

It was hoped that after monobromination, substitution of the opposite ***a*** ring of pyrene could be achieved, and by introducing polar functional groups, separation of isomeric 1,6 and 1,8-disubstituted pyrenes would be possible. To this end, pyrene was first brominated with NBS, in DMF to afford 1-bromopyene **29.1**, which was then acylated with AcCl in the presence of $AlCl_3$, to furnish a mixture of regioisomers **36.1** and **36.2**, which were not separable by

chromatography. Baeyer-Villiger oxidation using *m*-CPBA was carried out on the mixture of isomers producing an inseparable mixture of acetate esters. Cleavage of the ester using potassium carbonate yielded a mixture of alcohols **36.3** and **36.4** that were allylated and subjected directly to a Claisen rearrangement, to install a C-allyl group at the 2-position of pyrene.[25] To the best of our knowledge this is the first example of a Claisen rearrangement on the pyrene nucleus, and a rare example of primary C-2 alkylation. The mixture of alcohols were subjected to acetylation at which point the mixture of products was separable by chromatography. Despite the fact that **36.7** and **36.8** were separable, ascertaining the exact structures proved to be quite difficult in the absence of an X-ray crystal structure. While the ^{1}H and ^{13}C NMR spectra of these compound are different, 2-D NMR experiments including HSQC and HMBC did not establish unambiguous connectivity in these two regioisomers.

2.3.1 Regioselective synthesis of tetra- and pentasubstituted pyrenes by initial K-region functionalization

Drawing inspiration from the few known examples were initial K-region functionalization of pyrene had led to selective disubstitution reactions, we proposed that 4,5-dimethoxypyrene could be used to selectively introduce one functional group per reaction. It is known that formylation of pyrene only proceeds at one of the ***a*** rings of the PAH, unlike bromination reactions. Furthermore, we reasoned that the steric hindrance imposed by the K-region -OMe groups would attenuate substitution at the *peri*-position (C3). Access to this formyl pyrene derivative would provide a handle for which a hydroxyl group could be placed at the 1-position and subsequently used to direct a C-alkylation reaction at the 2-position, ultimately installing a primary alkyl group. These selective monofunctionalization reactions could provide a strategy to regioselective substitution of unsymmetrical pyrene derivatives.

The monofunctionalization strategy presented below provides access to unsymmetrically substituted pyrene derivatives, as well as sterically hindered or unhindered hydroxypyrene derivatives, which were successfully used for direct primary C-allylation. The C-allyl unit was shown to be a functional group handle for dimerization of two identical pyrene units via metathesis reaction. Furthermore, we were able to use sequential monofunctionalization reactions to prepare regioselective functionalized 1,2,4,5,8-pentasubstituted pyrene derivatives.

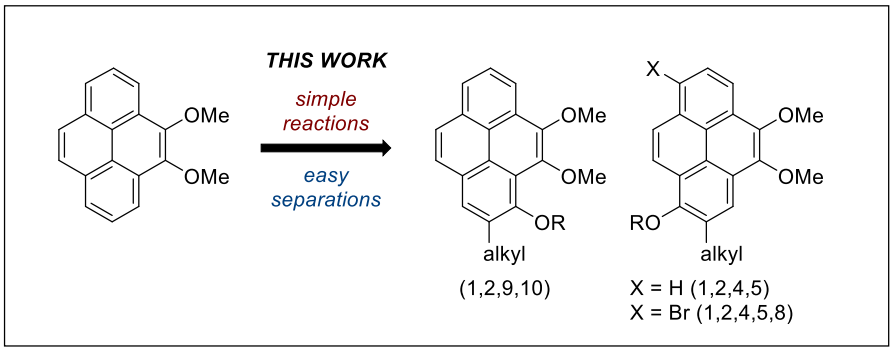

Figure 37. Unsymmetrical synthesis of tetra- and pentasubstituted pyrenes with C-2 alkylation

The observation that 4,5-alkoxypyrenes can be selectively substituted at the 1- and 8-position, blocking further substitution at the 3 and 6-position lead us predict that reaction of 4,5-dimethoxypyrene under Rieche formylation conditions, which is one of the most useful functionalization reactions of pyrene and has been used for the synthesis of several pyrene-1-carbaldehyde derivatives,[26,27] would produce predominately 4,5-dimethoxypyrene-1-carbaldehyde (**38.1**, Figure 38).

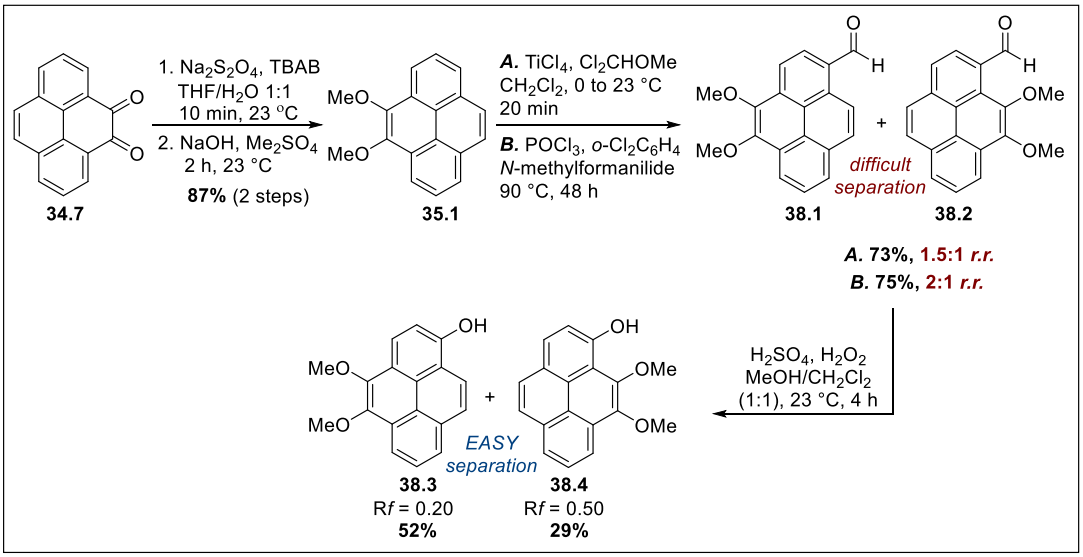

Figure 38. Synthesis of 1-Hydroxypyrenes **38.3** and **38.4**

However, when 4,5-dimethoxypyrene was subjected to Rieche formylation using dichloromethyl methyl ether in the presence of $TiCl_4$, a 1.5:1 ratio of regioisomers, in favor of the 1-formylpyrene derivative **38.1** was afforded (Figure 38). Changing the formylation conditions to a Vilsmeier-Haak-based protocol provided a slight increase (2:1 *r.r.*) in the formation of **38.1** but did not suppress the formation of the 3-formylpyrene derivative **38.2**. We then investigated the influence of the alkoxy substituent, reasoning that a bulkier alkyl unit at this position would slow down formylation at the 3-position.

We attempted to introduce the Bn, Nap, TIPS and TBDPS protecting groups at the 4 and 5-positions, however, only alkylated derivatives could be prepared. Indeed, the presence of a bulkier benzyl ether attenuated the rate of formylation at the 3-positon, producing a 4:1 ratio of regioisomers in 84% yield (Figure 39) under Vilsmeier-Haak conditions. Unfortunately, no comparison could be made to the Rieche formylation reaction of this substrate or the ONap derivative, as these compounds succumbed to dealkylation (Figure 39).

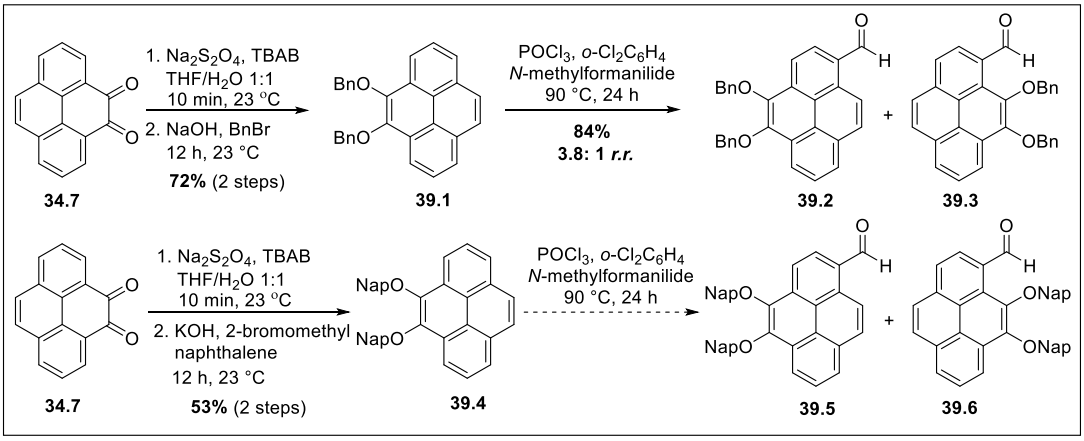

Figure 39. Influence of bulkier alkoxy substituents on formylation at the 3-position

During our investigations of regioselective functionalization and 1-bromopyrene (Figure 36), we had difficulty assigning (definitively) structures to the constitutional isomers produced. In the case of the mixture of formylpyrene derivatives produced after K-region functionalization, ^{1}H NMR analysis of the crude mixtures was sufficient to ascertain connectivity and determine the regiochemical outcome of the formylation reactions. Assignment of the structure to **38.1** and **38.2** was done first by the observation of that the major constitutional isomer displayed a doublet at 9.38 ppm, which is indicative of a K-region proton flanked by an aldehyde group at the 1-position of pyrene, being the structure of the

major isomer 4,5-dimethoxyoyrene-1-carbaldehyde. The absence of this signal from the minor regioisomer produced in this reaction suggested 9,10-dimethoxyoyrene-1-carbaldehyde as its structure.

Separation of the mixture of aldehyde regioisomers produced in these formylation reactions was possible, however, it required tedious chromatography. Our synthetic plan for the introduction of a primary alkyl group at the position called for the oxidation of the formyl group. To our delight, Dakin oxidation of the regioisomeric mixture of aldehydes, **38.1** and **38.2**, produced alcohols **38.3** and **38.4** that could be easily separated by silica gel chromatography. During ^{1}H NMR characterization of these two alcohols, it was observed that even though they were both soluble in $CDCl_3$, the ^{1}H NMR spectrum of **38.3** (R_f = 0.20 1:4 EtOAc/hexanes) was poorly resolved in this solvent. A well-resolved ^{1}H NMR of this compound was obtained in CD_3OD, while for alcohol **38.4** (R_f = 0.50 1:4 EtOAc/hexanes) the ^{1}H NMR was obtained in $CDCl_3$.

Monofuntionalization of 4,5-dimethoxypyrene was attempted using a Friedel-Crafts acylation reaction (Figure 40). Treating 4,5-dimethoxypyrene with AcCl and $AlCl_3$ in dichloromethane at 0 °C, successfully afforded monoacylated product **40.1** in 87% yield (Figure 40).

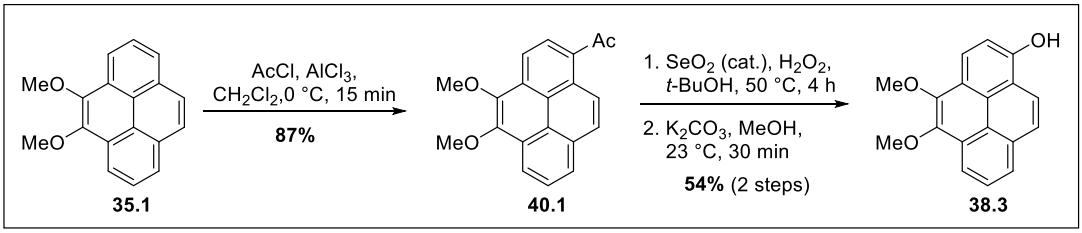

Figure 40. Monofunctionalization 4,5-dimethoxypyrene using a Friedel-Crafts acylation reaction

To convert the ketone **40.1** into the desired 1-hydroxypyrene derivative **38.3** alcohol, standard Baeyer-Villiger oxidation using *m*-CPBA or related peroxy acids were screened. Although the desired acetate ester was obtained, it was either obtained in poor yield or accompanied by the formation of numerous (unidentified) by-products. This transformation required several weeks of optimization. We examined the potential of a boric acid-mediated protocol reported by Harvey and co-workers for the synthesis of 1-hydroxypyrene.[28] In their study, treatment of 1-acetylpyrene with sodium perborate tetrahydrate in glacial acetic acid at room temperature yielded 1-acetoxypyrene in a 77% yield. Subjecting **40.1** to these

conditions, yielded the expected acetate ester, however, contrary to Harvey's results, complete consumption of the ketone starting material was not achieved. Furthermore, the separation of the acetate ester produced from the ketone starting material was not trivial. Finally, we tested a protocol employed by Kan and co-workers[29] for the successful oxidation of 1-(2,3,4,6-tetramethoxyphenyl)ethanone to the corresponding acetate ester, using a catalytic amount of SeO_2 and H_2O_2, followed by direct hydrolysis to produce the desired 2-hydroxy-3,4,5,6-tetramethoxybenzene. This procedure enabled the smooth conversion of 1-(4,5-dimethoxypyren-1-yl)ethanone (**40.1**) into desired alcohol **38.3** in 54% overall yield. The ^{1}H NMR spectrum obtained for the hydrolysis product was identical to that of **38.3**, thus validating our assumption that only 1-acetyl-4,5-dimethoxypyrene was afforded upon acylation of **35.1** with $AlCl_3$, and further supporting our earlier assignment of the structures of **38.3** and **38.4**.

One of the main objectives of this monofunctionalization-based approach was to develop a strategy that would allow primary alkylation at the 2-position of pyrene, which, to the best of our knowledge, had not been previously reported. With hydroxypyrenes **38.3** and **38.4** in hand, we focused our study to the incorporation of an allyl substituent at the 2-position via a Claisen rearrangement. To this end, both alcohols were subjected to identical reaction sequences (Figure 41). Upon *O*-allylation of **38.3** under standard conditions, 1-allyloxy-4,5-dimethoxypyrene **41.1** was afforded in 87% yield. A Claisen rearrangement was induced by heating allylated pyrene derivative **41.1** at 190 °C in *N,N*-diethylaniline for 6 h, which produced compound **41.2** in a 74% yield. The same two-step sequence was applied to hydroxypyrene **38.4** producing **41.3** in a comparable (65%) yield. It should be noted that **41.3** was moderately susceptible to deallylation. Approximately 10% of **38.4** was produced in this reaction, along with 18% of unreacted starting material (**41.3**).

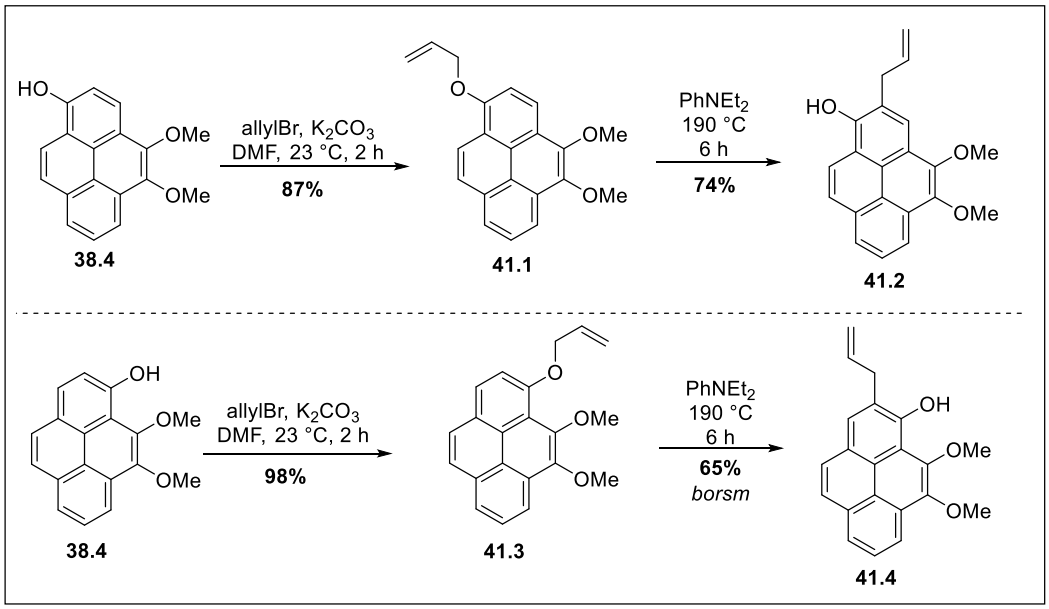

Figure 41. Direct C2-allylation of pyrene via a Claisen rearrangement

With the idea of using the allyl units as handles for dimerization, first, the free alcohols after Claisen rearrangement **41.2** and **41.3** were sulfonylated to give **42.1** and **42.3** in 89% and 51% yields, respectively (Figure 42). We examined olefin metathesis conditions using Grubbs first-generation catalyst, which gave a 4.7:1 mixture of alkene diastereomers, in the case of **42.1**. This mixture was directly subjected to transfer hydrogenation in the presence of Hoveyda-Grubbs second generation catalyst to afford **42.2** in 55% overall yield. A one-pot metathesis/transfer hydrogenation sequence employing only Hoveyda-Grubbs second generation catalyst was attempted.[30,31] Although the desired product was obtained the overall yield of the transformation was much lower. In the case of triflate **42.3**, a 2.7:1 mixture of alkene diastereomers was produced when subjected to olefin metathesis conditions using the Grubbs first-generation catalyst. Transfer hydrogenation of this mixture afforded **42.4** in 64% yield over two steps. A single crystal suitable for X-ray crystallographic analysis of **42.2** was obtained (Figure 42), allowing for the unambiguous assignment of the substitution pattern of the tetrasubstituted pyrenes synthesized.

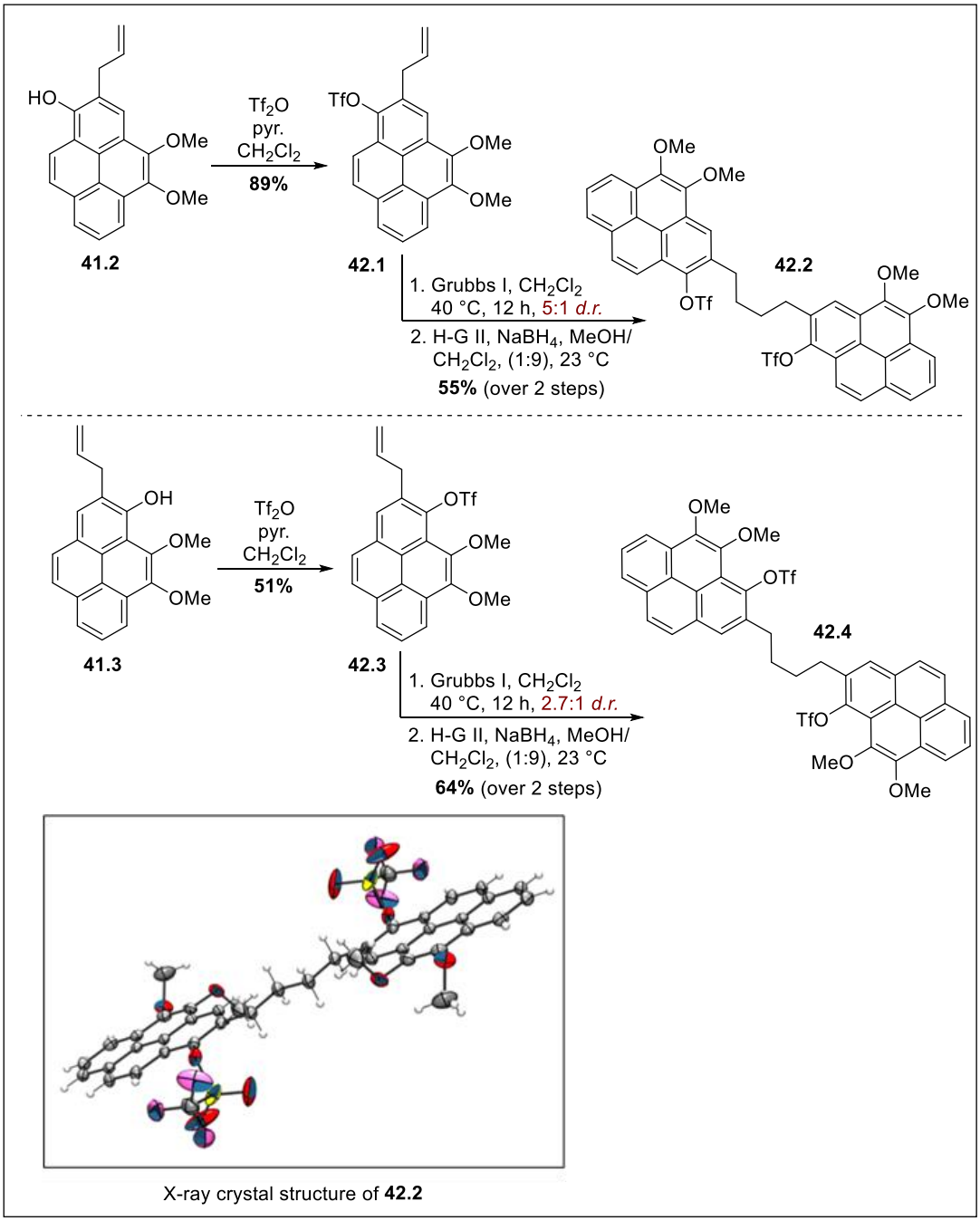

X-ray crystal structure of **42.2**

Figure 42. Synthesis of **42.2** and **42.4** via olefin methatesis

As previously mentioned, substituted pyrene derivatives are important in the development of pyrene-based materials for applications in optoelectronics, as the incorporation of substituents can be used to fine tune the optical properties of the pyrene chromophore. In the development of highly efficient pyrene-based photoelectric materials, cross-coupling reactions have been used to produce arylated pyrene derivatives with the purpose of extending π-conjugation, which translates into efficiently tunable emissive materials.[32] Access to triflated pyrene derivatives such as **42.2** and **42.4** should enable the synthesis of arylated derivatives via cross-coupling reaction that can find application in the development of new fluorophores.

2.4 Application of regioselectively functionalized pyrene dimers to carbon nanohoops and carbon nanobelts synthesis

The synthesis of π-extended carbon nanohoops that can serve as templates for the construction of carbon nanotubes have received considerable attention in recent years. In addition to their potential as starting materials in the bottom-up chemical synthesis of carbon nanotubes, these strained macrocyclic structures show interesting photophysical and electrochemical properties.[33] The groups of Yamago and Itami have independently reported the synthesis of cycloparaphenylene-2,7-pyrenylene, as the first pyrene containing carbon nanohoop.[34,35]

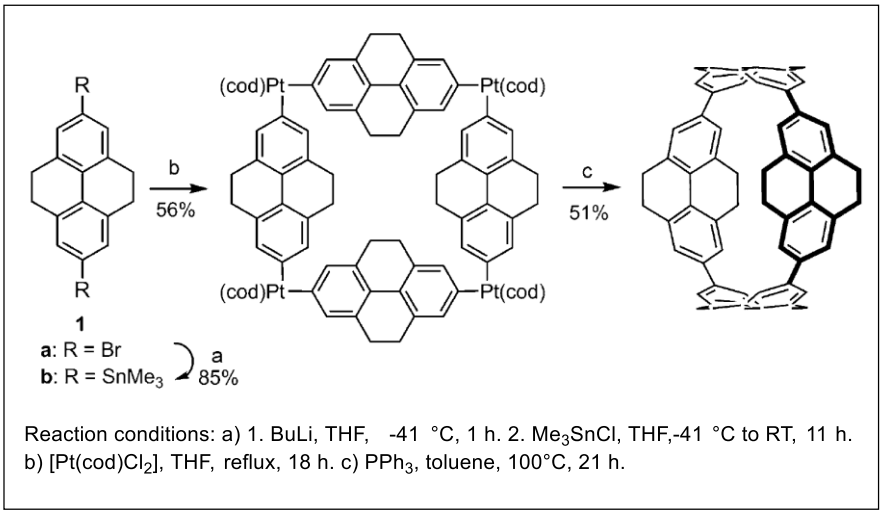

Reaction conditions: a) 1. BuLi, THF, -41 °C, 1 h. 2. Me_3SnCl, THF,-41 °C to RT, 11 h. b) [$Pt(cod)Cl_2$], THF, reflux, 18 h. c) PPh_3, toluene, 100°C, 21 h.

Figure 43. Yamago's synthesis of [4]Cyclo-2,7-Pyrenylene

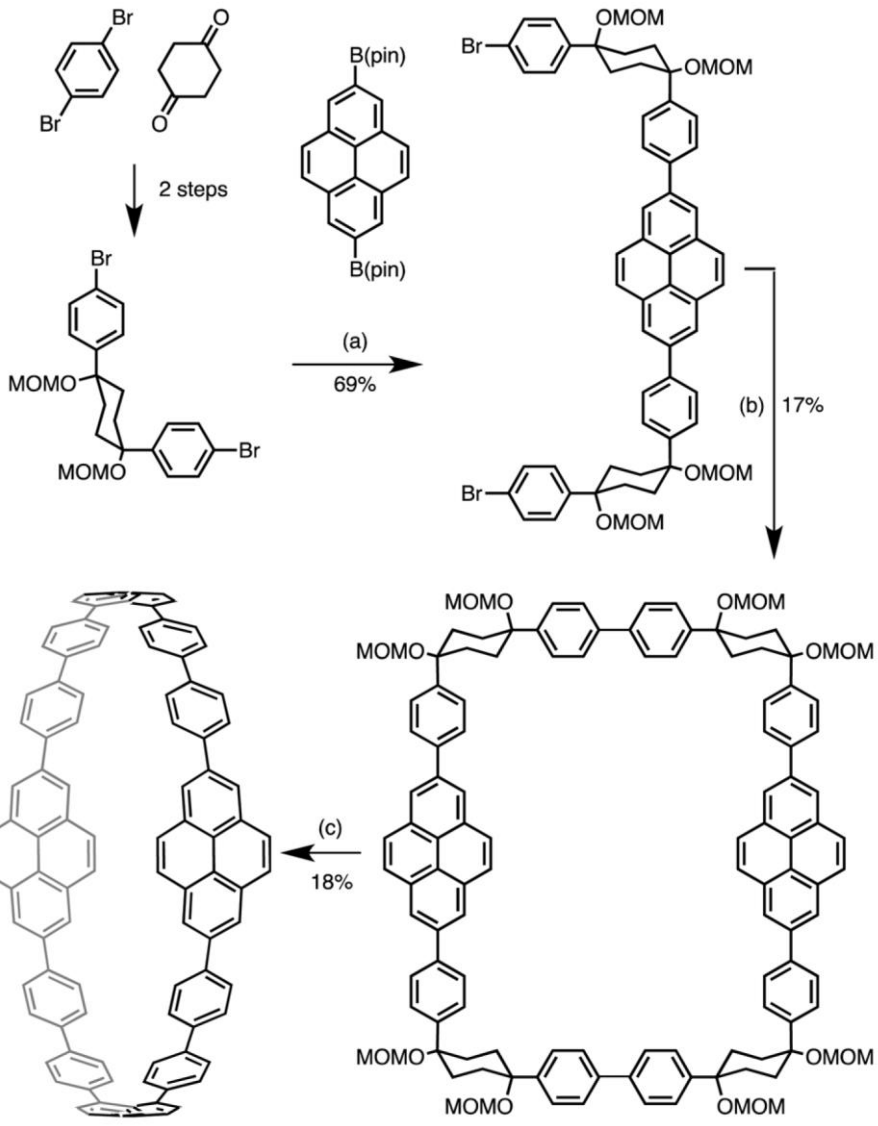

Reaction conditions: (a) $Pd(PPh_3)_4$, Ag_2O, THF, reflux. (b) $Ni(cod)_2$, 2,2′-bipyridyl, 1,4-dioxane, 90 °C. (c) $NaHSO_4 \cdot H_2O$, 1,2,3-trichlorobenzene, 150 °C. MOM = CH_2OCH_3

Figure 44. Itami's synthesis and of a pyrene-containing carbon nanoring

Our group has reported a strategy that employs 1,4-diketo-bridged macrocycles as precursors for the preparation of strained benzenoid macrocycles (Figure 45A).[36] The bridging butyl and butenyl units featured in compounds **36.2** and **36.4** and their unsaturated derivatives can be subjected to benzylic and allylic oxidation reactions to afford 1,4-diketones

that can be used as building blocks for the synthesis of carbon nanohoops that incorporate functionalized pyrene units, which, in turn, could be further extended into higher order nanostructures (Figure 45B).

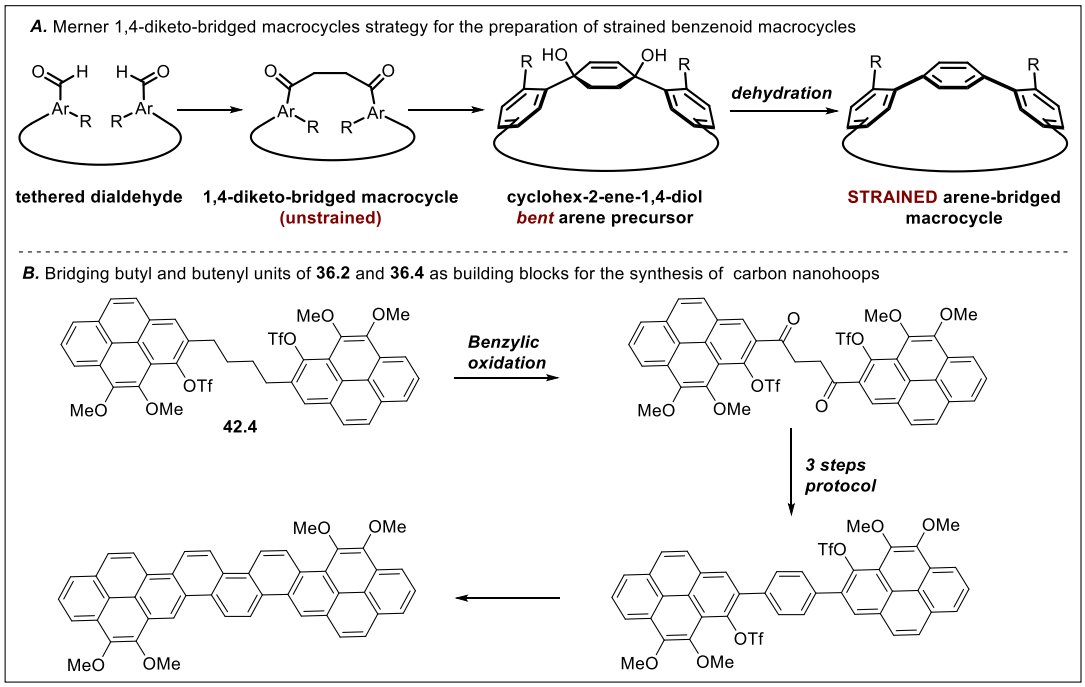

Figure 45. Future plans for **42.2** as a precursor for macrocyclic PAH synthesis

With this in mind, the synthesis of a pentasubstituted pyrene derivative, with both bromine and triflate cross-coupling handles, was pursued. Low temperature bromination of **35.1**, followed by acylation of the intermediate monobromide **46.1**, furnished bromoketone **46.2** in 70% overall yield. Subjecting **46.2** to the same reaction sequence as describe above gave 1,2,4,5,8-pentasubstituted pyrene **46.3** in 32% overall yield. Sulfonylation of the free alcohol in **46.3** afforded triflate **46.4** in 57% yield. The substitution pattern of **46.4**, and the orthogonal nature of aryl bromides and triflates in cross-coupling and functional group interconversion reactions, promise to be of great use in the development of synthetic approaches to p-extended macrocyclic systems, such as the above-mentioned carbon nanohoops and nanobelts.

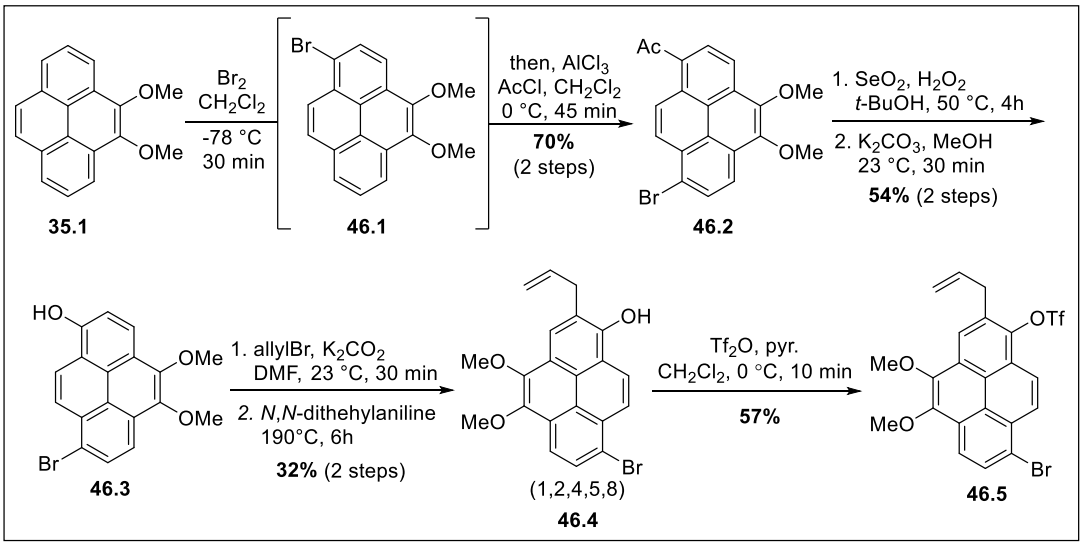

Figure 46. Synthesis of 1,2,4,5,8-pentasubstituted pyrene

2.5 FUTURE OUTLOOK CHAPTER 2

Access to unsymmetrical, regioselectively functionalized pyrene derivatives containing multiple functional group handles will put our research group in a position to synthesize contorted, π-extended PAHs or curved graphene nanoribbons (GNRs), as well as pyrene-containing carbon nanobelts.

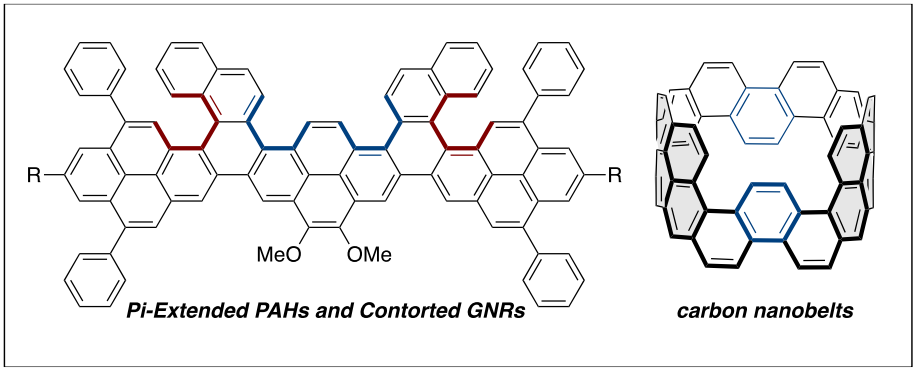

Figure 47. π-extended PAHs or curved graphene nanoribbons (GNRs), as well as pyrene-containing carbon nanobelts

Using the synthetic strategies that have been developed in this chapter and the 1,4-diketone approach that we have developed for the synthesis of highly strained benzenoid macrocycles, our group will focus on the synthesis of these new targets in the years to come.

2.6 CONCLUDING REMARKS CHAPTER 2

A strategy for the regioselective synthesis of tetra- and pentasubstituted pyrenes with primary C-alkylation of the 2-positon of pyrene has been developed. Access to 4,5-dimethoxypyren-1-ol and 9,10-dimethoxypyrene-1-ol allowed for *O*-allylation followed by a Claisen rearrangement to introduce a C2-allyll unit. A metathesis reaction of the allylated pyrene derivatives connects the 2-positions of two functionalized pyrenes with a butenyl or butyl unit after hydrogenation. When viewed as a p-extended building block of benzene, the 2 and 7 positions of pyrene can be viewed as the analogous 1 and 4 (para) carbons. Thus, selective substitution of these vertices in this manner should enable the synthesis of macrocyclic nanohoops, which can be used as key intermediates in the synthesis of CNBs.

REFERENCES CHAPTER 2

(1) Havenith, R. W. A.; Van Lenthe, J. H.; Dijkstra, F.; Jenneskens, L. W. Aromaticity of Pyréne and Its Cyclopentafused Congeners-Resonance and NICS Criteria. An Ab Initio Valence Bond Analysis in Terms of Kekulé Resonance Structures. *J. Phys. Chem. A* **2001**, *105* (15), 3838–3845.

(2) Wu, J.; Dobrowolski, M.; Cyrański, M.; Merner, B.; Bodwell, G.; Mo, Y.; Schleyer, P.; Cyran, M. On the Aromatic Stabilization Energy of the 4N π Electron Pyrene. *Mol. Phys.* **2009**, *107*, 1177–1186.

(3) Figueira-Duarte, T. M.; Klaus, M. Pyrene-Based Materials for Organic Electronics. *Chem. Rev.* **2011**, *111*, 7260–7314.

(4) Feng, X.; Hu, J. Y.; Redshaw, C.; Yamato, T. Functionalization of Pyrene To Prepare Luminescent Materials—Typical Examples of Synthetic Methodology. *Chem. - A Eur. J.* **2016**, *22* (34), 11898–11916.

(5) Casas-Solvas, J. M.; Howgego, J. D.; Davis, A. P. Synthesis of Substituted Pyrenes by Indirect Methods. *Org. Biomol. Chem.* **2014**, *12* (2), 212–232.

(6) Miyazawa, Akira; Yamato, Takehiko; Tashiro, M. Preparation of 4-Alkyl-2, 7-di-tert-butylpyrene from Pyrene. *Chem. Express* **1991**, *5* (6), 381–384.

(7) Maeda, H.; Maeda, T.; Mizuno, K.; Fujimoto, K.; Shimizu, H.; Inouye, M. Alkynylpyrenes as Improved Pyrene-Based Biomolecular Probes with the Advantages of High Fluorescence Quantum Yields and Long Absorption/Emission Wavelengths. *Chem. - A Eur. J.* **2006**, *12* (3), 824–831.

(8) Grimshaw, J.; Trocha-Grimshaw, J. Characterisation of 1,6- and 1,8-Dibromopyrenes. *J. Chem. Soc. Perkin Trans. 1* **1972**, *0* (0), 1622.

(9) Figueira-Duarte, T. M.; Simon, S. C.; Wagner, M.; Druzhinin, S. I.; Zachariasse, K. A.; Müllen, K. Polypyrene Dendrimers. *Angew. Chemie Int. Ed.* **2008**, *47* (52), 10175–10178.

(10) Coventry, D. N.; Batsanov, A. S.; Goeta, A. E.; Howard, J. A. K.; Marder, T. B.; Perutz, R. N. Selective Ir-Catalysed Borylation of Polycyclic Aromatic Hydrocarbons: Structures of Naphthalene-2,6-Bis(Boronate), Pyrene-2,7-Bis(Boronate) and Perylene-2,5,8,11-Tetra(Boronate) Esters. *Chem. Commun.* **2005**, No. 16, 2172.

(11) Minabe, M.; Mochizuki, H.; Yoshida, M.; Toda, T. Syntheses of Acetyl-1-Bromopyrenes. *Bull. Chem. Soc. Jpn.* **1989**, *62* (1), 68–72.

(12) Harvey, R. G.; Konieczny, M.; Pataki, J. Synthesis of the Isomeric Mono- and Bisoxiranylpyrenes. *J. Org. Chem.* **1983**, *48* (17), 2930–2932.

(13) Tashiro, M.; Yamato, T.; Kobayashi, K.; Arimura, T. Metacyclophanes and Related Compounds. 19. Reaction of 8-Methoxy[2.2]Metacyclophanes with Iodine in Benzene Solution. A Preparative Route of Pyrenes. *J. Org. Chem.* **1987**, *52* (15), 3196–3199.

(14) Musa, A.; Sridharan, B.; Lee, H.; Mattern, D. L. 7-Amino-2-Pyrenecarboxylic Acid. *J. Org. Chem.* **1996**, *61* (16), 5481–5484.

(15) Yang, W.; Monteiro, J. H. S. K.; de Bettencourt-Dias, A.; Catalano, V. J.; Chalifoux, W. A. Pyrenes, Peropyrenes, and Teropyrenes: Synthesis, Structures, and Photophysical Properties. *Angew. Chemie - Int. Ed.* **2016**, *55* (35), 10427–10430.

(16) Walker, D. B.; Howgego, J.; Davis, A. P. Synthesis of Regioselectively Functionalized Pyrenes via Transition-Metal-Catalyzed Electrocyclization. *Synthesis (Stuttg).* **2010**, No. 21, 3686–3692.

(17) Maeda, H.; Maeda, T.; Mizuno, K.; Fujimoto, K.; Shimizu, H.; Inouye, M. Alkynylpyrenes as Improved Pyrene-Based Biomolecular Probes with the Advantages of High Fluorescence Quantum Yields and Long Absorption/Emission Wavelengths. *Chem. - A Eur. J.* **2006**, *12* (3), 824–831.

(18) Bernhardt, S.; Kastler, M.; Enkelmann, V.; Baumgarten, M.; Müllen, K. Pyrene as Chromophore and Electrophore: Encapsulation in a Rigid Polyphenylene Shell. *Chem. - A Eur. J.* **2006**, *12* (23), 6117–6128.

(19) Crawford, A. G.; Liu, Z.; Mkhalid, I. A. I.; Thibault, M. H.; Schwarz, N.; Alcaraz, G.; Steffen, A.; Collings, J. C.; Batsanov, A. S.; Howard, J. A. K.; et al. Synthesis of 2-and 2,7-Functionalized Pyrene Derivatives: An Application of Selective C-H Borylation. *Chem. - A Eur. J.* **2012**, *18* (16), 5022–5035.

(20) Kumar Mitra, N.; Lawrence Merner, B.; Mitra Caroline P Merryman Bradley L Merner, N. K. Highly Strained Para-Phenylene-Bridged Macrocycles from Unstrained 1,4-Diketo Macrocycles Synthesis of the Building Block of CabonNano Tubes View Project Synpacts Syn Lett Highly Strained Para-Phenylene-Bridged Macrocycles from Unstrained 1,4-Diketo Macrocycles. **2017**, *28*, 2205–2211.

(21) Ozaki, K.; Kawasumi, K.; Shibata, M.; Ito, H.; Itami, K. One-Shot K-Region-Selective Annulative π-Extension for Nanographene Synthesis and Functionalization. *Nat. Commun.* **2015**, *6* (1), 6251.

(22) Venkataramana, G.; Dongare, P.; Dawe, L. N.; Thompson, D. W.; Zhao, Y.; Bodwell, G. J. 1,8-Pyrenylene-Ethynylene Macrocycles. *Org. Lett.* **2011**, *13* (9), 2240–2243.

(23) Keller, S. N.; Veltri, N. L.; Sutherland, T. C. Tuning Light Absorption in Pyrene: Synthesis and Substitution Effects of Regioisomeric Donor-Acceptor Chromophores. *Org. Lett.* **2013**, *15* (18), 4798–4801.

(24) Zöphel, L.; Beckmann, D.; Enkelmann, V.; Chercka, D.; Rieger, R.; Müllen, K. Asymmetric Pyrene Derivatives for Organic Field-Effect Transistors. *Chem. Commun.* **2011**, *47* (24), 6960.

(25) Meudom, R. Synthesis of Functionalized Benzenoid Macrocycles: An Approach to Accessing Functionalized Cycloparaphenylenes. **2016**.

(26) Merner, B. L.; Dawe, L. N.; Bodwell, G. J. 1,1,8,8-Tetramethyl[8](2,11)Teropyrenophane: Half of an Aromatic Belt and a Segment of an (8,8) Single-Walled Carbon Nanotube. *Angew. Chemie - Int. Ed.* **2009**, *48* (30), 5487–5491.

(27) Merner, B. L.; Unikela, K. S.; Dawe, L. N.; Thompson, D. W.; Bodwell, G. J. 1,1,n,n-Tetramethyl[n](2,11)Teropyrenophanes (n = 7–9): A Series of Armchair SWCNT Segments. *Chem. Commun.* **2013**, *49* (53), 5930.

(28) Harvey, R. G.; Hahn, J. T.; Bukowska, M.; Jackson, H. Full-Text. *J. Org. Chem.* **1990**, *55* (25), 6161–6166.

(29) Asakawa, T.; Hiza, A.; Nakayama, M.; Inai, M.; Oyama, D.; Koide, H.; Shimizu, K.; Wakimoto, T.; Harada, N.; Tsukada, H.; et al. PET Imaging of Nobiletin Based on a Practical Total Synthesis. *Chem. Commun.* **2011**, *47* (10), 2868.

(30) Connolly, T.; Wang, Z.; Walker, M. A.; McDonald, I. M.; Peese, K. M. Tandem Ring-Closing Metathesis/Transfer Hydrogenation: Practical Chemoselective Hydrogenation of Alkenes. *Org. Lett.* **2014**, *16* (17), 4444–4447.

(31) Mitra, N. K.; Meudom, R.; Corzo, H. H.; Gorden, J. D.; Merner, B. L. Overcoming Strain-Induced Rearrangement Reactions: A Mild Dehydrative Aromatization Protocol for Synthesis of Highly Distorted p-Phenylenes. *J. Am. Chem. Soc.* **2016**, *138* (9), 3235–3240.

(32) Wang, C. Z.; Feng, X.; Kowser, Z.; Wu, C.; Akther, T.; Elsegood, M. R. J.; Redshaw, C.; Yamato, T. Pyrene-Based Color-Tunable Dipolar Molecules: Synthesis, Characterization and Optical Properties. *Dye. Pigment.* **2018**, *153* (January), 125–131.

(33) Golder, M. R.; Jasti, R. Syntheses of the Smallest Carbon Nanohoops and the Emergence of Unique Physical Phenomena. *Acc. Chem. Res.* **2015**, *48* (3), 557–566.

(34) Yagi, A.; Venkataramana, G.; Segawa, Y.; Itami, K. Synthesis and Properties of Cycloparaphenylene-2,7-Pyrenylene: A Pyrene-Containing Carbon Nanoring. *Chem. Commun.* **2014**, *50* (8), 957–959.

(35) Iwamoto, T.; Kayahara, E.; Yasuda, N.; Suzuki, T.; Yamago, S. Synthesis, Characterization, and Properties of [4]Cyclo-2,7-Pyrenylene: Effects of Cyclic Structure on the Electronic Properties of Pyrene Oligomers. *Angew. Chemie Int. Ed.* **2014**, *53* (25), 6430–6434.

(36) Mitra, N. K.; Corzo, H. H.; Merner, B. L. A Macrocyclic 1,4-Diketone Enables the Synthesis of a p-Phenylene Ring That Is More Strained than a Monomer Unit of [4]Cycloparaphenylene. *Org. Lett.* **2016**, *18* (13), 3278–3281.

Appendix Chapter 1

General experimental conditions

All reactions were run in flame or oven-dried (120 °C) glassware and cooled under a positive pressure of ultra high pure nitrogen or argon gas. All chemicals were used as received from commercial sources, unless otherwise stated. Anhydrous reaction solvents were purified and dried by passing HPLC grade solvents through activated columns of alumina (Glass Contour SDS). All solvents used for chromatographic separations were HPLC grade (hexanes, ethyl acetate and dichloromethane). Chromatographic separations were preformed using flash chromatography, as originally reported by Still and co-workers,[1] on silica gel 60 (particle size 43-60 μm), and all chromatography conditions have been reported as diameter × height in centimeters. Reaction progress was monitored by thin layer chromatography (TLC), on glass-backed silica gel plates (pH = 7.0). TLC plates were visualized using a handheld UV lamp (254 nm or 365 nm) and stained using an aqueous ceric ammonium molybdate (CAM) solution. Plates were dipped, wiped clean, and heated from the back. ^{1}H and ^{13}C nuclear magnetic resonance (NMR) spectra were recorded at 400 or 600 MHz, calibrated using residual undeuterated solvent as an internal reference ($CHCl_3$, δ 7.27 and 77.2 ppm), reported in parts per million relative to trimethylsilane (TMS, δ 0.00 ppm), and presented as follows: chemical shift (δ, ppm), multiplicity (s = singlet, d = doublet, dd = doublet of doublets, ddt = doublet of doublet of triplets, bs = broad singlet, m = multiplet), coupling constants (*J*, Hz), and integration. High-resolution mass spectrometric (HRMS) data were obtained using a quadrupole time-of-flight (Q-TOF) spectrometer and electrospray ionization (ESI).

[1] Still, W. C.; Kahn, M.; Mitra, A.; *J. Org. Chem.* **1978**, *43*, 2923-2925.

Experimental Procedures Chapter 1

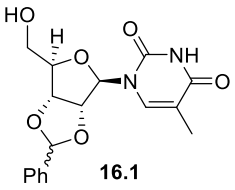

16.1

Compound 16.1: To 5-methyluridine (2.00 g, 7.74 mmol) in acetonitrile (40 mL), benzaldehyde (3.55 mL, 38.8 mmol), *p*-toluenesulfonic acid (0.235 g, 10.2 mmol) and trimethyl orthoformate (4.23 mL, 38.7 mmol) were added and the resulting mixture was stirred at 40 °C. After 6 hours, the reaction mixture was poured directly into water (50 mL) and further diluted with a saturated solution of $NaHCO_3$ (50 mL). The resulting mixture was extracted with dichloromethane (3 × 40 mL). The combined organic extracts were dried over $MgSO_4$, filtered and concentrated under reduced pressure. The residue was purified by flash chromatography (3.8 cm × 15 cm; 60% EtOAc/ Hexanes) to afford compound **16.1** as a yellow oil (2.0 g, 74%, 1.6:1 *d.r.*): R_f = 0.40 (60% EtOAc/ Hexanes); ^{1}H NMR (600 MHz, $CDCl_3$) δ 9.32 – 9.22 (m, 3H), 7.57 – 7.53 (m, 2H), 7.53 – 7.39 (m, 12H), 7.16 (s, 2H), 7.14 (s, 1H), 6.12 (s, 2H), 6.05 (s, 1H), 5.65 – 5.59 (m, 3H), 5.30 (dd, *J* = 6.8, 3.0 Hz, 1H), 5.24 – 5.17 (m, 3H), 5.15 (dd, *J* = 6.8, 3.3 Hz, 1H), 4.52 – 4.46 (m, 1H), 4.39 – 4.32 (m, 2H), 4.07 – 3.83 (m, 6H), 3.25 (s, 1H), 3.04 (s, 2H), 1.95 (d, *J* = 7.2 Hz, 8H); ^{13}C{^{1}H}NMR (151 MHz, $CDCl_3$) δ 163.78, 150.57, 150.52, 139.46, 139.03, 135.74, 135.67, 130.03, 129.90, 128.63, 128.57, 126.66, 126.56, 111.56, 111.42, 107.85, 104.09, 96.57, 95.83, 86.66, 85.09, 83.83, 83.33, 81.48, 79.90, 62.65, 12.41, 12.37; HRMS (ESI) calculated for $C_{17}H_{19}N_2O_6$ ([M + H]$^+$) *m/z* = 347.1243, found 347.1241 (sample 02-86).

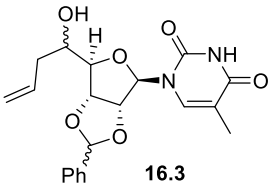

16.3

Compound 16.3: To a stirred solution of **16.1** (1.99 g, 5.75 mmol) in dichloromethane (20 mL), DMP (3.68 g, 8.68 mmol) was added. After 22 h, the reaction mixture was directly poured into a 10% solution of $Na_2S_2O_3$ (50 mL) and the resulting mixture was stirred until a clear organic phase was observed, the layers were separated, and the aqueous layer was extracted with dichloromethane (3 × 35 mL). The combined organic extracts were washed with a saturated solution of $NaHCO_3$ (2 × 60), dried over $MgSO_4$, filtered and concentrated under reduce pressure to afford the corresponding aldehyde**.** 5'-formylated nucleoside (0.91 g, 2.6 mmol) was dissolved in dichloromethane (8 mL), and trimethylallylsilane (0.58 mL, 3.9 mmol) and Boron trifluoride diethyl etherate (0.66 mL, 5.2 mmol) were added. After 1 h, the reaction mixture was poured into water (50 mL), the layers were separated, and the aqueous layer was extracted with dichloromethane (3 ×

40 mL). The combined organic extracts were dried over $MgSO_4$, filtered and concentrated under reduce pressure. The residue was purified by flash chromatography (2.5 cm × 20 cm; 15% acetone/dichloromethane) to afford compound **16.3** as white foam (1.5 g, 75%): R_f = 0.41 (20% acetone/dichloromethane); ^{1}H NMR (600 MHz, $CDCl_3$) δ 9.82 – 9.61 (m, 4H), 7.56 – 7.52 (m, 3H), 7.52 – 7.48 (m, 7H), 7.47 – 7.40 (m, 12H), 7.22 (dd, *J* = 4.8, 1.4 Hz, 2H), 7.18 (dd, *J* = 6.2, 1.5 Hz, 2H), 6.12 (s, 1H), 6.09 (s, 1H), 6.03 (s, 2H), 5.94 – 5.82 (m, 4H), 5.71 (d, *J* = 3.0 Hz, 1H), 5.69 (d, *J* = 3.3 Hz, 1H), 5.68 – 5.64 (m, 2H), 5.29 (dd, *J* = 6.8, 4.6 Hz, 1H), 5.24 – 5.06 (m, 15H), 4.31 (dt, *J* = 15.2, 3.3 Hz, 2H), 4.21 – 4.15 (m, 2H), 4.11 – 4.05 (m, 1H), 4.01 (d, *J* = 2.7 Hz, 1H), 3.98 – 3.89 (m, 1H), 3.58 (s, 1H), 3.43 (s, 1H), 3.32 (d, *J* = 6.9 Hz, 1H), 3.13 (d, *J* = 6.4 Hz, 1H), 2.48 – 2.35 (m, 8H), 2.03 (s, 2H), 1.93 (ddd, *J* = 5.8, 3.9, 1.2 Hz, 12H); ^{13}C{^{1}H}NMR (151 MHz, $CDCl_3$) δ 164.05, 164.02, 163.98, 150.71, 150.59, 150.56, 139.24, 139.10, 138.77, 138.67, 135.89, 135.81, 135.78, 135.76, 133.97, 133.66, 133.64, 129.95, 129.93, 129.84, 129.83, 128.52, 126.73, 126.64, 126.56, 118.59, 118.53, 118.42, 118.34, 111.59, 111.48, 111.40, 111.31, 107.96, 107.88, 104.17, 104.04, 95.58, 95.37, 94.72, 94.65, 88.30, 87.26, 86.37, 85.84, 83.99, 83.60, 83.29, 83.23, 82.46, 80.00, 78.66, 71.21, 71.19, 70.37, 70.23, 38.29, 38.19, 37.54, 37.50, 12.38, 12.35; HRMS (ESI) calculated for $C_{20}H_{23}N_2O_6$ ([M + H]$^+$) *m/z* = 387.1556, found 387.1563.

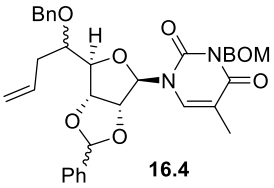

16.4

Compound 16.4: To a stirred 0 °C solution of **16.3** (1.74 g, 4.51 mmol) in DMF (20 mL), BOMCl (0.83 mL, 5.4 mmol) and DBU (0.84 mL, 5.6 mmol) were added. After 1 h, the reaction mixture was poured into water (100 mL) and further diluted with 1 M HCl (100 mL). The resulting mixture was extracted with EtOAc (3 × 60 mL). The combined organic extracts were washed with brine (3 × 100 mL), dried over $MgSO_4$, filtered and concentrated under reduced pressure to afford the NBOM protected nucleoside as a yellow oil: R_f = 0.53 (60% EtOAc/Hexanes). The NBOM protected nucleoside (2.00 g, 3.95 mmol) was dissolved in 1:1 DMF-THF (20 mL) and cooled to 0 °C. Sodium borohydride (0.250 g, 6.26 mmol), TBAI (0.783 g, 1.97 mmol) and benzylbromide (0.71 mL, 5.9 mmol) were added. After 4 h, MeOH (5 mL) was added and stirred for 5 min. The mixture was poured into water (100 mL) and further diluted with 1 M HCl (100 mL). The resulting mixture was extracted with dichloromethane (3 × 60 mL) and the combined organic extracts were washed with brine (2 × 60 mL), dried over $MgSO_4$, filtered and concentrated under reduced pressure. The product of this reaction was purified by flash chromatography (1.5 cm × 15 cm; 30% EtOAc/Hexanes) to afford compound **16.4** as clear oil (1.6 g, 70%): R_f = 0.38 (40%

EtOAc/Hexanes); ^{1}H NMR (600 MHz, $CDCl_3$) δ 7.62 – 7.58 (m, 6H), 7.56 – 7.50 (m, 17H), 7.49 – 7.32 (m, 176H), 7.13 (d, *J* = 1.4 Hz, 2H), 7.03 (d, *J* = 1.6 Hz, 6H), 6.29 (d, *J* = 3.4 Hz, 1H), 6.22 (d, *J* = 3.3 Hz, 3H), 6.19 (s, 3H), 6.15 (d, *J* = 3.5 Hz, 7H), 6.13 (d, *J* = 3.3 Hz, 5H), 6.07 (s, 2H), 6.05 (s, 1H), 5.97 – 5.82 (m, 11H), 5.56 – 5.50 (m, 16H), 5.50 – 5.46 (m, 8H), 5.32 – 5.15 (m, 31H), 4.94 (ddt, *J* = 12.3, 6.8, 3.2 Hz, 6H), 4.88 (dd, *J* = 6.6, 2.6 Hz, 1H), 4.85 (dd, *J* = 6.9, 3.3 Hz, 5H), 4.84 – 4.80 (m, 7H), 4.79 – 4.72 (m, 25H), 4.70 (s, 11H), 4.64 (s, 3H), 4.62 (s, 2H), 4.60 – 4.53 (m, 7H), 4.53 – 4.51 (m, 1H), 4.43 – 4.41 (m, 2H), 4.40 – 4.39 (m, 3H), 4.28 (dd, *J* = 4.8, 3.6 Hz, 5H), 3.95 – 3.85 (m, 7H), 3.81 – 3.71 (m, 4H), 2.71 – 2.64 (m, 4H), 2.63 – 2.53 (m, 10H), 2.53 – 2.39 (m, 7H), 1.71 – 1.64 (m, 33H); ^{13}C{^{1}H}NMR (151 MHz, $CDCl_3$) δ 163.44, 163.33, 163.28, 151.06, 150.97, 141.14, 138.15, 138.12, 138.09, 138.08, 137.62, 137.52, 136.28, 136.08, 135.90, 135.80, 135.53, 135.48, 135.11, 135.04, 133.42, 133.36, 133.30, 133.18, 130.39, 130.03, 129.99, 129.85, 129.81, 128.76, 128.70, 128.68, 128.67, 128.62, 128.59, 128.57, 128.51, 128.46, 128.44, 128.37, 128.36, 128.28, 128.17, 128.14, 127.95, 127.88, 127.86, 127.83, 127.76, 127.72, 127.71, 127.68, 127.65, 127.61, 127.16, 127.02, 126.97, 126.93, 126.92, 126.74, 126.61, 126.58, 118.93, 118.86, 118.78, 118.72, 111.15, 110.69, 110.67, 110.31, 108.13, 107.85, 104.37, 104.26, 91.81, 91.50, 90.98, 90.64, 86.57, 85.67, 85.21, 85.13, 85.04, 84.62, 83.85, 83.41, 81.31, 80.50, 79.17, 79.03, 78.96, 78.46, 78.12, 77.44, 77.23, 77.02, 76.94, 72.57, 72.52, 72.37, 72.35, 72.31, 72.27, 72.03, 70.77, 70.71, 70.67, 65.28; HRMS (ESI) calculated for $C_{35}H_{37}N_2O_7$ ([M + H]$^+$) *m/z* = 597.2601, found 597.2572.

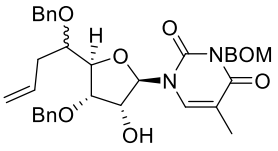

16.5

Compound 16.5: To a C stirred 0 ° solution of **16.4** (1.60 g, 2.68 mmol) in MeCN (12 mL), $NaBH_3CN$ (0.74 g, 10 mmol), and $TiCl_4$ (0.86 mL, 8.0 mmol) were added. After 3 h, the reaction mixture was poured into water (100 mL) and CH_2Cl_2 (60 mL) was added, the layers were separated, and the aqueous portion was extracted with dichloromethane (2 × 60 mL). The combined organic extracts were washed with brine (2 × 100 mL), dried over $MgSO_4$, filtered and concentrated under reduced pressure to afford **16.5** as a clear oil (1.63 g, 95%): R_f = 0.55 (60% EtOAc/Hexanes); ^{1}H NMR (600 MHz, $CDCl_3$) δ 7.59 – 7.56 (m, 1H), 7.44 – 7.22 (m, 54H), 7.14 – 7.09 (m, 2H), 6.05 – 5.98 (m, 3H), 5.93 – 5.73 (m, 3H), 5.53 – 5.44 (m, 6H), 5.44 (s, 1H), 5.26 – 5.12 (m, 7H), 4.84 (s, 1H), 4.81 (s, 1H), 4.79 – 4.58 (m, 17H), 4.55 (s, 1H), 4.51 (d, *J* = 2.9 Hz, 2H), 4.31 (d, *J* = 10.8 Hz, 1H), 4.30 – 4.20 (m, 7H), 4.19 (dd, *J* = 4.5, 1.6 Hz, 1H), 4.01 – 3.94 (m, 1H), 3.52 – 3.45 (m, 1H), 3.22 – 3.16 (m, 3H), 2.69 – 2.44 (m, 4H), 2.39 – 2.26 (m, 3H), 1.60 – 1.51 (m, 9H); ^{13}C{^{1}H}NMR (101 MHz, $CDCl_3$)

δ 163.48, 163.32, 151.59, 151.40, 141.01, 138.07, 138.00, 137.83, 137.36, 136.82, 136.81, 134.69, 134.34, 133.48, 133.42, 128.76, 128.71, 128.65, 128.61, 128.52, 128.47, 128.34, 128.30, 128.28, 128.16, 128.01, 127.88, 127.72, 127.69, 127.65, 127.61, 127.58, 127.55, 126.97, 126.84, 118.68, 118.49, 110.69, 110.15, 89.75, 89.19, 83.60, 82.57, 78.78, 77.81, 77.73, 77.47, 77.35, 77.15, 76.83, 76.44, 73.95, 73.52, 72.73, 72.50, 72.33, 72.19, 71.99, 70.66, 70.54, 65.23, 34.88, 34.69, 12.76, 12.70; HRMS (ESI) calculated for $C_{35}H_{39}N_2O_7$ ([M + H]$^+$) *m/z* 599.2757, found 599.2770.

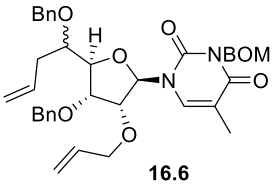

16.6

Compound 16.6: To a stirred 0 °C solution of **16.5** (0.82 g, 1.7 mmol) in 1:1 DMF-THF (7 mL), sodium borohydride (0.0819 g, 2.05 mmol), TBAI (0.252 g, 0.683 mmol) and allylbromide (0.18 mL, 2.05 mmol) were added. After 4 h, MeOH (5 mL) was added and stirred for 5 min. The mixture was poured into water (75 mL) and further diluted with 1 M HCl (60 mL). The resulting mixture was extracted with dichlromethane (3 × 50 mL) and the combined organic extracts were washed with water (60 mL), dried over $MgSO_4$, filtered and concentrated under reduced pressure. The product of this reaction was purified by flash chromatography (2.5 cm × 18 cm; 30% EtOAc/Hexanes) to afford **16.6** as clear oil (0.661 g, 90%): R_f = 0.67 (60% EtOAc/Hexanes); ^{1}H NMR (600 MHz, $CDCl_3$) δ 7.44 – 7.28 (m, 22H), 7.22 – 7.16 (m, 1H), 6.10 (d, *J* = 4.0 Hz, 1H), 6.03 – 5.78 (m, 3H), 5.57 – 5.45 (m, 3H), 5.46 – 5.09 (m, 6H), 4.90 – 4.78 (m, 1H), 4.78 – 4.49 (m, 9H), 4.49 – 4.35 (m, 1H), 4.38 – 4.08 (m, 5H), 4.11 – 3.93 (m, 2H), 3.88 (ddd, *J* = 8.2, 5.8, 2.7 Hz, 1H), 3.73 – 3.64 (m, 1H), 2.62 – 2.48 (m, 2H), 2.50 – 2.37 (m, 1H), 1.49 – 1.38 (m, 3H); HRMS (ESI) calculated for $C_{38}H_{43}N_2O_7$ ([M + H]$^+$) *m/z* 639.3070, found 639.3066.

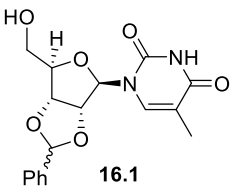

16.1

Compound 16.1 (modified procedure): To a stirred solution of 5-methyluridine (5.00 g, 19.4 mmol) in 1,2-dichloroethane (60 mL), *p*-toluenesulfonic acid (0.62 g, 3.3 mmol) and benzaldehyde dimethyl acetal (10.2 mL, 67.8 mmol) were added and the resulting mixture was stirred at 80 °C. After 24 h, the reaction mixture was poured directly into water (200 mL) and further diluted with a saturated solution of $NaHCO_3$ (200 mL). The mixture was stirred for 5 min, the layers were separated, and the aqueous portion was extracted with dichloromethane (3 × 80 mL). The combined organic extracts were washed with brine (200 mL), dried over $MgSO_4$, filtered and concentrated under reduced pressure.

The residue was purified by flash chromatography (5 cm × 15 cm; 80% EtOAc/Hexanes) to afford compound **16.1** as white foam (6.80 g, >95%): R_f = 0.42 (100% EtOAc).

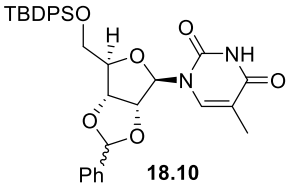

18.10

Compound 18.10: To a stirred solution of **16.1** (1.00 g, 2.88 mmol) in THF (11 mL), Imidazole (0.501 g, 7.36 mmol) and TBDPSCl (1.1 mL, 1.3 mmol) were added. The reaction mixture was stirred at room temperature for 15 min. before MeOH (5 mL) was added. After 5 min, the resulting mixture was poured into water (100 mL), and the resulting mixture was extracted with CH_2Cl_2 (3 × 60 mL). The combined organic extracts were dried over $MgSO_4$ and concentrated under reduced pressure. The residue was purified by flash chromatography (15 cm × 2.5 cm; 20% EtOAc/Hexanes) to afford **18.10** as a colorless oil (1.7 g, 98% yield): R_f = 0.82 (20% EtOAc/Hexanes); ^{1}H NMR (600 MHz, $CDCl_3$) δ 8.92 – 8.80 (m, 3H), 7.71 – 7.66 (m, 13H), 7.61 – 7.57 (m, 2H), 7.54 – 7.50 (m, 5H), 7.50 – 7.36 (m, 30H), 7.34 – 7.30 (m, 1H), 7.29 (s, 1H), 6.15 (s, 2H), 6.11 (d, *J* = 3.4 Hz, 1H), 6.08 (s, 1H), 6.06 (d, *J* = 3.4 Hz, 2H), 5.13 (dd, *J* = 6.7, 4.3 Hz, 2H), 5.03 (dd, *J* = 6.6, 2.9 Hz, 1H), 4.99 (dd, *J* = 6.7, 3.4 Hz, 1H), 4.95 (dd, *J* = 6.7, 3.4 Hz, 2H), 4.46 (dd, *J* = 3.2 Hz, 1H), 4.32 (dd, *J* = 3.8 Hz, 2H), 4.08 (dd, *J* = 11.6, 2.9 Hz, 2H), 4.04 (dd, *J* = 11.6, 3.0 Hz, 1H), 3.97 (dd, *J* = 11.6, 4.1 Hz, 2H), 3.92 (dd, *J* = 11.6, 3.9 Hz, 1H), 1.73 (s, 8H), 1.70 (s, 3H), 1.14 – 1.09 (m, 29H); ^{13}C{^{1}H}NMR (151 MHz, $CDCl_3$) δ 163.72, 163.61, 150.12, 136.48, 136.40, 135.77, 135.68, 135.58, 135.39, 135.36, 132.95, 132.90, 132.54, 132.44, 130.16, 130.09, 130.03, 129.87, 128.63, 128.55, 127.99, 127.97, 127.93, 126.84, 126.63, 111.71, 111.36, 108.05, 104.17, 91.47, 90.67, 85.52, 84.82, 84.23, 83.99, 81.88, 79.81, 64.04, 63.76, 26.96, 19.40, 12.19; HRMS (ESI) calculated for $C_{33}H_{37}N_2O_6Si$ ([M + H]$^+$) *m/z* 585.2421, found 585.2400.

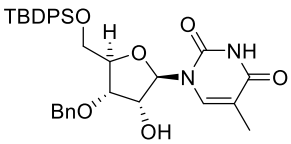

18.1

Compound 18.1: To a stirred 0 °C solution of **18.10** (1.66 g, 2.84 mmol) in MeCN (25 mL), $TiCl_4$ (0.81 mL, 7.6 mmol) was added and the mixture was stirred for 5 min before $NaBH_3CN$ (0.763 g, 12.1 mmol) was added. The mixture was allowed to warm to room temperature and stirred for 18 h. Then, it was poured into water (250 mL) and further diluted with 1 M HCl (150 mL), the resulting mixture was extracted with dichloromethane (3 × 60 mL). The combined organic extracts were sequentially washed with brine (50 mL) and a saturated solution of $NaHCO_3$ (50 mL), dried over $MgSO_4$ and

concentrated under reduced pressure. The residue was purified by flash chromatography (15 cm × 2.5 cm; 30% EtOAc/Hexanes) to afford **18.1** as a colorless oil (0.74 g, 44% yield): R_f = 0.45 (20% EtOAc/Hexanes); ^{1}H NMR (600 MHz, $CDCl_3$) δ 10.01 (s, 1H), 7.70 – 7.61 (m, 4H), 7.53 – 7.39 (m, 7H), 7.40 – 7.31 (m, 5H), 6.11 (d, *J* = 6.1 Hz, 1H), 4.76 (d, *J* = 11.8 Hz, 1H), 4.64 (d, *J* = 11.8 Hz, 1H), 4.34 (dd, *J* = 6.4 Hz, 1H), 4.19 (ddd, *J* = 16.0, 5.8, 3.1 Hz, 2H), 4.06 (d, *J* = 11.7 Hz, 1H), 4.00 (dd, *J* = 11.7, 2.4 Hz, 1H), 3.71 (dd, *J* = 11.7, 2.4 Hz, 1H), 1.59 (s, 3H), 1.11 (s, 9H); ^{13}C{^{1}H}NMR (151 MHz, $CDCl_3$) δ 164.25, 151.23, 137.11, 135.56, 135.29, 132.84, 132.26, 130.23, 130.12, 128.66, 128.23, 128.17, 128.10, 128.05, 111.54, 88.38, 83.15, 76.79, 74.46, 72.84, 63.67, 27.06, 19.43, 12.03; HRMS (ESI) calculated for $C_{33}H_{39}N_2O_6Si$ ([M + H]$^+$) *m/z* 587.2577, found 587.2562.

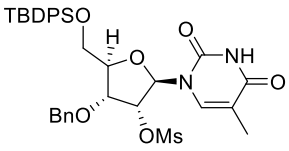

18.2

Compound 18.2: To a stirred 0 °C solution of **18.1** (0.0435 g, 0.0654 mmol) in MeCN (2.2 mL), DBU (0.02 mL, 0.1 mmol) was added. After 2 h, 1 M HCl (5 mL) was added and stirred for 5 min. The resulting mixture was extracted with dichloromethane (3 × 10 mL), and the combined organic extracts were washed with brine (20 mL), dried over $MgSO_4$ and concentrated under reduced pressure. The residue was purified by flash column chromatography (15 cm × 1.3 cm; 30% hexanes/ethyl acetate) to afford **18.2** as a colorless oil (0.023 g, 63% yield): R_f = 0.12 (20% EtOAc/Hexanes); ^{1}H NMR (600 MHz, $CDCl_3$) δ 7.59 – 7.54 (m, 4H), 7.49 – 7.44 (m, 2H), 7.43 – 7.33 (m, 10H), 7.16 (d, *J* = 1.6 Hz, 1H), 6.14 (d, *J* = 5.8 Hz, 1H), 5.30 (dd, *J* = 5.8, 1.3 Hz, 1H), 4.69 (d, *J* = 11.6 Hz, 1H), 4.62 (d, *J* = 11.6 Hz, 1H), 4.47 (dd, *J* = 3.0, 1.4 Hz, 1H), 4.34 (ddd, *J* = 8.3, 5.5, 3.0 Hz, 1H), 3.57 (dd, *J* = 11.2, 5.4 Hz, 1H), 3.44 (dd, *J* = 11.1, 7.1 Hz, 1H), 1.94 (d, *J* = 1.4 Hz, 3H), 0.99 (s, 9H); ^{13}C{^{1}H}NMR (151 MHz, $CDCl_3$) δ 172.13, 159.00, 136.22, 135.46, 135.45, 132.68, 132.31, 130.10, 130.07, 129.96, 128.79, 128.51, 128.09, 128.00, 127.96, 127.91, 119.50, 90.07, 86.52, 85.82, 82.10, 72.57, 62.39, 26.64, 19.15, 14.13; HRMS (ESI) calculated for $C_{33}H_{37}N_2O_5Si$ ([M + H]$^+$) *m/z* 569.2472, found 569.2445.

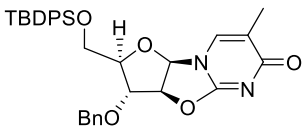

18.3

Compound 18.3: To a stirred solution of **18.2** (0.0392 g, 0.0667 mmol) in pyridine (1.5 mL), MsCl (0.03 mL, 0.04 mmol) was added. After 1 h, 1 M HCl (15 mL) was added and stirred for 5 min. The resulting mixture was extracted with dichloromethane (3 × 10 mL), and the combined organic extracts were washed with brine (10 mL), dried over

$MgSO_4$ and concentrated under reduced pressure to afford **18.3** as a colorless oil (0.044 g, 98% yield): R_f = 0.72 (20% EtOAc/Hexanes); ^{1}H NMR (600 MHz, $CDCl_3$) δ 9.47 (s, 1H), 7.67 (d, *J* = 7.3 Hz, 2H), 7.65 – 7.60 (m, 2H), 7.54 – 7.44 (m, 3H), 7.44 – 7.32 (m, 9H), 6.16 (d, *J* = 3.7 Hz, 1H), 5.33 (dd, *J* = 4.4 Hz, 1H), 4.87 (d, *J* = 11.1 Hz, 1H), 4.52 (d, *J* = 11.2 Hz, 1H), 4.35 (dd, *J* = 5.5 Hz, 1H), 4.22 (d, *J* = 5.7 Hz, 1H), 4.15 – 4.11 (m, 1H), 3.84 (dd, *J* = 12.2, 2.3 Hz, 1H), 1.49 (s, 3H), 1.28 (s, 3H), 1.13 (s, 9H); ^{13}C{^{1}H}NMR (151 MHz, $CDCl_3$) δ 163.74, 150.66, 136.76, 135.47, 135.22, 134.49, 132.82, 132.11, 130.30, 130.19, 128.65, 128.37, 128.32, 128.17, 128.09, 111.89, 87.35, 82.86, 79.14, 74.67, 73.31, 62.28, 39.06, 29.76, 27.10, 19.50, 11.94; HRMS (ESI) calculated for $C_{34}H_{41}N_2O_8SSi$ ([M + H]$^+$) *m/z* 665.2353, found 665.2347.

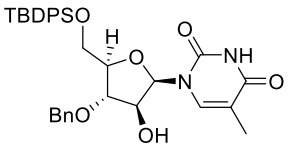

18.4

Compound 18.4: To a stirred solution of **18.3** (0.150 g, 0.264 mmol) in THF (2 mL), an aqueous 3 M solution of CF_3COOH (0.2 mL, 0.6 mmol) was added. The resulting solution was stirred at 45 °C for 16 h. Then, it was poured into water (10 mL) and further diluted with a saturated solution of $NaHCO_3$ (15 mL). The resulting mixture was extracted with dichloromethane (3 × 10 mL), and the combined organic extracts were dried over $MgSO_4$, filtered and concentrated under reduced pressure. The residue was purified by flash chromatography (15 cm × 2.5 cm; 70% EtOAc/Hexanes) to afford **18.4** as a white solid (0.15 g, 95% yield): R_f = 0.56 (100% EtOAc); ^{1}H NMR (600 MHz, $CDCl_3$) δ 11.17 (s, 1H), 7.78 – 7.72 (m, 4H), 7.58 – 7.26 (m, 11H), 6.26 (d, *J* = 3.5 Hz, 1H), 5.07 (s, 1H), 4.96 (s, 1H), 4.81 (d, *J* = 11.7 Hz, 1H), 4.59 (d, *J* = 11.7 Hz, 1H), 4.19 (d, *J* = 3.0 Hz, 2H), 4.00 (dd, *J* = 10.9, 4.1 Hz, 1H), 3.92 (dd, *J* = 10.9, 4.5 Hz, 1H), 1.63 (s, 3H), 1.12 (s, 9H); ^{13}C{^{1}H}NMR (151 MHz, $CDCl_3$) δ 166.17, 150.61, 139.60, 137.60, 135.65, 135.59, 134.88, 133.08, 133.00, 129.98, 129.92, 128.56, 128.14, 127.94, 127.90, 127.89, 107.59, 87.17, 84.22, 83.40, 73.24, 71.67, 63.32, 26.83, 19.35, 12.28; HRMS (ESI) calculated for $C_{33}H_{39}N_2O_6Si$ ([M + H]$^+$) *m/z* 587.2577, found 587.2573.

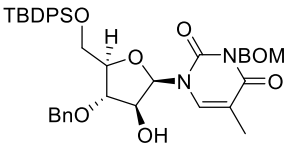

18.11

Compound 18.11: To a stirred 0 °C solution of **18.4** (0.030g, 0.052 mmol) in DMF (1.5 mL), BOMCl (0.01 mL, 0.06 mmol) and DBU (0.01 mL, 0.06 mmol) were added. After 10 min, the reaction mixture was poured into water (2 mL) and further diluted with 1 M HCl (2 mL). The resulting mixture was extracted with

dichloromethane (3 × 8 mL), and the combined organic extracts were washed with brine (10 mL), dried over $MgSO_4$, filtered and concentrated under reduced pressure to afford **18.11** as a white solid (0.046 g, 95% yield): R_f = 0.66 (60% EtOAc/Hexanes); ^{1}H NMR (600 MHz, $CDCl_3$) δ 7.78 – 7.74 (m, 2H), 7.72 – 7.67 (m, 2H), 7.62 – 7.30 (m, 17H), 6.25 (d, *J* = 3.2 Hz, 1H), 5.59 – 5.49 (m, 2H), 4.80 (d, *J* = 11.8 Hz, 1H), 4.76 (s, 2H), 4.69 (s, 1H), 4.63 (d, *J* = 11.8 Hz, 1H), 4.50 (dd, *J* = 9.0, 3.4 Hz, 1H), 4.30 – 4.24 (m, 1H), 4.23 – 4.20 (m, 1H), 4.20 – 4.17 (m, 1H), 4.06 (dd, *J* = 11.5, 3.0 Hz, 1H), 3.80 (dd, *J* = 11.6, 2.5 Hz, 1H), 1.83 (s, 3H), 1.14 (s, 9H); ^{13}C{^{1}H}NMR (151 MHz, $CDCl_3$) δ 163.78, 151.02, 141.00, 137.94, 137.16, 136.34, 135.57, 135.49, 131.77, 131.64, 130.45, 128.69, 128.57, 128.40, 128.23, 128.19, 128.17, 127.95, 127.87, 127.76, 127.61, 127.02, 108.49, 87.10, 84.00, 83.25, 72.81, 72.22, 72.09, 70.48, 64.03, 26.77, 19.18, 13.12; HRMS (ESI) calculated for $C_{41}H_{47}N_2O_7Si$ ($[M + H]^+$) *m/z* 707.3153, found 707.3137.

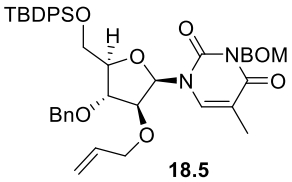

18.5

Compound 18.5: To a stirred 0 °C solution of **18.11** (0.046 g, 0.065 mmol) in 1:1 DMF-THF (2 mL), sodium hydride (0.0089 g, 0.2230 mmol), TBAI (0.0164 g, 0.0444 mmol) and allylbromide (0.02 mL, 0.23 mmol) were added. After 2 h, the mixture was poured into water (5 mL) and further diluted with 1 M HCl (5 mL). The resulting mixture was extracted with dichloromethane (3 × 10 mL) and the combined organic extracts were washed with brine (10 mL), dried over $MgSO_4$, filtered and concentrated under reduced pressure. The residue was purified by flash chromatography (15 cm × 1.3 cm; 100% hexanes, 20% EtOAc/Hexanes) to afford **18.5** as a residue (0.030 g, 61% yield): R_f = 0.29 (20% EtOAc/Hexanes); ^{1}H NMR (600 MHz, $CDCl_3$) δ 7.71 (d, *J* = 7.4 Hz, 4H), 7.53 – 7.47 (m, 2H), 7.47 – 7.35 (m, 14H), 7.34 – 7.30 (m, 1H), 6.33 (d, *J* = 4.2 Hz, 1H), 5.71 (ddt, *J* = 17.6, 10.4, 5.3 Hz, 1H), 5.56 (s, 2H), 5.18 – 5.11 (m, 2H), 4.74 (s, 2H), 4.70 (d, *J* = 11.9 Hz, 1H), 4.63 (d, *J* = 11.8 Hz, 1H), 4.21 (d, *J* = 4.1 Hz, 2H), 4.13 – 4.06 (m, 1H), 3.98 – 3.89 (m, 3H), 3.82 (dd, *J* = 12.9, 4.3, 1.6 Hz, 1H), 1.82 (s, 3H), 1.12 (s, 9H); ^{13}C{^{1}H}NMR (151 MHz, $CDCl_3$) δ 163.67, 151.11, 137.91, 137.31, 136.73, 135.61, 135.54, 134.88, 133.36, 133.10, 132.89, 130.04, 129.97, 128.65, 128.38, 128.12, 127.94, 127.91, 127.82, 127.77, 127.75, 117.51, 108.63, 85.21, 82.04, 81.52, 81.44, 72.08, 71.44, 70.42, 62.63, 26.90, 19.40, 13.03; HRMS (ESI) calculated for $C_{44}H_{51}N_2O_7Si$ ($[M + H]^+$) *m/z* 747.3466, found 747.3468.

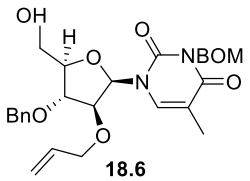

18.6

Compound 18.6: To a stirred 0 °C solution of **18.5** (0.201 g, 0.269 mmol) in THF (3 mL), a 1 M solution of TBAF in THF (0.31 mL, 0.31 mmol) was added. After 2 h, the reaction mixture was poured into water (20 mL) and the resulting mixture was extracted with dichloromethane (3 × 15 mL). The combined organic extracts were dried over $MgSO_4$, filtered and concentrated under reduced pressure. The residue was purified by flash chromatography (15 cm × 1.3 cm; 30% EtOAc/Hexanes) to afford **18.6** (0.13 g, 94% yield): R_f = 0.50 (60% EtOAc/Hexanes); ^{1}H NMR (600 MHz, Chloroform-*d*) δ 7.52 – 7.48 (m, 1H), 7.43 – 7.31 (m, 10H), 7.32 – 7.27 (m, 1H), 6.29 (d, *J* = 4.6 Hz, 1H), 5.71 (ddt, *J* = 16.3, 5.4 Hz, 1H), 5.53 (s, 2H), 5.21 – 5.10 (m, 2H), 4.76 – 4.68 (m, 3H), 4.63 (d, *J* = 11.8 Hz, 1H), 4.20 (dd, *J* = 4.6, 2.7 Hz, 1H), 4.12 – 4.05 (m, 2H), 3.95 (dd, *J* = 12.8, 5.6 Hz, 1H), 3.91 (dd, *J* = 12.0, 3.5 Hz, 1H), 3.86 (dd, *J* = 12.7, 5.4 Hz, 1H), 3.80 (dd, *J* = 12.0, 4.3 Hz, 1H), 2.69 (s, 1H), 1.96 (s, 3H); ^{13}C{^{1}H}NMR (151 MHz, $CDCl_3$) δ 163.62, 151.09, 137.80, 137.20, 136.55, 133.09, 128.67, 128.38, 128.22, 127.83, 127.80, 127.77, 118.05, 108.84, 85.16, 82.33, 81.37, 81.03, 72.29, 72.08, 71.71, 70.42, 62.04, 13.33; HRMS (ESI) calculates for $C_{28}H_{33}N_2O_7$ ([M+H]$^+$) *m/z* 509.2288, found 509.2278.

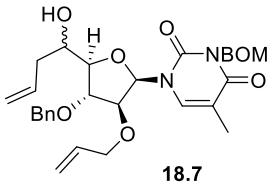

18.7

Compound 18.7: To a stirred solution of **18.6** (0.106 g, 0.209 mmol) in dichloromethane (2 mL), Dess-Martin periodinate (0.266 g, 0.626 mmol) was added. After 24 h, the reaction mixture was poured into water (30 mL) and further diluted with 10% $Na_2S_2O_3$ (30 mL). The resulting mixture was stirred until a clear organic phase was observed. The layers were separated, and the aqueous portion was extracted with dichloromethane (3 × 20 mL). The combined organic extracts were washed with brine (20 mL), dried over $MgSO_4$, filtered and concentrated under reduced pressure to afford **7** as an oily residue (0.11 g, 94% yield): R_f = 0.58 (10% acetone/dichloromethane). Compound 7 was dissolved in dichloromethane (2 mL) and the solution was cooled to 0 °C. Boron trifluoride diethyl etherate (0.03 mL, 0.24 mmol) was added and the mixture was stirred for 5 min. before trimethylallylsilane (0.04 mL, 0.31 mmol) was added. After 20 min., the mixture was poured into water (40 mL), the layers were separated, and the aqueous portion was extracted with dichloromethane (3 × 20 mL). The combined organic extracts were dried over $MgSO_4$, filtered and concentrated under reduced pressure. The product of this reaction was purified by flash chromatography (1.3 cm × 15 cm; 40% EtOAc/Hexanes) to yield compound **18.7** as an oily residue (0.084 g, 73% yield): R_f = 0.72 (70% EtOAc/Hexanes), and N-deprotected compound

(0.011 g, 12% yield); ^{1}H NMR (600 MHz, $CDCl_3$) δ 7.54 (s, 1H), 7.49 – 7.32 (m, 36H), 7.32 – 7.26 (m, 4H), 6.30 (d, *J* = 4.6 Hz, 1H), 6.24 (d, *J* = 4.0 Hz, 2H), 5.89 (ddt, *J* = 17.1, 10.3, 6.9 Hz, 3H), 5.72 (ddt, 3H), 5.54 (s, 6H), 5.26 – 5.12 (m, 14H), 4.72 (d, *J* = 2.3 Hz, 9H), 4.70 – 4.59 (m, 5H), 4.21 (dt, *J* = 9.9, 2.7 Hz, 3H), 4.17 (dd, *J* = 3.9, 1.8 Hz, 2H), 4.12 (dd, *J* = 4.9, 3.0 Hz, 1H), 4.01 – 3.91 (m, 10H), 3.91 – 3.81 (m, 5H), 2.52 – 2.47 (m, 1H), 2.47 – 2.37 (m, 7H), 2.31 – 2.22 (m, 2H), 2.01 – 1.93 (m, 10H); ^{13}C{^{1}H}NMR (151 MHz, $CDCl_3$) δ 163.54, 151.12, 151.05, 137.87, 137.14, 137.12, 136.51, 136.48, 134.03, 133.65, 133.05, 132.94, 128.68, 128.63, 128.36, 128.27, 128.20, 127.96, 127.89, 127.76, 127.72, 118.99, 118.61, 118.32, 118.10, 109.00, 108.75, 85.26, 84.91, 84.71, 83.46, 82.11, 80.99, 80.69, 80.58, 72.44, 72.11, 72.08, 71.99, 71.84, 71.44, 70.45, 70.43, 70.22, 70.16, 38.50, 38.12, 13.37, 13.33; HRMS (ESI) calculated for $C_{31}H_{37}N_2O_7$ ([M + H]$^{+}$) *m/z* 549.2601, found 549.2619.

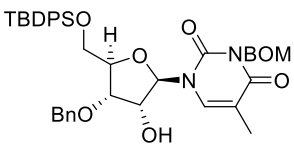

20.2

Compound 20.2: To a stirred 0 °C solution of **18.1** (0.311 g, 0.531 mmol) in DMF (5 mL), BOMCl (0.12 g, 0.69 mmol) and DBU (0.11 g, 0.69 mmol) were added. After 15 min., the reaction mixture was poured into water (20 mL) and further diluted with 1 M HCl (20 mL). The resulting mixture was extracted with dichloromethane (3 × 20 mL) and the combined organic extracts were washed with brine (40 mL), dried over $MgSO_4$, filtered and concentrated under reduced pressure to afford **20.2** as a white solid (0.39 g, 95% yield): R_f = 0.36 (30% EtOAc/Hexanes); ^{1}H NMR (600 MHz, $CDCl_3$) δ 7.74 – 7.66 (m, 4H), 7.56 – 7.35 (m, 15H), 7.34 – 7.29 (m, 2H), 6.12 (d, *J* = 6.0 Hz, 1H), 5.57 (d, *J* = 9.8 Hz, 1H), 5.53 (d, *J* = 9.6 Hz, 1H), 4.76 (s, 2H), 4.71 (d, *J* = 11.7 Hz, 1H), 4.65 (d, *J* = 11.6 Hz, 1H), 4.37 – 4.31 (m, 1H), 4.24 – 4.18 (m, 2H), 4.03 (dd, *J* = 11.7, 2.5 Hz, 1H), 3.73 (dd, *J* = 11.8, 2.5 Hz, 1H), 3.38 (s, 1H), 1.66 (s, 3H), 1.15 (s, 9H); ^{13}C{^{1}H}NMR (151 MHz, $CDCl_3$) δ 163.46, 151.61, 138.07, 136.84, 135.60, 135.33, 134.13, 132.82, 132.30, 130.31, 130.19, 128.77, 128.45, 128.36, 128.18, 128.15, 128.09, 127.79, 127.68, 110.74, 89.39, 82.87, 76.99, 74.09, 72.89, 72.26, 70.71, 63.70, 27.11, 19.46, 12.79; HRMS (ESI) calculated for $C_{41}H_{47}N_2O_7Si$ ([M + H]$^{+}$) *m/z* = 707.3153, found 707.3137.

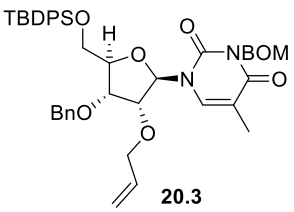

20.3

Compound 20.3: To a stirred 0 °C solution of **20.2** (0.150 g, 0.212 mmol) in 1:1 DMF-THF (2 mL), NaH (60% dispersion in oil) (0.018 g, 0.14 mmol), TBAI (0.039 g, 0.11 mmol) and allylbromide (0.039 g, 0.32 mmol) were added. After 2 h, the mixture was poured into water (15 mL) and further diluted with 1 M HCl (15

mL). The resulting mixture was extracted with CH_2Cl_2 (3 × 15 mL) and the combined organic extracts were washed with brine (30 mL), dried over $MgSO_4$, filtered and concentrated under reduced pressure. The residue was purified by flash chromatography (18 cm × 2.5 cm; 20% EtOAc/Hexanes) to afford **20.3** as a residue (0.11 g, 72% yield): R_f = 0.40 (20% EtOAc/Hexanes); ^{1}H NMR (600 MHz, $CDCl_3$) δ 7.71 – 7.68 (m, 2H), 7.66 – 7.63 (m, 2H), 7.52 (s, 1H), 7.50 – 7.45 (m, 2H), 7.44 – 7.36 (m, 13H), 7.33 – 7.27 (m, 1H), 6.12 (d, *J* = 3.2 Hz, 1H), 6.03 – 5.93 (m, 1H), 5.59 – 5.51 (m, 2H), 5.41 – 5.36 (m, 1H), 5.26 (dd, *J* = 10.5, 1.7 Hz, 1H), 4.78 – 4.71 (m, 3H), 4.59 (d, *J* = 11.6 Hz, 1H), 4.43 – 4.35 (m, 1H), 4.30 (dt, *J* = 6.7, 2.2 Hz, 1H), 4.26 (ddt, *J* = 12.9, 6.2, 1.4 Hz, 1H), 4.22 (dd, *J* = 6.7, 5.0 Hz, 1H), 4.18 (dd, *J* = 12.0, 2.0 Hz, 1H), 4.10 (dd, *J* = 5.0, 3.2 Hz, 1H), 3.93 (dd, *J* = 12.0, 2.4 Hz, 1H), 1.48 (s, 3H), 1.15 (s, 9H); ^{13}C{^{1}H}NMR (151 MHz, $CDCl_3$) δ 163.50, 150.95, 138.03, 137.39, 135.46, 135.24, 134.08, 133.88, 133.15, 132.44, 130.18, 130.08, 128.58, 128.34, 128.11, 128.09, 128.03, 128.00, 127.75, 127.69, 118.28, 110.28, 88.51, 82.48, 79.54, 74.64, 72.45, 72.24, 71.17, 70.53, 62.57, 27.18, 19.59, 12.56; HRMS (ESI) calculated for $C_{44}H_{51}N_2O_7Si$ ([M + H]$^+$) *m/z* = 747.3466, found 747.3453.

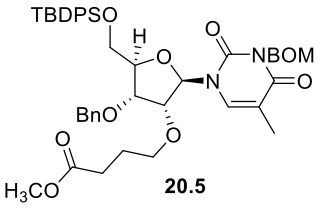

20.5

Compound 20.5: To a stirred 50 °C solution of **20.3** (0.100 g, 0.134 mmol) in methyl acrylate (1.3 mL), Hoveyda-Grubbs second-generation catalyst (0.0021g, 0.0033 mmol) was added. After 4 h, the solvent was evaporated and the residue was dissolved in 1:9 MeOH-CH_2Cl_2 (1.3 mL), and $NaBH_4$ (0.015 g, 0.04 mmol) was added. After 23 h, the reaction mixture was poured into water (10 mL), and the resulting mixture was extracted with dichloromethane (3 × 10 mL). The combined organic extracts were washed a saturated solution of $NaHCO_3$ (10 mL), dried over $MgSO_4$, filtered and concentrated under reduced pressure. The product was purified by flash chromatography (1.3 × 20 cm; 30% EtOAc/Hexanes) to afford **20.5** as colorless residue (0.075 g, 70% yield): R_f = 0.62 (40% EtOAc/Hexanes); ^{1}H NMR (400 MHz, $CDCl_3$) δ 7.71 – 7.65 (m, 2H), 7.66 – 7.60 (m, 2H), 7.50 (d, *J* = 1.4 Hz, 1H), 7.50 – 7.39 (m, 2H), 7.42 – 7.30 (m, 12H), 7.32 – 7.23 (m, 1H), 6.04 (d, *J* = 3.0 Hz, 1H), 5.57 – 5.47 (m, 2H), 4.74 (s, 2H), 4.69 (d, *J* = 11.5 Hz, 1H), 4.55 (d, *J* = 11.5 Hz, 1H), 4.28 – 4.21 (m, 1H), 4.22 – 4.12 (m, 2H), 3.99 (dd, *J* = 4.9, 3.1 Hz, 1H), 3.95 – 3.83 (m, 2H), 3.65 (s, 3H), 3.62 (dd, *J* = 9.1, 5.8 Hz, 1H), 2.52 – 2.44 (m, 2H), 1.98 (p, *J* = 8.0, 7.5 Hz, 2H), 1.48 (d, *J* = 1.1 Hz, 3H), 1.13 (s, 9H); ^{13}C{^{1}H}NMR (101 MHz, $CDCl_3$) δ 173.79, 163.47, 150.91, 138.05, 137.41, 135.45, 135.24, 133.83, 133.13, 132.45, 130.18, 130.08, 128.57, 128.32, 128.09, 128.08, 128.00, 127.91,

127.73, 127.68, 110.29, 88.56, 82.35, 80.86, 74.82, 72.54, 72.24, 70.53, 69.55, 62.50, 51.59, 30.59, 27.16, 25.22, 19.57, 12.61; HRMS (ESI) calculated for $C_{46}H_{55}N_2O_9Si$ ([M + H]$^+$) *m/z* = 807.3677, found 807.3661.

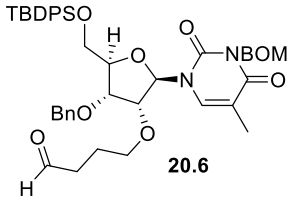

20.6

Compound 20.6: To a stirred -78 °C solution of **20.5** (0.040 g, 0.050 mmol) in Toluene (0.5 mL), a 1 M solution of DIBAL-H 1 M in hexanes (0.05 mL, 0.05 mmol) was added. After 1h, the reaction mixture was poured into 1 M HCl (6 mL) and the resulting mixture was extracted with dichloromethane (3 × 7 mL). The combined organic extracts were washed brine (10 mL), dried over $MgSO_4$, filtered and concentrated under reduced pressure. The product was purified by flash chromatography (0.5 × 20 cm; 40% EtOAc/Hexanes) to afford **20.6** as colorless residue (0.018 g, 46% yield): R_f = 0.48 (40% EtOAc/Hexanes); ^{1}H NMR (400 MHz, $CDCl_3$) δ 9.72 (s, 1H), 7.70 – 7.58 (m, 4H), 7.52 – 7.30 (m, 17H), 6.02 (d, *J* = 3.0 Hz, 1H), 5.56 – 5.46 (m, 2H), 4.73 (s, 2H), 4.65 (d, *J* = 11.5 Hz, 1H), 4.55 (d, *J* = 11.5 Hz, 1H), 4.25 – 4.19 (m, 1H), 4.21 – 4.12 (m, 2H), 3.97 (dd, *J* = 4.9, 3.1 Hz, 1H), 3.90 (dd, *J* = 12.1, 2.5 Hz, 1H), 3.89 – 3.80 (m, 1H), 3.61 (dt, *J* = 9.2, 5.9 Hz, 1H), 2.61 – 2.51 (m, 2H), 2.01 – 1.92 (m, 2H), 1.48 (d, *J* = 1.1 Hz, 3H), 1.12 (s, 9H); ^{13}C{^{1}H}NMR (101 MHz, $CDCl_3$) δ 202.17, 163.46, 150.91, 138.01, 137.36, 135.45, 135.23, 133.76, 133.09, 132.42, 130.18, 130.08, 128.58, 128.32, 128.12, 128.07, 127.99, 127.82, 127.72, 127.69, 110.33, 88.54, 82.32, 80.87, 74.89, 72.56, 72.24, 70.52, 69.63, 62.48, 40.70, 27.15, 22.61, 19.55, 12.61.

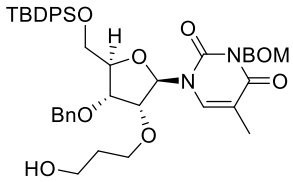

21.1

Compound 21.1: A 0.5 M solution of 9-BBN in THF (25.0 mL, 12.5 mmol) was added to a stirred solution of **20.3** (4.67 g, 6.25 mmol) in THF (63 mL). After 10 min., the reaction mixture was cooled to 0 °C, and a 35% (w/w) solution of hydrogen peroxide in water (0.59 mL, 8.7 mmol) was added followed by a 3 M aqueous solution of NaOH (2.1 mL, 6.3 mmol). After 30 min., the mixture was poured into water (50 mL) and neutralized with 1 M HCl (7 mL). The resulting mixture was extracted with dichloromethane (3 × 50 mL), washed with brine (100 mL), dried over $MgSO_4$, filtered and concentrated under reduced pressure. The residue was purified by flash chromatography (5 × 15 cm; 4% acetone/dichloromethane) to afford **21.1** as a white foam (3.7 g, 77%): R_f = 0.20

(4% acetone/dichloromethane); ^{1}H NMR (600 MHz, $CDCl_3$) δ 7.70 – 7.65 (m, 2H), 7.65 – 7.60 (m, 2H), 7.52 – 7.50 (m, 1H), 7.49 – 7.44 (m, 2H), 7.43 – 7.31 (m, 14H), 6.04 (d, *J* = 2.9 Hz, 1H), 5.59 – 5.44 (m, 2H), 4.74 (s, 2H), 4.71 (d, *J* = 11.5 Hz, 1H), 4.57 (d, *J* = 11.6 Hz, 1H), 4.26 – 4.18 (m, 2H), 4.17 (dd, *J* = 12.0, 1.8 Hz, 1H), 4.09 – 4.03 (m, 1H), 3.98 (dd, *J* = 4.9, 2.9 Hz, 1H), 3.91 (dd, *J* = 12.0, 2.3 Hz, 1H), 3.86 – 3.77 (m, 2H), 3.78 – 3.71 (m, 1H), 2.62 – 2.56 (m, 1H), 1.98 – 1.81 (m, 2H), 1.47 (s, 3H), 1.13 (s, 9H); ^{13}C{^{1}H}NMR (151 MHz, $CDCl_3$) δ 163.39, 150.94, 137.95, 137.14, 135.43, 135.22, 133.66, 133.06, 132.39, 130.19, 130.09, 128.63, 128.34, 128.23, 128.08, 128.03, 128.00, 127.73, 127.71, 110.42, 88.62, 82.30, 81.33, 74.72, 72.79, 72.28, 70.50, 69.91, 62.36, 61.16, 32.11, 27.15, 19.56, 12.57; HRMS (ESI) calculated for $C_{44}H_{53}N_2O_8Si$ ([M + H]$^+$) m/z = 765.3571, found xx.

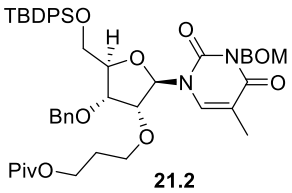

21.2

Compound 21.2: Pivaloyl chloride (0.48 g, 4.0 mmol) was added to a stirred solution of **21.1** (2.55 g, 3.33 mmol) in pyridine (12 mL). After 6 h, the reaction mixture was poured into water (50 mL) and neutralized with 1 M HCl (15 mL). The resulting mixture was extracted with dichloromethane (3 × 50 mL), and the combined organic extracts were sequentially washed with 1 M HCl (50 mL), a saturated solution of $NaHCO_3$ (50 mL) and brine (70 mL), dried over $MgSO_4$, filtered and concentrated under reduced pressure. The residue was purified by flash chromatography (5 × 13 cm; 20% EtOAc/hexanes) To afford **21.2** as a light yellow oil (2.5 g, 88%): R_f = 0.44 (20% EtOAc/hexanes). ^{1}H NMR (600 MHz, CDCl3) δ 7.69 (d, *J* = 6.7 Hz, 2H), 7.64 (d, *J* = 7.3 Hz, 2H), 7.53 (s, 1H), 7.50 – 7.43 (m, 2H), 7.43 – 7.30 (m, 14H), 6.04 (d, *J* = 2.7 Hz, 1H), 5.54 (d, *J* = 9.6 Hz, 1H), 5.51 (d, *J* = 9.6 Hz, 1H), 4.74 (s, 2H), 4.71 (d, *J* = 11.5 Hz, 1H), 4.56 (d, *J* = 11.5 Hz, 1H), 4.31 – 4.14 (m, 5H), 4.01 (dd, *J* = 5.0, 2.8 Hz, 1H), 3.97 (dt, *J* = 9.5, 6.1 Hz, 1H), 3.93 (dd, *J* = 12.0, 2.4 Hz, 1H), 3.70 – 3.63 (m, 1H), 2.00 (p, *J* = 6.2 Hz, 2H), 1.48 (s, 3H), 1.21 (s, 9H), 1.14 (s, 9H); ^{13}C{^{1}H}NMR (151 MHz, $CDCl_3$) δ 178.48, 163.49, 150.88, 138.02, 137.33, 135.45, 135.23, 133.82, 133.13, 132.43, 130.17, 130.07, 128.60, 128.33, 128.14, 128.07, 127.99, 127.95, 127.72, 127.69, 110.26, 88.61, 82.29, 80.92, 74.67, 72.55, 72.25, 70.52, 67.11, 62.37, 61.17, 38.76, 29.27, 27.23, 27.15, 19.57, 12.59; HRMS (ESI) calculated for $C_{49}H_{61}N_2O_9Si$ ([M + H]$^+$) m/z = 849.4146, found.

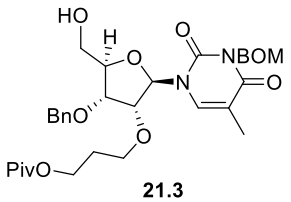

21.3

Compound 21.3: A 1 M solution of TBAF in THF (1.3 mL, 1.31 mmol) was added to a stirred 0 °C solution of **21.2** (0.93 g, 1.09 mmol) in THF (11 mL). After 1 h, the reaction mixture was poured into water (50 mL) and further diluted with 1 M HCl (10 mL). The resulting mixture was extracted with dichloromethane (3 × 20 mL), and the combined organic extracts were sequentially washed with a saturated solution of $NaHCO_3$ (40 mL), and brine (50 mL), dried over $MgSO_4$, filtered and concentrated under reduced pressure. The residue was purified by flash chromatography (2.5 × 11 cm; 40% EtOAc/hexanes) To afford **21.3** as a light yellow oil (0.60 g, 90%): R_f = 0.23 (40% EtOAc/hexanes); ^{1}H NMR (600 MHz, $CDCl_3$) δ 7.56 (d, *J* = 1.5 Hz, 1H), 7.42 – 7.35 (m, 6H), 7.37 – 7.32 (m, 3H), 7.31 – 7.26 (m, 1H), 5.71 (d, *J* = 3.3 Hz, 1H), 5.54 – 5.45 (m, 2H), 4.72 (s, 2H), 4.68 (d, *J* = 11.6 Hz, 1H), 4.59 (d, *J* = 11.6 Hz, 1H), 4.25 (dt, *J* = 6.4, 2.2 Hz, 1H), 4.24 – 4.13 (m, 4H), 4.03 (dd, *J* = 12.2, 2.2 Hz, 1H), 3.84 (dt, *J* = 9.4, 6.2 Hz, 1H), 3.79 – 3.73 (m, 1H), 3.67 – 3.61 (m, 1H), 2.74 (s, 1H), 1.97 (tt, *J* = 6.2, 3.5 Hz, 2H), 1.93 (d, *J* = 1.3 Hz, 3H), 1.19 (s, 9H); ^{13}C{^{1}H}NMR (151 MHz, $CDCl_3$) δ 178.55, 163.46, 150.89, 137.89, 137.42, 136.34, 128.59, 128.35, 128.19, 127.93, 127.74, 127.73, 110.00, 91.81, 82.87, 79.93, 74.99, 72.58, 72.30, 70.46, 67.11, 61.24, 61.13, 38.75, 29.24, 27.21, 13.24; HRMS (ESI) calculated for $C_{33}H_{43}N_2O_9$ ($[M + H]^+$) m/z = 611.2969, found.

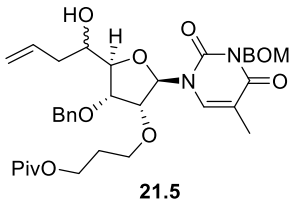

21.5

Compound 21.5: Dess-Martin periodinane (0.929 g, 2.19 mmol) was added to a stirred solution of compound **21.4** (0.669 g, 1.09 mmol) in dichloromethane (15 mL). After 1h, the reaction mixture was directly poured into a 10% solution of $Na_2S_2O_3$ (50 mL) and the resulting mixture was stirred until a clear organic phase was observed. The layers were separated, and the aqueous layer was extracted with CH_2Cl_2 (3 × 20 mL). The combined organic extracts were washed with water (2 × 50), dried over $MgSO_4$, filtered and concentrated under reduce pressure to afford the corresponding aldehyde yy. Compound yy was dissolved in dichloromethane (18 mL) and the resulting solution was cooled to 0 °C. Trimetylallylsilane (0.24 mL, 1.6 mmol) and boron trifluoride diethyl etherate (0.21 mL, 1.6 mmol) were added and the resulting mixture was allowed to warm to room temperature. After 10 min., the reaction mixture was poured into water (75 mL), the layers were separated, and the aqueous layer was extracted with CH_2Cl_2 (3 × 20 mL). The combined organic extracts were dried over $MgSO_4$, filtered and concentrated under

reduce pressure. The residue was purified by flash chromatography (2.5 cm × 12 cm; 40% EtOAc/hexanes) to afford compound **21.5** as clear oil *d.r*. 6:1 (0.34 g, 48%): R_f = 0.43 (40% EtOAc/hexanes); ^{1}H NMR (600 MHz, $CDCl_3$) δ 7.66 (s, 7H), 7.43 – 7.30 (m, 79H), 5.85 (ddt, *J* = 17.3, 10.3, 7.1 Hz, 8H), 5.76 (d, *J* = 2.3 Hz, 6H), 5.70 (d, *J* = 4.5 Hz, 1H), 5.55 – 5.48 (m, 14H), 5.23 – 5.16 (m, 16H), 4.81 (d, *J* = 4.4 Hz, 1H), 4.73 (s, 17H), 4.68 (d, *J* = 11.6 Hz, 7H), 4.63 (d, *J* = 8.3 Hz, 1H), 4.59 (d, *J* = 11.5 Hz, 7H), 4.27 (d, *J* = 4.7 Hz, 1H), 4.25 – 4.12 (m, 37H), 4.09 – 4.00 (m, 2H), 3.88 – 3.78 (m, 12H), 3.66 – 3.58 (m, 7H), 2.50 – 2.37 (m, 14H), 2.37 – 2.23 (m, 2H), 2.01 – 1.91 (m, 37H), 1.92 – 1.86 (m, 1H), 1.32 – 1.24 (m, 2H), 1.19 (d, *J* = 4.7 Hz, 64H); ^{13}C{^{1}H}NMR δ 178.51, 178.48, 163.48, 163.41, 151.02, 150.90, 137.95, 137.44, 137.35, 136.84, 136.33, 134.26, 134.19, 128.57, 128.48, 128.43, 128.34, 128.15, 128.12, 127.98, 127.95, 127.74, 127.70, 118.80, 118.75, 110.19, 109.91, 91.85, 91.32, 85.50, 83.87, 83.73, 79.95, 76.18, 74.44, 72.60, 72.34, 72.29, 72.26, 70.45, 70.27, 69.45, 69.32, 67.21, 67.12, 61.15, 61.08, 38.88, 38.75, 37.45, 29.24, 27.21, 13.30, 13.23; HRMS (ESI) calculated for $C_{36}H_{47}N_2O_9$ ([M + H]$^+$) m/z = 651.3282, found 651.3278.

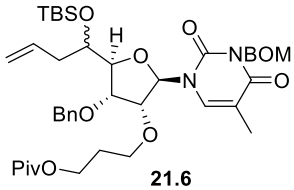

21.6

Compound 21.6: TBS-OTf (0.14 mL, 0.59 mmol) and pyridine (0.05 mL, 0.59 mmol) were added to a stirred 0 °C solution of **21.5** (0.321 g, 0.493 mmol) in dichloromethane (10 mL). After 1 h, the reaction mixture was directly poured into water (40 mL), the layers were separated, and the aqueous portion was extracted with dichloromethane (3 × 20 mL). The combined organic extracts were washed with brine (60 mL), dried over MgSO4, filtered and concentrated under reduced pressure. The residue was purified by flash chromatography (2.5 cm × 18 cm; 20% EtOAc/hexanes) to afford ***diastereomer 21.6a*** as clear oil (0.31 g, 82%): R_f = 0.34 (20% EtOAc/hexanes); ^{1}H NMR (600 MHz, $CDCl_3$) δ 7.67 (d, *J* = 1.5 Hz, 1H), 7.45 – 7.27 (m, 10H), 6.02 (d, *J* = 3.2 Hz, 1H), 5.78 (ddt, *J* = 17.3, 10.2, 7.3 Hz, 1H), 5.55 (d, *J* = 9.7 Hz, 1H), 5.52 (d, *J* = 9.6 Hz, 1H), 5.17 (dd, *J* = 17.1, 1.7 Hz, 1H), 5.12 (dd, *J* = 10.2, 2.0 Hz, 1H), 4.75 (s, 2H), 4.63 (d, *J* = 11.1 Hz, 1H), 4.53 (d, *J* = 11.0 Hz, 1H), 4.25 – 4.14 (m, 3H), 3.99 (dd, *J* = 4.9, 3.2 Hz, 1H), 3.96 (t, *J* = 5.5 Hz, 1H), 3.92 (dt, *J* = 9.3, 6.1 Hz, 1H), 3.85 (ddd, *J* = 9.9, 4.8, 1.8 Hz, 1H), 3.61 (dt, *J* = 9.4, 6.2 Hz, 1H), 2.64 – 2.55 (m, 1H), 2.44 – 2.36 (m, 1H), 2.02 – 1.93 (m, 5H), 1.19 (s, 9H), 0.96 (s, 9H), 0.17 (s, 3H), 0.11 (s, 3H); ^{13}C{^{1}H}NMR (151 MHz, $CDCl_3$) δ 178.40, 163.59, 150.96, 138.08, 137.27, 134.17, 133.21, 128.54, 128.31, 128.11, 128.06, 127.69, 127.65, 118.58, 109.77, 87.91, 82.76, 81.19, 75.70, 72.23, 72.19, 71.50, 70.51, 67.03, 61.14, 38.88,

38.73, 29.25, 27.20, 26.00, 18.24, 13.53, -4.14, -4.71; HRMS (ESI) calculated for $C_{42}H_{61}N_2O_9Si$ ([M+H]+) m/z = 765.4146, found.

Diastereomer 21.6b as a clear oil (0.045 g, 12%): R_f = 0.22 (20% EtOAc/hexanes); ^{1}H NMR (600 MHz, $CDCl_3$) δ 7.43 – 7.30 (m, 10H), 7.05 (d, *J* = 1.6 Hz, 1H), 5.98 (d, *J* = 5.6 Hz, 1H), 5.80 (ddt, *J* = 16.1, 11.5, 7.2 Hz, 1H), 5.54 (d, *J* = 9.6 Hz, 1H), 5.51 (d, *J* = 9.6 Hz, 1H), 5.14 – 5.08 (m, 2H), 4.71 (d, *J* = 15.9 Hz, 3H), 4.61 (d, *J* = 11.5 Hz, 1H), 4.21 – 4.13 (m, 3H), 4.10 (dd, *J* = 4.8, 3.3 Hz, 1H), 4.00 – 3.94 (m, 2H), 3.65 (dt, *J* = 9.1, 6.1 Hz, 1H), 3.55 (dt, *J* = 9.2, 6.3 Hz, 1H), 2.35 (d, *J* = 7.0 Hz, 2H), 1.97 – 1.91 (m, 5H), 1.18 (s, 9H), 0.94 (s, 9H), 0.14 (s, 3H), 0.08 (s, 3H); ^{13}C NMR (151 MHz, $CDCl_3$) δ 178.39, 163.34, 150.94, 137.94, 137.67, 134.94, 133.62, 128.48, 128.33, 127.93, 127.83, 127.75, 127.69, 118.28, 110.54, 88.48, 83.26, 80.20, 74.78, 72.37, 72.21, 71.38, 70.64, 67.23, 61.02, 38.73, 38.35, 29.26, 27.18, 25.99, 18.10, 13.15, -2.92, -4.10.

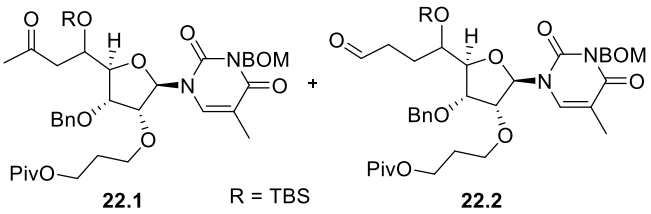

22.1 R = TBS **22.2**

Compounds 22.1 and 22.2: $PdCl_2$ (0.0039 g, 0.022 mmol) and $Cu(OAc)_2$ (0.0081 g, 0.044 mmol) were added to a stirred 40 °C solution of **21.6a** (0.170 g, 0.222 mmol) in 7:1 DMA-H_2O (4 mL), the resulting mixture was stirred for 3 h under an oxygen atmosphere. The reaction mixture was allowed to cool to room temperature and filtered through a pad of Celite, rinsing with ether. The filtrate was concentrated under reduce pressure and the residue obtained was re-dissolved in dichloromethane (25 mL). The organic solution was washed with water (25 mL). The layers were separated, and the aqueous phase was extracted with dichloromethane (3 × 15 mL), the combined organic extracts were sequentially washed with 1 M HCl (20 mL), and brine (20 mL), dried over MgSO4, filtered and concentrated under reduced pressure. The residue was purified by flash chromatography (1.5 cm × 17 cm; 20% EtOAc/hexanes) to afford **22.1** and **22.2** (mixture of ketone and aldehyde 1.8:1 by NMR) as clear oil (0.16 g, 92%): R_f = 0.21 (20% EtOAc/hexanes); ^{1}H NMR (600 MHz, $CDCl_3$δ 9.80 (d, *J* = 1.4 Hz, 1H), 7.59 (s, 1H), 7.53 (s, 2H), 7.43 – 7.31 (m, 29H), 7.31 – 7.24 (m, 4H), 6.04 (d, *J* = 3.8 Hz, 2H), 5.95 (d, *J* = 2.7 Hz, 1H), 5.57 – 5.48 (m, 6H), 4.74 (s, 4H), 4.62 (dd, *J* = 11.1, 4.4 Hz, 3H), 4.57 (d, *J* = 11.3 Hz, 2H), 4.50 (d, *J* = 10.9 Hz, 1H), 4.38 (ddd, *J* = 8.6, 4.5, 2.4 Hz, 2H), 4.24 (dd, *J* = 5.4, 2.5 Hz, 2H), 4.24 – 4.11 (m, 5H),

3.99 (dd, *J* = 5.0, 2.7 Hz, 1H), 3.98 – 3.89 (m, 6H), 3.80 (dt, *J* = 9.2, 6.1 Hz, 2H), 3.61 (dt, *J* = 9.4, 6.1 Hz, 1H), 3.56 (dt, *J* = 9.2, 6.2 Hz, 2H), 3.08 (dd, *J* = 17.5, 8.5 Hz, 2H), 2.66 (dd, *J* = 17.5, 4.5 Hz, 2H), 2.64 – 2.53 (m, 2H), 2.18 (s, 5H), 2.01 – 1.91 (m, 13H), 1.25 – 1.13 (m, 26H), 1.00 – 0.88 (m, 26H), 0.17 (s, 3H), 0.14 – 0.09 (m, 9H), 0.07 (s, 6H); $^{13}C\{^{1}H\}$NMR ^{13}C NMR (151 MHz, $CDCl_3$) δ 206.11, 201.31, 178.43, 178.37, 163.49, 163.48, 150.96, 150.88, 138.03, 137.16, 137.09, 133.90, 133.86, 128.59, 128.54, 128.31, 128.21, 128.12, 128.08, 128.00, 127.70, 127.68, 127.66, 110.08, 109.88, 88.27, 87.59, 83.61, 83.04, 81.15, 80.80, 75.66, 75.42, 72.33, 72.26, 72.21, 71.87, 70.55, 70.51, 69.92, 67.85, 67.04, 67.01, 61.09, 47.42, 39.43, 38.74, 38.71, 30.96, 29.27, 29.22, 27.21, 27.18, 27.08, 26.48, 25.99, 25.97, 18.22, 18.14, 13.55, 13.46, -4.26, -4.62, -4.71, -4.74; HRMS (ESI) calculated for $C_{42}H_{60}N_2O_{10}Si$ ($[M + H]^+$) m/z = 780.4017, found.

Compounds 22.1 and 22.2 (Fernandes Wacker oxidation): $Pd(OAc)_2$ (0.0001 g, 0.0003 mmol) and Dess-Martin periodinane (0.0033 g, 0.0078 mmol) were added to a stirred 50 °C solution of **19.6a** (0.005 g, 0.007 mmol) in 7:1 CH_3CN-H_2O (0.5 mL). After 2 days, water was added (1 mL) and the resulting mixture was extracted with dichloromethane (3 × 2 mL). The combined organic extracts were dried over $MgSO_4$, filtered and concentrated under reduced pressure. The residue was purified by flash chromatography (0.5 cm × 6 cm; 1% acetone/dichloromethane) to afford compound **22.1** and **22.2** (mixture of ketone and aldehyde 7:1) as clear residue (0.0039 g, 69%): R_f = 0.48 (1% acetone/dichloromethane); ^{1}H NMR (600 MHz, $CDCl_3$) δ 9.81 (s, 1H), 7.54 (d, *J* = 1.4 Hz, 7H), 7.43 – 7.32 (m, 77H), 6.04 (d, *J* = 3.7 Hz, 7H), 5.97 (d, *J* = 4.7 Hz, 1H), 5.59 – 5.43 (m, 17H), 4.74 (s, 17H), 4.64 – 4.54 (m, 15H), 4.41 – 4.36 (m, 7H), 4.24 (dd, *J* = 5.5, 2.4 Hz, 7H), 4.23 – 4.09 (m, 16H), 3.94 (d, *J* = 4.6 Hz, 6H), 3.95 – 3.88 (m, 9H), 3.81 (dt, *J* = 9.2, 6.2 Hz, 7H), 3.56 (dt, *J* = 9.2, 6.2 Hz, 7H), 3.08 (dd, *J* = 17.5, 8.4 Hz, 6H), 2.67 (d, *J* = 4.5 Hz, 4H), 2.65 (d, *J* = 4.4 Hz, 3H), 2.20 (s, 7H), 2.18 (s, 21H), 2.00 – 1.91 (m, 51H), 1.17 (s, 57H), 0.92 (s, 55H), 0.12 (s, 21H), 0.07 (s, 21H); $^{13}C\{^{1}H\}$NMR; HRMS (ESI) calculated for $C_{42}H_{60}N_2O_{10}Si$ ($[M + H]^+$) m/z = 780.4017, found.

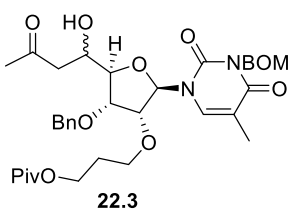

22.3

Compound 22.3 (Wacker on free homoallylic alcohol): $PdCl_2$ (0.0023 g, 0.013 mmol) and $Cu(OAc)_2$ (0.0047 g, 0.026 mmol) were added to a stirred 40 °C solution of **21.5** (0.100 g, 0.131 mmol) in 7:1 DMA-H_2O (2 mL). The resulting mixture was stirred for 3 h under an oxygen atmosphere. The reaction mixture was

allowed to cool to room temperature and filtered through a pad of Celite, rinsing with ether. The filtrated was washed with water (20 mL), the layers were separated, and the aqueous portion was extracted with ether (3 × 15 mL). The combined organic extracts were dried over MgSO4, filtered and concentrated under reduced pressure. The residue was purified by flash chromatography (1.5 cm × 15 cm; 50% EtOAc/hexanes) to afford compound **22.3** (only ketone observed, *d.r.* 6:1 from Sakurai) as clear residue (0.069 g, 67%): R_f = 0.29 (50% EtOAc/hexanes); ^{1}H NMR (600 MHz, $CDCl_3$) δ δ 7.87 (s, 6H), 7.42 – 7.31 (m, 93H), 7.31 – 7.25 (m, 14H), 5.87 (d, *J* = 2.3 Hz, 6H), 5.82 (d, *J* = 2.6 Hz, 1H), 5.55 – 5.47 (m, 16H), 4.72 (s, 17H), 4.68 – 4.60 (m, 8H), 4.62 – 4.53 (m, 8H), 4.32 – 4.26 (m, 7H), 4.25 – 4.13 (m, 26H), 4.10 – 4.03 (m, 9H), 3.98 (dd, *J* = 4.8, 2.3 Hz, 6H), 3.93 (dt, *J* = 9.5, 6.2 Hz, 6H), 3.67 (d, *J* = 3.9 Hz, 6H), 3.67 – 3.57 (m, 6H), 3.00 – 2.92 (m, 7H), 2.76 – 2.68 (m, 7H), 2.27 – 2.22 (m, 28H), 2.01 – 1.89 (m, 48H), 1.20 (s, 64H); ^{13}C{^{1}H}NMR (151 MHz, $CDCl_3$) δ 209.90, 209.36, 178.61, 178.52, 163.51, 163.41, 150.87, 150.85, 138.01, 137.98, 137.34, 137.27, 135.29, 135.15, 128.59, 128.56, 128.54, 128.32, 128.15, 128.09, 127.91, 127.88, 127.71, 127.69, 127.68, 127.66, 109.82, 109.75, 99.04, 89.90, 89.60, 88.90, 88.67, 83.82, 82.28, 81.27, 80.77, 80.50, 80.47, 75.22, 72.67, 72.64, 72.25, 72.23, 70.45, 70.41, 66.99, 66.90, 66.72, 65.78, 61.21, 61.16, 46.71, 45.05, 38.75, 34.50, 33.28, 30.72, 30.70, 29.24, 29.21, 27.21, 27.18, 25.45, 24.63, 13.33, 13.28; HRMS (ESI) calculated for $C_{36}H_{47}N_2O_{10}$ ([M + H]$^+$) m/z = 667.3231, found 667.3152 (error -11.8 ppm).

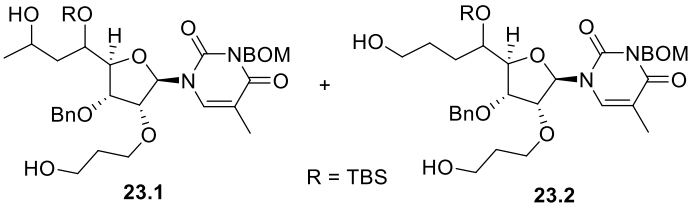

Compounds 23.1 and 23.2: A 1 M solution of DIBAL-H in dichloromethane (1.1 mL, 1.1 mmol) was added dropwise to a stirred -78 °C solution of **22.1** and **22.2** (0.274 g, 0.351 mmol) in dichloromethane (12 mL). After 5 min., the reaction was allowed to warm to room temperature and water was added (20 mL) and further diluted with 1 M HCl (20 mL). The layers were separated, and the aqueous portion was extracted with dichloromethane (3 x 25 mL). The combined organic extracts were washed with brine (60 mL), dried over $MgSO_4$, filtered and concentrated under reduced pressure. The residue was purified by flash chromatography (2.5 cm × 18 cm; 60% EtOAc/hexanes) to afford secondary alcohol **23.1** (0.099 g, 40%) as clear residue: R_f = 0.28 (60% EtOAc/hexanes); ^{1}H NMR (600 MHz, $CDCl_3$) δ 7.55 (s, 1H), 7.44 – 7.32 (m, 10H), 6.02 (d, *J* = 3.3 Hz, 1H), 5.56 – 5.49 (m, 2H), 4.75 (s, 2H), 4.67 (d, *J* = 11.2 Hz, 1H), 4.54 (d, *J* = 11.1 Hz, 1H), 4.27 (dd, *J* = 6.2, 2.5

Hz, 1H), 4.07 – 3.91 (m, 5H), 3.79 (th, *J* = 10.8, 5.0 Hz, 2H), 3.72 – 3.65 (m, 1H), 2.43 (q, *J* = 5.1 Hz, 1H), 2.03 – 1.92 (m, 6H), 1.92 – 1.80 (m, 1H), 1.76 – 1.68 (m, 1H), 1.21 (d, *J* = 6.1 Hz, 3H), 0.95 (s, 9H), 0.16 (s, 3H), 0.09 (s, 3H); (ESI) calculated for $C_{37}H_{55}N_2O_9Si$ ([M + H]$^+$) m/z = 699.3677, found.

Compound 23.2: (0.054 g, 54%) as clear residue: and R_f = 0.18 (60% EtOAc/hexanes); ^{1}H NMR (600 MHz, $CDCl_3$) δ 7.64 (s, 1H), 7.44 – 7.33 (m, 10H), 6.02 (d, *J* = 2.9 Hz, 1H), 5.53 (d, *J* = 3.3 Hz, 2H), 4.75 (s, 2H), 4.67 (d, *J* = 11.1 Hz, 1H), 4.63 – 4.56 (m, 1H), 4.55 (d, *J* = 11.0 Hz, 1H), 4.23 (d, *J* = 5.3 Hz, 1H), 4.02 – 3.95 (m, 3H), 3.83 – 3.74 (m, 2H), 3.73 – 3.64 (m, 3H), 2.46 (s, 1H), 2.20 (s, 1H), 1.95 (s, 4H), 1.93 – 1.80 (m, 3H), 1.76 – 1.62 (m, 2H), 0.95 (s, 9H), 0.15 (s, 3H), 0.09 (s, 3H); HRMS (ESI) calculated for $C_{37}H_{55}N_2O_9Si$ ([M + H]$^+$) m/z = 699.3677, found.

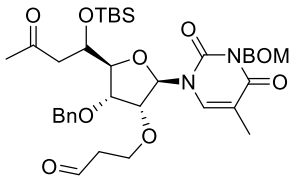

23.3

Compound 23.3: (0.091 g, 0.21 mmol) was added to a stirred solution of **23.1** (0.050 g, 0.072 mmol) in dichloromethane (3 mL). After 24 h a 10% solution of $Na_2S_2O_3$ (9 mL) was added, and the resulting mixture was stirred until a clear organic phase was observed. The layers were separated, and the aqueous layer was extracted with CH_2Cl_2 (3 × 10 mL). The combined organic extracts were washed with water (20 mL), and brine (20 mL), dried over $MgSO_4$, filtered and concentrated under reduce pressure. The residue was purified by flash chromatography (0.5 cm × 16 cm; 40% EtOAc/hexanes) to afford ketoaldehyde **23.3** (0.029 g, 59%) as clear residue: R_f = 0.33 (40% EtOAc/hexanes); ^{1}H NMR (600 MHz, $CDCl_3$) δ 9.78 (s, 1H), 7.54 (s, 1H), 7.43 – 7.32 (m, 10H), 6.03 (d, *J* = 3.5 Hz, 1H), 5.57 – 5.49 (m, 2H), 4.74 (s, 2H), 4.56 (q, *J* = 11.2 Hz, 2H), 4.42 – 4.35 (m, 1H), 4.21 (dd, *J* = 5.9, 2.5 Hz, 1H), 4.07 (dt, *J* = 10.7, 5.8 Hz, 1H), 4.00 (t, *J* = 4.3 Hz, 1H), 3.91 (t, *J* = 5.6 Hz, 1H), 3.88 – 3.81 (m, 1H), 3.07 (dd, *J* = 17.5, 8.4 Hz, 1H), 2.72 (dt, *J* = 12.5, 5.8 Hz, 2H), 2.67 (dd, *J* = 17.7, 4.4 Hz, 1H), 2.17 (s, 3H), 1.97 (s, 3H), 0.93 (s, 9H), 0.13 (s, 3H), 0.08 (s, 3H); HRMS (ESI) calculated for $C_{37}H_{51}N_2O_9Si$ ([M + H]$^+$) m/z = 695.3364, found.

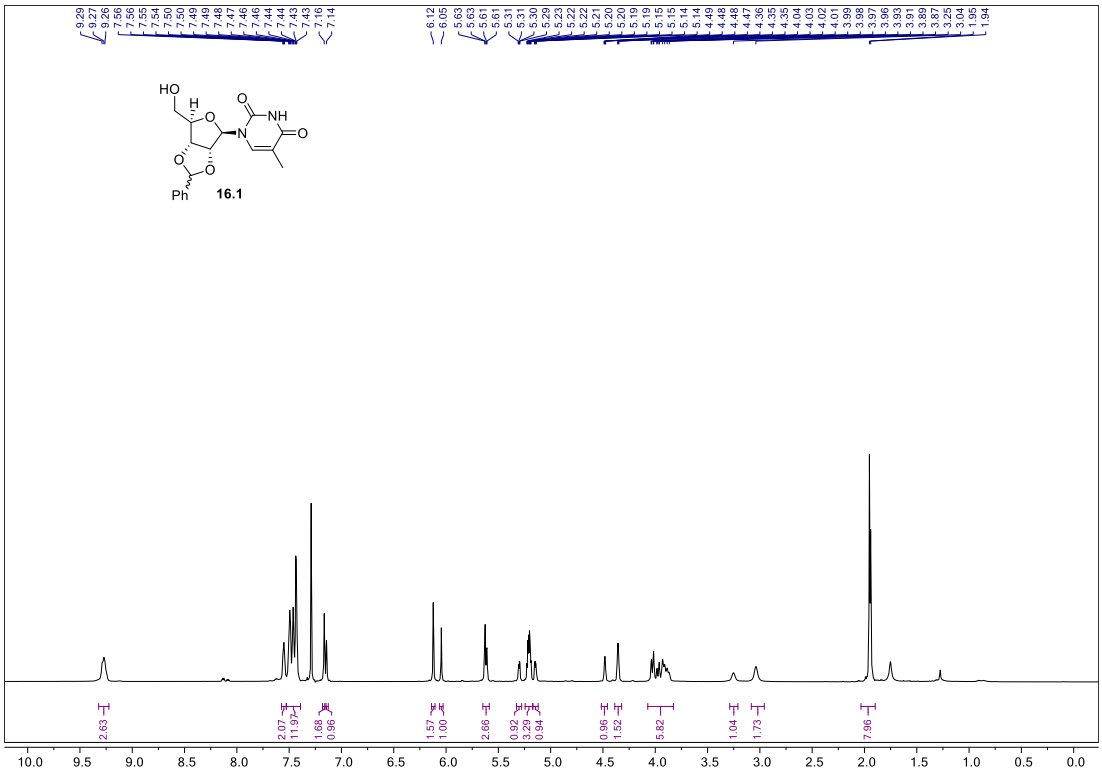
HO
O
NH
N
O
O
O
Ph
16.1

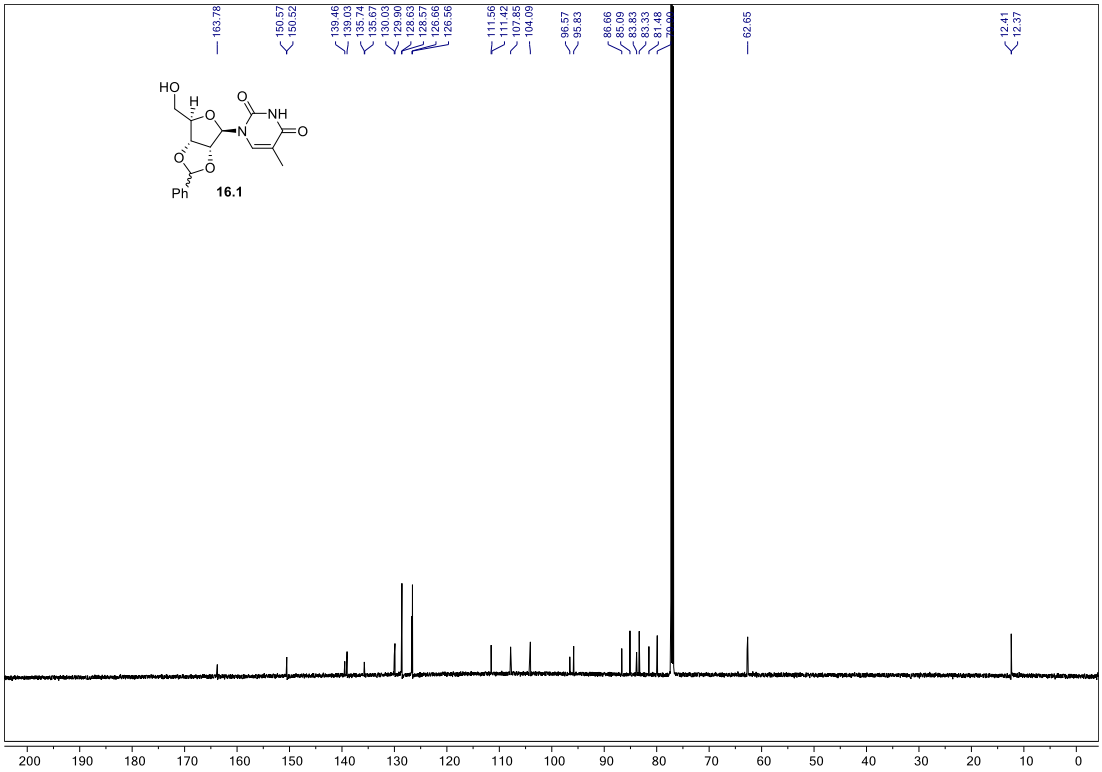
HO
O
NH
N
O
O
O
Ph
16.1

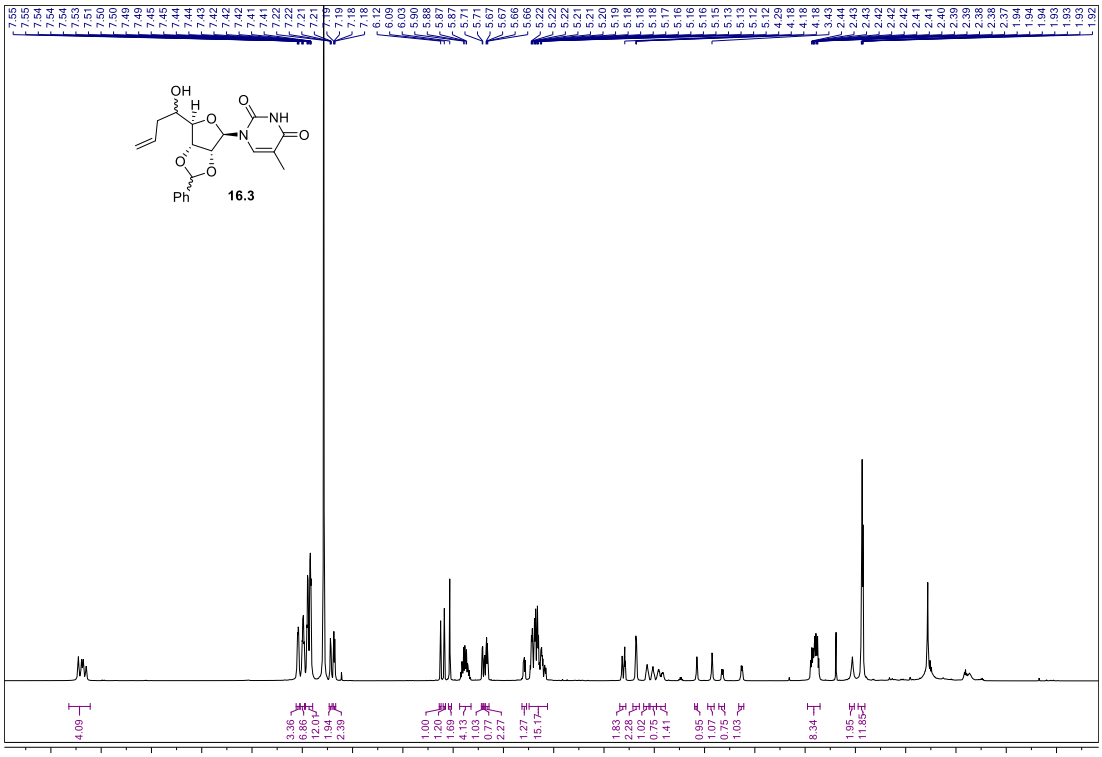
16.3

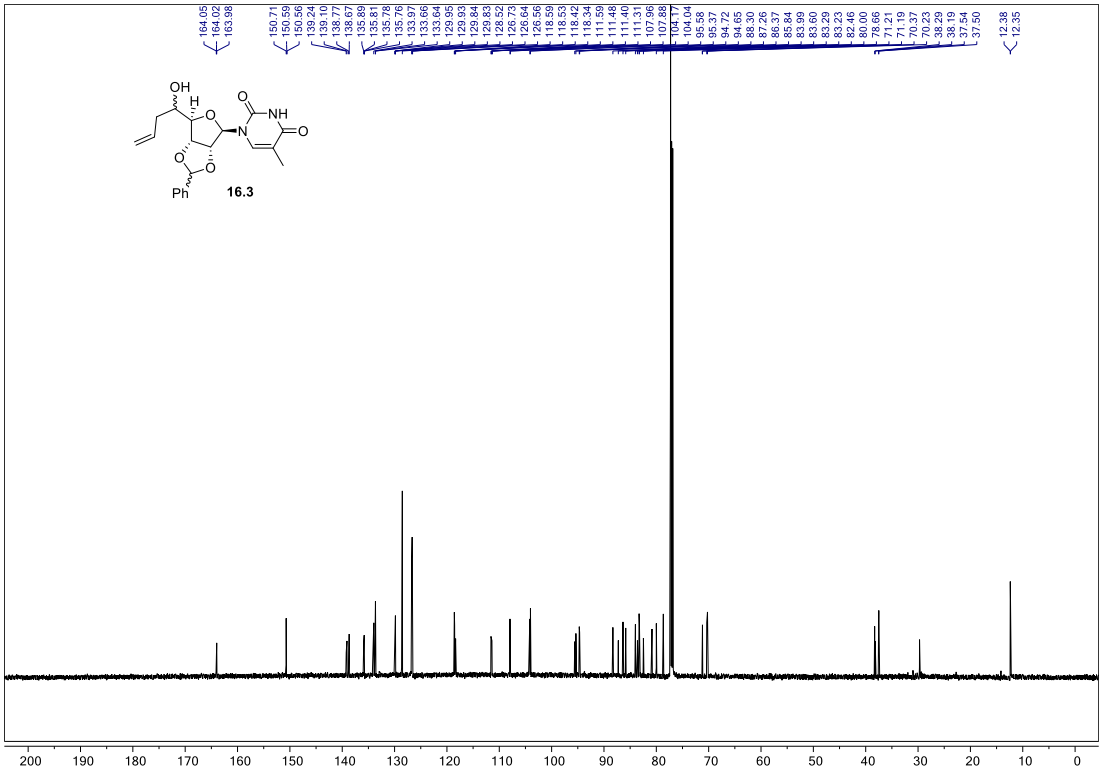
16.3

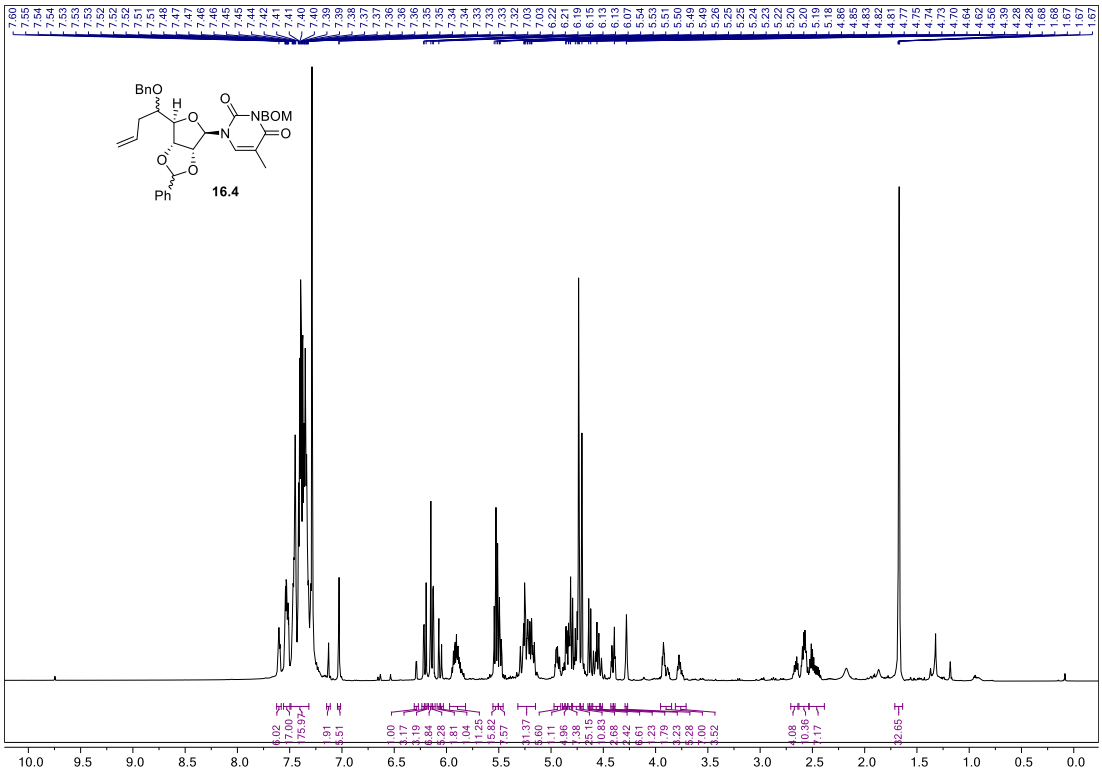
BnO
H
O
NBOM
O
O
O
Ph
16.4

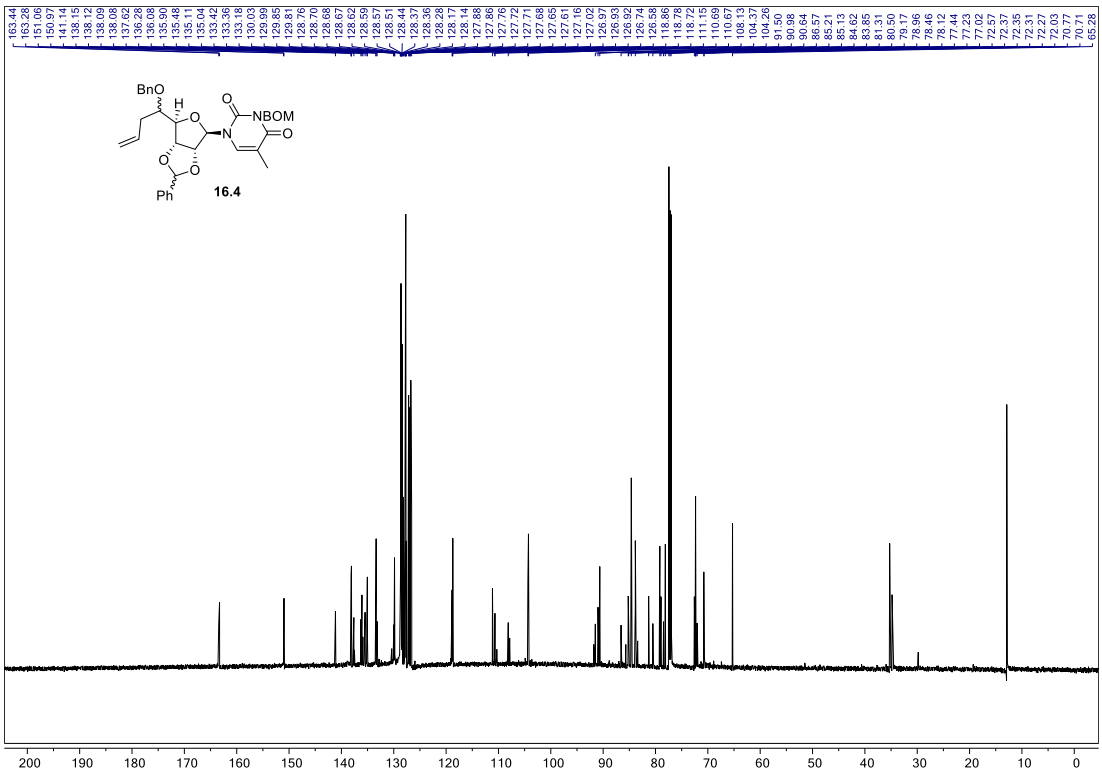
BnO
H
O
NBOM
O
O
O
Ph
16.4

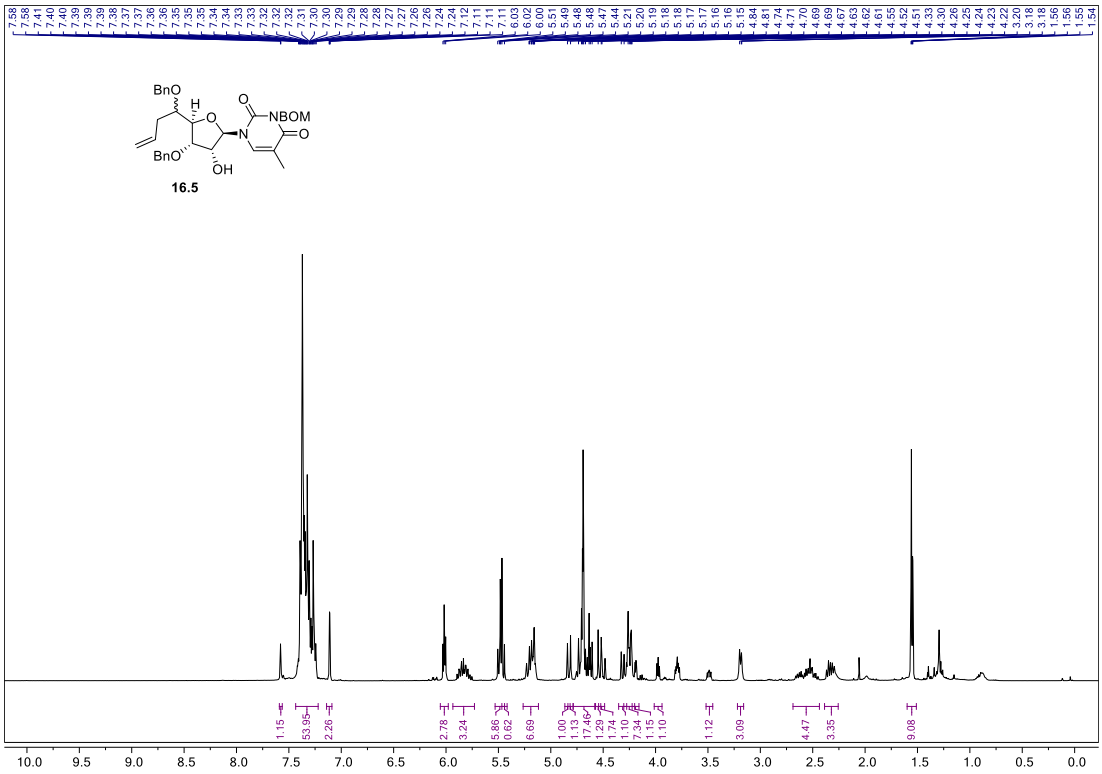
BnO
H
O
NBOM
N
O
BnO
OH
16.5

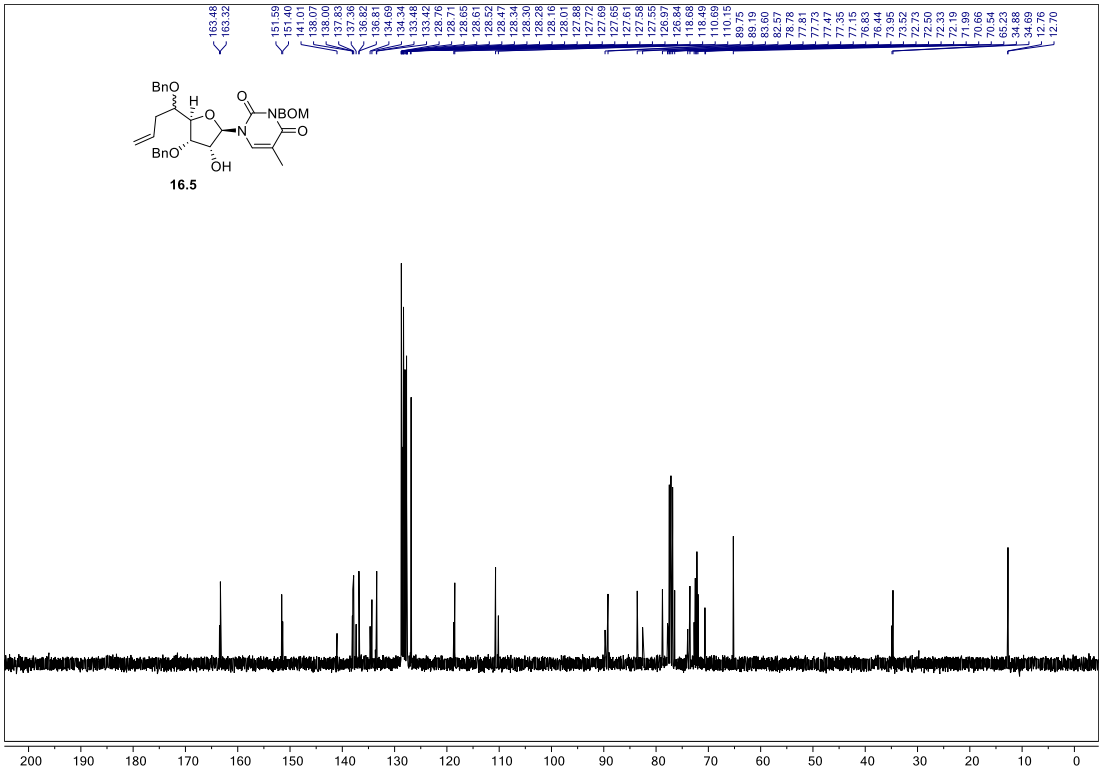
BnO
H
O
NBOM
N
O
BnO
OH
16.5

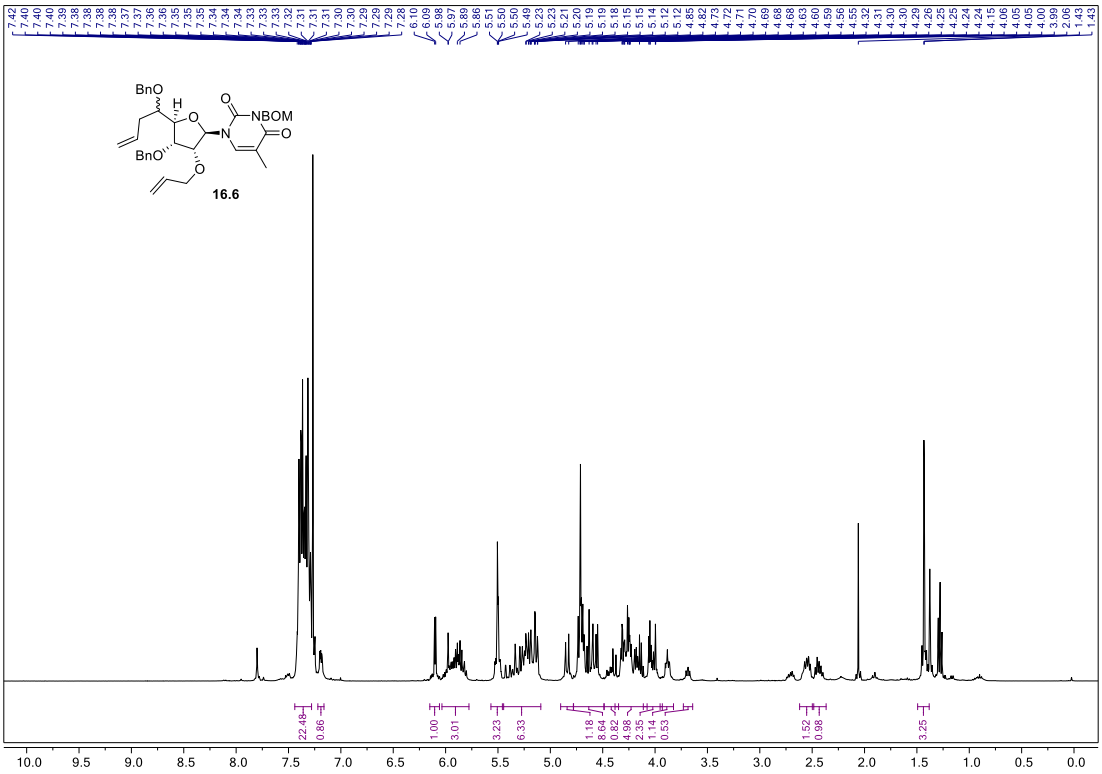
BnO
H
O
O
NBOM
N
O
BnO
O
16.6
22.48
0.86
1.00
3.01
3.23
6.33
1.18
8.64
0.82
4.98
2.35
2.14
0.53
1.52
0.98
3.25
10.0
9.5
9.0
8.5
8.0
7.5
7.0
6.5
6.0
5.5
5.0
4.5
4.0
3.5
3.0
2.5
2.0
1.5
1.0
0.5
0.0

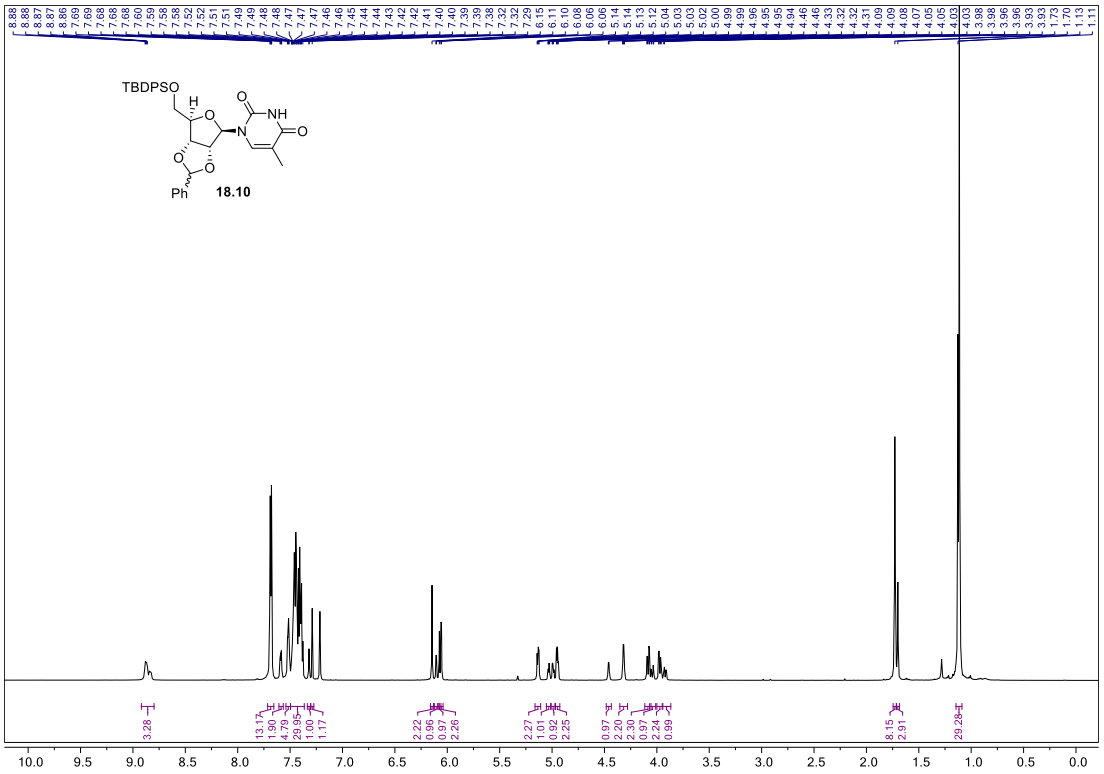
TBDPSO
NH
O
Ph
18.10

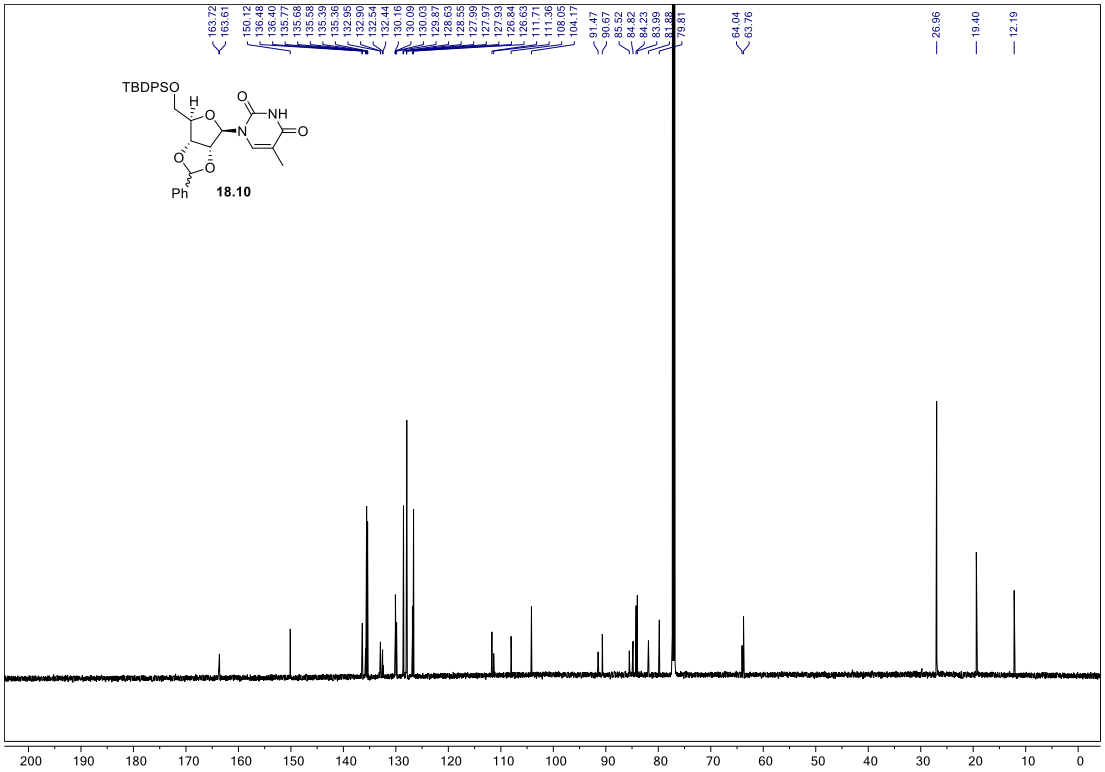
TBDPSO
NH
O
Ph
18.10

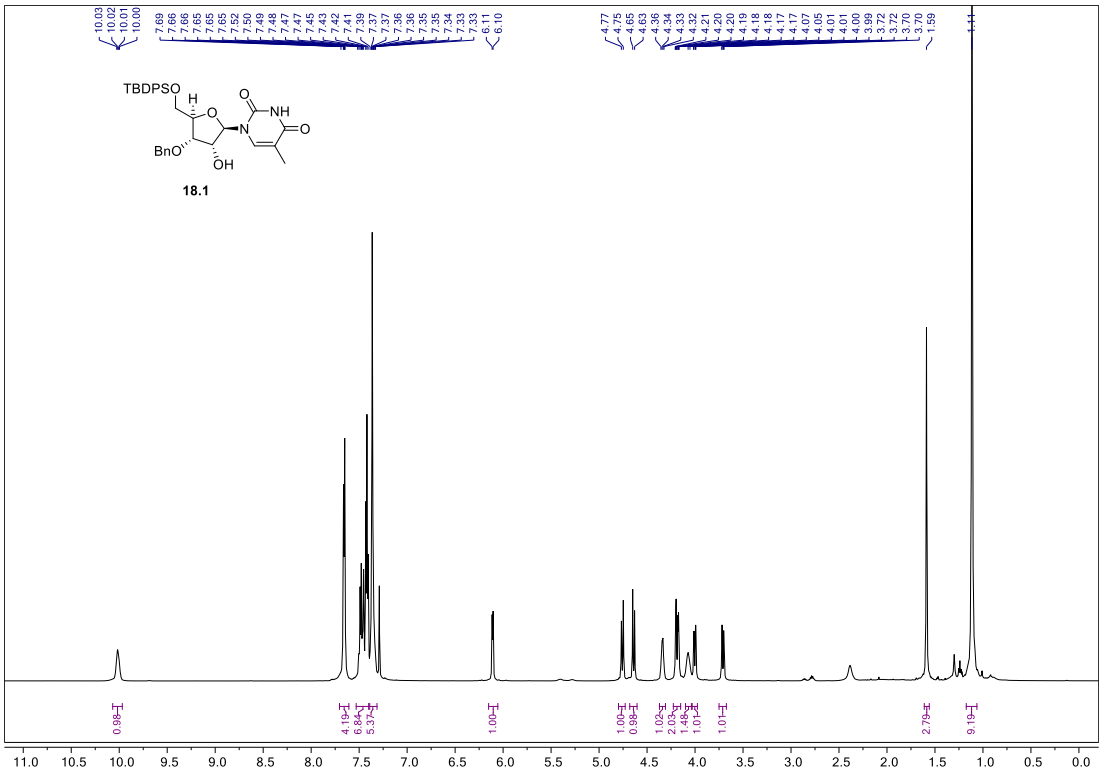
TBDPSO
BnO
OH
NH
O
18.1

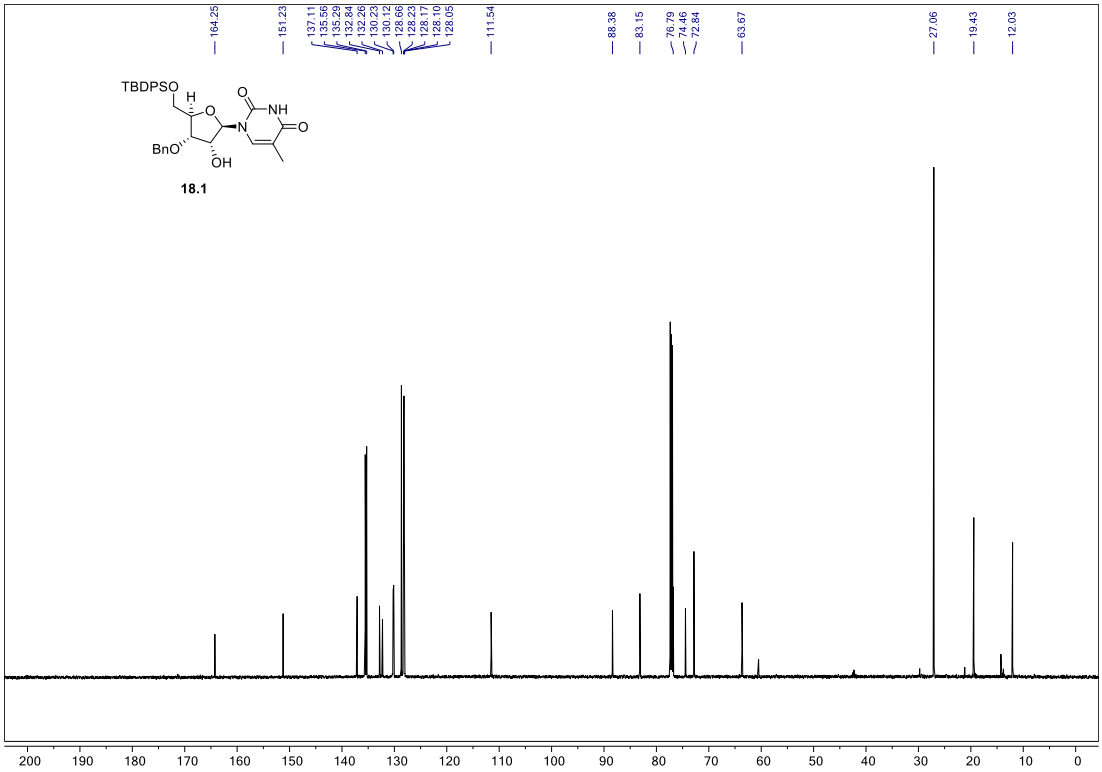
TBDPSO
BnO
OH
NH
O
18.1

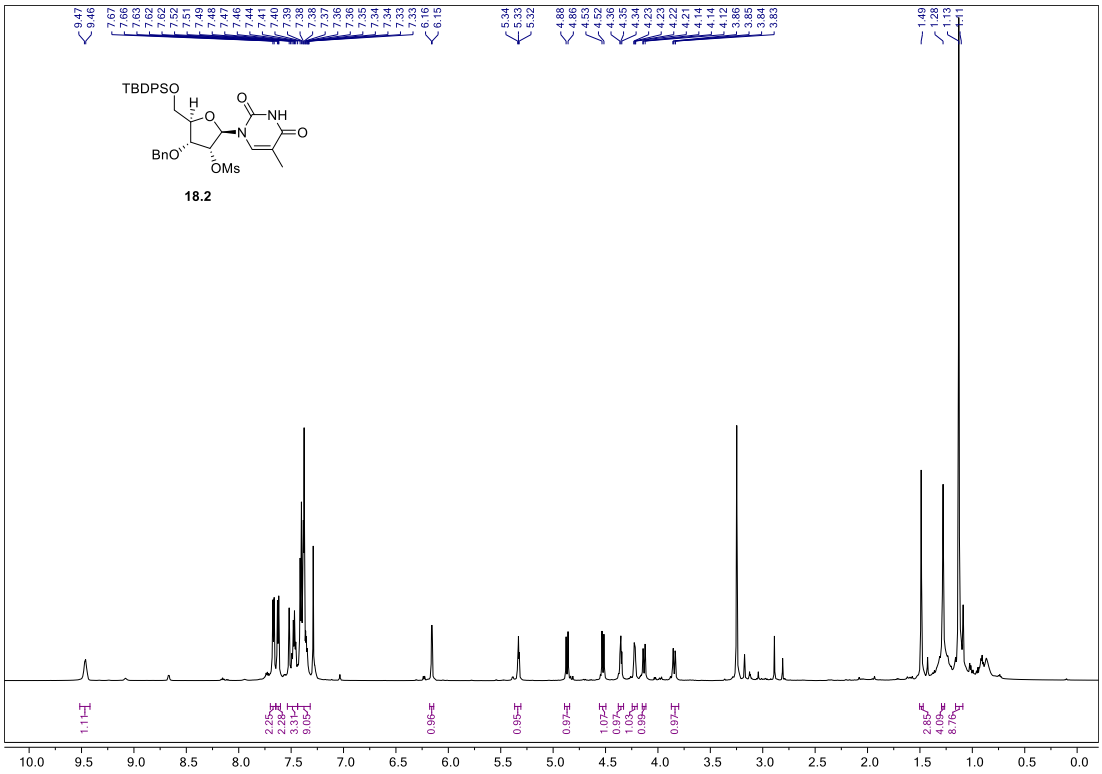
TBDPSO
BnO
OMs
NH
O
18.2

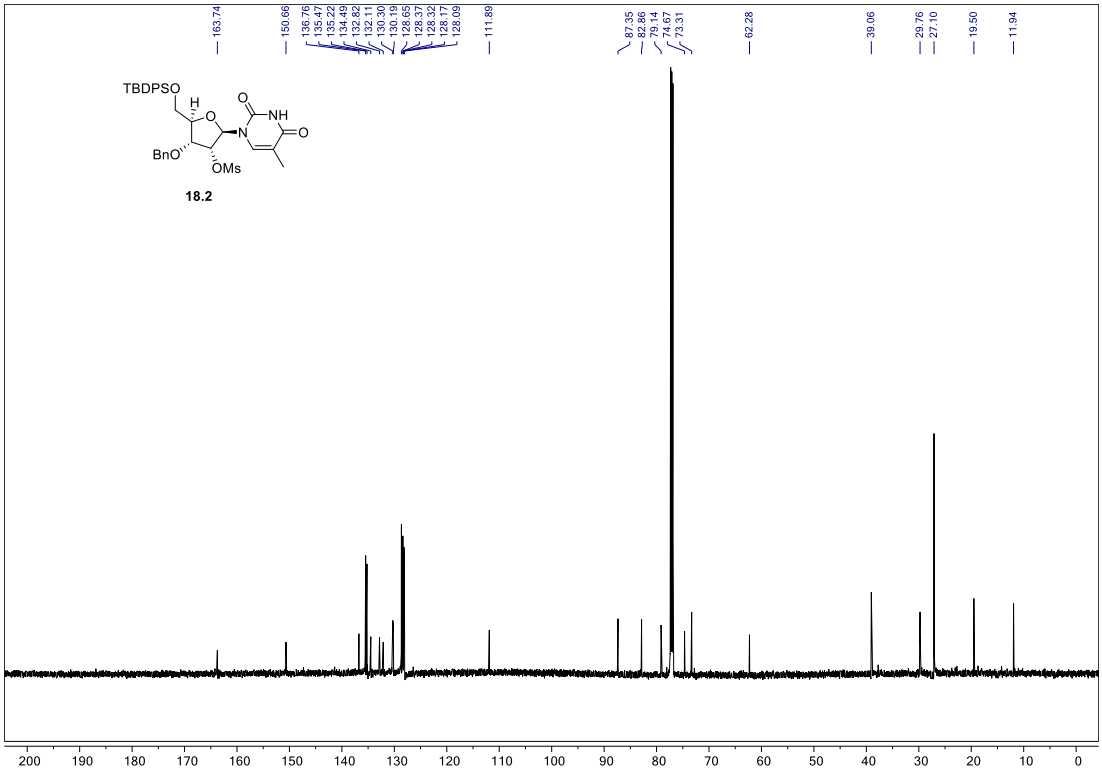
TBDPSO
BnO
OMs
NH
O
18.2

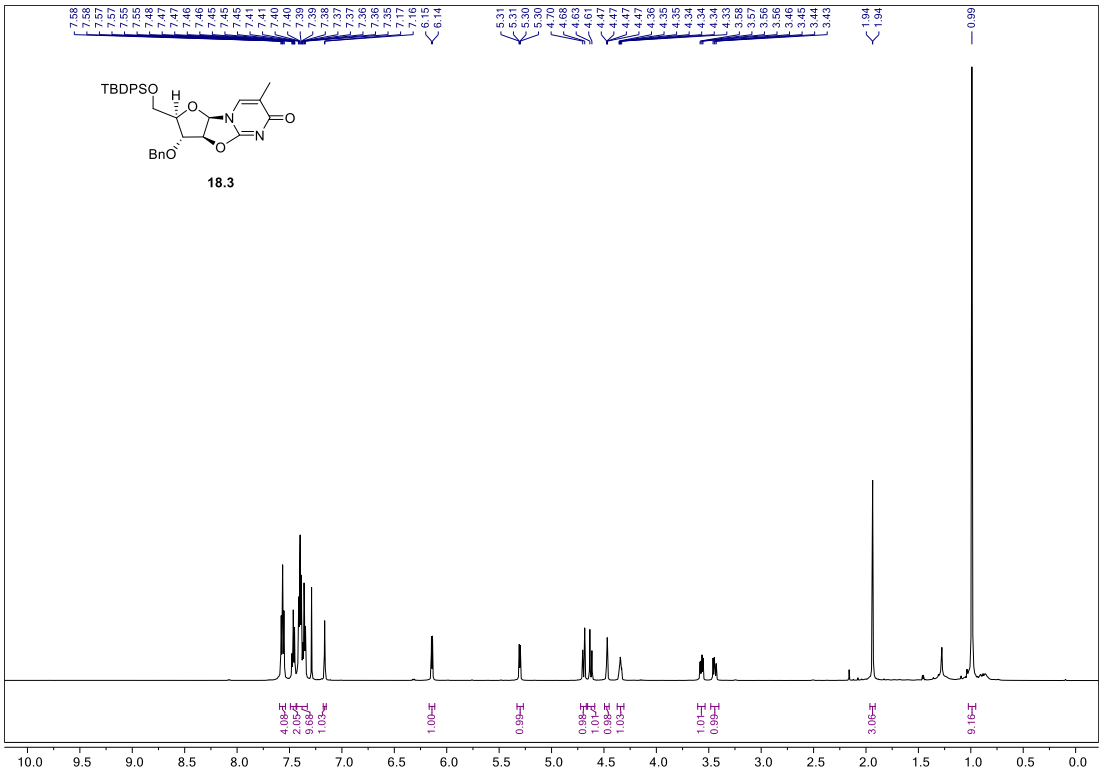
TBDPSO
BnO
18.3

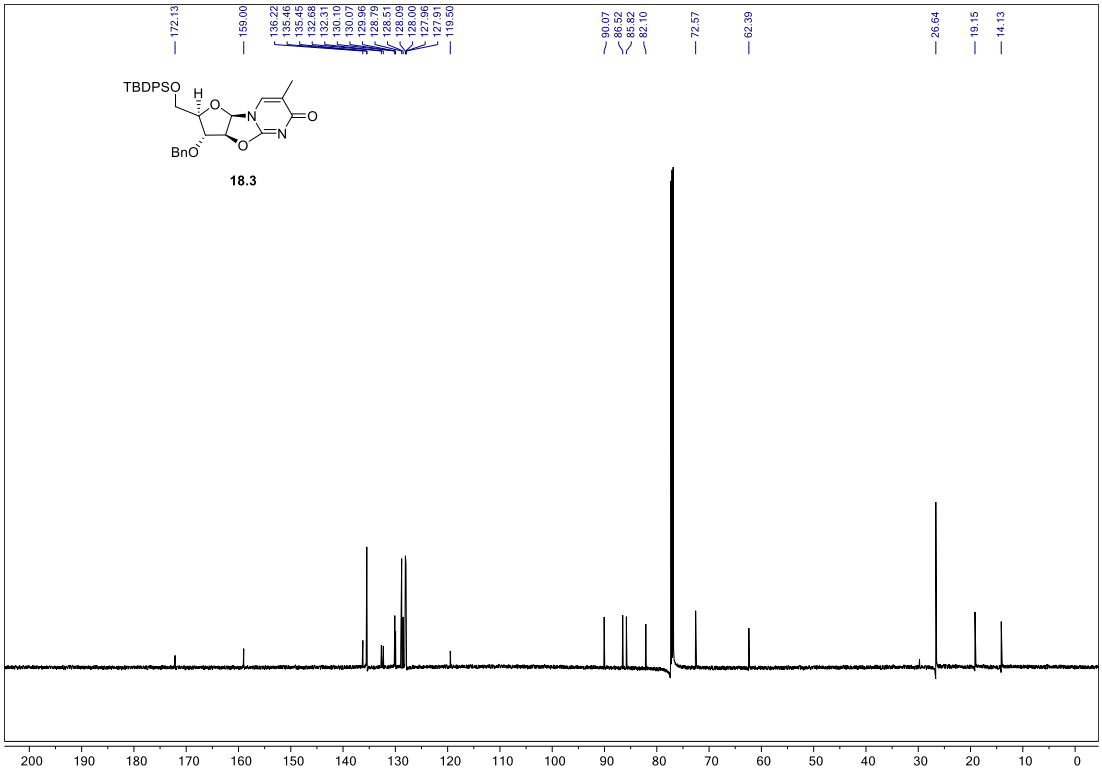
TBDPSO
BnO
18.3

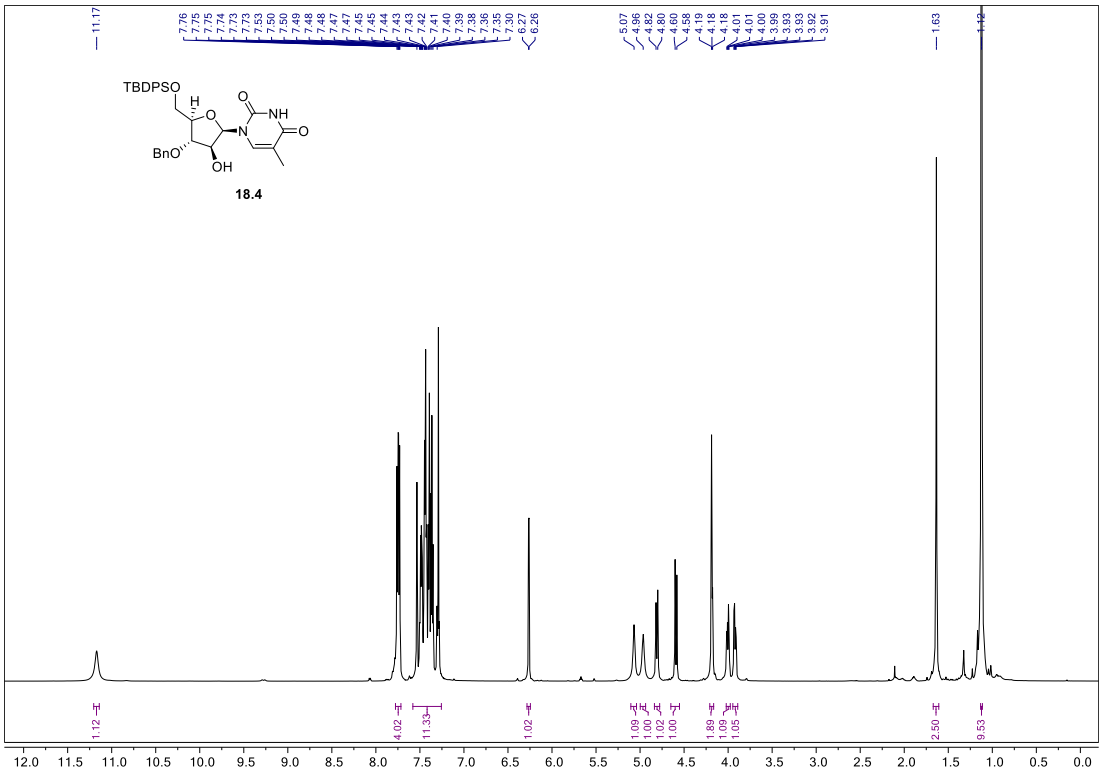
TBDPSO
BnO
OH
NH
18.4

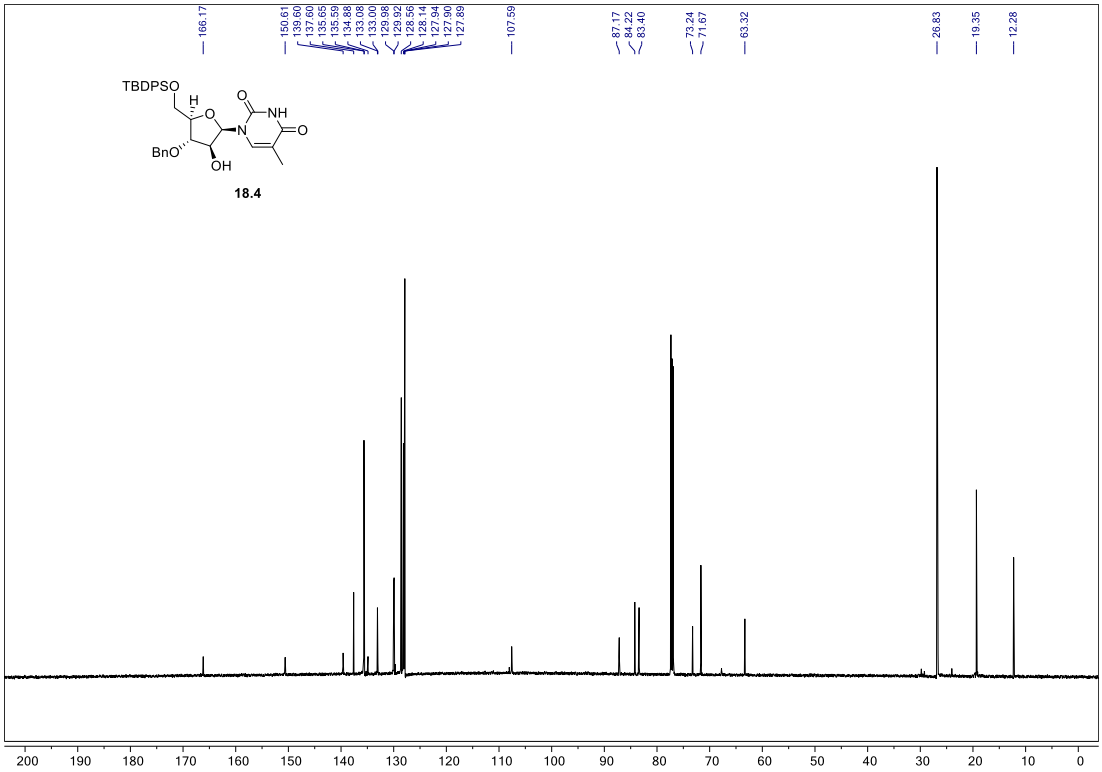
TBDPSO
BnO
OH
NH
18.4

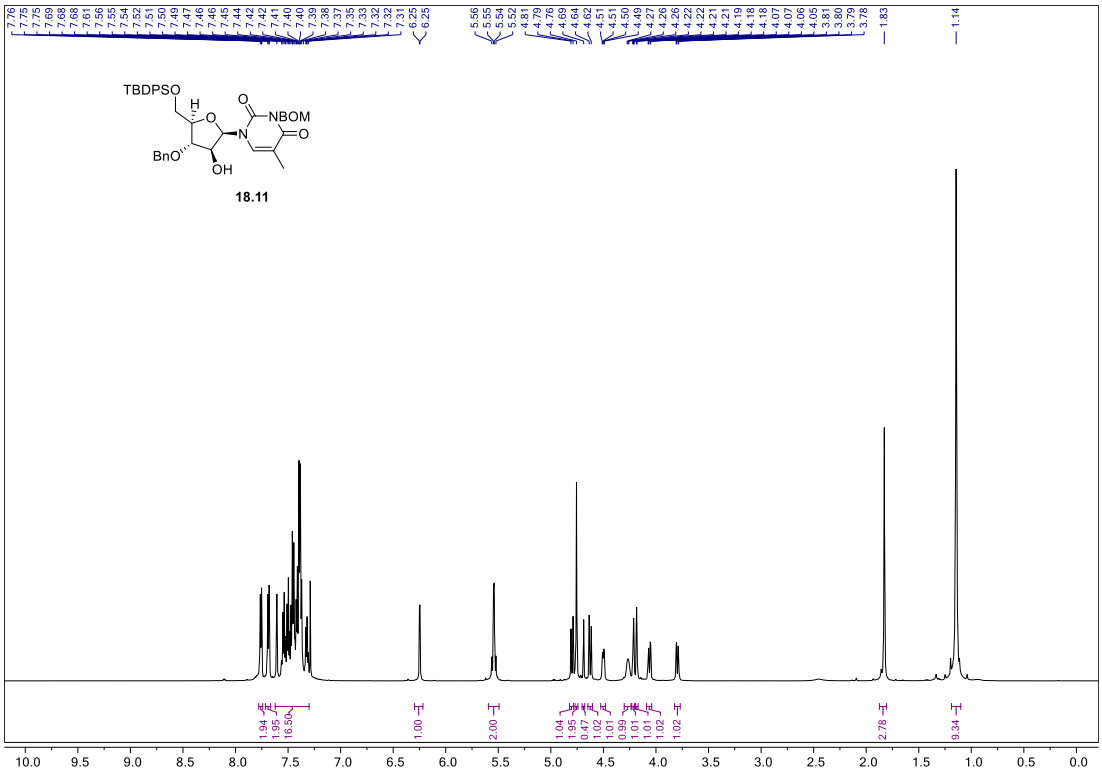
TBDPSO
NBOM
BnO
OH
18.11

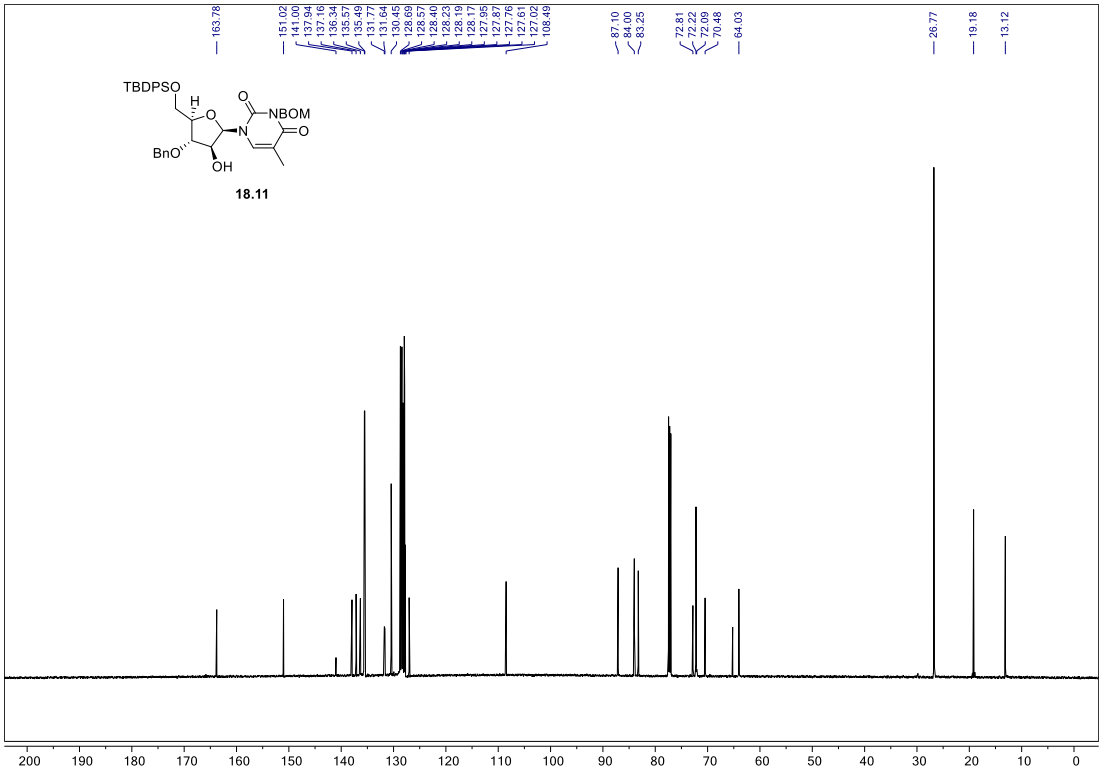
TBDPSO
NBOM
BnO
OH
18.11

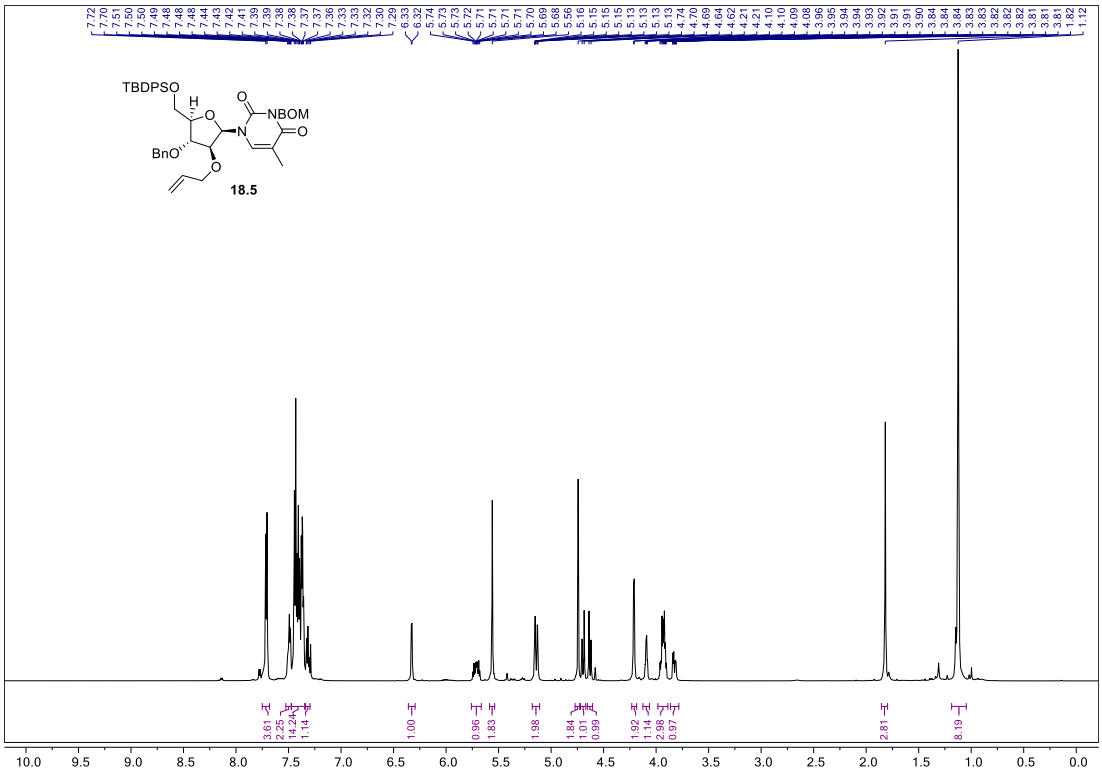
TBDPSO
NBOM
BnO
18.5

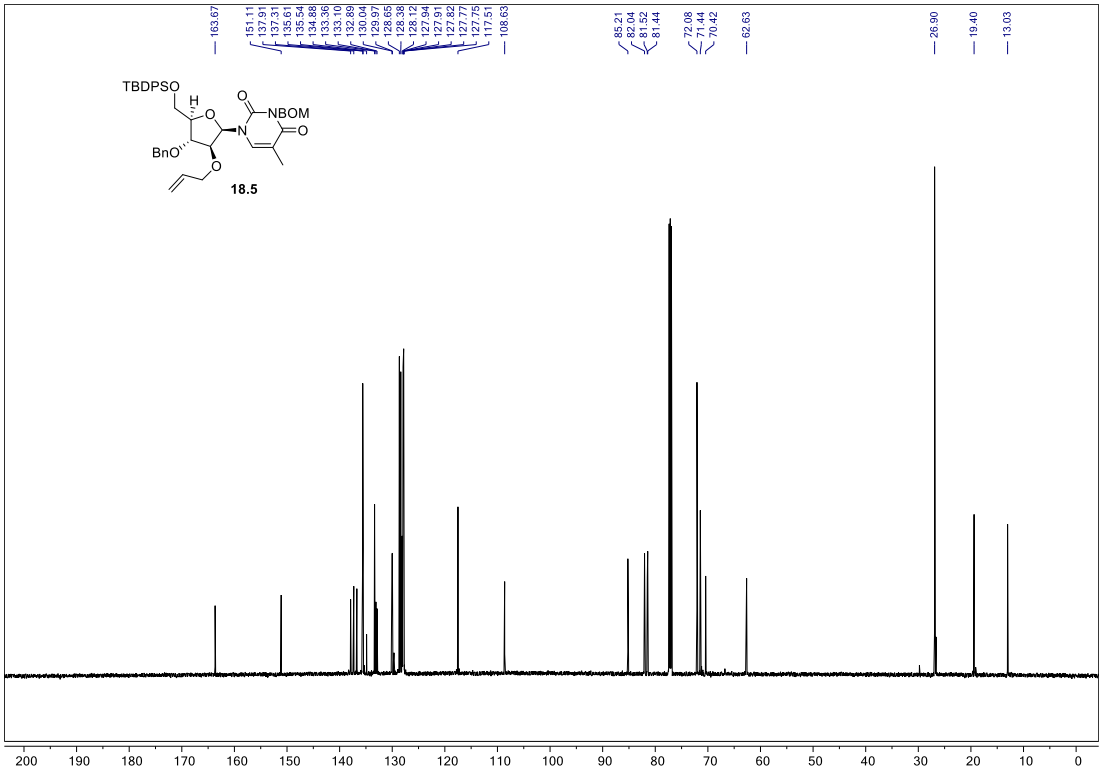
TBDPSO
NBOM
BnO
18.5

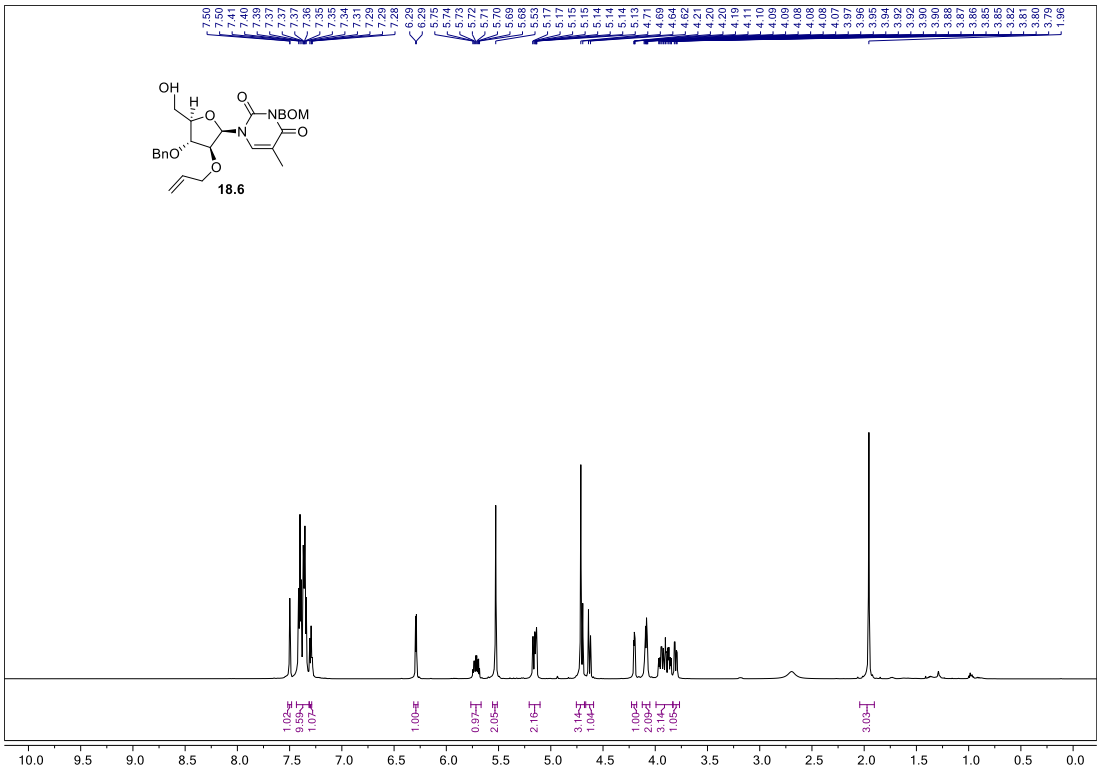
OH
H
O
NBOM
N
O
BnO
O
18.6

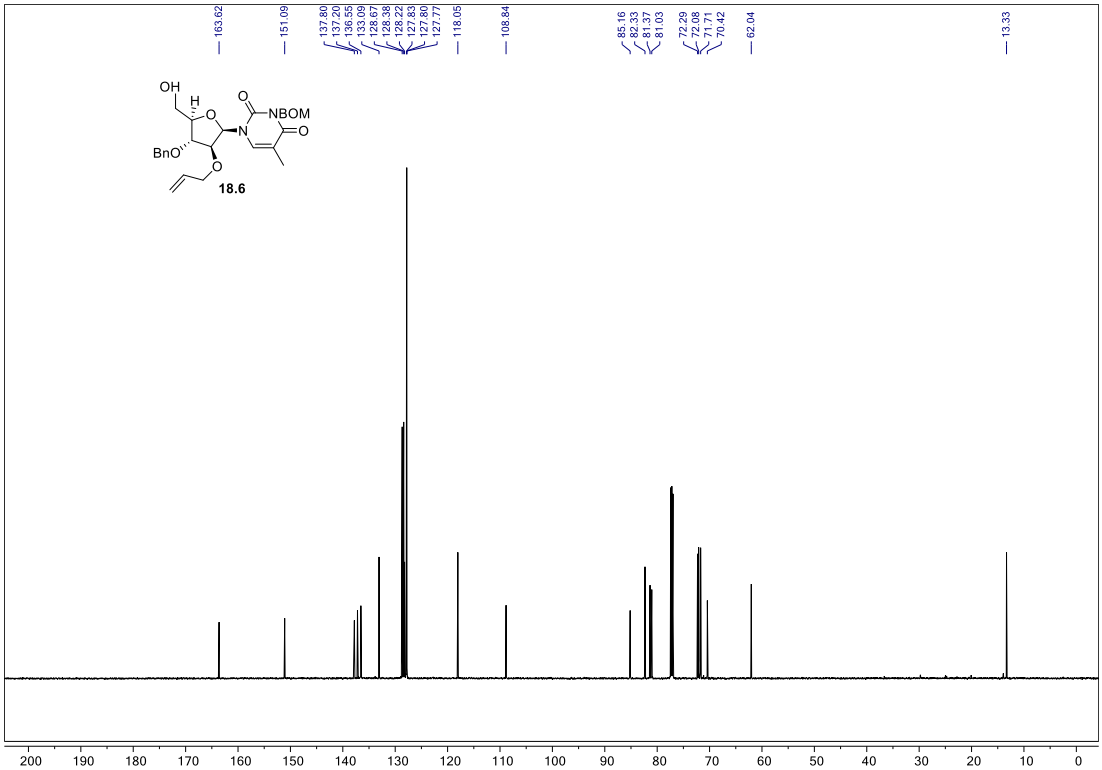
OH
H
O
NBOM
N
O
BnO
O
18.6

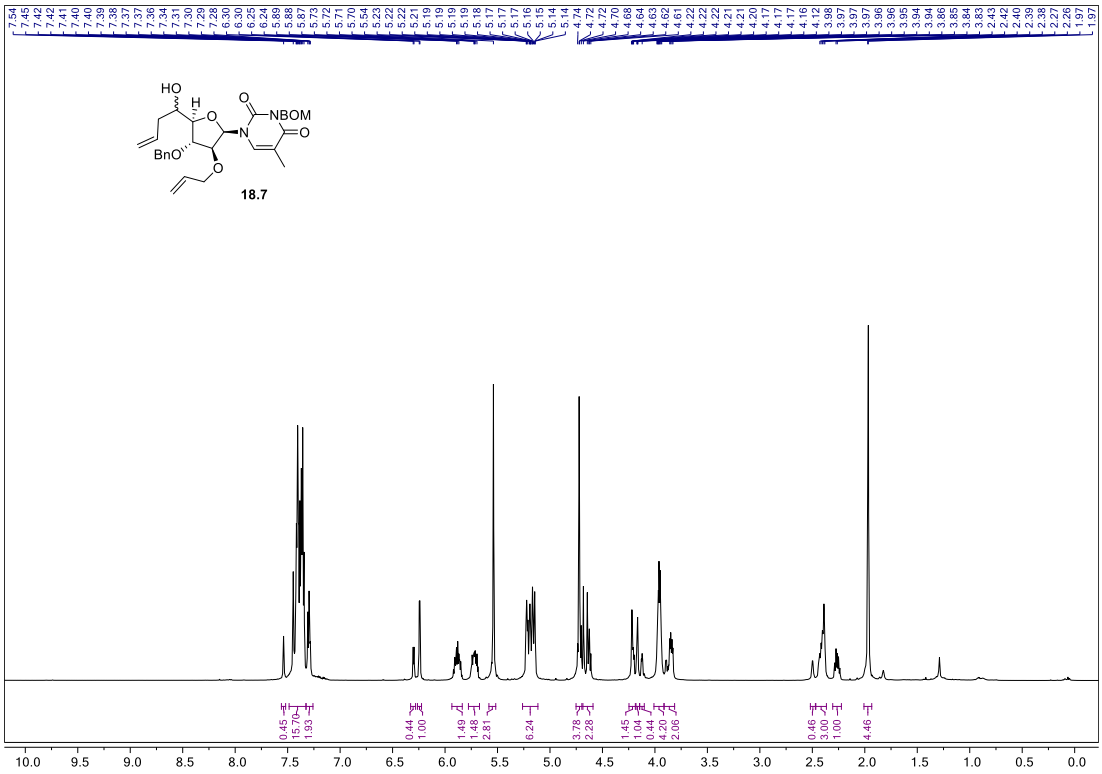
HO
H
O
NBOM
N
O
BnO
O
18.7

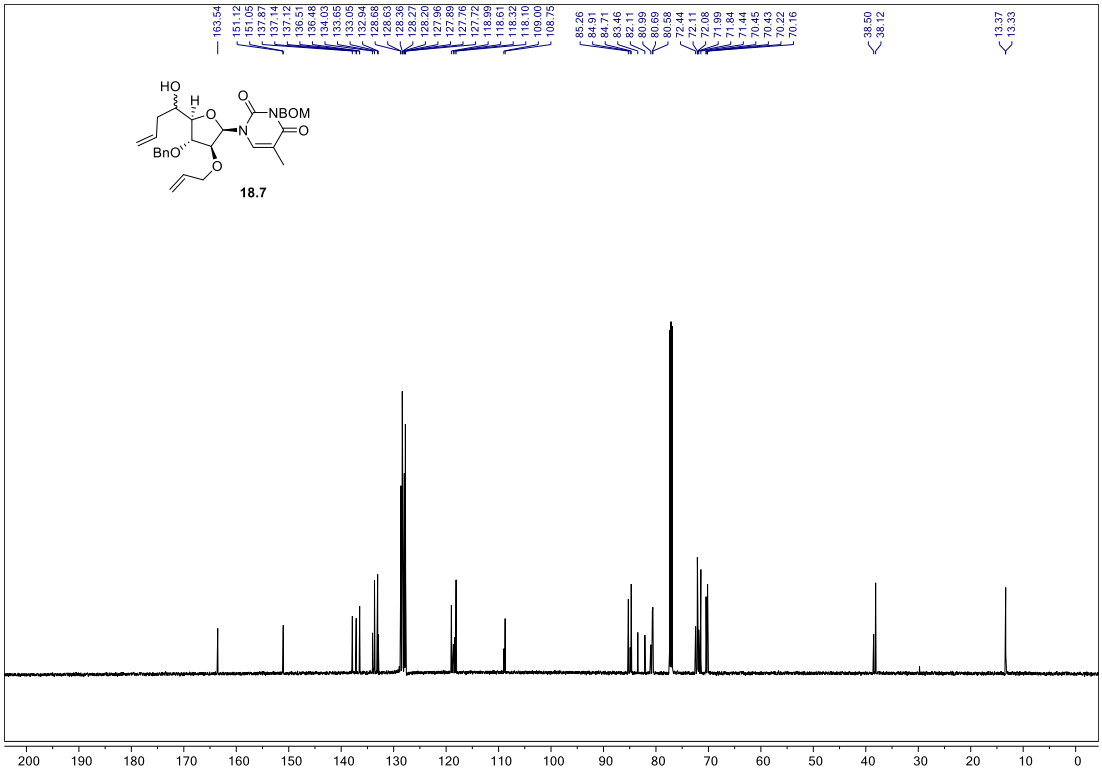
HO
H
O
NBOM
N
O
BnO
O
18.7

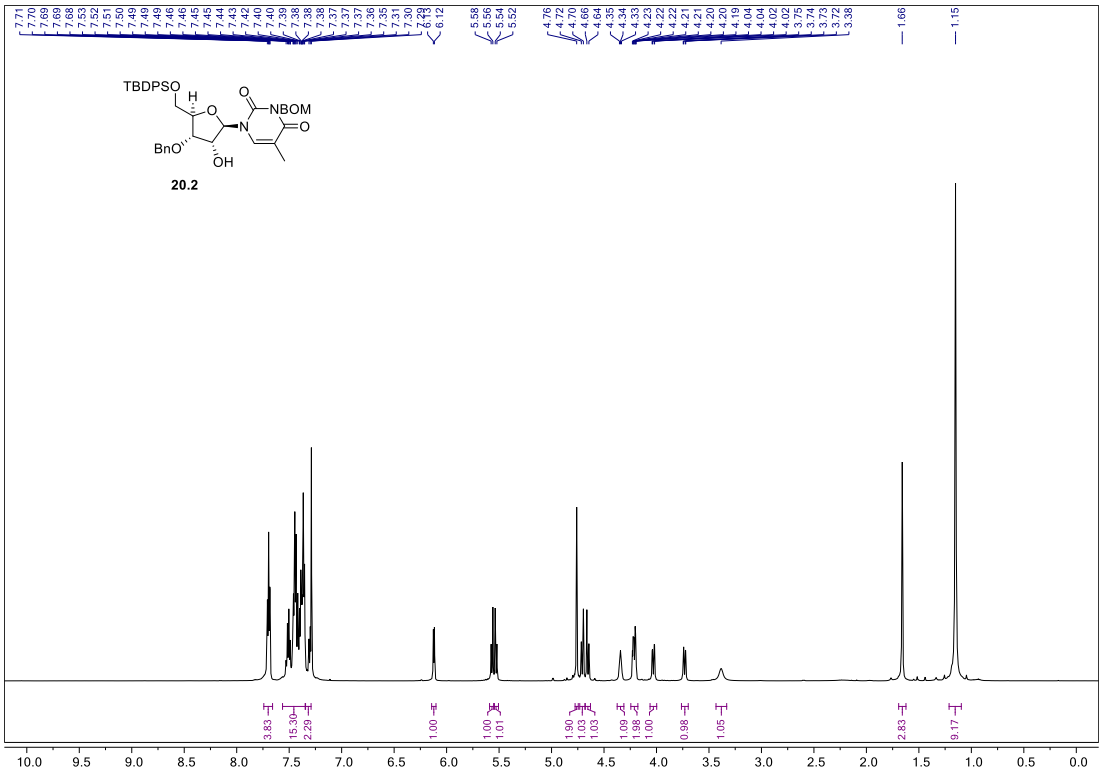
TBDPSO
H
O
NBOM
O
BnO
OH
20.2

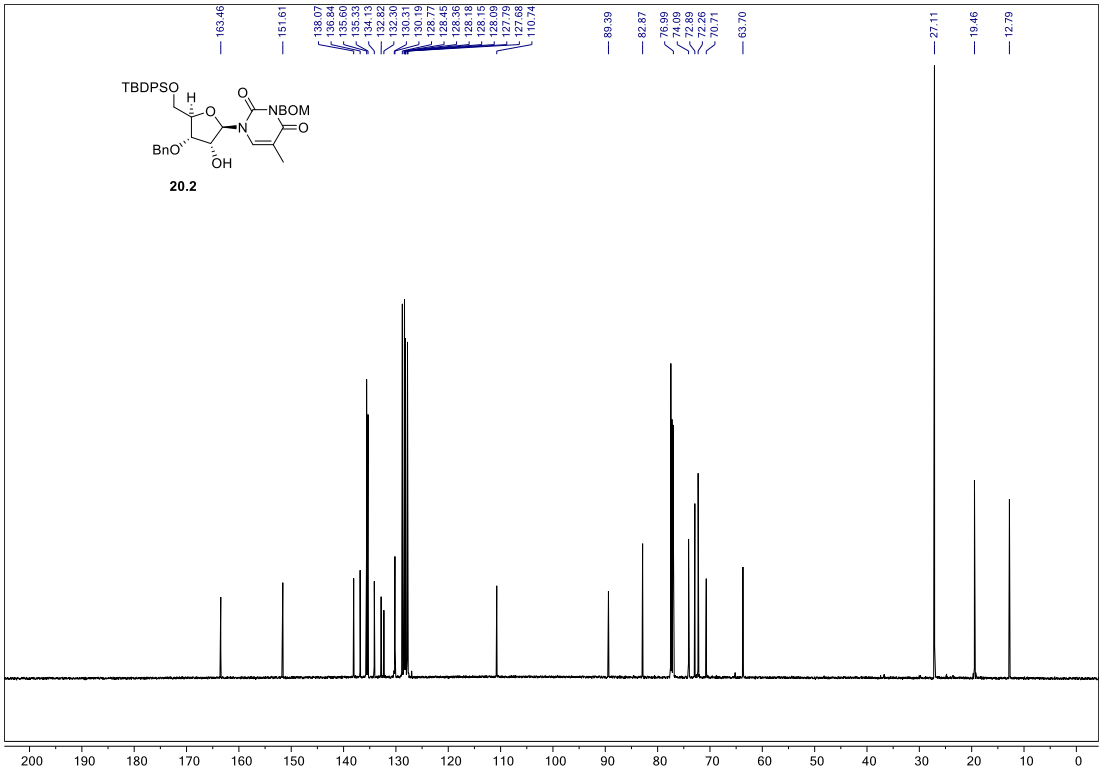
TBDPSO
H
O
NBOM
O
BnO
OH
20.2

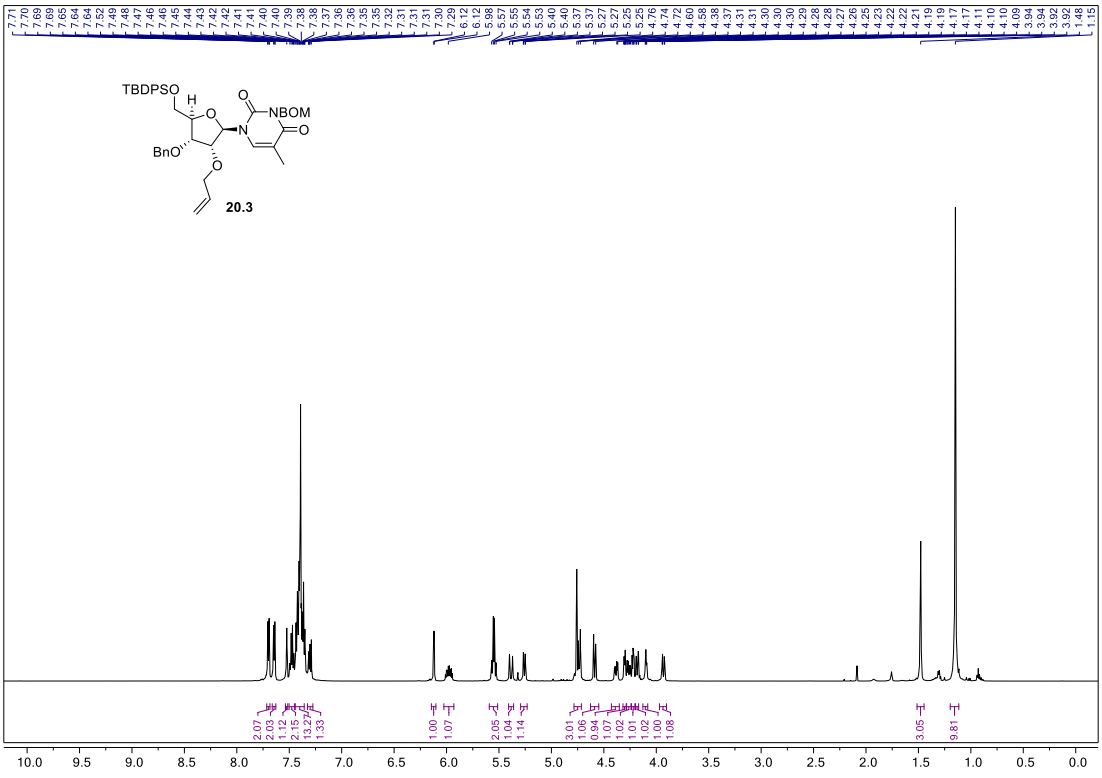
TBDPSO
H
O
NBOM
O
N
O
BnO
O
20.3

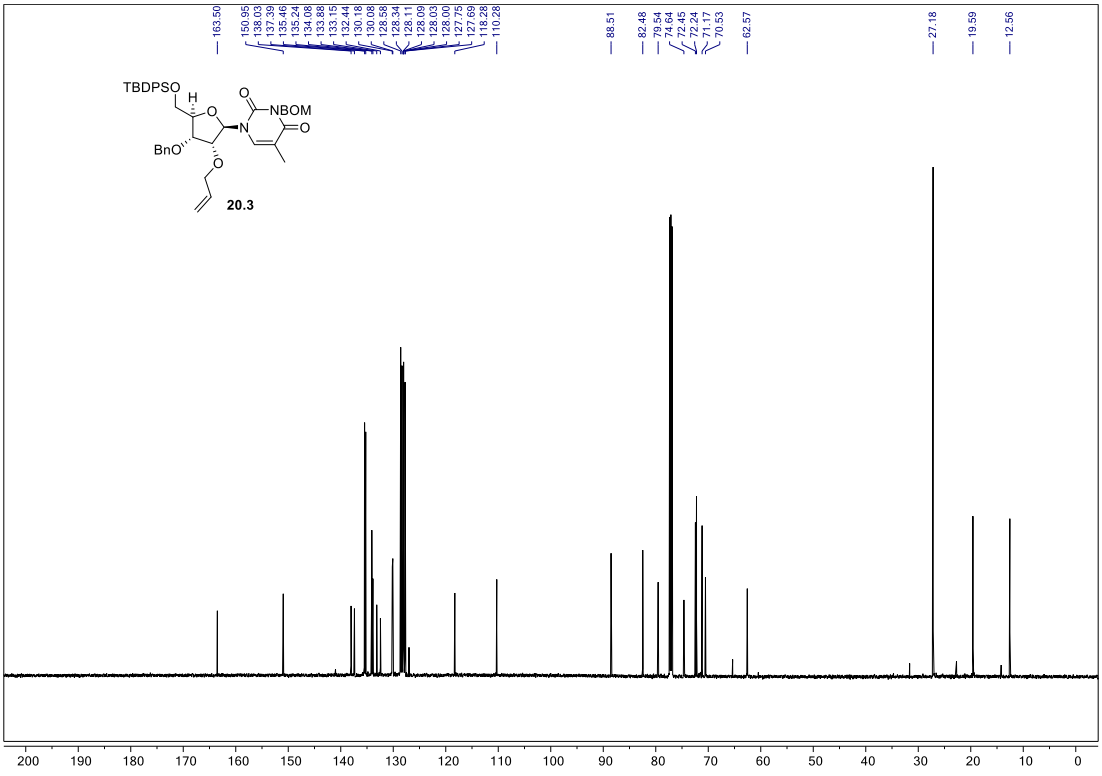
TBDPSO
H
O
NBOM
O
N
O
BnO
O
20.3

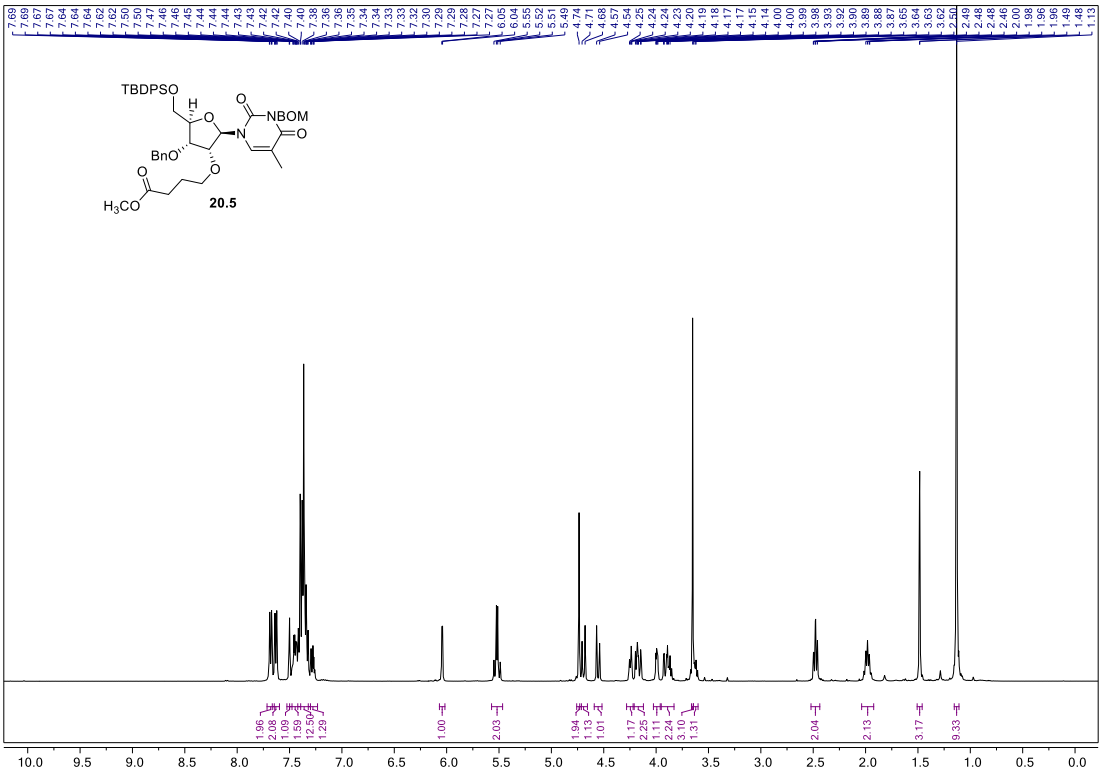
TBDPSO
H
O
N
NBOM
O
BnO
O
O
H3CO
20.5

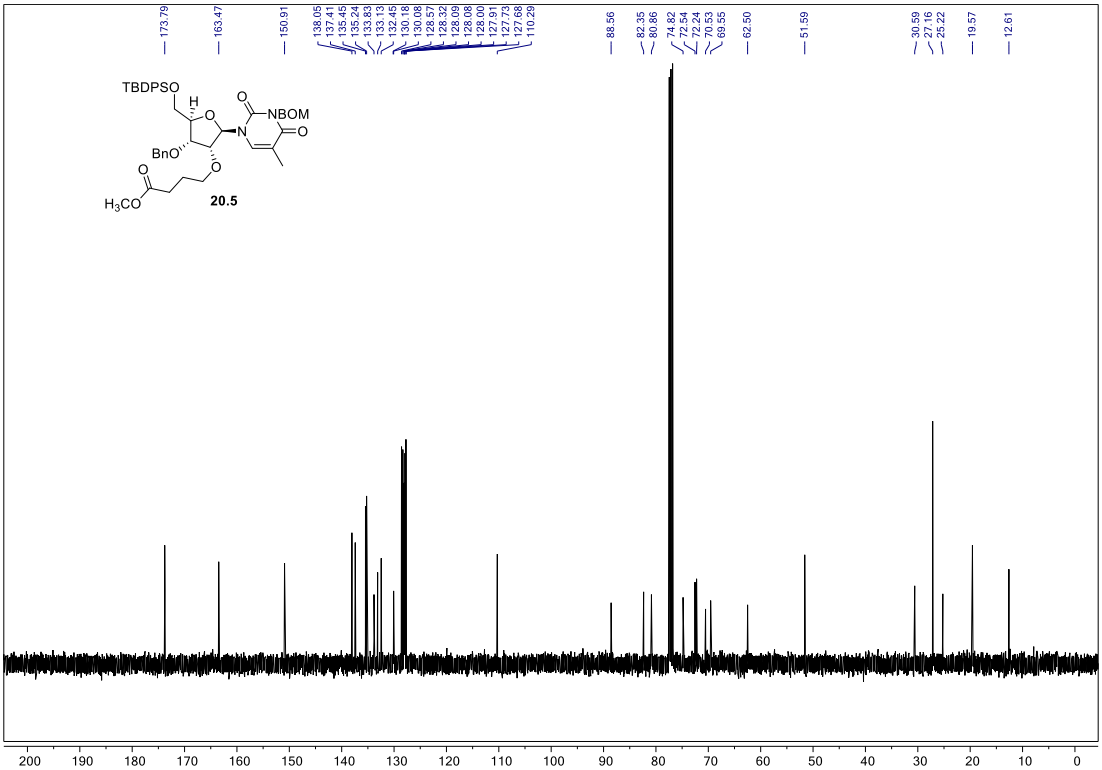
TBDPSO
H
O
N
NBOM
O
BnO
O
O
H3CO
20.5

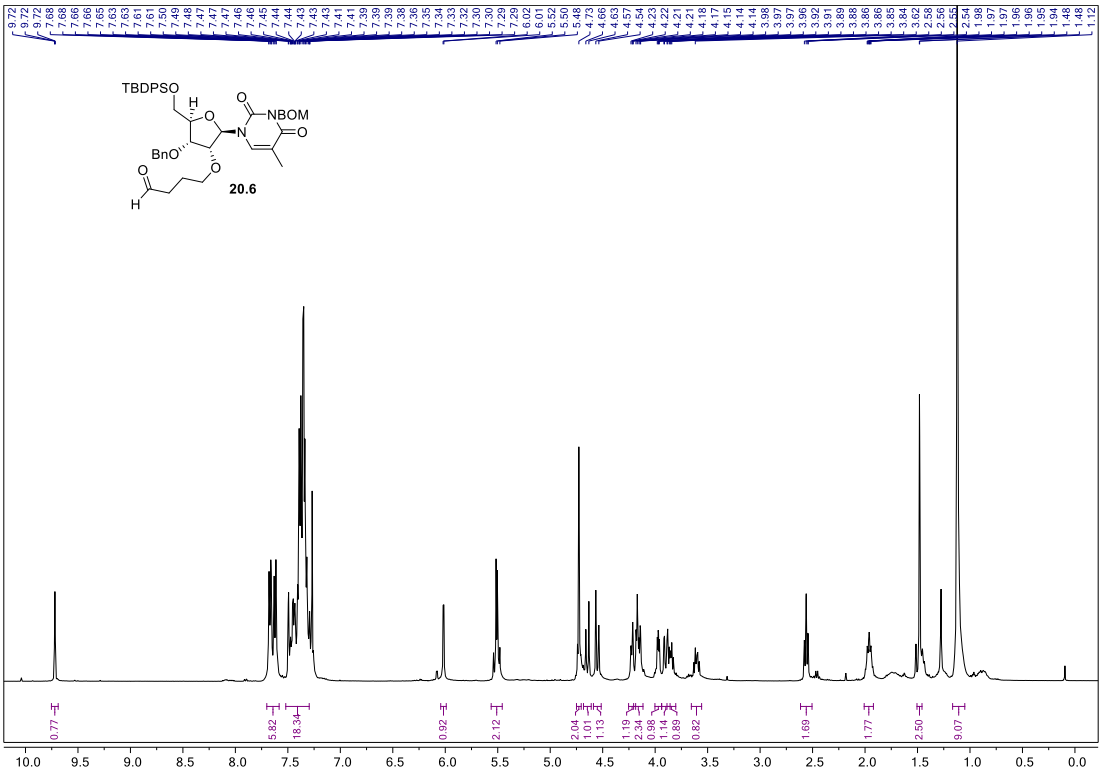
TBDPSO
NBOM
BnO
20.6

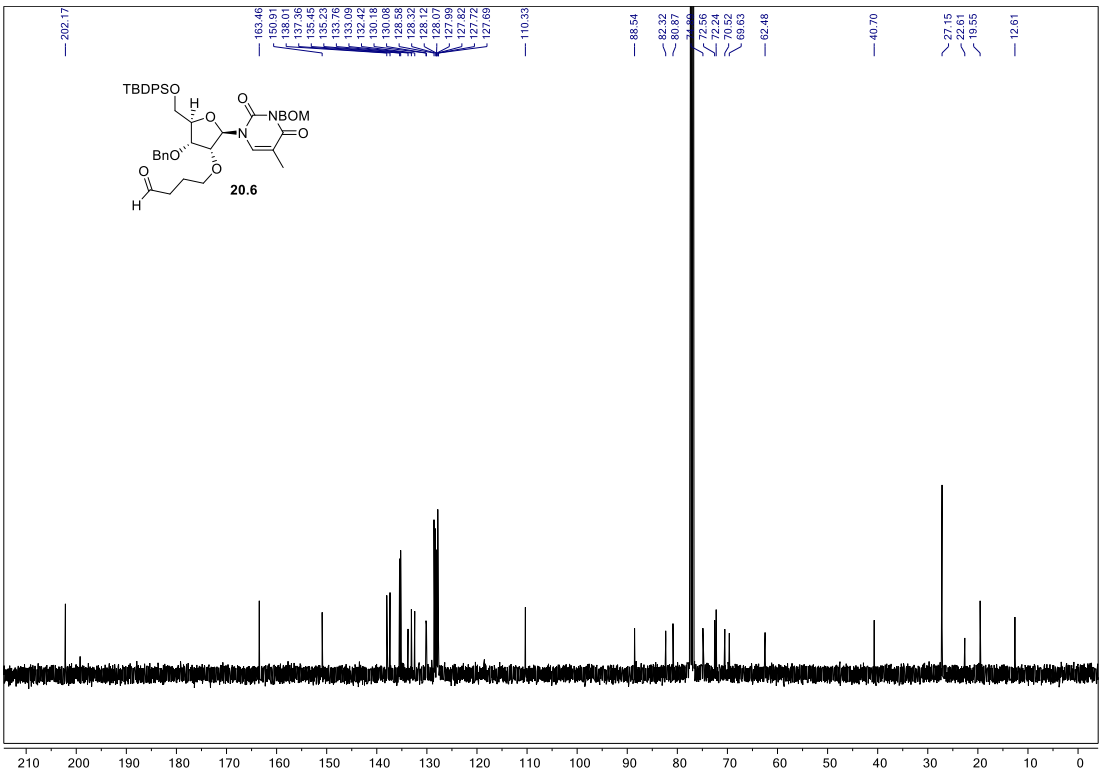
TBDPSO
NBOM
BnO
20.6

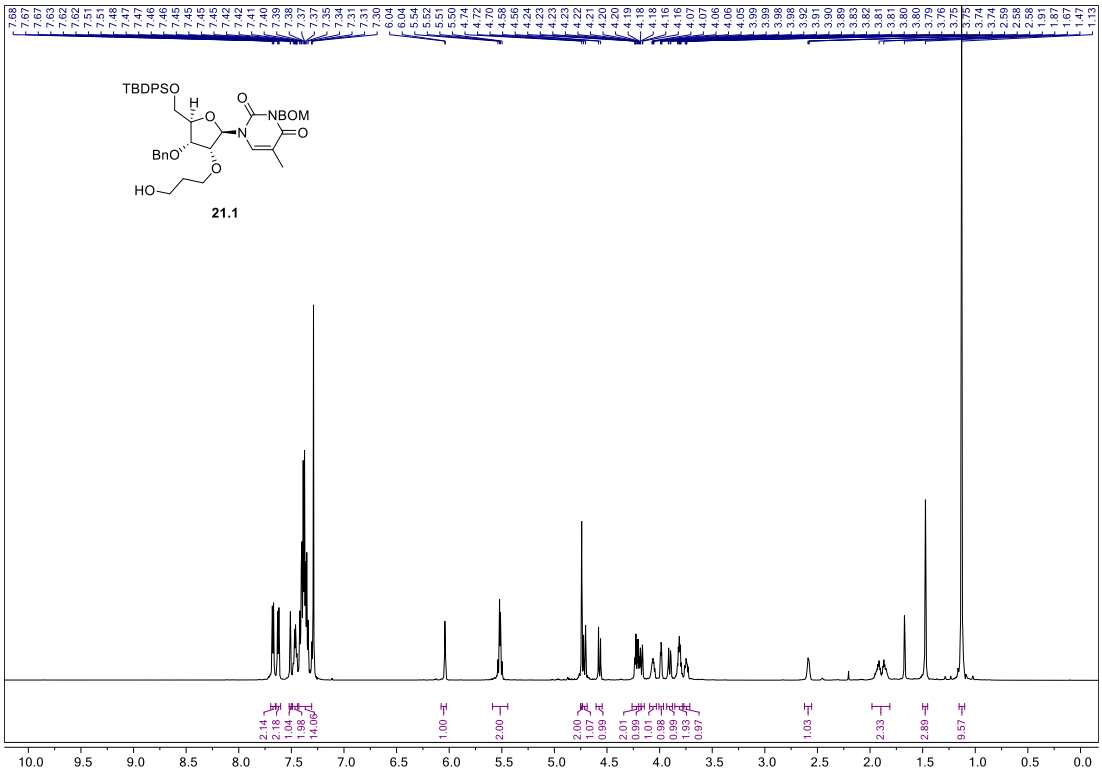
TBDPSO
NBOM
BnO
HO
21.1

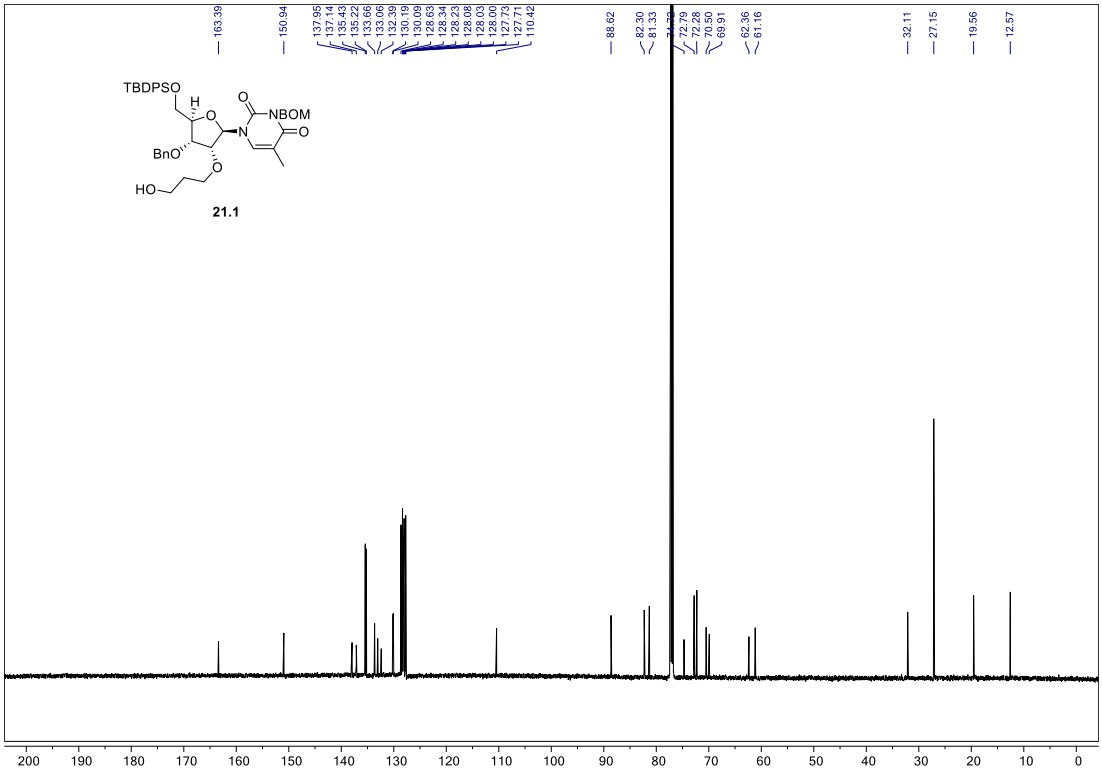
TBDPSO
NBOM
BnO
HO
21.1

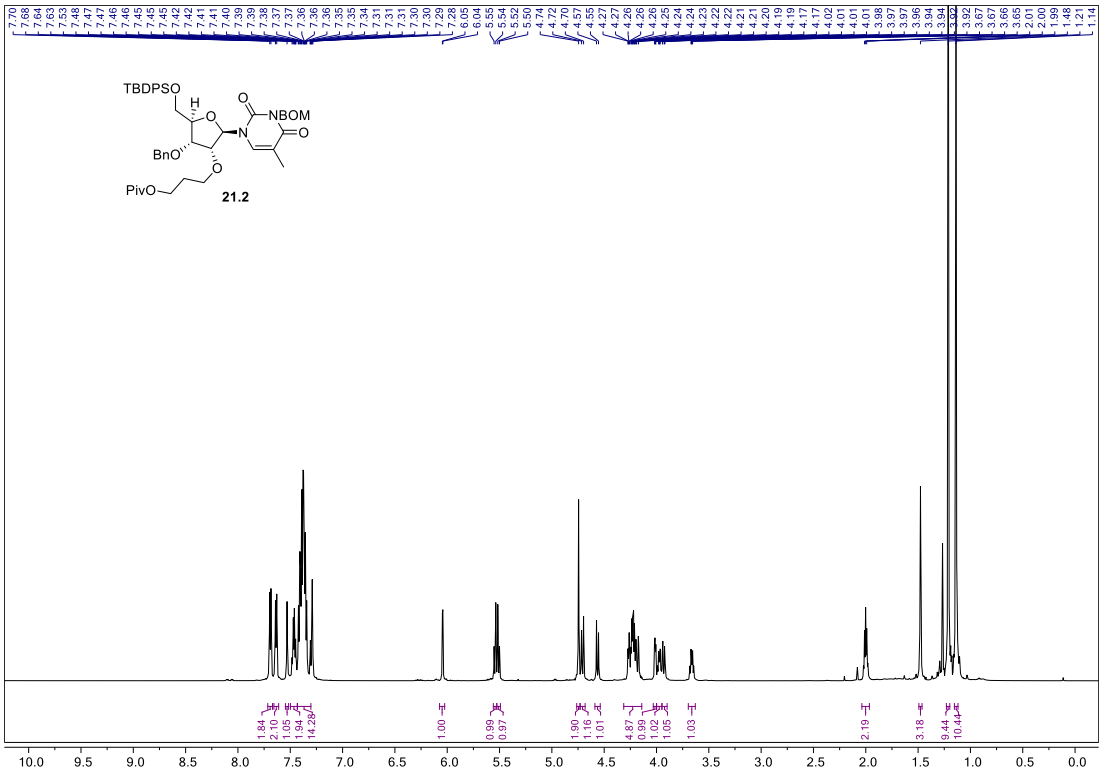
TBDPSO
NBOM
BnO
PivO
21.2

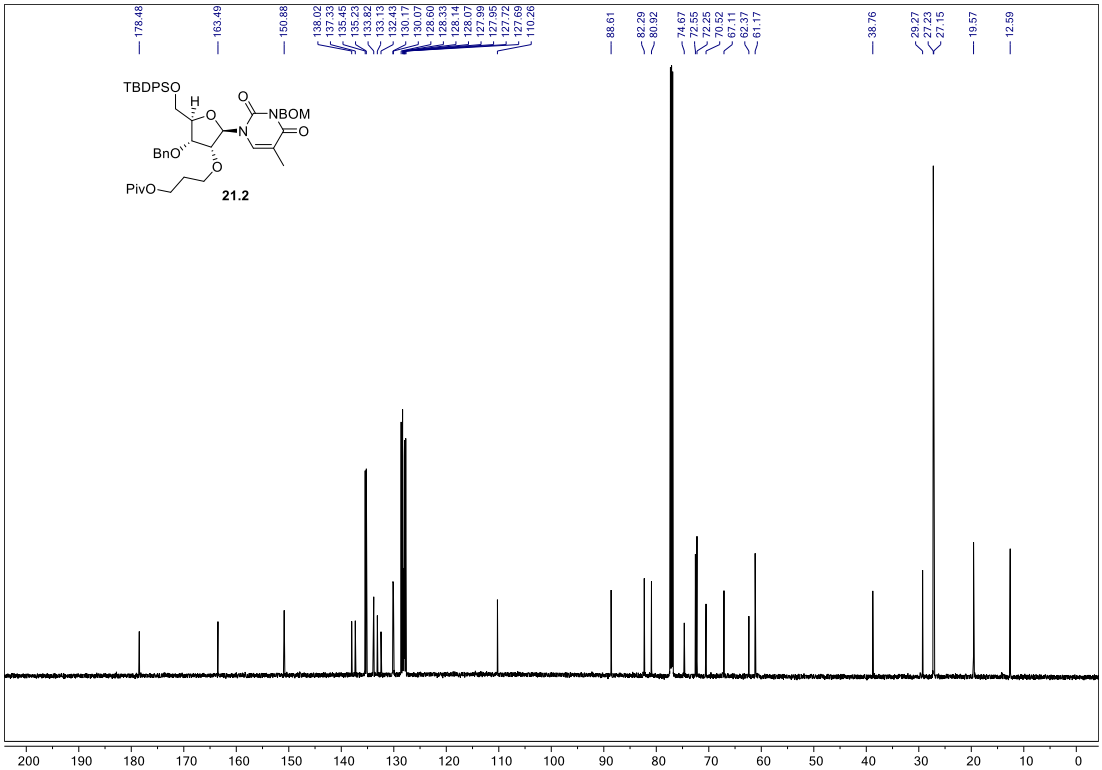
TBDPSO
NBOM
BnO
PivO
21.2

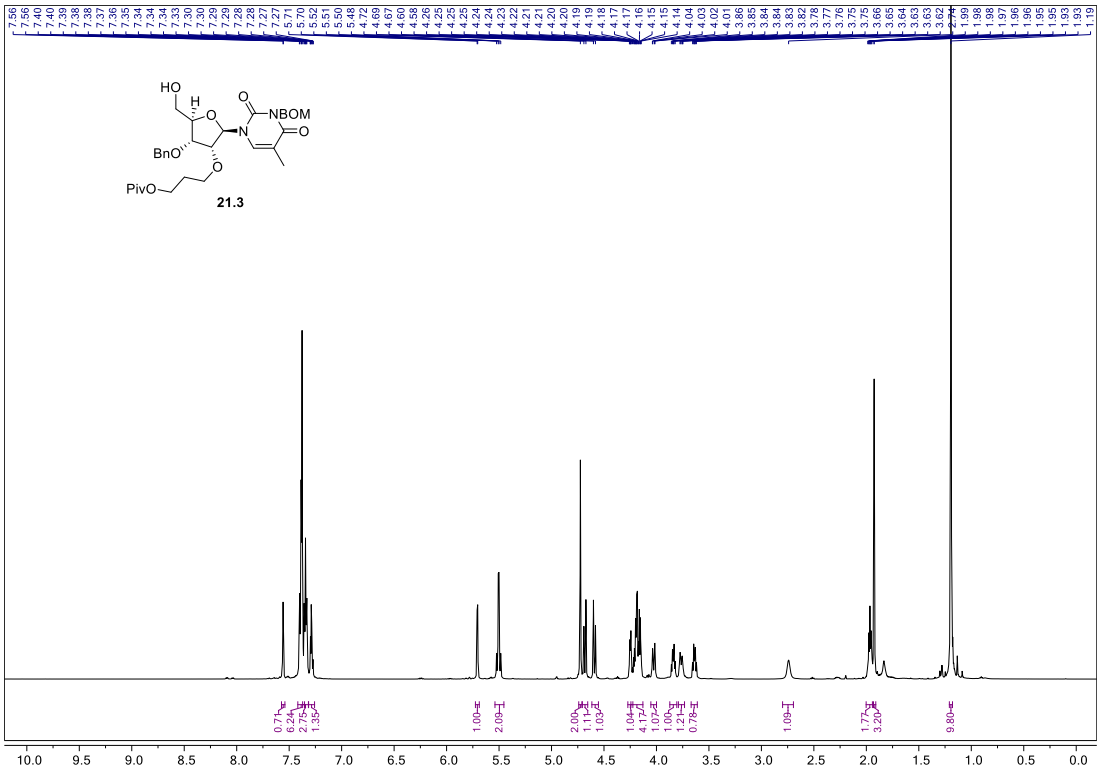
HO
H
O
NBOM
O
N
BnO
O
PivO
21.3

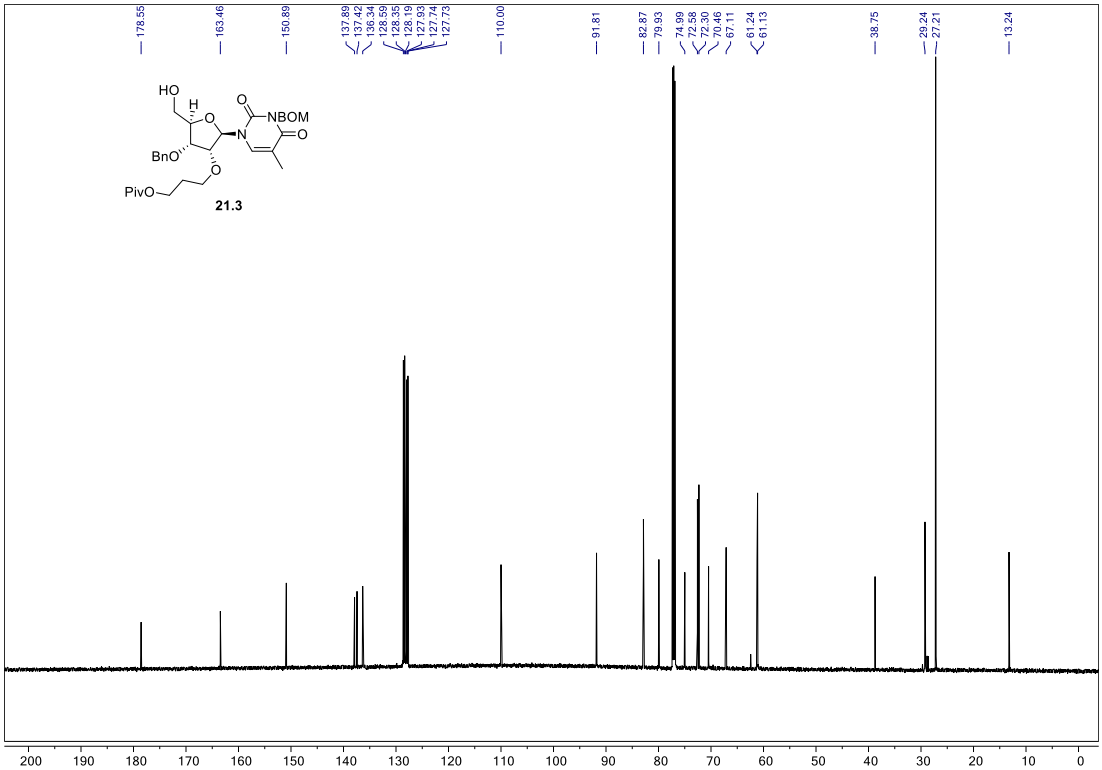
HO
H
O
NBOM
O
N
BnO
O
PivO
21.3

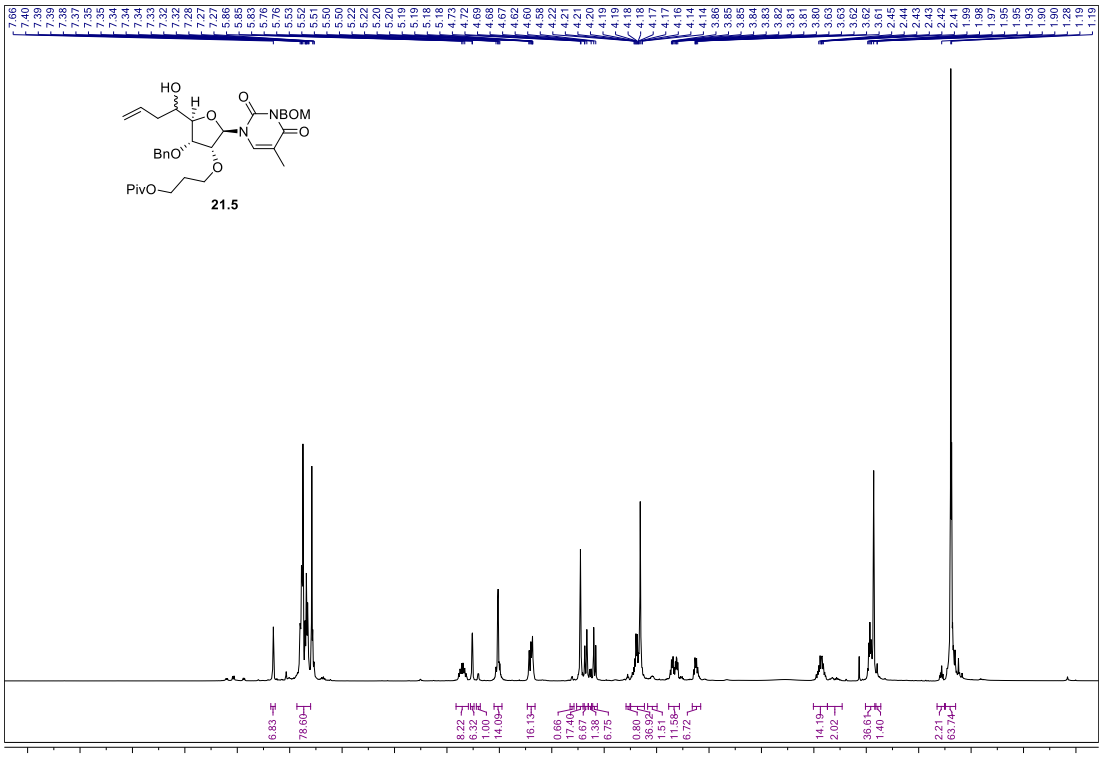
HO
H
O
NBOM
O
N
O
BnO
O
PivO
21.5

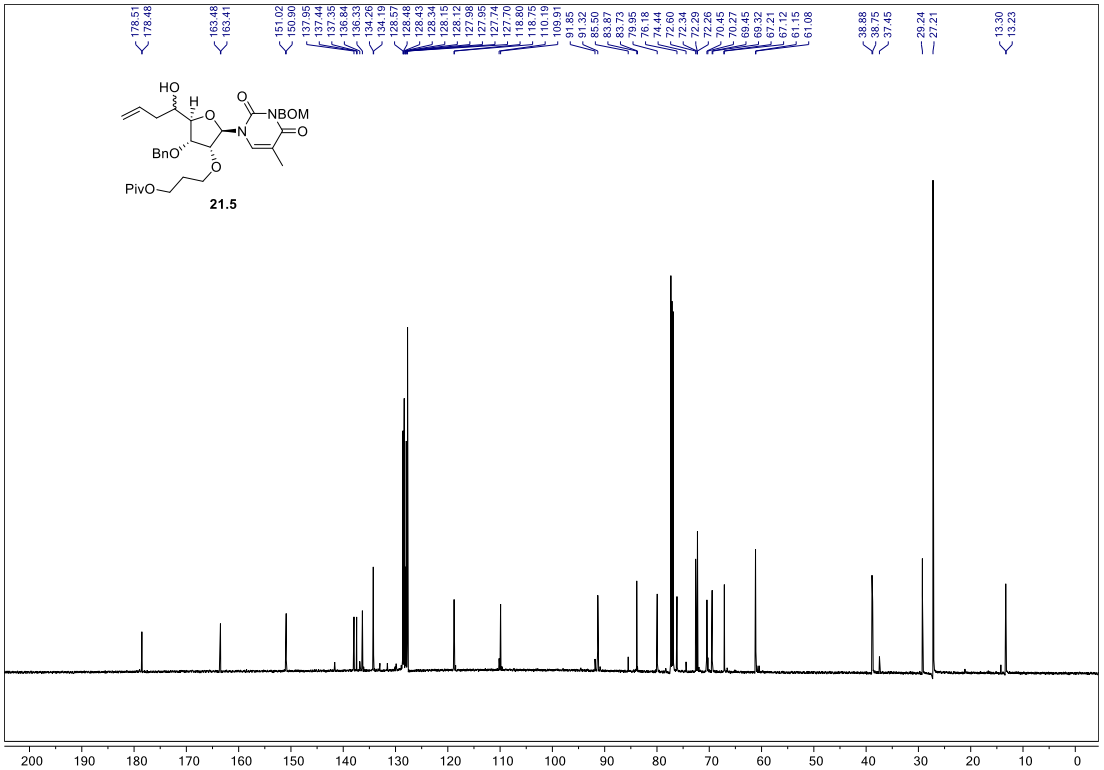
HO
H
O
NBOM
O
N
O
BnO
O
PivO
21.5

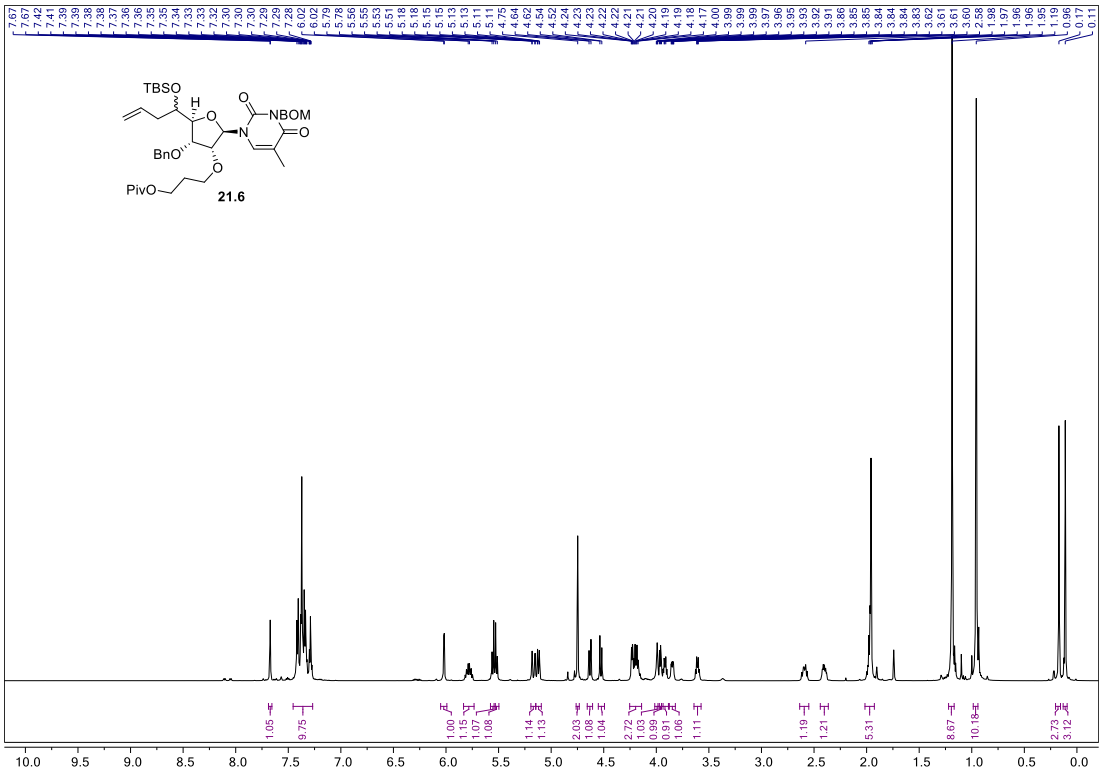
TBSO
H
O
NBOM
O
BnO
O
PivO
21.6

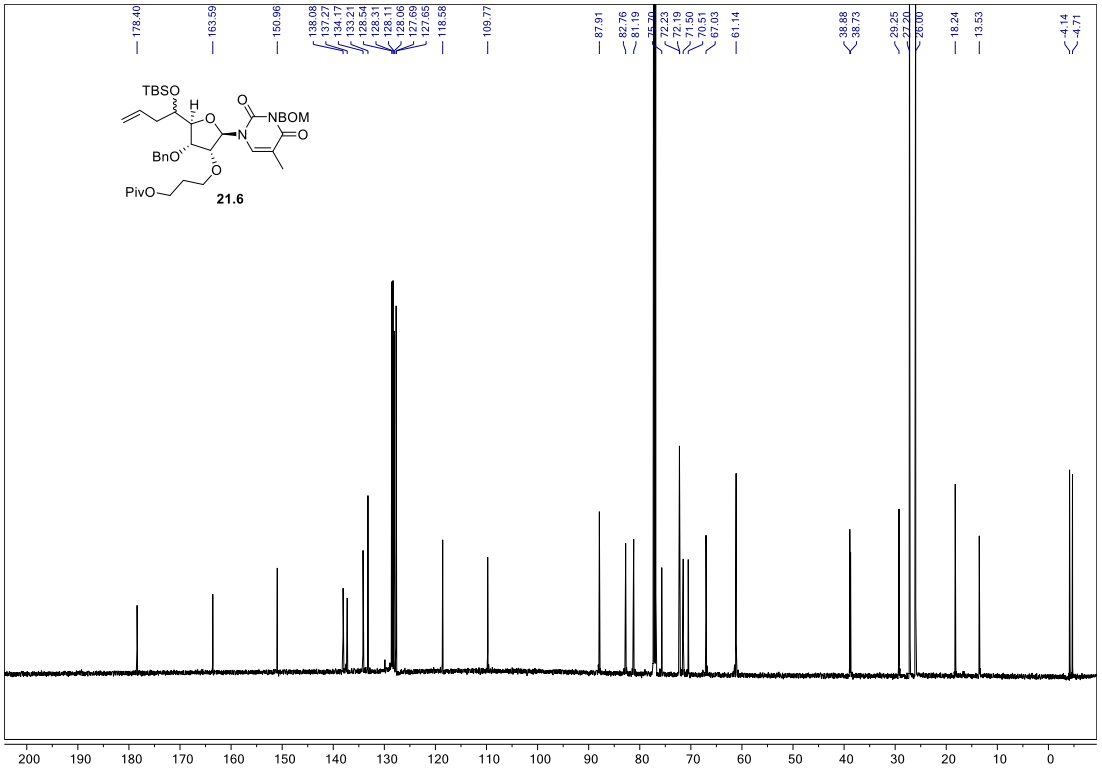
TBSO
H
O
NBOM
O
BnO
O
PivO
21.6

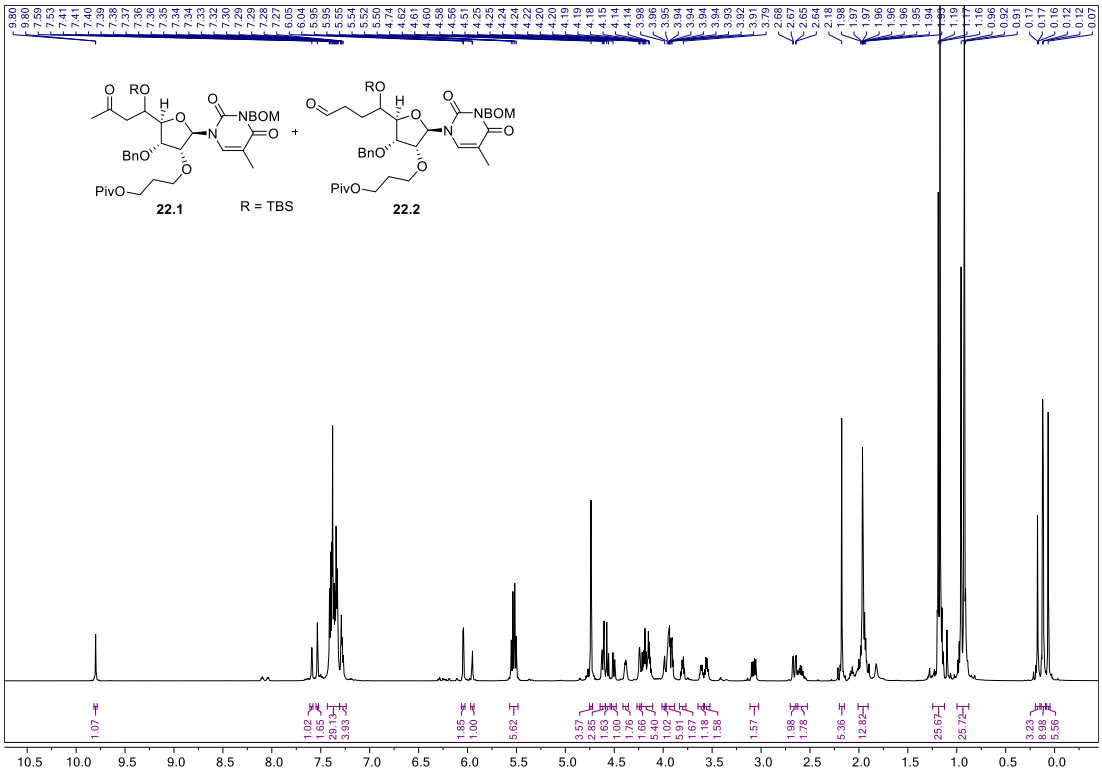
RO
H
O
NBOM
BnO
PivO
22.1
R = TBS
22.2

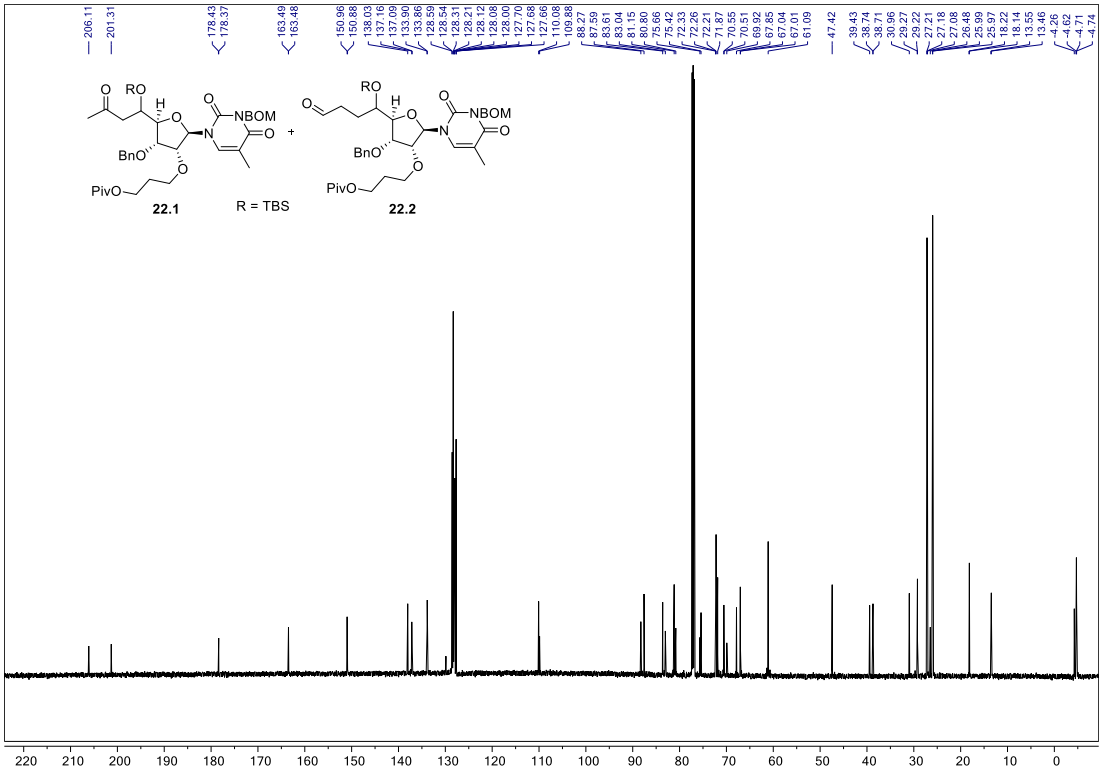
RO
H
O
NBOM
BnO
PivO
22.1
R = TBS
22.2

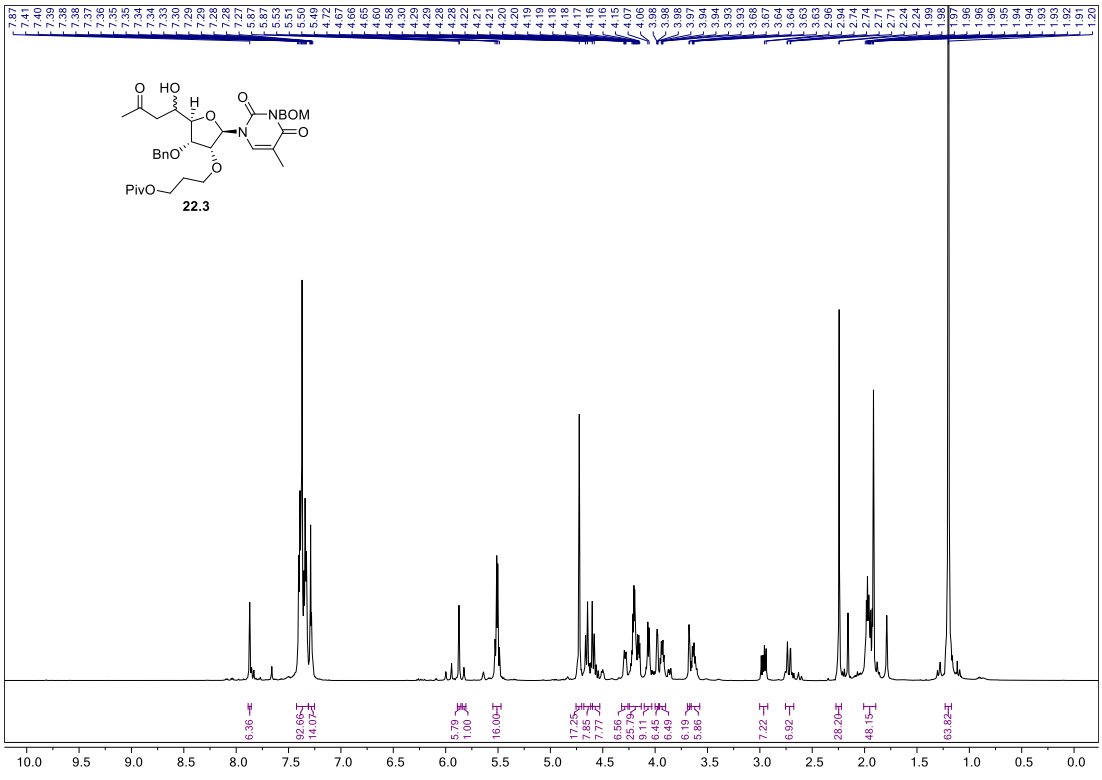
22.3

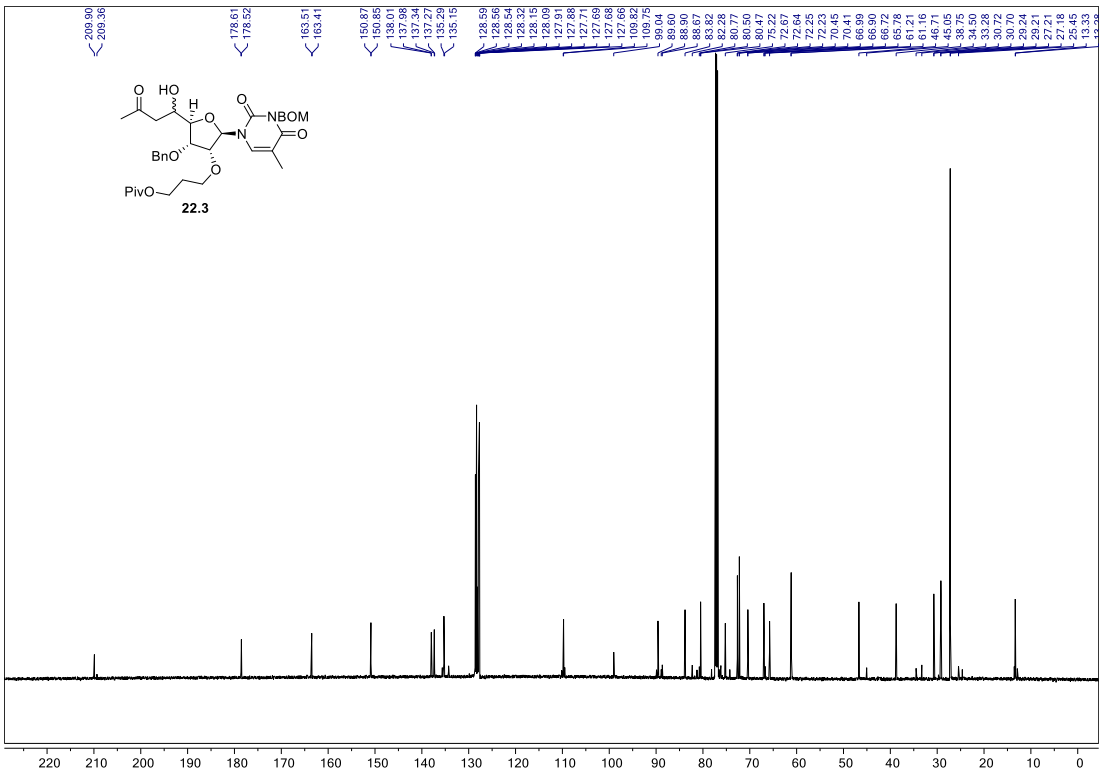
22.3

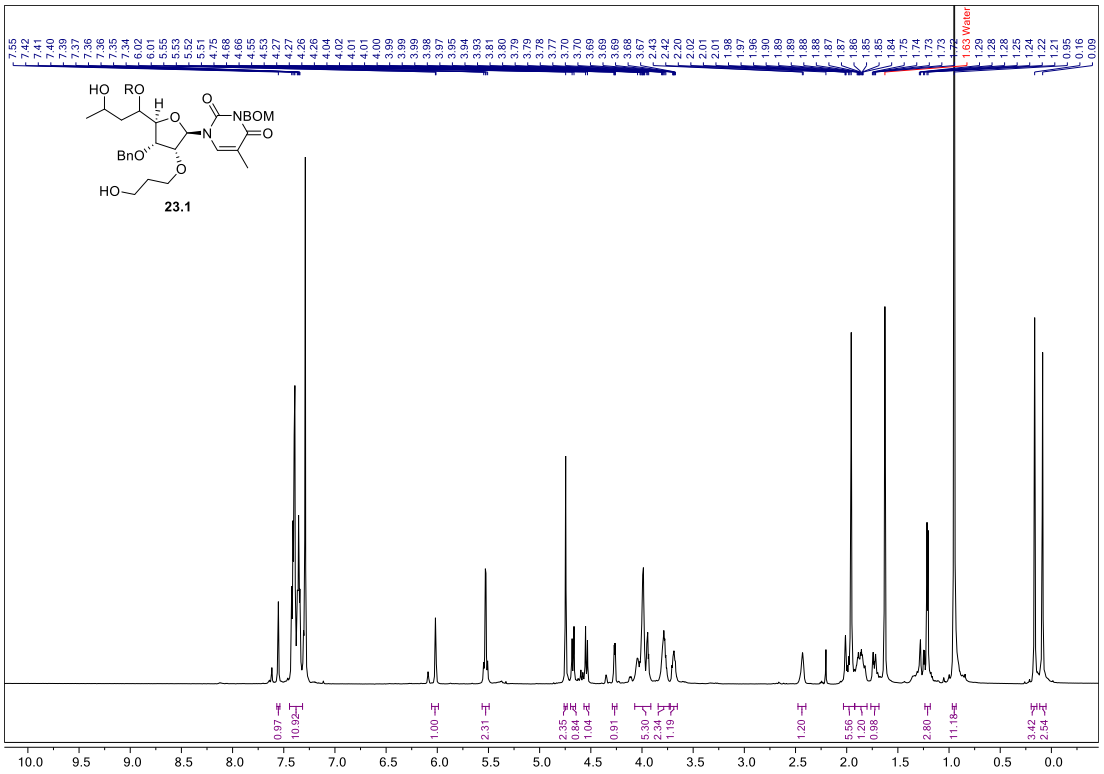
HO
RO
H
O
NBOM
O
N
BnO
O
HO
23.1

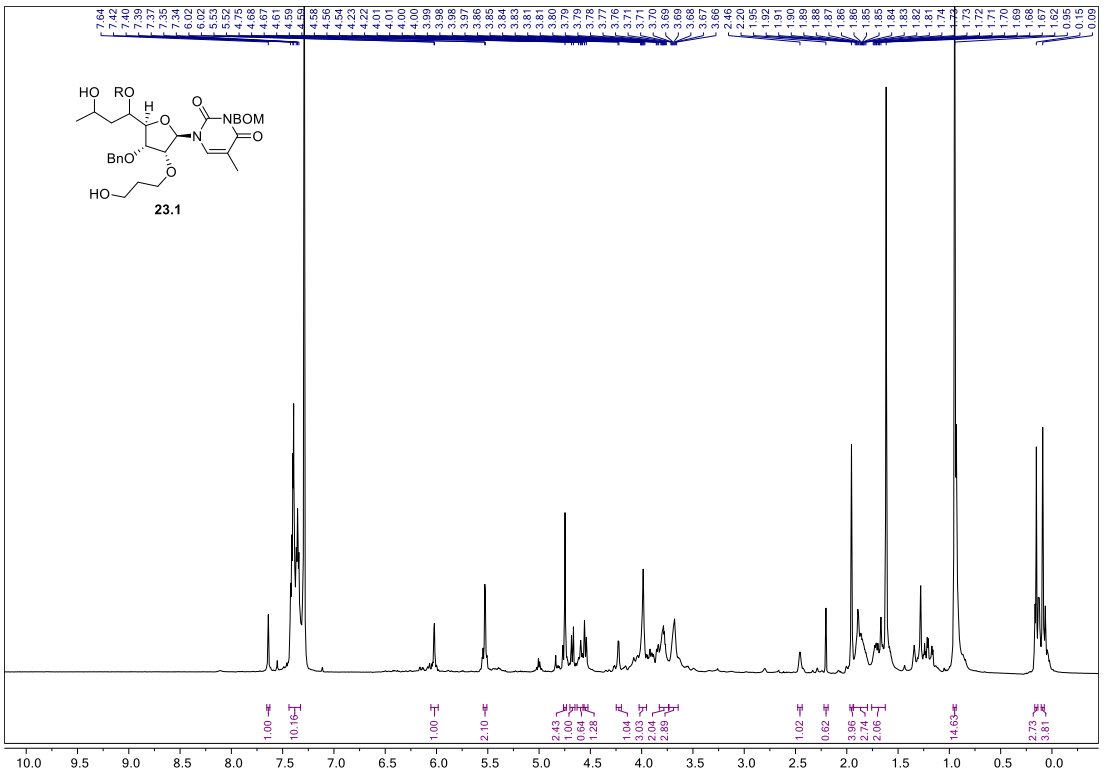
HO
RO
H
O
NBOM
O
N
BnO
O
HO
23.1

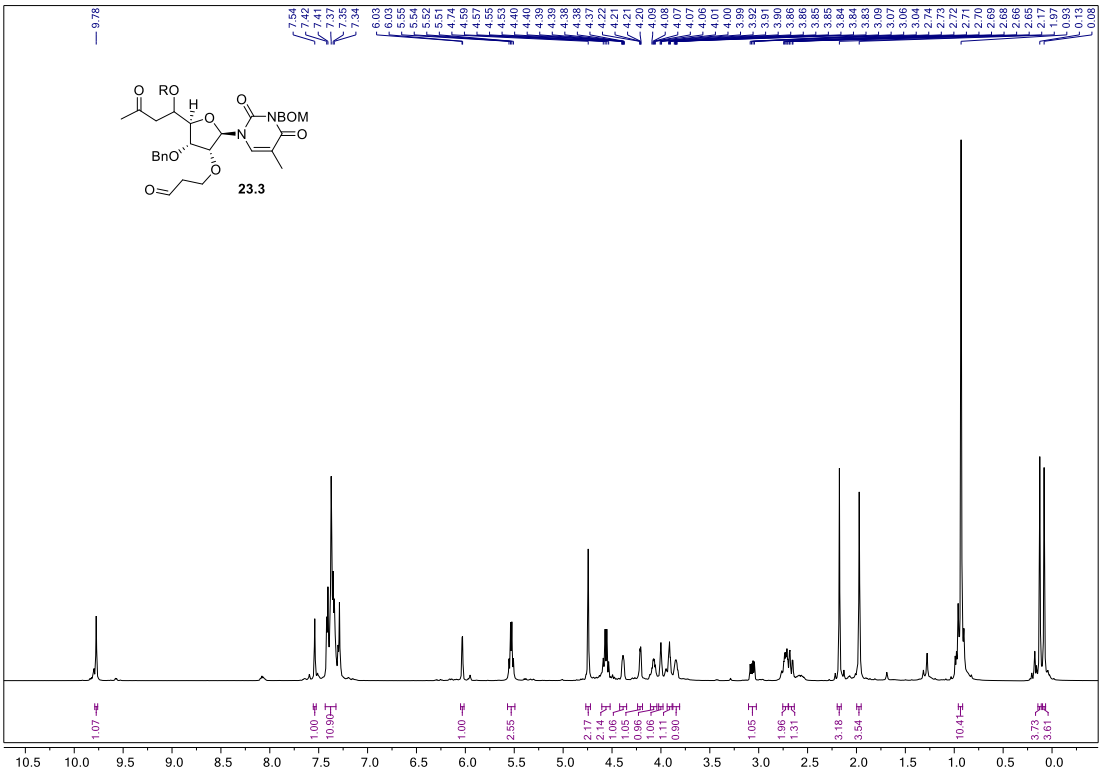
9.78
7.54
7.42
7.41
7.37
7.35
7.34
6.03
6.03
5.55
5.54
5.52
5.51
4.74
4.59
4.57
4.55
4.53
4.40
4.40
4.39
4.39
4.38
4.38
4.37
4.22
4.21
4.21
4.20
4.09
4.08
4.07
4.07
4.06
4.01
4.00
3.99
3.92
3.91
3.90
3.86
3.86
3.85
3.85
3.84
3.84
3.83
3.09
3.07
3.06
3.04
2.74
2.73
2.72
2.71
2.70
2.69
2.68
2.66
2.65
2.17
1.97
0.93
0.13
0.08
O
RO
H
O
O
NBOM
N
O
BnO
O
O
23.3
1.07
1.00
10.90
1.00
2.55
2.17
2.14
1.06
1.05
0.96
1.06
1.11
0.90
1.05
1.96
1.31
3.18
3.54
10.41
3.73
3.61
10.5
10.0
9.5
9.0
8.5
8.0
7.5
7.0
6.5
6.0
5.5
5.0
4.5
4.0
3.5
3.0
2.5
2.0
1.5
1.0
0.5
0.0

Optimized bicyclo[6.2.1]undecane simplified structures for SE calculations

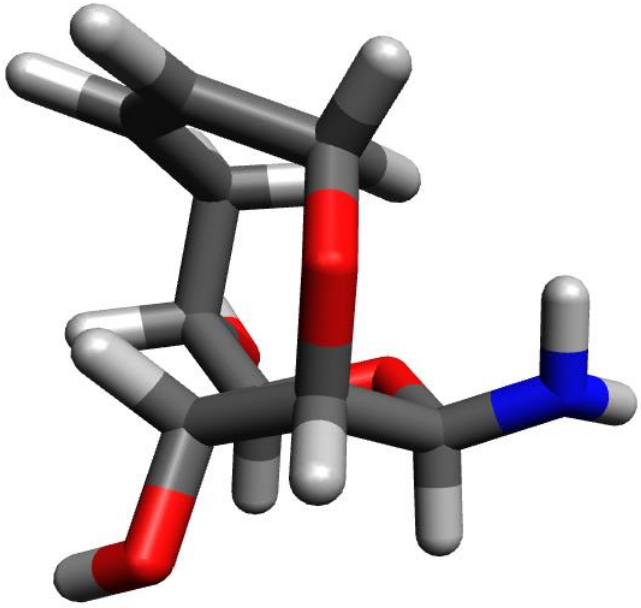

cis-bicyclo[6.2.1]undecane framework with Z configured olefin

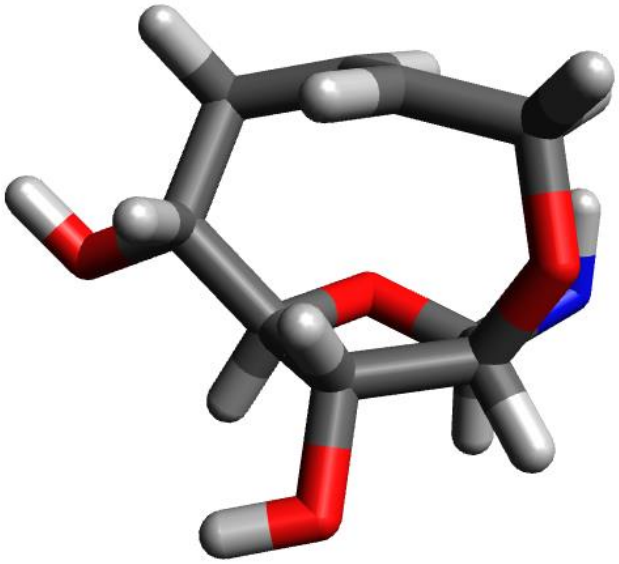

cis-bicyclo[6.2.1]undecane framework with E configured olefin

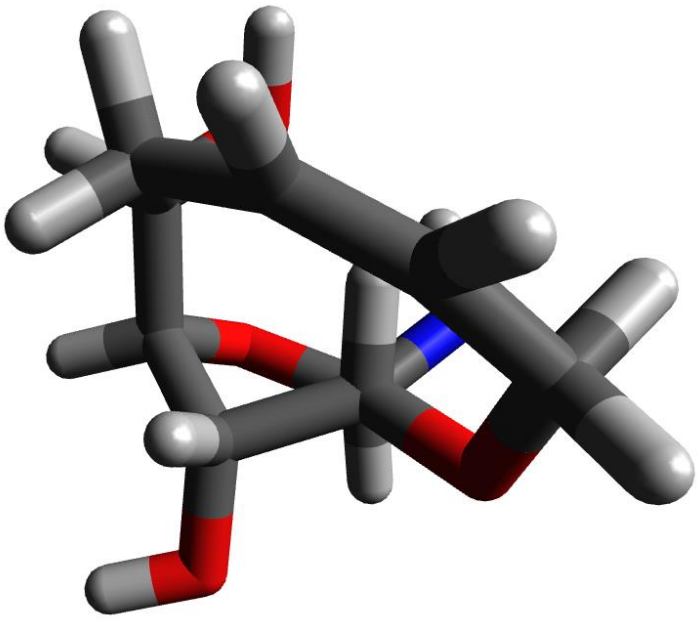

trans-bicyclo[6.2.1]undecane framework with *Z* configured olefin (exo)

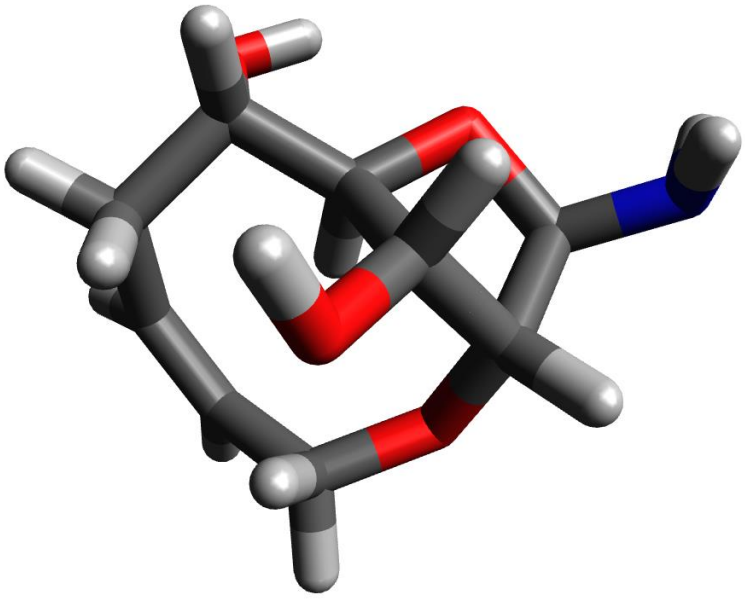

trans-bicyclo[6.2.1]undecane framework with *Z* configured olefin (endo)

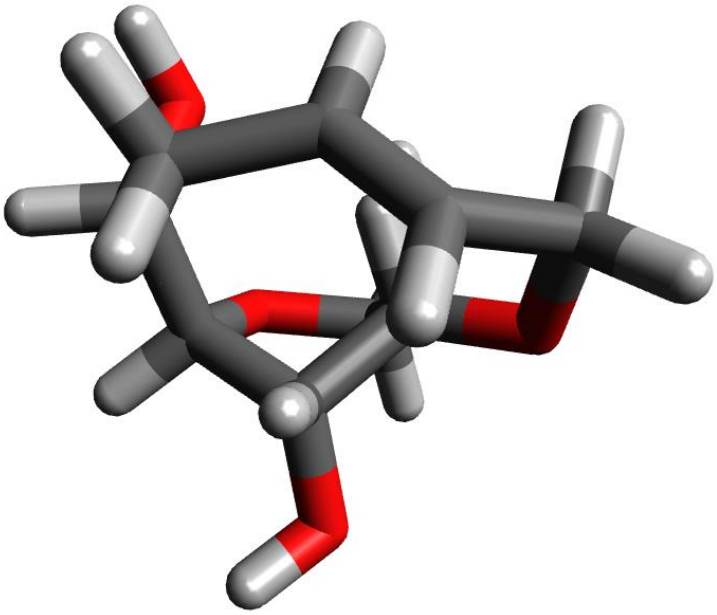

trans-bicyclo[6.2.1]undecane framework with *E* configured olefin (endo)

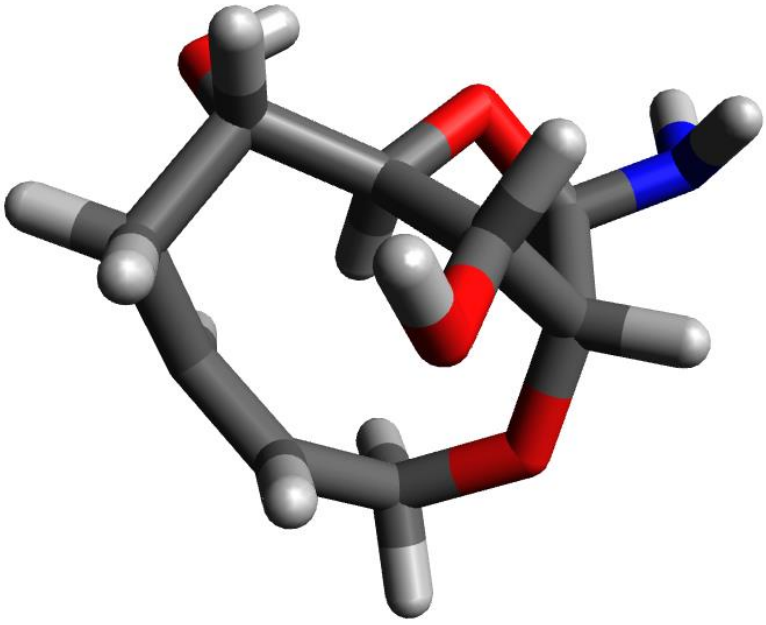

trans-bicyclo[6.2.1]undecane framework with *E* configured olefin (endo)

Appendix Chapter 2

Experimental Procedures Chapter 2

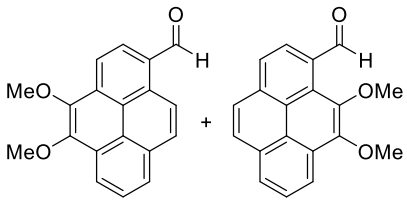

38.1 **38.2**

Compounds 38.1 and 38.2: $POCl_3$ (9.8 g, 64 mmol) was added dropwise to a stirred 0 °C solution of *N*-methylformanilide (4.3 g, 32 mmol) in 1,2-dichlorobenzene (15 mL). After 10 min., the cooling bath was removed and a solution of 4,5-dimethoxypyrene (2.66 g, 10.1 mmol) in 1,2-dichlorobenzene (10 mL) was added. The reaction was then heated at 90 °C. After 48 h, the reaction mixture was poured into ice, neutralized with 1 M NaOH, and diluted with EtOAc (60 mL). The layers were separated, and the aqueous phase was extracted with EtOAc (2 × 60 mL). The combined organic extracts were washed with brine (80 mL), dried over $MgSO_4$, filtered and concentrated under reduced pressure. The residue was purified by flash chromatography (5 cm × 15 cm; 80% dichloromethane/hexanes) to afford a mixture of **38.1** and **38.2** (2:1 *r.r*) as a yellow solid (2.2 g, 75%): R_f = 0.31 (80% dichloromethane/hexanes); a small portion of **38.1** was isolated from a single chromatography fraction and characterized: ^{1}H NMR (600 MHz, $CDCl_3$) δ 10.74 (s, 1H), 9.41 (d, *J* = 9.2 Hz, 1H), 8.60 (dd, *J* = 7.8, 1.1 Hz, 1H), 8.56 (d, *J* = 8.1 Hz, 1H), 8.45 (d, *J* = 8.2 Hz, 1H), 8.28 (d, *J* = 9.2 Hz, 1H), 8.25 (dd, *J* = 7.6, 1.1 Hz, 1H), 8.11 – 8.07 (m, 1H), 4.26 (s, 3H), 4.18 (s, 3H); ^{13}C NMR (151 MHz, $CDCl_3$) δ 193.35, 147.80, 144.32, 133.44, 132.10, 131.16, 131.01, 130.57, 128.34, 127.07, 126.84, 126.56, 123.23, 122.92, 122.49, 121.65, 118.85, 61.58, 61.44; HRMS (ESI) calculated for the mixture of constitutional isomers $C_{19}H_{15}O_3$ ($[M+H]^+$) *m/z* = 291.1021, found 291.1057.

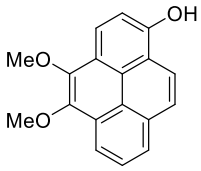

38.3

Compound 38.3: Concentrated $H_2S_2O_4$ (5 drops) and a 35% solution (w/w) of hydrogen peroxide in water (5 drops) were added to a stirred solution of **38.1** and **38.2** (2:1 *r.r*, 0.212 g, 0.731 mmol) in 1:1 methanol/dichloromethane (8 mL) at room temperature. After 4 h, the reaction mixture was poured into water (50 mL), the layers were separated, and the aqueous phase was extracted with dichloromethane (3 × 35 mL). The combined organic extracts were sequentially washed with water (2 × 30 mL), a saturated solution of $NaHCO_3$ (60 mL) and brine (60 mL), dried over $MgSO_4$, filtered and concentrated under reduced pressure. The residue was purified by flash chromatography (2.5 × 18 cm;

10% EtOAc/hexanes) to afford **38.3** as a brown solid (0.11 g, 52%): R_f = 0.20 (20% EtOAc/hexanes); ^{1}H NMR (400 MHz, CD_3OD) δ 8.35 (d, *J* = 9.1 Hz, 1H), 8.29 – 8.23 (m, 2H), 7.98 (dd, *J* = 7.8, 1.2 Hz, 1H), 7.94 – 7.87 (m, 2H), 7.51 (d, *J* = 8.5 Hz, 1H), 4.14 (s, 3H), 4.09 (s, 3H); ^{13}C NMR (101 MHz, CD_3OD) δ 151.74, 144.97, 141.99, 131.75, 128.77, 125.72, 125.12, 124.21, 123.01, 122.91, 121.04, 120.70, 119.92, 118.80, 117.78, 112.42, 60.10, 59.92; HRMS (ESI) calculated for $C_{18}H_{15}O_3$ ([M+H]$^+$) *m/z* = 279.1021, found 279.1009.

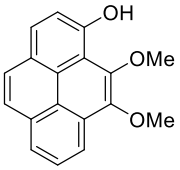

38.4

Compound 38.4: isolated as a yellow solid (0.058 g, 29%): R_f = 0.50 (20% EtOAc/hexanes); ^{1}H NMR (400 MHz, $CDCl_3$) δ 10.01 (s, 1H), 8.30 (dd, *J* = 7.7, 1.2 Hz, 1H), 8.07 – 8.00 (m, 2H), 7.99 – 7.93 (m, 1H), 7.91 (d, *J* = 8.9 Hz, 1H), 7.83 (d, *J* = 8.9 Hz, 1H), 7.52 (d, *J* = 8.4 Hz, 1H), 4.29 (s, 3H), 4.14 (s, 3H); ^{13}C NMR (101 MHz, $CDCl_3$) δ 153.19, 145.58, 143.92, 132.18, 128.71, 127.67, 126.92, 126.45, 124.71, 124.59, 124.50, 124.27, 123.96, 117.73, 115.26, 112.68, 62.14, 61.13; HRMS (ESI) calculated for $C_{18}H_{15}O_3$ ([M+H]$^+$) *m/z* = 279.1021, found 279.1021.

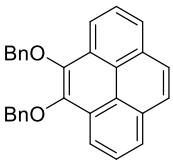

39.1

Compound 39.1: Sodium dithionite (0.56 g, 3.2 mmol) and tetrabutylammonium bromide (0.11 g, 0.32 mmol) were added to a stirred solution of pyrene-4,5-dione (0.25 g, 1.1 mmol) in THF (10 mL) and H_2O (10 mL) at room temperature. After 15 min., a solution of NaOH (0.52 g, 13 mmol) in water (10 mL) was added to the reaction mixture followed by benzyl bromide (0.94 g, 5.4 mmol). The resulting mixture was stirred at room temperature for 12 h. The reaction was diluted with EtOAc (20 mL), the layers were separated, and the aqueous phase was extracted with EtOAc (3 × 20 mL). The combined organic extracts were washed with H_2O (30 mL) and brine (30 mL), dried over $MgSO_4$, filtered and concentrated under reduced pressure. The residue was purified by flash chromatography (2.5 × 18 cm, 50% dichloromethane/hexanes) to afford **39.1** as a light brown solid (0.064 g, 33%) and the monobenzylated side product (0.19 g, 54%): R_f = 0.21 (60% dichloromethane/hexanes). The monobenzylated compound (0.19 g, 0.60 mmol) was re-subjected to the alkylation conditions described above to afford **34.1b** (0.098 g, 39%): R_f = 0.82 (60% dichloromethane/hexanes); ^{1}H NMR (600 MHz, $CDCl_3$) δ 8.54 (d, *J* = 7.8 Hz, 2H), 8.18 (d, *J* = 7.7, Hz, 2H), 8.09 (s, 2H), 8.07 – 8.01 (m, 2H), 7.64 (d, *J* = 7.4 Hz, 4H), 7.47 – 7.44 (m, 4H), 7.42 – 7.38 (m, 2H), 5.43 (s, 4H); ^{13}C NMR (151 MHz, $CDCl_3$) δ 144.28, 137.57, 131.09, 128.67, 128.52, 128.50,

128.26, 127.41, 126.12, 124.66, 123.03, 119.65, 75.64; HRMS (ESI) calculated for $C_{30}H_{23}O_2$ ($[M+H]^+$) *m/z* = 415.1698, found 415.1701.

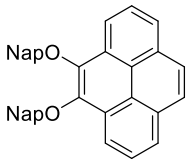

39.4

Compound 39.4: Sodium dithionite (0.34 g, 1.9 mmol) and tetrabutylammonium bromide (0.065 g, 0.19 mmol) were added to a stirred solution of pyrene-4,5-dione (0.14 g, 0.59 mmol) in THF (7 mL) and H_2O (7 mL) at room temperature. After 15 min., a solution of KOH (0.27 g, 4.8 mmol) in water (10 mL) was added to the reaction mixture, followed by 2-(bromomethyl)naphthalene (0.69 g, 3.1 mmol). The resulting mixture was stirred at room temperature for 12 h. The reaction was diluted with EtOAc (20 mL), the layers were separated, and the aqueous phase was extracted with EtOAc (3 × 20 mL). The combined organic extracts were washed with H_2O (30 mL) and brine (30 mL), dried over $MgSO_4$, filtered and concentrated under reduced pressure. The residue was purified by flash chromatography (2.5 × 18 cm, 70% dichloromethane/hexanes) to afford **39.4** as a white solid (0.050 g, 17%) and mononaphtylated side product (0.020 g, 9%): R_f = 0.28 (60% dichloromethane/hexanes). The mononaphtylated compound (0.020 g, 0.053 mmol) was re-subjected to the alkylation conditions described above to afford **39.4** (0.010 g, 36%): R_f = 0.80 (60% dichloromethane/hexanes); ^{1}H NMR (600 MHz, $CDCl_3$) δ 8.65 (d, *J* = 7.8 Hz, 2H), 8.20 (d, *J* = 7.6 Hz, 2H), 8.11 (s, 2H), 8.10 – 8.05 (m, 4H), 7.94 – 7.90 (m, 4H), 7.81 (d, *J* = 7.8 Hz, 2H), 7.78 (d, *J* = 8.3 Hz, 2H), 7.57 – 7.51 (m, 4H), 5.61 (s, 4H); ^{13}C NMR (151 MHz, $CDCl_3$) δ 144.47, 135.11, 133.37, 133.20, 131.16, 128.55, 128.43, 128.17, 127.80, 127.46, 127.32, 126.30, 126.25, 126.20, 124.74, 123.10, 119.68, 75.87 (only 18 of 19 carbons observed); HRMS (ESI) calculated for $C_{38}H_{27}O_2$ ($[M+H]^+$) *m/z* = 515.2011, found 515.2015.

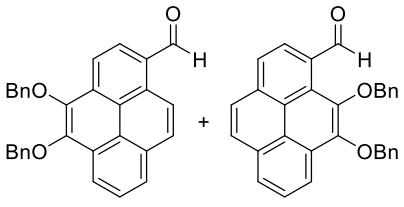

39.2 **39.3**

Compounds 39.2 and 39.3: $POCl_3$ (0.022 g, 0.14 mmol) was added dropwise to a stirred 0 °C solution of *N*-methylformanilide (0.009 g, 0.07 mmol) in 1,2-dichlorobenzene (0.6 mL). After 10 min., the cooling bath was removed, and the temperature was increased to 80 °C. After 15 min., a solution of **39.1** (0.010 g, 0.024 mmol) in 1,2-dichlorobenzene (0.3 mL) was added and the reaction was heated at 80 °C for 24 h. The reaction mixture was cooled to room temperature, diluted with dichloromethane (10 mL), then poured into ice water (10 mL), and the layers were separated. The aqueous

phase was extracted with dichloromethane (3 × 5 mL). The combined organic extracts were washed with brine (25 mL), dried over $MgSO_4$, filtered and concentrated under reduced pressure. The residue was purified by flash chromatography (1.3 × 18 cm; 60% dichloromethane/hexanes) to afford an inseparable mixture of constitutional isomers **39.2** and **39.3** (3.8:1 *r.r*) as a yellow solid (0.0084 g, 84%): R_f = 0.36 (60% dichloromethane/hexanes); ^{1}H NMR (600 MHz, $CDCl_3$) δ 11.51 (s, 1H), 10.77 (s, 3H), 9.47 (d, *J* = 9.2 Hz, 4H), 8.66 (d, *J* = 7.8 Hz, 4H), 8.63 – 8.61 (m, 5H), 8.52 (d, *J* = 8.1 Hz, 1H), 8.46 (d, *J* = 8.1 Hz, 4H), 8.34 (d, *J* = 9.2 Hz, 4H), 8.30 (d, *J* = 7.6 Hz, 4H), 8.27 (d, *J* = 7.6 Hz, 1H), 8.23 – 8.18 (m, 3H), 8.13 – 8.08 (m, 7H), 7.63 – 7.60 (m, 18H), 7.50 – 7.48 (m, 3H), 7.47 – 7.43 (m, 19H), 7.42 – 7.38 (m, 10H), 5.53 (s, 2H), 5.49 (s, 7H), 5.41 (s, 7H), 5.29 (s, 2H); HRMS (ESI) calculated for the mixture of constitutional isomers $C_{31}H_{23}O_3$ ($[M+H]^+$) *m/z* = 443.1647, found 443.1642.

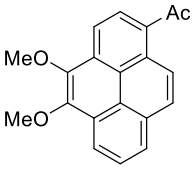

40.1

Compound 40.1: Acetyl chloride (0.065 g, 0.84 mmol) was added to a stirred 0 °C solution of $AlCl_3$ (0.25 g, 1.7 mmol) and 4,5-dimethoxypyrene (0.20 g, 0.76 mmol) in dichloromethane (8 mL). After 15 min., the reaction mixture was poured into ice water (10 mL), the layers were separated, and the aqueous phase was extracted with dichloromethane (3 × 10 mL). The combined organic extracts were washed with a saturated solution of $NaHCO_3$ (20 mL) and brine (20 mL), dried over $MgSO_4$, filtered and concentrated under reduced pressure. The residue was purified by flash chromatography (2.5 × 15 cm, dichloromethane) to afford **6** as a bright yellow solid (0.20 g, 87%): R_f = 0.12 (80% dichloromethane/hexane); ^{1}H NMR (600 MHz, $CDCl_3$) δ 9.09 (d, *J* = 9.3 Hz, 1H), 8.58 (d, *J* = 7.8 Hz, 1H), 8.49 (d, *J* = 8.3 Hz, 1H), 8.43 (d, *J* = 8.3 Hz, 1H), 8.25 – 8.18 (m, 2H), 8.11 – 8.06 (m, 1H), 4.26 (s, 3H), 4.21 (s, 3H), 2.92 (s, 3H); ^{13}C NMR (151 MHz, $CDCl_3$) δ 202.25, 146.73, 144.24, 131.79, 131.45, 130.64, 129.91, 129.69, 128.40, 127.68, 126.67, 125.80, 125.13, 123.29, 122.71, 120.85, 118.32, 61.48, 61.38, 30.65; HRMS (ESI) calculated for **6** $C_{20}H_{17}O_3$ ($[M+H]^+$) *m/z* = 305.1178, found 305.1231.

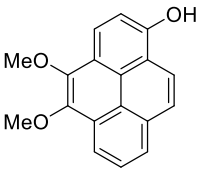

38.3

Alternative synthesis of Compound 38.1: SeO_2 (0.001 g, 0.001 mmol) and a 30% solution (w/w) of hydrogen peroxide in water (0.13 mL, 1.1 mmol) were added to a stirred 50 °C solution of **40.1** (0.086 g, 0.28 mmol) in *t*-BuOH (3 mL). After 4 h, the reaction mixture was cooled to room temperature, poured into water (30 mL) and further diluted with dichloromethane (15 mL). The layers were separated, and the aqueous phase was extracted

with dichloromethane (3 × 15 mL). The combined organic extracts were washed with water (50 mL) and brine (50 mL), dried over $MgSO_4$, filtered and concentrated under reduced pressure to afford the corresponding acetate ester as a light brown solid: R_f = 0.45 (dichloromethane); ^{1}H NMR (400 MHz, $CDCl_3$) δ 8.63 – 8.39 (m, 2H), 8.16 (d, *J* = 7.7, 1H), 8.13 – 8.07 (m, 2H), 8.05 (d, *J* = 7.8 Hz, 1H), 7.83 (d, *J* = 8.5 Hz, 1H), 4.23 (s, 3H), 4.22 (s, 3H) 2.58 (s, 3H); ^{13}C NMR (101 MHz, $CDCl_3$) δ 169.97, 144.70, 144.56, 144.06, 130.93, 128.62, 128.14, 126.58, 126.46, 124.75, 123.79, 123.13, 122.69, 120.14, 119.91, 119.86, 119.60, 61.22, 21.16; HRMS (ESI) calculated for $C_{20}H_{17}O_4$ ($[M+H]^+$) *m/z* = 321.1127, found 321.1111. Potassium carbonate (0.64 g, 4.6 mmol) was added to a stirred solution of the acetate ester derivative in MeOH (20 mL) at room temperature. After 30 min., the reaction mixture was poured into ice water (10 mL) and neutralized with 1 M HCl (10 mL), the layers were separated and the aqueous phase was extracted with dichloromethane (3 × 10 mL). The combined organic extracts were washed with a saturated solution of $NaHCO_3$ (20 mL), dried over $MgSO_4$, filtered and concentrated under reduced pressure. The residue was purified by flash chromatography (1.3 cm × 15 cm, dichloromethane) to afford **38.3** as a light yellow solid (0.042 g, 54% overall).

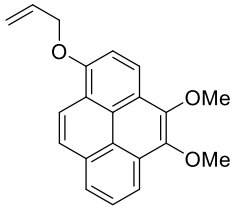

41.1

Compound 41.1: K_2CO_3 (0.126 g, 0.912 mmol) and allyl bromide (0.11 g, 0.91 mmol) were added to a stirred solution of **38.4** (0.168 g, 0.603 mmol) in DMF (13 mL) at room temperature. After 2 h, the reaction mixture was poured into water (100 mL) and further diluted with 1 M HCl (50 mL). The resulting mixture was extracted with EtOAc (5 × 20 mL), the combined organic extracts were washed with 1 M HCl (3 × 30 mL) and a saturated solution of $NaHCO_3$ (50 mL), dried over $MgSO_4$, filtered and concentrated under reduced pressure. The residue was purified by flash chromatography (2.5 cm × 15 cm; 50% dichloromethane/hexanes) to afford **41.1** as a yellow solid (0.15 g, 87%): R_f = 0.39 (50% dichloromethane/hexanes); ^{1}H NMR (600 MHz, $CDCl_3$) δ 8.53 (d, *J* = 9.1 Hz, 1H), 8.46 – 8.39 (m, 2H), 8.11 (d, *J* = 7.6 Hz, 1H), 8.08 – 8.00 (m, 2H), 7.55 (d, *J* = 8.6 Hz, 1H), 6.27 (ddt, *J* = 17.3, 10.4, 5.1 Hz, 1H), 5.62 (dd, *J* = 17.3, 1.6 Hz, 1H), 5.42 (dd, *J* = 10.6, 1.5 Hz, 1H), 4.94 – 4.85 (m, 2H), 4.26 (s, 3H), 4.22 (s, 3H); ^{13}C NMR (151 MHz, $CDCl_3$) δ 152.57, 145.08, 143.01, 133.53, 131.76, 129.24, 126.50, 126.42, 124.34, 123.91, 123.21, 122.31, 121.37, 120.84, 120.11, 118.81, 117.78, 109.72, 69.85, 61.32, 61.21; HRMS (ESI) calculated for $C_{21}H_{19}O_3$ ($[M+H]^+$) *m/z* = 319.1334, found 319.1348.

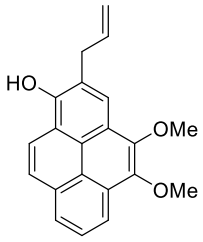

41.2

Compound 41.2: Compound **41.1** (0.105 g, 0.331 mmol) was dissolved in *N*,*N*-diethylaniline (0.2 mL) and heated to 190 °C. After 12 h, the solvent was evaporated under a gentle stream of nitrogen and the residue was purified by flash chromatography (1.3 × 15 cm; 10% EtOAc/hexanes) to afford **41.2** as an off-white solid (0.078 g, 74%): R_f = 0.27 (10% EtOAc/hexanes); ^{1}H NMR (600 MHz, $CDCl_3$) δ 8.47 – 8.21 (m, 3H), 8.16 – 7.89 (m, 3H), 6.22 (ddt, *J* = 16.6, 10.1, 6.2 Hz, 1H), 5.94 – 5.89 (m, 1H), 5.39 – 5.29 (m, 2H), 4.24 (s, 3H), 4.19 (s, 3H), 3.89 (bs, 2H); ^{13}C NMR (151 MHz, $CDCl_3$) δ 148.80, 144.99, 143.06, 136.44, 131.42, 128.88, 126.68, 126.26, 123.85, 123.54, 123.14, 122.69, 122.19, 121.35, 120.83, 119.64, 118.91, 117.70, 61.39, 61.24, 36.99; HRMS (ESI) calculated for $C_{21}H_{19}O_3$ ($[M+H]^+$) *m/z* = 319.1334, found 319.1336.

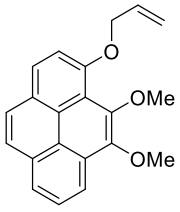

41.3

Compound 41.3: K_2CO_3 (0.091 g, 0.66 mmol) and allyl bromide (0.08 g, 0.7 mmol) were added to a stirred solution of **38.4** (0.061 g, 0.22 mmol) in DMF (7 mL) at room temperature. After 20 h, the reaction mixture was poured into water (20 mL) and further diluted with 1 M HCl (25 mL). The resulting mixture was extracted with diethyl ether (3 × 15 mL), the combined organic extracts were washed with brine (40 mL), dried over $MgSO_4$, filtered and concentrated under reduced pressure. The residue was purified by flash chromatography (1.3 × 15 cm; 40% dichloromethane/hexanes) to afford **41.3** as a light brown solid (0.045 g, 98%): R_f = 0.22 (40% dichloromethane/hexanes); ^{1}H NMR (400 MHz, $CDCl_3$) δ 8.40 (d, *J* = 7.5 Hz, 1H), 8.11 – 7.85 (m, 5H), 7.60 (d, *J* = 8.5 Hz, 1H), 6.40 – 6.23 (m, 1H), 5.62 (d, *J* = 17.2 Hz, 1H), 5.41 (d, *J* = 10.1 Hz, 1H), 4.89 (d, *J* = 5.6 Hz, 2H), 4.23 (s, 3H), 4.10 (s, 3H); ^{13}C NMR (101 MHz, $CDCl_3$) δ 153.59, 146.87, 146.33, 133.74, 132.01, 128.84, 127.56, 126.45, 126.02, 125.76, 125.39, 125.35, 124.22, 123.59, 118.38, 118.09, 117.95, 112.68, 71.41, 61.97, 61.53; HRMS (ESI) calculated for $C_{21}H_{19}O_3$ ($[M+H]^+$) *m/z* = 319.1334, found 319.1324.

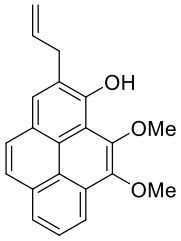

41.4

Compound 41.4: Compound **41.3** (0.229 g, 0.719 mmol) was dissolved in *N*,*N*-diethylaniline (0.3 mL) and heated to 190 °C. After 9 h, the solvent was evaporated under a gentle stream of nitrogen and the residue was purified by flash chromatography (1.3 × 15 cm; 40% dichloromethane/hexanes) to afford **41.4** as a dark yellow solid (0.13 g, 62% BORSM, 0.022 g recovered of **41.3** and 0.041 g of **38.4**): R_f = 0.35 (40% dichloromethane/hexanes); ^{1}H NMR (400 MHz, $CDCl_3$) δ 10.31 (s, 1H), 8.28 (d, *J* = 7.2 Hz, 1H), 8.04 (d, *J* = 7.5 Hz, 1H), 7.98 – 7.88 (m, 3H), 7.84 (d, *J* = 8.8 Hz, 1H), 6.24 (ddt, *J* = 16.7, 10.1, 6.5 Hz, 1H), 5.24 – 5.13 (m, 2H), 4.30 (s, 3H), 4.14 (s, 3H), 3.81 (d, *J* = 6.4 Hz, 2H); ^{13}C NMR (101 MHz, $CDCl_3$) δ 151.06, 145.71, 144.05, 137.13, 131.92, 128.48, 127.50, 127.41, 126.17, 126.14, 124.48, 124.38, 124.24, 123.87, 123.50, 117.65, 116.00, 112.39, 62.21, 61.17, 34.79; HRMS (ESI) calculated for $C_{21}H_{19}O_3$ ($[M+H]^+$) *m/z* = 319.1334, found 319.1319.

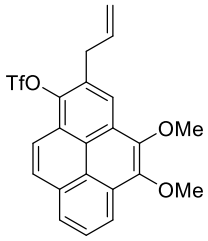

42.1

Compound 42.1: Triflic anhydride (0.14 g, 0.35 mmol) and pyridine (0.03 g, 0.3 mmol) were added to a stirred 0 °C solution of **41.2** (0.056 g, 0.18 mmol) in dichloromethane (3.5 mL). The cooling bath was removed and 10 min. later the reaction mixture was poured into 1 M HCl (30 mL). The resulting mixture was extracted with dichloromethane (3 × 15 mL), the combined organic extracts were washed with and brine (35 mL), dried over $MgSO_4$, filtered and concentrated under reduced pressure. The residue was purified by flash chromatography (1.3 × 12 cm; 20% dichloromethane/hexanes) to afford **42.1** as a yellow solid (0.071 g, 89%): R_f = 0.32 (20% dichloromethane/hexanes); ^{1}H NMR (600 MHz, $CDCl_3$) δ 8.54 (d, *J* = 7.8, 1.1 Hz, 1H), 8.41 (s, 1H), 8.28 (d, *J* = 9.2 Hz, 1H), 8.22 – 8.15 (m, 2H), 8.10 – 8.02 (m, 1H), 6.17 (ddt, *J* = 16.1, 10.6, 6.6 Hz, 1H), 5.33 – 5.26 (m, 2H), 4.23 – 4.21 (m, 6H), 4.00 (d, 2H); ^{13}C NMR (151 MHz, $CDCl_3$) δ 145.78, 144.12, 140.12, 135.45, 131.43, 130.47, 129.66, 128.55, 128.52, 126.91, 125.66, 124.66, 122.87, 122.17, 121.28, 120.93, 120.14, 119.02 (J_{C-F} = 318 Hz), 117.78, 61.41, 61.39, 35.44; HRMS (ESI) calculated for $C_{22}H_{16}O_5F_3S$ ($[M-H]^-$) *m/z* = 449.0676, found 449.0667.

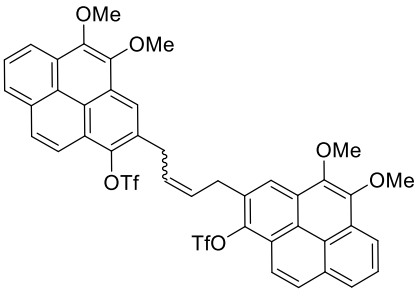

Compound 42.5: Grubbs first-generation catalyst (0.001 g, 0.001 mmol) was added to a stirred 40 °C solution of **42.1** (0.020 g, 0.043 mmol) in dichloromethane (0.8 mL). After 12 h, the reaction mixture was cooled to room temperature and the solvent was evaporated under reduced pressure. The residue was purified by flash chromatography (1.3 × 10 cm; 30% dichloromethane/hexanes) to afford **42.5** (dark yellow solid, 0.014 g, 78%, 4.7:1 *d.r*) as an inseparable mixture of diastereomers: R_f = 0.27 (35% dichloromethane/hexanes); ^{1}H NMR (400 MHz, $CDCl_3$) δ 8.52 – 8.48 (m, 5H), 8.43 – 8.40 (m, 1H), 8.37 (s, 5H), 8.28 – 8.23 (m, 6H), 8.18 (d, *J* = 1.4 Hz, 5H), 8.16 (d, *J* = 1.1 Hz, 5H), 8.07 – 7.94 (m, 9H), 6.19 – 6.15 (m, 1H), 6.02 – 5.96 (m, 5H), 4.15 (s, 14H), 4.13 – 4.10 (m, 2H), 4.07 – 4.04 (m, 18H), 4.02 – 3.98 (m, 13H); ^{13}C NMR (151 MHz, $CDCl_3$) δ 145.79, 145.55, 144.14, 143.99, 140.10, 139.85, 131.80, 131.73, 130.51, 130.31, 130.21, 129.69, 129.42, 129.41, 128.62, 128.55, 128.43, 128.38, 126.96, 126.81, 125.69, 125.58, 124.71, 124.40, 122.90, 122.52, 122.20, 121.91, 121.33, 120.96, 120.80, 120.72, 120.19, 120.06, 119.75, 117.94, 61.40, 61.28, 61.25, 61.15, 34.37, 29.93, 29.05; HRMS (ESI) calculated for $C_{42}H_{31}O_{10}F_6S_2$ ($[M+H]^+$) *m/z* = 873.1263, found 873.1262.

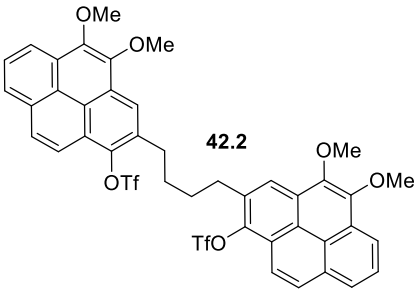

Compound 42.2: Hoveyda-Grubbs second-generation catalyst (0.010 g, 0.016 mmol) and $NaBH_4$ (0.025 g, 0.66 mmol) were added to stirred solution of **42.1** (0.110 g, 0.126 mmol) in 1:9 methanol/dichloromethane (14 mL). After 2 h, the reaction mixture was poured into water (30 mL) and further diluted with 1 M HCl (15 mL). The resulting mixture was extracted with dichloromethane (3 × 10 mL), and the combined organic extracts were washed with brine (20 mL), dried over $MgSO_4$, filtered and concentrated under reduced pressure. The residue was purified by flash chromatography (1.3 × 15 cm; 40% dichloromethane/hexanes) to afford **42.2** as an off-white solid (0.070 g, 70% BORSM, 0.010 g of **42.1**): R_f = 0.21 (40% dichloromethane/hexanes); ^{1}H NMR (600 MHz, $CDCl_3$) δ 8.55 (d, *J* = 7.9, 1.1 Hz, 2H), 8.40 (s, 2H), 8.26 (d, *J* = 9.2 Hz, 2H), 8.23 – 8.17 (m, 4H), 8.13 – 8.07 (m, 2H), 4.22 (s, 6H), 4.19 (s, 6H), 3.32 (t, 4H), 2.12 – 2.02 (m, 4H); ^{13}C NMR (151 MHz, $CDCl_3$) δ 148.14, 142.93, 140.12, 133.56, 130.74, 130.64, 128.57, 127.81, 126.62, 126.42,

125.95, 125.72, 123.03, 122.16, 121.17, 120.27, 117.87 ($J_{C\text{-}F}$ = 318 Hz), 61.71, 60.76, 30.50, 30.23; HRMS (ESI) calculated for $C_{42}H_{33}O_{10}F_6S_2$ ([M+H]$^+$) *m/z* = 875.1419, found 875.1459.

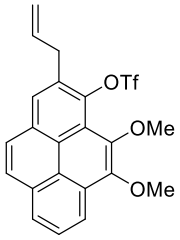

42.3

Compound 42.3: Triflic anhydride (0.22 g, 0.60 mmol) was added to a stirred 0 °C solution of **41.3** (0.064 g, 0.20 mmol) in pyridine (2 mL). The cooling bath was removed, and the temperature increased to 40 °C. After 4 h, the reaction mixture was cooled to room temperature, diluted with dichloromethane (10 mL), and poured into 1 M HCl (50 mL). The layers were separated, and the aqueous phase was extracted with dichloromethane (3 × 15 mL), the combined organic extracts were washed with 1 M HCl (20 mL), a saturated solution of $NaHCO_3$ (20 mL) and brine (20 mL), dried over $MgSO_4$, filtered and concentrated under reduced pressure. The residue was purified by flash chromatography (1.3 × 15 cm; 20% dichloromethane/hexanes) to afford **42.3** as a light yellow solid (0.046 g, 51%): R_f = 0.23 (20% dichloromethane/hexanes); ^{1}H NMR (600 MHz, $CDCl_3$) δ 8.54 (d, *J* = 7.7 Hz, 1H), 8.18 (d, *J* = 7.5 Hz, 1H), 8.10 – 8.01 (m, 3H), 7.99 (d, *J* = 9.0 Hz, 1H), 7.81 (d, *J* = 8.8 Hz, 1H), 6.12 – 6.08 (m, 1H), 5.37 – 5.25 (m, 2H), 4.32 (s, 3H), 3.99 (s, 3H), 3.95 (d, *J* = 7.0 Hz, 2H); ^{13}C NMR (151 MHz, $CDCl_3$) δ 148.36, 143.17, 140.11, 135.69, 131.61, 130.97, 130.76, 128.77, 128.05, 126.84, 126.69, 126.26, 126.13, 123.40, 122.34, 121.42, 120.45, 119.06 ($J_{C\text{-}F}$ = 317 Hz), 117.99, 61.90, 61.07, 34.61; HRMS (ESI) calculated for $C_{22}H_{18}O_5F_3S$ ([M+H]$^+$) *m/z* = 451.0827, found 451.0825.

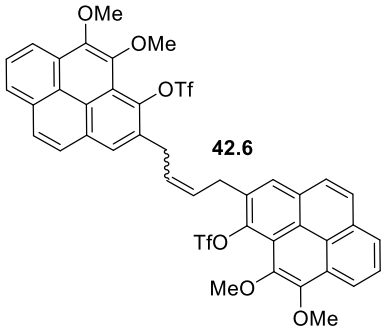

42.6

Compound 42.6: Grubbs first-generation catalyst (0.003 g, 0.003 mmol) was added to a stirred 40 °C solution of **42.3** (0.047 g, 0.10 mmol) in dichloromethane (0.8 mL). After 12 h, the reaction mixture was cooled to room temperature and the solvent was evaporated under reduced pressure. The residue was purified by flash chromatography (1.3 × 15 cm; 30% dichloromethane/hexanes) to afford **42.6** (light yellow solid, 0.031 g, 67%, 2.7:1 *d.r.*) as an inseparable mixture of diastereomers: R_f = 0.38 (30% dichloromethane/hexanes); ^{1}H NMR (600 MHz, $CDCl_3$ δ 8.54 (d, *J* = 7.7 Hz, 4H), 8.20 (d, *J* = 7.5 Hz, 3H), 8.16 (d, *J* = 7.6 Hz, 1H), 8.12 – 8.04 (m, 10H), 7.99 (d, *J* = 9.0 Hz, 5H), 7.81 (d, *J* = 8.8 Hz, 1H), 6.12 – 6.08 (m, 1H), 6.02 – 5.97 (m, 3H), 4.32 – 4.27 (m, 12H), 4.18 –

4.14 (m, 2H), 4.04 – 3.98 (m, 6H), 3.95 (s, 3H), 3.89 (s, 9H); ^{13}C NMR (151 MHz, $CDCl_3$) δ 148.44, 148.41, 143.13, 140.12, 140.09, 131.93, 130.99, 130.93, 130.84, 130.56, 129.61, 128.87, 128.80, 128.06, 128.04, 126.89, 126.71, 126.54, 126.26, 126.20, 126.18, 125.85, 123.43, 122.34, 122.29, 121.53, 121.46, 120.51, 120.50, 120.12, 117.99, 61.89, 61.02, 60.99, 33.57, 28.27; HRMS (ESI) calculated for $C_{42}H_{31}O_{10}F_6S_2$ ([M+H]$^+$) *m/z* = 873.1263, found 873.1257.

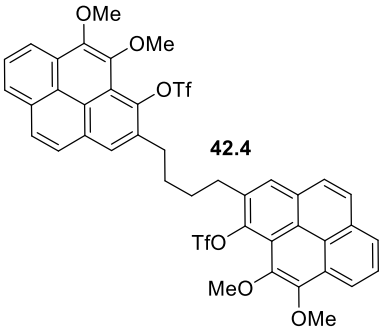

42.4

Compound 42.4: Hoveyda-Grubbs second-generation catalyst (0.0005 g, 0.0009 mmol) and $NaBH_4$ (0.006 g, 0.1 mmol) were added to stirred solution of **42.6** (0.025 g, 0.029 mmol) in 1:9 methanol/dichloromethane (1.5 mL). After 2 h, the reaction mixture was poured into water (25 mL) and diluted with 1 M HCl (15 mL). The resulting mixture was extracted with dichloromethane (3 × 12 mL), the combined organic extracts were washed with brine (20 mL), dried over $MgSO_4$, filtered and concentrated under reduced pressure. The residue was purified by flash chromatography (0.5 × 10 cm; 40% dichloromethane/hexanes) to afford **42.4** as an off-white solid (0.012 g, 95%): R_f = 0.30 (40% dichloromethane/hexanes); ^{1}H NMR (600 MHz, $CDCl_3$) δ 8.52 (d, *J* = 7.8, 1.2 Hz, 2H), 8.17 (d, *J* = 8.0, 7.6 Hz, 2H), 8.08 – 8.02 (m, 4H), 7.99 (s, 2H), 7.91 (d, *J* = 8.9 Hz, 2H), 4.29 (s, 6H), 3.90 (s, 6H), 3.26 (t, *J* = 6.8 Hz, 4H), 2.10 – 1.94 (m, 4H).; ^{13}C NMR (151 MHz, $CDCl_3$) δ 148.14, 142.93, 140.12, 133.55, 130.73, 130.64, 128.57, 127.80, 126.62, 126.42, 125.96, 125.73, 123.03, 122.16, 121.17, 120.27, 118.88 ($J_{C\text{-}F}$ = 317 Hz), 61.72, 60.77, 30.51, 30.23, 29.74; HRMS (ESI) calculated for $C_{42}H_{32}O_{10}F_6S_2Na$ ([M+Na]) *m/z* = 897.1239, found 897.1194.

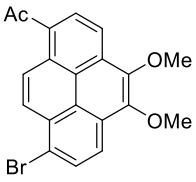

46.2

Compound 46.2: Bromine (0.06 g, 0.4 mmol) was added dropwise to a stirred –78 °C solution of 4,5-dimethoxypyrene (0.10 g, 0.38 mmol) in dichloromethane (20 mL). After 10 min., the reaction mixture was directly poured into an aqueous saturated solution of Na_2SO_3 (10 mL), and the resulting mixture was extracted with dichloromethane (3 × 10 mL). The combined organic extracts were washed with water (20 mL) and brine (20 mL), dried over $MgSO_4$, filtered and concentrated under reduced pressure. The residue was dissolved in dichloromethane (10 mL) and cooled to 0 °C, followed by addition of acetyl chloride (0.031 g,

0.42 mmol) and $AlCl_3$ (0.14 g, 0.83 mmol). After 30 min., the reaction mixture was directly poured into ice water (20 mL), the layers were separated, and the aqueous phase was extracted with dichloromethane (3 × 10 mL). The combined organic extracts were washed water (20 mL) and brine (20 mL), dried over $MgSO_4$, filtered and concentrated under reduced pressure. The residue was purified by flash chromatography (1.3 × 18 cm; 50% dichloromethane/hexanes) to afford **46.2** as a bright yellow solid (0.10 g, 70%): R_f = 0.29 (60% dichloromethane/hexanes); ^{1}H NMR (600 MHz, $CDCl_3$) δ 9.09 (d, *J* = 9.6 Hz, 1H), 8.51 – 8.45 (m, 2H), 8.41 (d, *J* = 8.2 Hz, 1H), 8.36 (d, *J* = 8.4 Hz, 1H), 8.24 (d, *J* = 8.4 Hz, 1H), 4.24 (s, 3H), 4.19 (s, 3H), 2.91 (s, 3H); ^{13}C NMR (151 MHz, $CDCl_3$) δ 201.86, 146.08, 143.93, 131.66, 131.39, 130.61, 129.27, 128.84, 128.08, 128.01, 127.75, 126.42, 123.57, 122.40, 121.23, 120.88, 118.80, 61.35, 61.23, 30.49; HRMS (ESI) calculated for $C_{20}H_{16}BrO_3$ ($[M+H]^+$) *m/z* = 383.0283, found 383.0276.

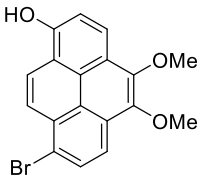

46.3

Compound 46.3: SeO_2 (0.009 g, 0.08 mmol) and a 30% solution (w/w) of hydrogen peroxide in water (1.0 mL, 12 mmol) were added to a stirred 50 °C solution of **46.2** (0.89 g, 2.9 mmol) in *t*-BuOH (12 mL). After 3 days, the reaction mixture was cooled to room temperature, poured into water (30 mL) and further diluted with dichloromethane (15 mL). The layers were separated, and the aqueous phase was extracted with dichloromethane (3 × 15 mL). The combined organic extracts were washed with water (50 mL) and brine (50 mL), dried over $MgSO_4$, filtered and concentrated under reduced pressure. The residue was purified by flash chromatography (2.5 × 18 cm, 80% dichloromethane/hexane) to afford the acetate ester (0.533 g, 57%): R_f = 0.48 (80% dichloromethane/hexanes); ^{1}H NMR (600 MHz, $CDCl_3$) δ 8.53 (d, *J* = 8.5 Hz, 1H), 8.47 (d, *J* = 9.4 Hz, 1H), 8.35 (d, *J* = 8.4 Hz, 1H), 8.27 (d, *J* = 8.4 Hz, 1H), 8.17 (d, *J* = 9.3 Hz, 1H), 7.85 (d, *J* = 8.5 Hz, 1H), 4.21 (s, 3H), 4.19 (s, 3H), 2.58 (s, 3H); ^{13}C NMR (151 MHz, $CDCl_3$) δ 170.00, 144.72, 144.37, 144.22, 130.66, 129.42, 128.23, 126.75, 123.89, 123.18, 123.11, 121.79, 120.65, 120.53, 120.40, 119.83, 61.30, 61.27, 21.25; HRMS (ESI) calculated for the acetate ester $C_{20}H_{16}BrO_4$ ($[M+H]^+$) *m/z* = 399.0232, found 399.0215. The acetate ester derivative was dissolved in MeOH (20 mL) and K_2CO_3 (0.641 g, 4.64 mmol) was added, the resulting mixture was stirred for 30 min. The reaction mixture was directly poured into ice water (50 mL) and neutralized with 1 M HCl (40 mL), the layers were separated and the aqueous phase was extracted with dichloromethane (3 × 30 mL). The combined organic extracts were washed with a saturated solution of $NaHCO_3$ (50 mL), dried over $MgSO_4$, filtered and concentrated under reduced pressure to afford **46.3** as a light brown solid

(0.393 g, 82%): R_f = 0.24 (dichloromethane); HRMS (ESI) calculated for $C_{18}H_{13}BrO_3$ ($[M]^+$) *m/z* = 356.0048, found 356.0041. The ^1H and ^{13}C NMR spectra for **46.3** were poorly resolved. As such it was subjected to allylation and characterized at a later stage.

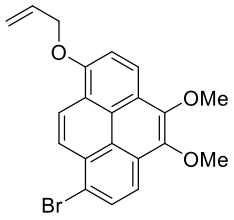

46.7

Compound 46.7: NaH (0.031 g, 1.3 mmol) and allyl bromide (0.17 g, 1.4 mmol) were added to a stirred solution of **46.3** (0.29 g, 0.82 mmol) in DMF (22 mL) at room temperature. After 30 min., the reaction mixture was poured into water (20 mL) and neutralized with 1 M HCl (20 mL). The resulting mixture was extracted with dichloromethane (3 × 15 mL), the combined organic extracts were washed with water (40 mL) and a saturated solution of $NaHCO_3$ (40 mL), dried over $MgSO_4$, filtered and concentrated under reduced pressure. The residue was purified by flash chromatography (2.5 × 18 cm; dichloromethane) to afford **76.7** as a yellow solid (0.30 g, 91%): R_f = 0.70 (dichloromethane); ^1H NMR (400 MHz, $CDCl_3$) δ 8.59 (d, *J* = 9.4 Hz, 1H), 8.43 (d, *J* = 8.7 Hz, 1H), 8.38 (d, *J* = 9.4 Hz, 1H), 8.25 – 8.20 (m, 2H), 7.58 (d, *J* = 8.7 Hz, 1H), 6.26 (ddt, *J* = 17.3, 10.4, 5.1 Hz, 1H), 5.60 (dd, *J* = 17.3, 1.6 Hz, 1H), 5.41 (dd, *J* = 10.6, Hz, 1H), 4.95 – 4.88 (m, 2H), 4.22 (s, 3H), 4.16 (s, 3H); ^{13}C NMR (151 MHz, $CDCl_3$) δ 152.77, 144.94, 142.42, 133.16, 130.42, 130.01, 128.71, 124.89, 124.22, 123.57, 122.89, 122.17, 120.82, 120.58, 119.34, 118.59, 117.91, 110.01, 69.71, 61.23, 61.13; HRMS (ESI) calculated for $C_{21}H_{18}BrO_3$ ($[M+H]^+$) *m/z* = 397.0439, found 397.0422.

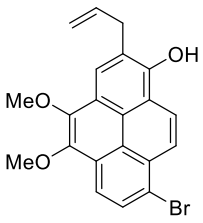

46.4

Compound 46.4: Compound **46.7** (0.29 g, 0.74 mmol) was dissolved in *N*,*N*-diethylaniline (2 mL) and heated to 190 °C. After 48 h, the solvent was evaporated under a gentle stream of nitrogen and the residue was purified by flash chromatography (2.5 × 18 cm; 50% dichloromethane/hexanes) to afford **46.4** as an off-white solid (0.21 g, 74%): R_f = 0.33 (50% dichloromethane/hexanes); HRMS (ESI) calculated for $C_{21}H_{17}BrO_3$ ($[M]^+$) *m/z* = 396.0361, found 396.0365. The ^1H and ^{13}C NMR spectra for **46.4** were poorly resolved. As such, it was subjected to triflation and characterized at a later stage.

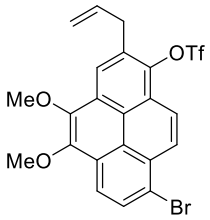

46.5

Compound 46.5: Trifluoromethanesulfonic anhydride (0.03 g, 0.1 mmol) and pyridine (0.01 g, 0.1 mmol) were added to a stirred 0 °C solution of **46.4** (0.021 g, 0.053 mmol) in dichloromethane (1.5 mL). After 10 min., the reaction mixture was diluted with dichloromethane (5 mL) and neutralized with 1 M HCl (10 mL). The layers were separated and the aqueous phase was extracted with dichloromethane (3 × 7 mL). The combined organic extracts were washed with 1 M HCl (10 mL), $NaHCO_3$ (10 mL), and brine (10 mL), dried over $MgSO_4$, filtered and concentrated under reduced pressure. The residue was purified by flash chromatography (0.5 × 10 cm; dichloromethane) to afford **46.5** as a yellow solid (0.027 g, 57%): R_f = 0.78 (dichloromethane); ^{1}H NMR (600 MHz, $CDCl_3$) δ 8.58 (d, *J* = 9.4 Hz, 1H), 8.43 (s, 1H), 8.41 – 8.35 (m, 2H), 8.30 (d, *J* = 8.3 Hz, 1H), 6.13 (ddt, *J* = 16.7, 9.9, 6.7 Hz, 1H), 5.31 – 5.25 (m, 2H), 4.22 – 4.18 (m, 6H), 3.98 (d, *J* = 6.6 Hz, 2H); ^{13}C NMR (151 MHz, $CDCl_3$) δ 145.25, 143.95, 140.09, 135.04, 132.06, 130.94, 128.93, 128.55, 128.16, 127.96, 124.49, 123.23, 122.13, 121.86, 121.56, 121.46, 120.72, 118.78 (J_{C-F} = 253 Hz), 117.88, 61.32, 61.27, 35.24; HRMS (ESI) calculated for $C_{22}H_{17}BrF_3O_5S$ ($[M+H]^+$) *m/z* = 528.9932, found 528.9926.

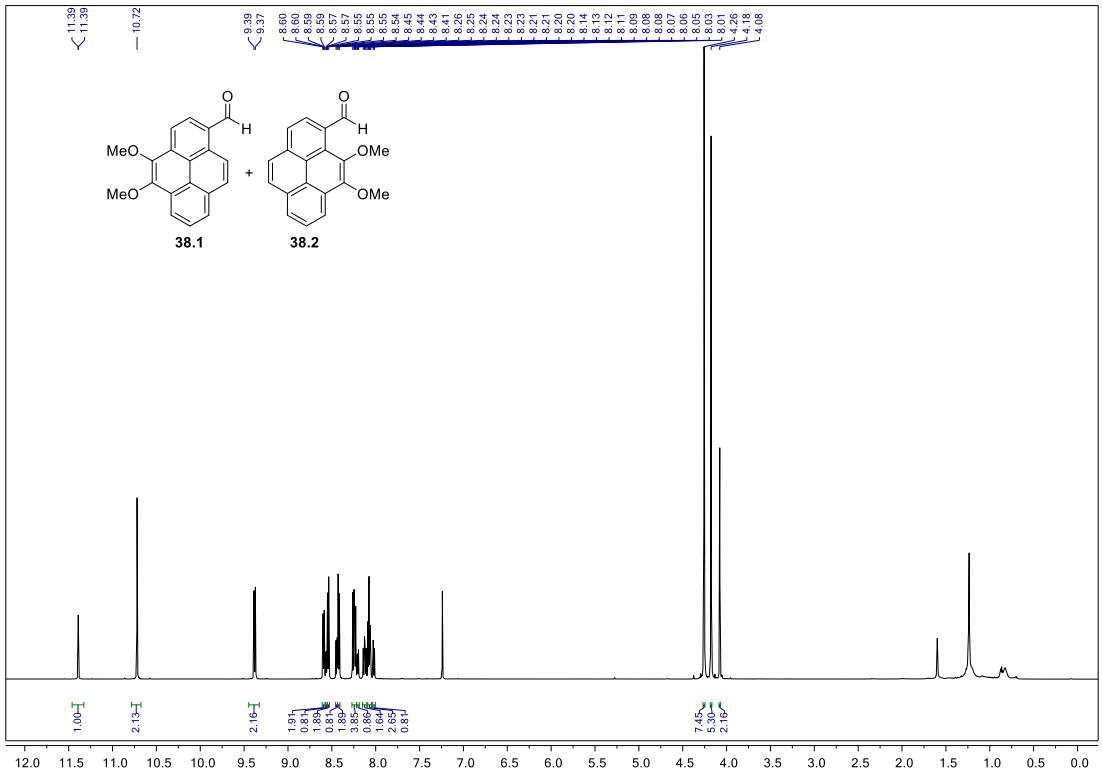
11.39
11.39
10.72
9.39
9.37
8.60
8.60
8.59
8.59
8.57
8.57
8.55
8.55
8.55
8.54
8.45
8.44
8.43
8.41
8.26
8.25
8.24
8.24
8.23
8.23
8.21
8.21
8.20
8.20
8.14
8.13
8.12
8.11
8.09
8.08
8.08
8.07
8.06
8.05
8.03
8.01
4.26
4.18
4.08
O
H
MeO
MeO
+
O
H
OMe
OMe
38.1
38.2
1.00
2.13
2.16
1.91
0.87
1.89
0.81
1.89
3.85
0.86
1.64
2.65
0.81
7.45
5.39
2.16
12.0
11.5
11.0
10.5
10.0
9.5
9.0
8.5
8.0
7.5
7.0
6.5
6.0
5.5
5.0
4.5
4.0
3.5
3.0
2.5
2.0
1.5
1.0
0.5
0.0

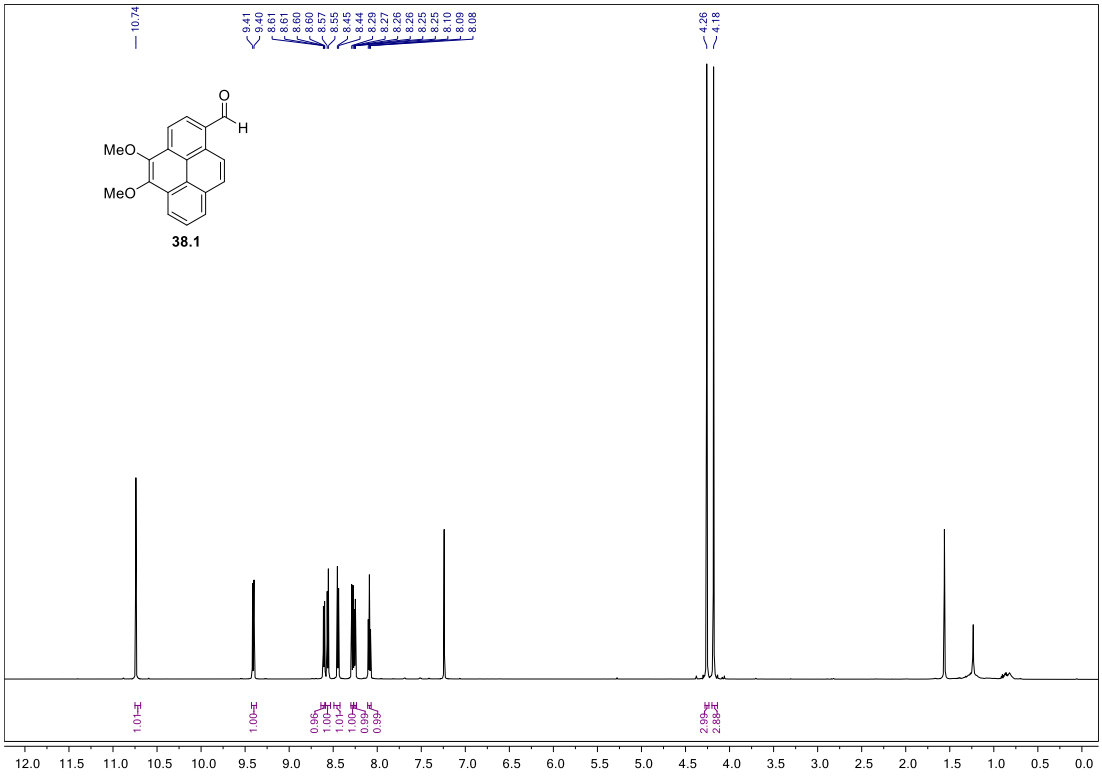
10.74
9.41
9.40
8.61
8.61
8.60
8.60
8.57
8.55
8.45
8.44
8.29
8.27
8.26
8.26
8.25
8.25
8.10
8.09
8.08
4.26
4.18
MeO
MeO
O
H
38.1
1.01
1.00
0.96
1.00
1.01
1.00
0.99
0.99
2.99
2.89
12.0 11.5 11.0 10.5 10.0 9.5 9.0 8.5 8.0 7.5 7.0 6.5 6.0 5.5 5.0 4.5 4.0 3.5 3.0 2.5 2.0 1.5 1.0 0.5 0.0

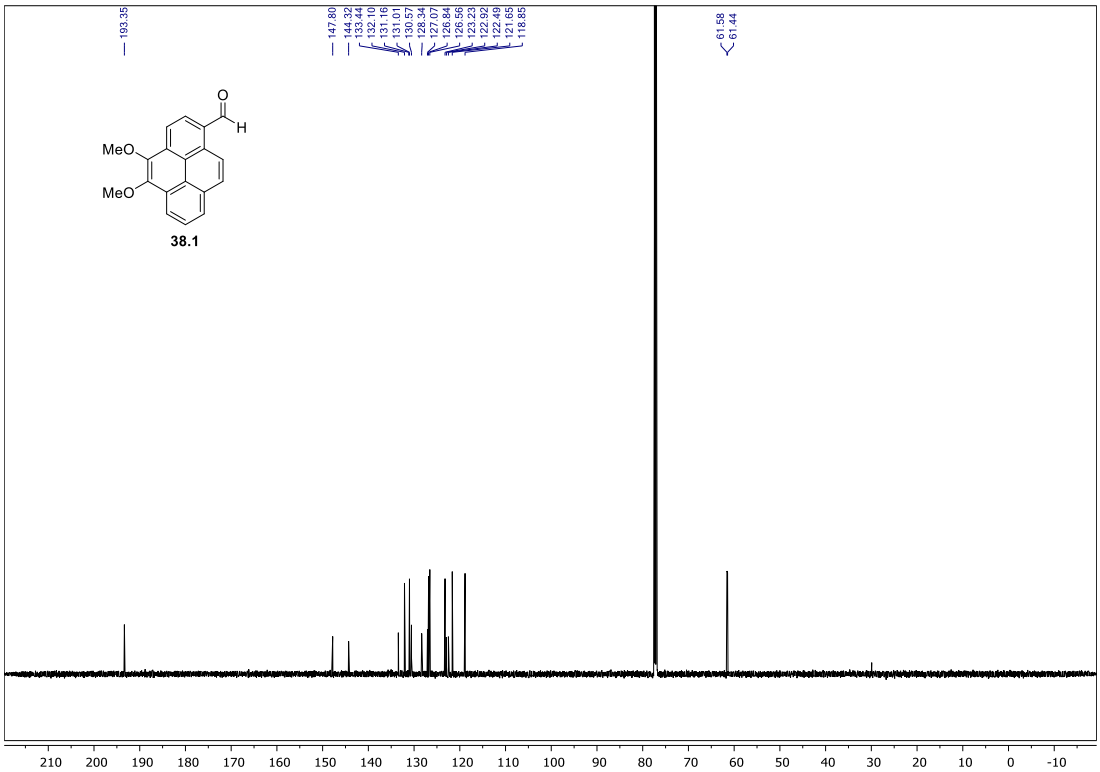
193.35
147.80
144.32
133.44
132.10
131.16
131.01
130.57
128.34
127.07
126.84
126.56
123.23
122.90
122.49
121.65
118.85
61.58
61.44
MeO
MeO
O
H
38.1
210 200 190 180 170 160 150 140 130 120 110 100 90 80 70 60 50 40 30 20 10 0 -10

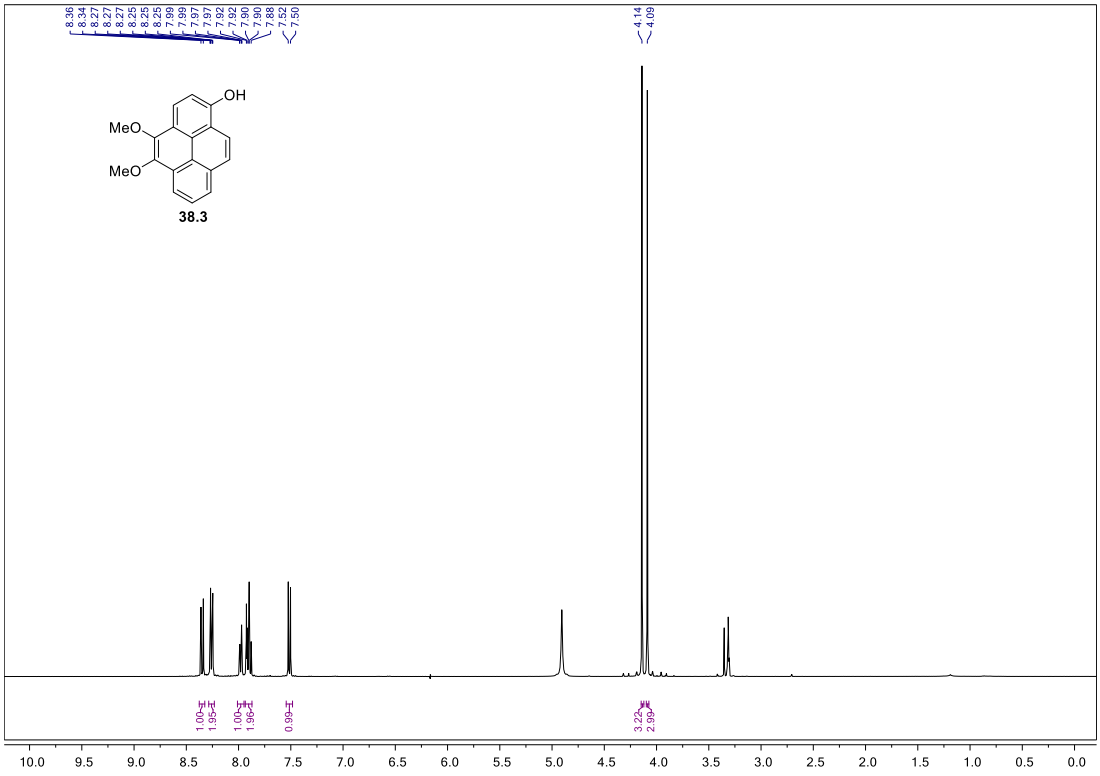
8.36
8.34
8.27
8.27
8.27
8.27
8.25
8.25
8.25
7.99
7.99
7.97
7.97
7.92
7.92
7.90
7.90
7.88
7.52
7.50
4.14
4.09
OH
MeO
MeO
38.3
1.00
1.95
1.00
1.96
0.99
3.23
2.99
10.0
9.5
9.0
8.5
8.0
7.5
7.0
6.5
6.0
5.5
5.0
4.5
4.0
3.5
3.0
2.5
2.0
1.5
1.0
0.5
0.0

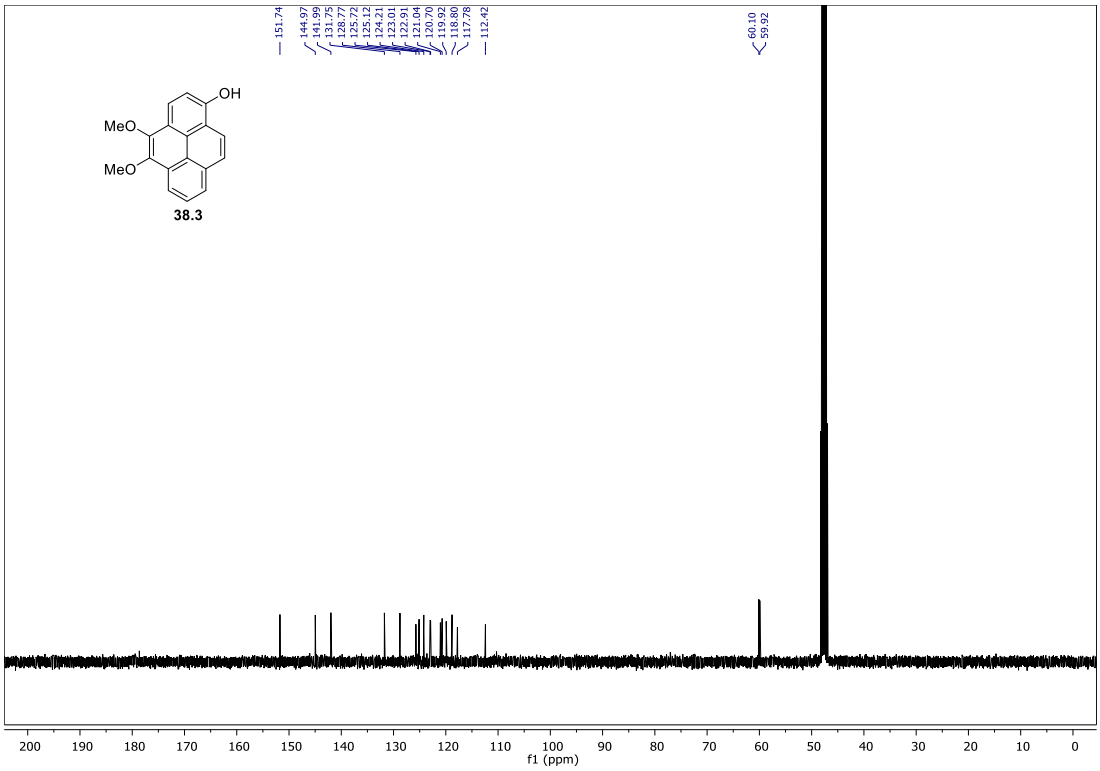
151.74
144.97
141.99
131.75
128.77
125.72
125.12
124.21
123.01
122.91
121.04
120.70
119.92
118.80
117.78
112.42
60.10
59.92
OH
MeO
MeO
38.3
200
190
180
170
160
150
140
130
120
110
100
90
80
70
60
50
40
30
20
10
0
f1 (ppm)

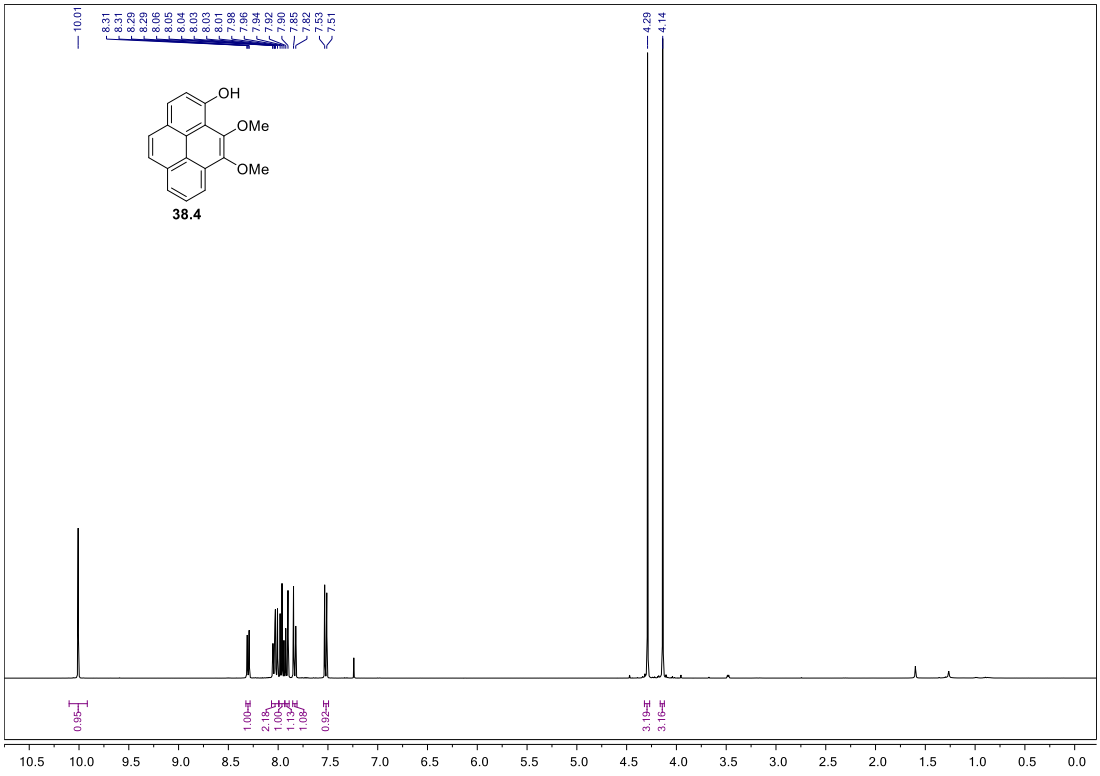
10.01
8.31
8.31
8.29
8.29
8.06
8.05
8.04
8.03
8.03
8.01
7.98
7.96
7.94
7.92
7.90
7.85
7.82
7.53
7.51
4.29
4.14
OH
OMe
OMe
38.4
0.95
1.00
2.18
1.00
1.13
1.09
0.92
3.19
3.16
10.5
10.0
9.5
9.0
8.5
8.0
7.5
7.0
6.5
6.0
5.5
5.0
4.5
4.0
3.5
3.0
2.5
2.0
1.5
1.0
0.5
0.0

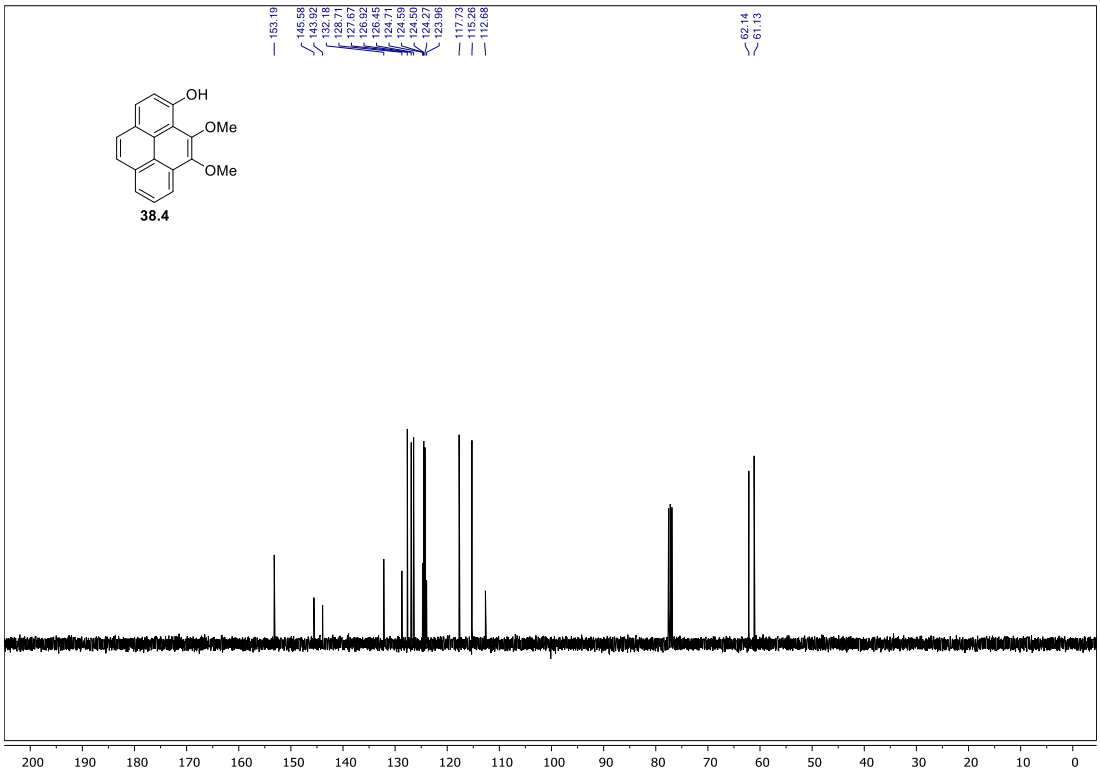
153.19
145.58
143.92
132.18
128.71
127.67
126.92
126.45
124.71
124.59
124.50
124.27
123.96
117.73
115.26
112.68
62.14
61.13
OH
OMe
OMe
38.4
200
190
180
170
160
150
140
130
120
110
100
90
80
70
60
50
40
30
20
10
0

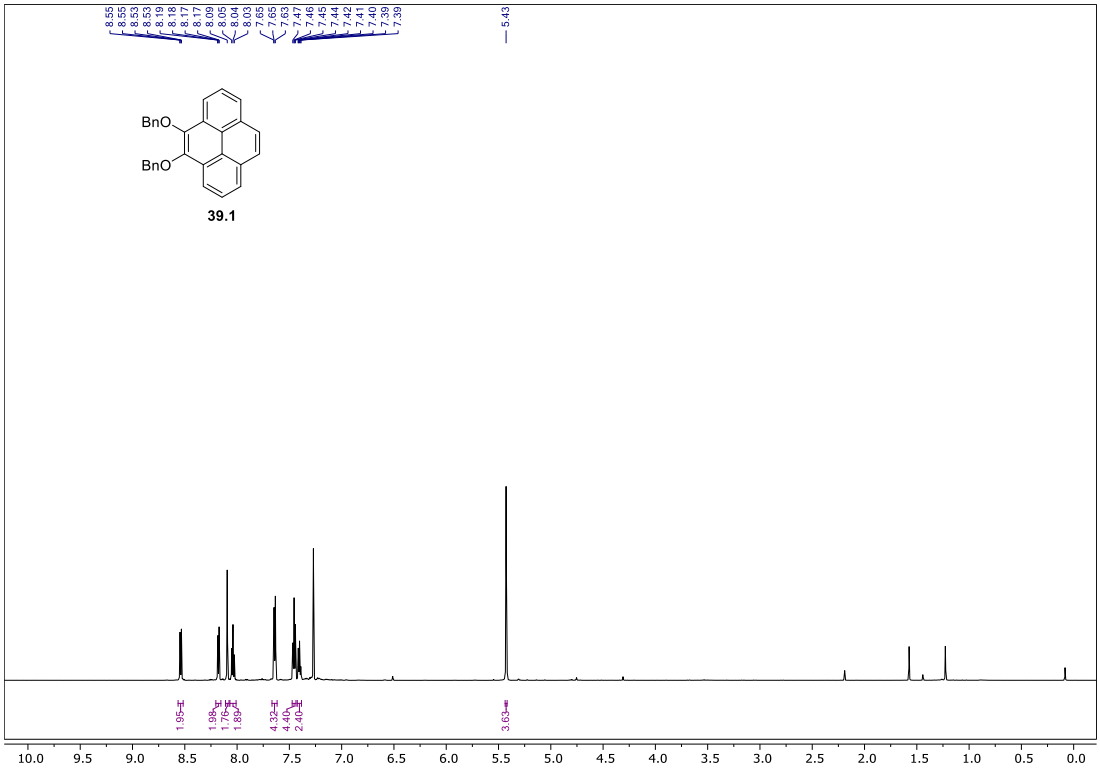
8.55
8.55
8.53
8.53
8.19
8.18
8.17
8.17
8.09
8.05
8.04
8.03
7.65
7.63
7.47
7.46
7.45
7.44
7.42
7.41
7.40
7.39
7.39
5.43
BnO
BnO
39.1
1.95
1.98
1.76
1.89
4.32
4.40
2.40
3.63
10.0 9.5 9.0 8.5 8.0 7.5 7.0 6.5 6.0 5.5 5.0 4.5 4.0 3.5 3.0 2.5 2.0 1.5 1.0 0.5 0.0

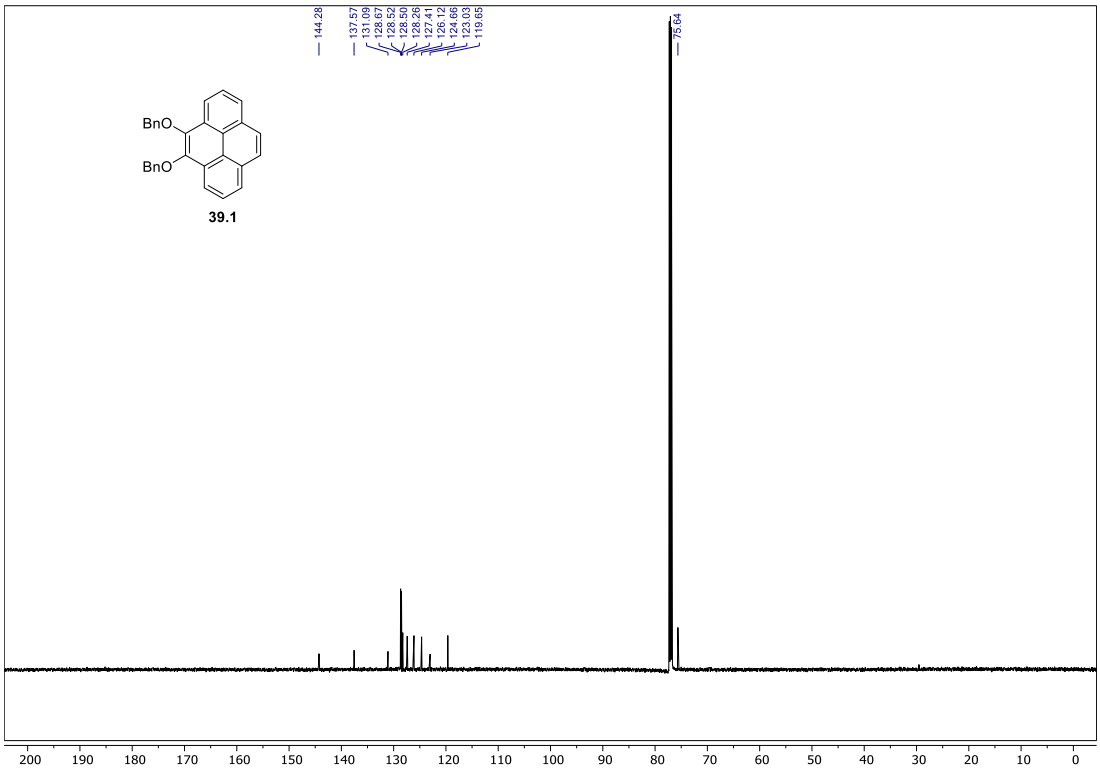
144.28
137.57
131.09
128.67
128.52
128.50
128.26
127.41
126.12
124.66
123.03
119.65
75.64
BnO
BnO
39.1
200 190 180 170 160 150 140 130 120 110 100 90 80 70 60 50 40 30 20 10 0

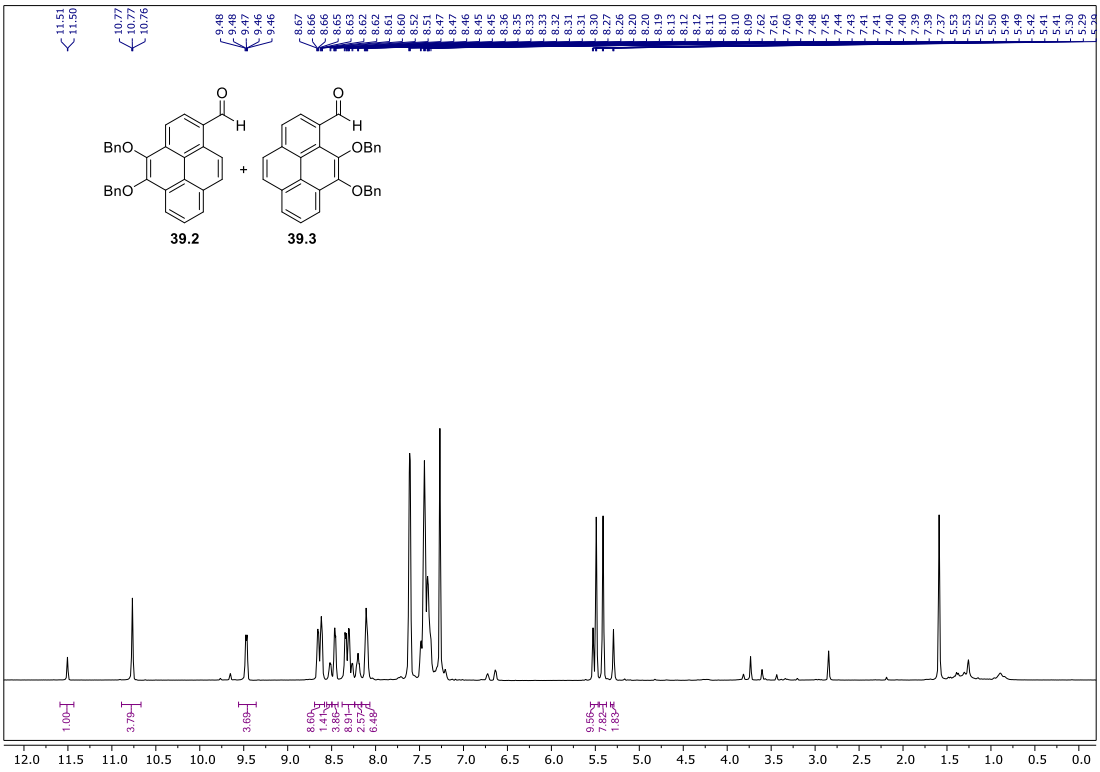
BnO
BnO
OBn
OBn
39.2
39.3

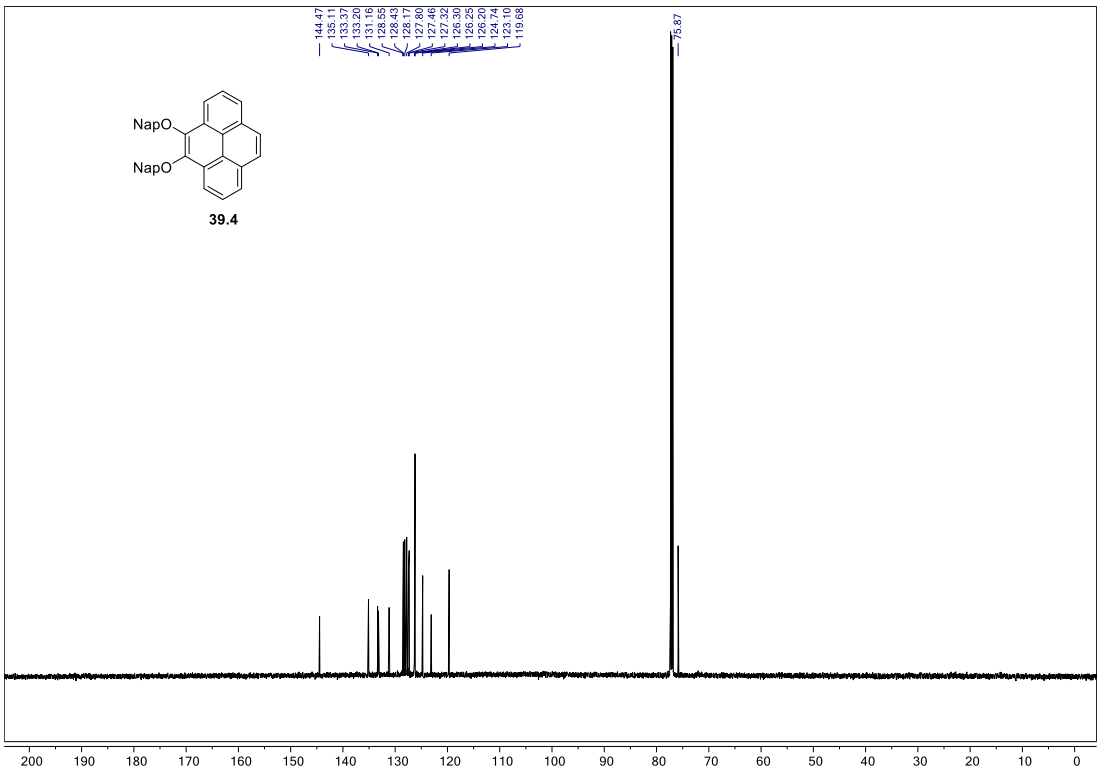
144.47
135.11
133.37
133.20
131.16
128.55
128.43
128.17
127.80
127.46
127.32
126.30
126.25
126.20
124.74
123.10
119.68
75.87
NapO
NapO
39.4
200
190
180
170
160
150
140
130
120
110
100
90
80
70
60
50
40
30
20
10
0

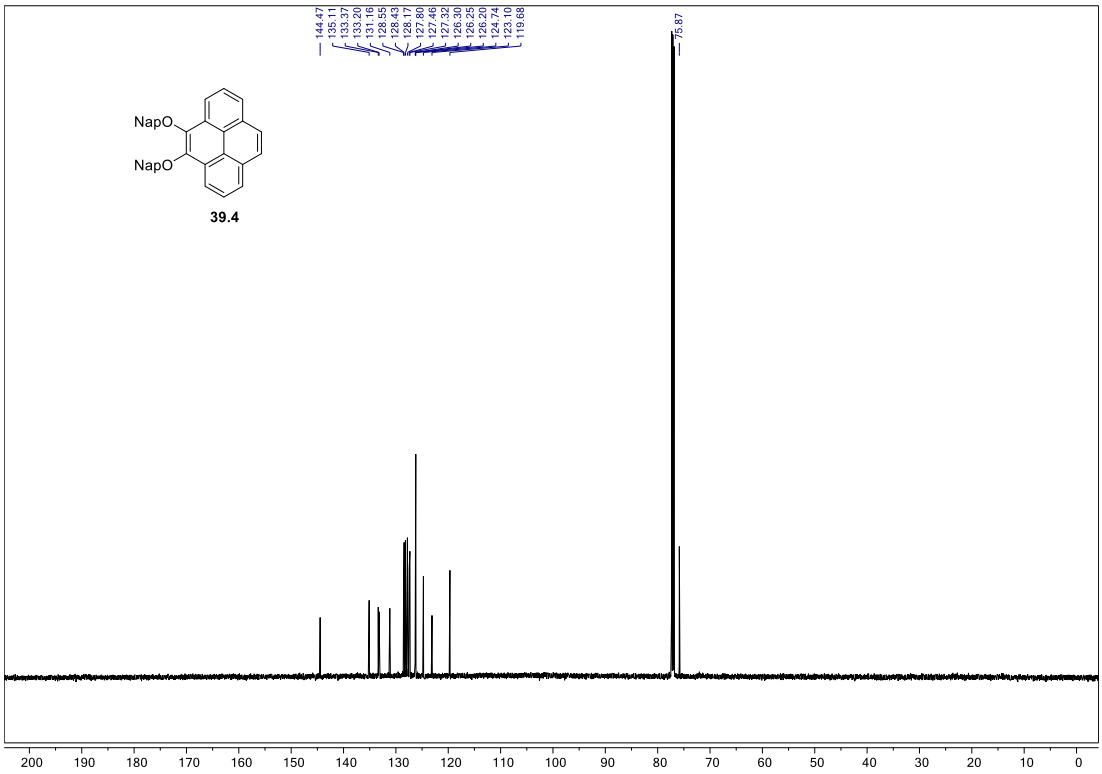
144.47
135.11
133.37
133.20
131.16
128.55
128.43
128.17
127.80
127.46
127.32
126.30
126.25
126.20
124.74
123.10
119.68
75.87
NapO
NapO
39.4
200
190
180
170
160
150
140
130
120
110
100
90
80
70
60
50
40
30
20
10
0

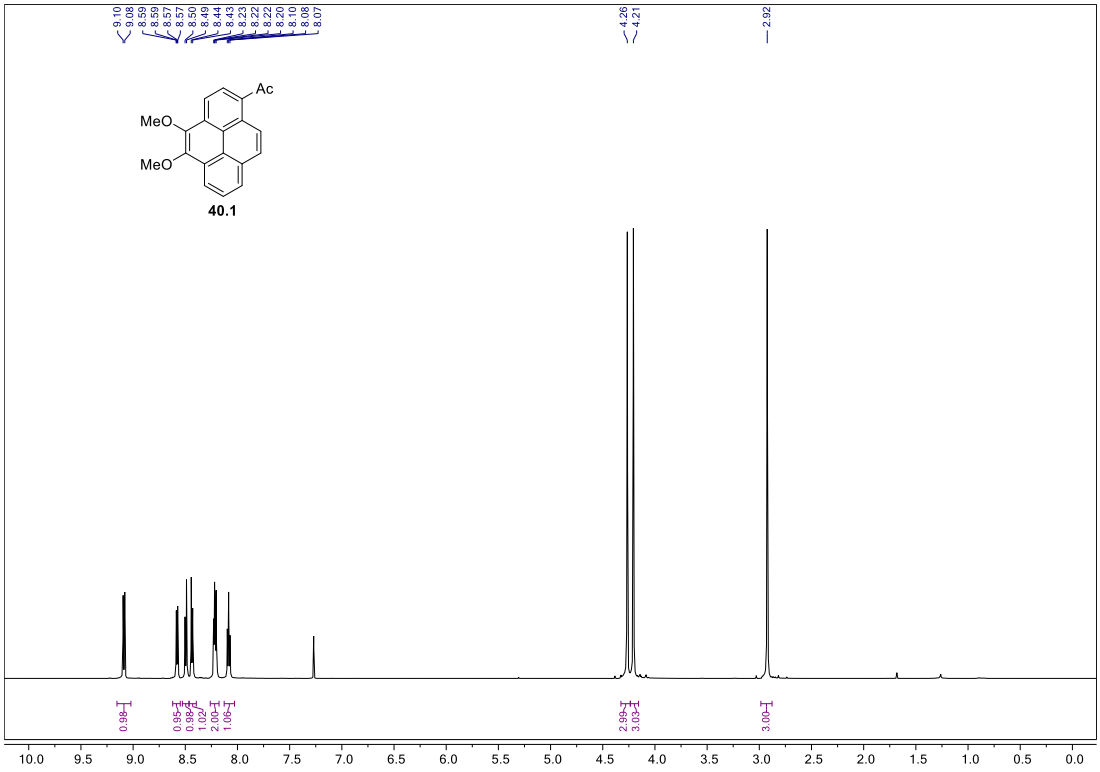
9.10
9.08
8.59
8.59
8.59
8.57
8.57
8.50
8.49
8.44
8.43
8.23
8.22
8.22
8.20
8.10
8.08
8.07
4.26
4.21
2.92
Ac
MeO
MeO
40.1
0.98
0.95
0.89
1.02
2.00
1.06
2.99
3.03
3.00
10.0
9.5
9.0
8.5
8.0
7.5
7.0
6.5
6.0
5.5
5.0
4.5
4.0
3.5
3.0
2.5
2.0
1.5
1.0
0.5
0.0

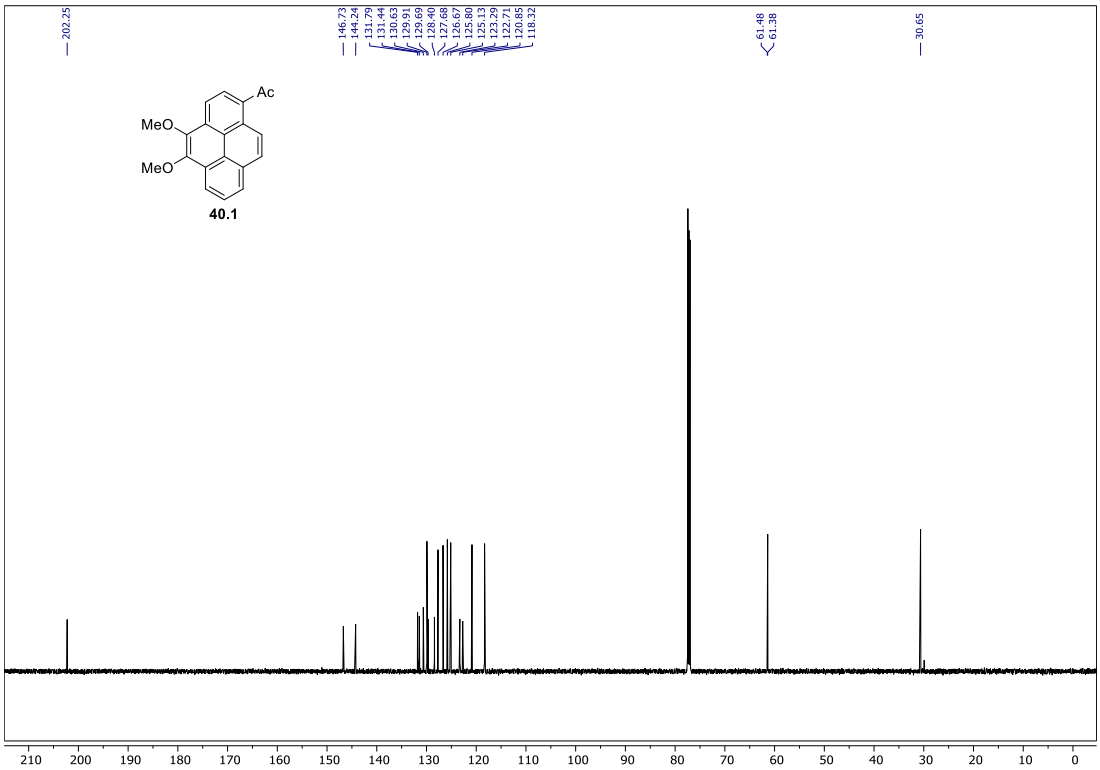
202.25
146.73
144.24
131.79
131.44
130.63
129.91
129.69
128.40
127.68
126.67
125.80
125.13
123.29
122.71
120.85
118.32
61.48
61.38
30.65
Ac
MeO
MeO
40.1
210
200
190
180
170
160
150
140
130
120
110
100
90
80
70
60
50
40
30
20
10
0

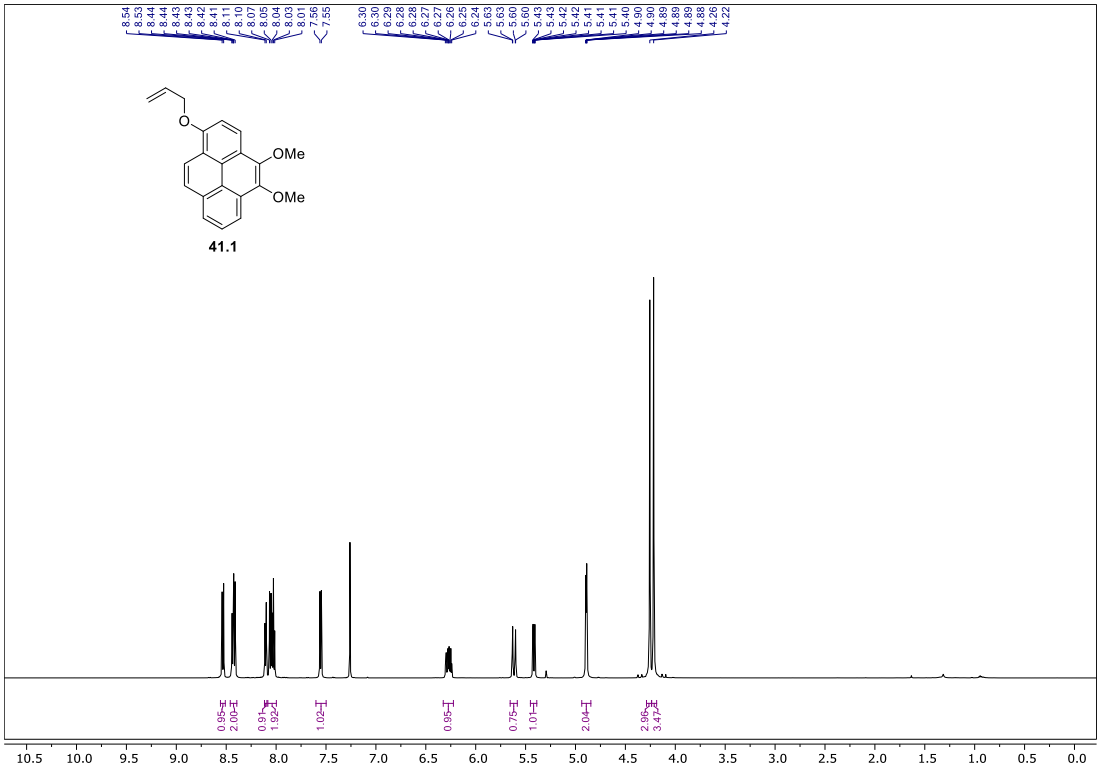
8.54
8.53
8.44
8.44
8.44
8.43
8.42
8.41
8.11
8.10
8.07
8.05
8.04
8.03
8.01
7.56
7.55
6.30
6.30
6.29
6.28
6.28
6.27
6.27
6.26
6.25
6.24
5.63
5.63
5.60
5.60
5.43
5.43
5.42
5.42
5.41
5.41
5.41
5.40
4.90
4.90
4.89
4.89
4.89
4.88
4.26
4.22
O
OMe
OMe
41.1
0.95
2.00
0.91
1.92
1.02
0.95
0.75
1.01
2.04
2.96
3.47
10.5
10.0
9.5
9.0
8.5
8.0
7.5
7.0
6.5
6.0
5.5
5.0
4.5
4.0
3.5
3.0
2.5
2.0
1.5
1.0
0.5
0.0

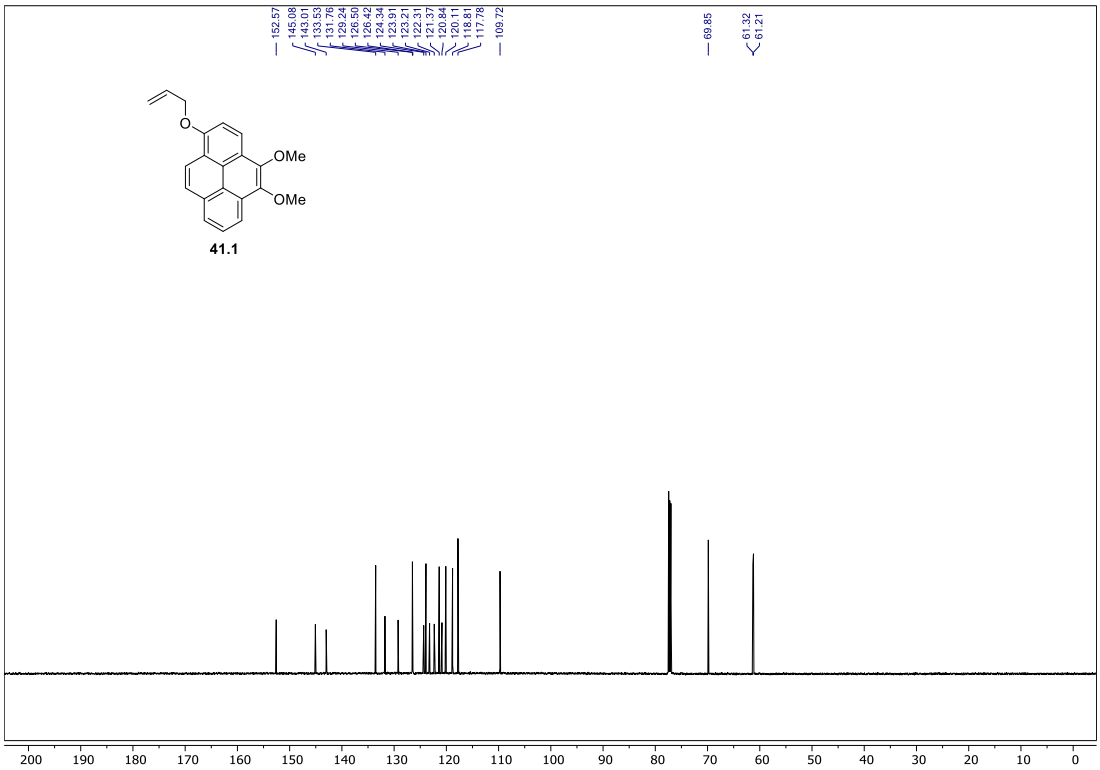
152.57
145.08
143.01
133.53
131.75
129.24
126.50
126.42
124.34
123.91
123.21
122.31
121.37
120.84
120.11
118.81
117.78
109.72
69.85
61.32
61.21
O
OMe
OMe
41.1
200
190
180
170
160
150
140
130
120
110
100
90
80
70
60
50
40
30
20
10
0

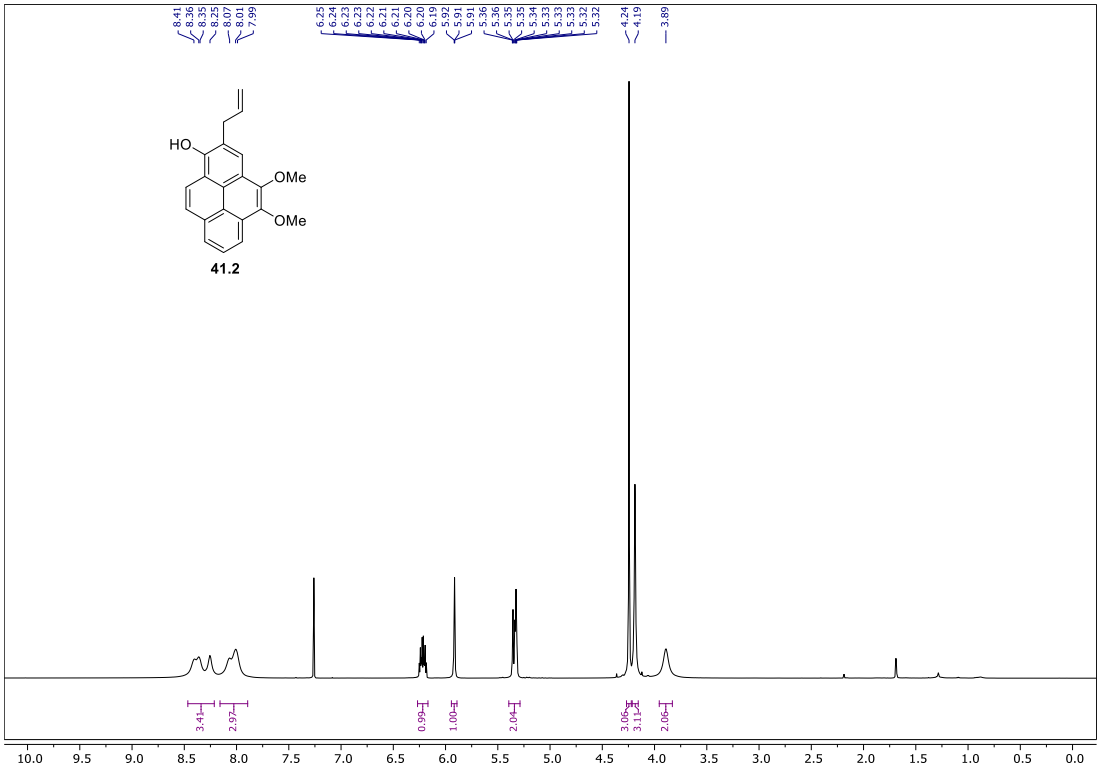
8.41
8.36
8.35
8.25
8.07
8.01
7.99
6.25
6.24
6.23
6.23
6.22
6.21
6.21
6.20
6.20
6.19
5.92
5.91
5.91
5.36
5.36
5.35
5.35
5.34
5.33
5.33
5.33
5.32
5.32
4.24
4.19
3.89
HO
OMe
OMe
41.2
3.41
2.97
0.99
1.00
2.04
3.06
3.11
2.06
10.0
9.5
9.0
8.5
8.0
7.5
7.0
6.5
6.0
5.5
5.0
4.5
4.0
3.5
3.0
2.5
2.0
1.5
1.0
0.5
0.0

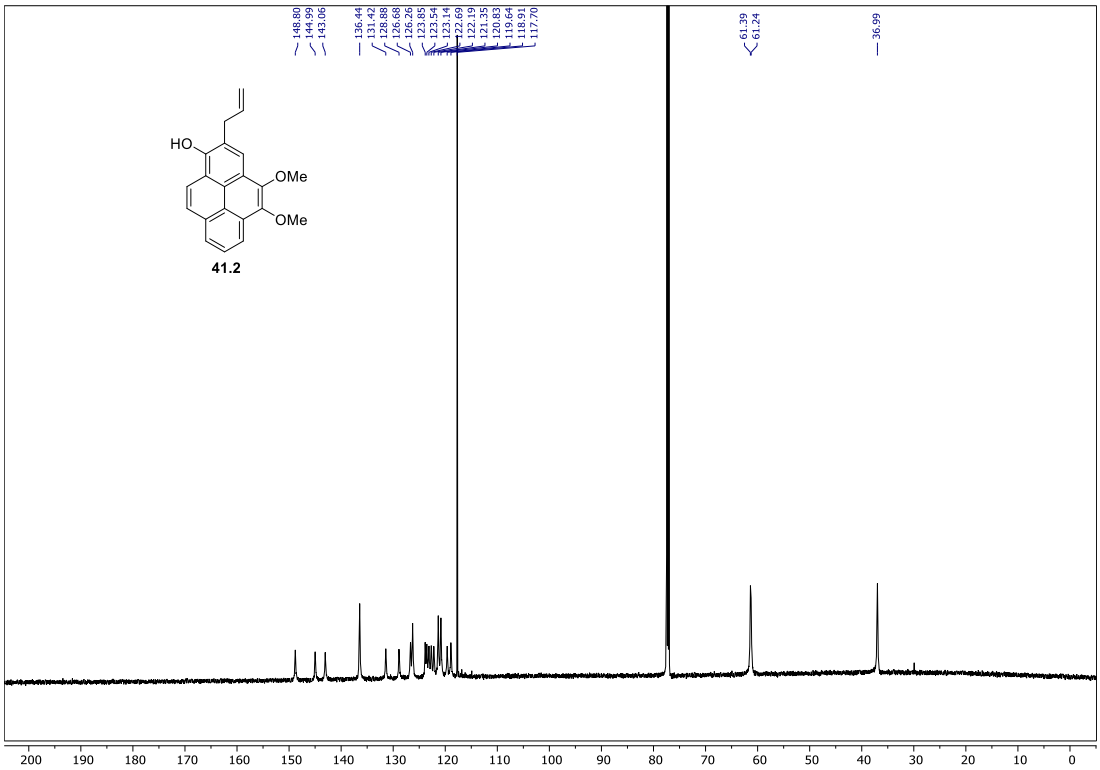
148.80
144.99
143.06
136.44
131.42
128.88
126.68
126.26
123.85
123.54
123.14
122.69
121.19
121.35
120.83
119.64
118.91
117.70
61.39
61.24
36.99
HO
OMe
OMe
41.2
200
190
180
170
160
150
140
130
120
110
100
90
80
70
60
50
40
30
20
10
0

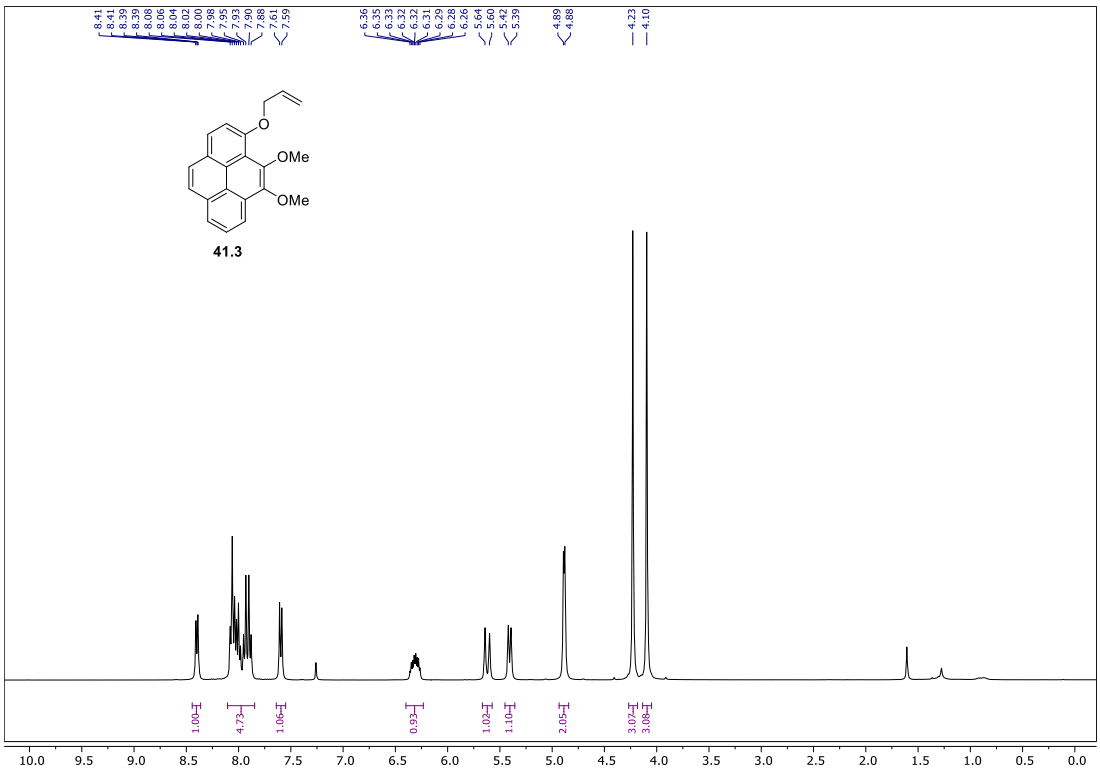
8.41
8.41
8.39
8.39
8.08
8.06
8.04
8.02
8.00
7.98
7.95
7.93
7.90
7.88
7.61
7.59
6.36
6.35
6.33
6.32
6.32
6.31
6.29
6.28
6.26
5.64
5.60
5.42
5.39
4.89
4.88
4.23
4.10
O
OMe
OMe
41.3
1.00
4.73
1.06
0.93
1.02
1.10
2.05
3.07
3.08
10.0
9.5
9.0
8.5
8.0
7.5
7.0
6.5
6.0
5.5
5.0
4.5
4.0
3.5
3.0
2.5
2.0
1.5
1.0
0.5
0.0

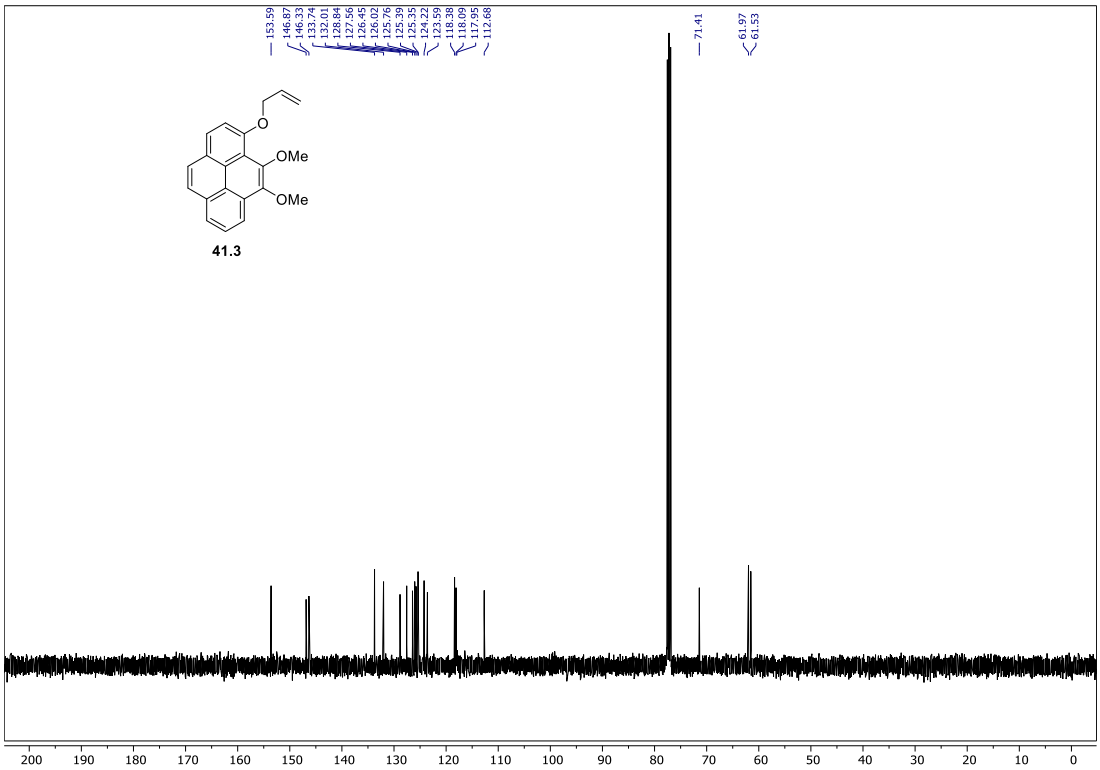
153.59
146.87
146.33
133.74
132.01
128.84
127.56
126.45
126.02
125.56
125.39
125.35
124.22
123.59
118.38
118.09
117.95
112.68
71.41
61.97
61.53
O
OMe
OMe
41.3
200
190
180
170
160
150
140
130
120
110
100
90
80
70
60
50
40
30
20
10
0

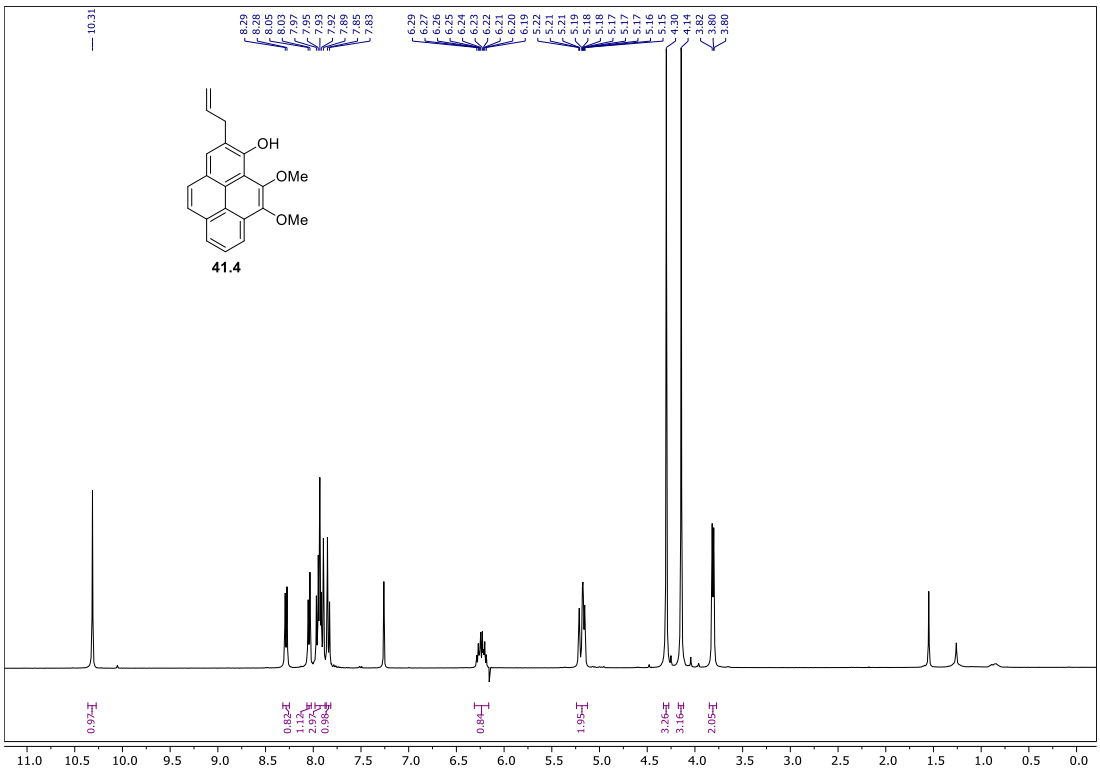
10.31
8.29
8.28
8.05
8.03
7.97
7.95
7.93
7.92
7.89
7.85
7.83
6.29
6.27
6.26
6.25
6.24
6.23
6.22
6.21
6.20
6.19
5.22
5.21
5.21
5.19
5.18
5.17
5.17
5.17
5.16
5.15
4.30
4.14
3.82
3.80
3.80
OH
OMe
OMe
41.4
0.97
0.83
1.12
2.97
0.98
0.84
1.95
3.26
3.16
2.05
11.0
10.5
10.0
9.5
9.0
8.5
8.0
7.5
7.0
6.5
6.0
5.5
5.0
4.5
4.0
3.5
3.0
2.5
2.0
1.5
1.0
0.5
0.0

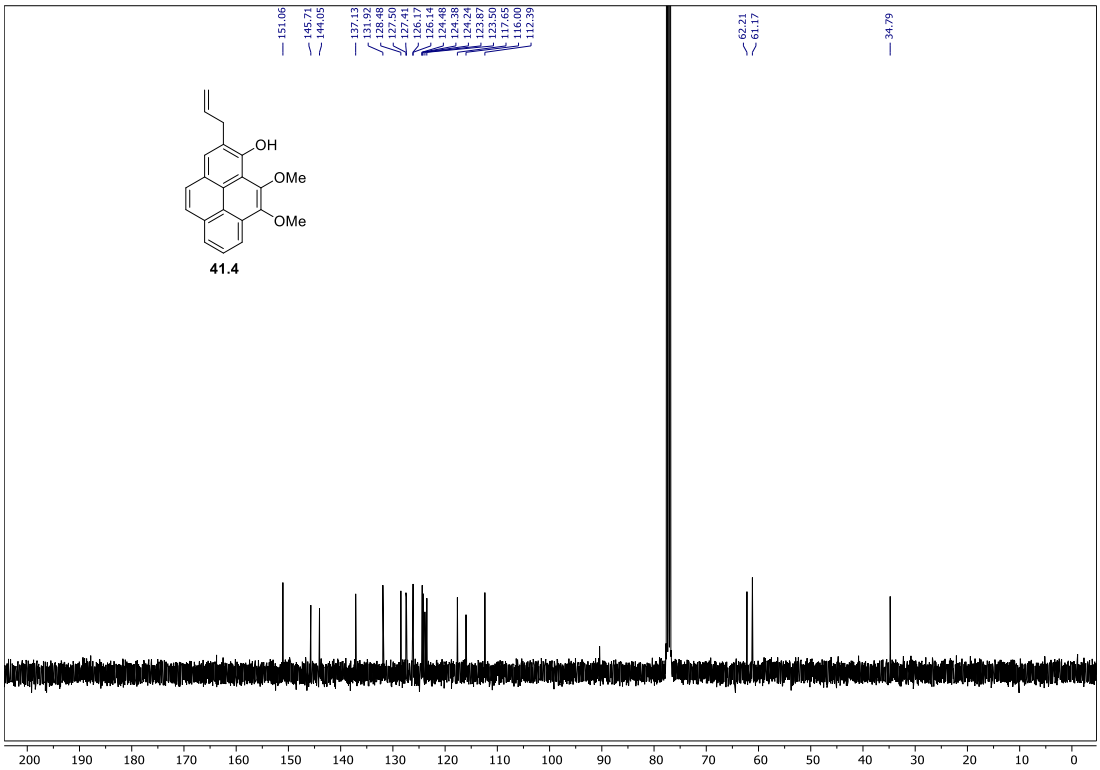
151.06
145.71
144.05
137.13
131.92
128.48
127.50
127.41
126.17
126.14
124.48
124.38
124.24
123.87
123.50
117.65
116.00
112.39
62.21
61.17
34.79
OH
OMe
OMe
41.4
200
190
180
170
160
150
140
130
120
110
100
90
80
70
60
50
40
30
20
10
0

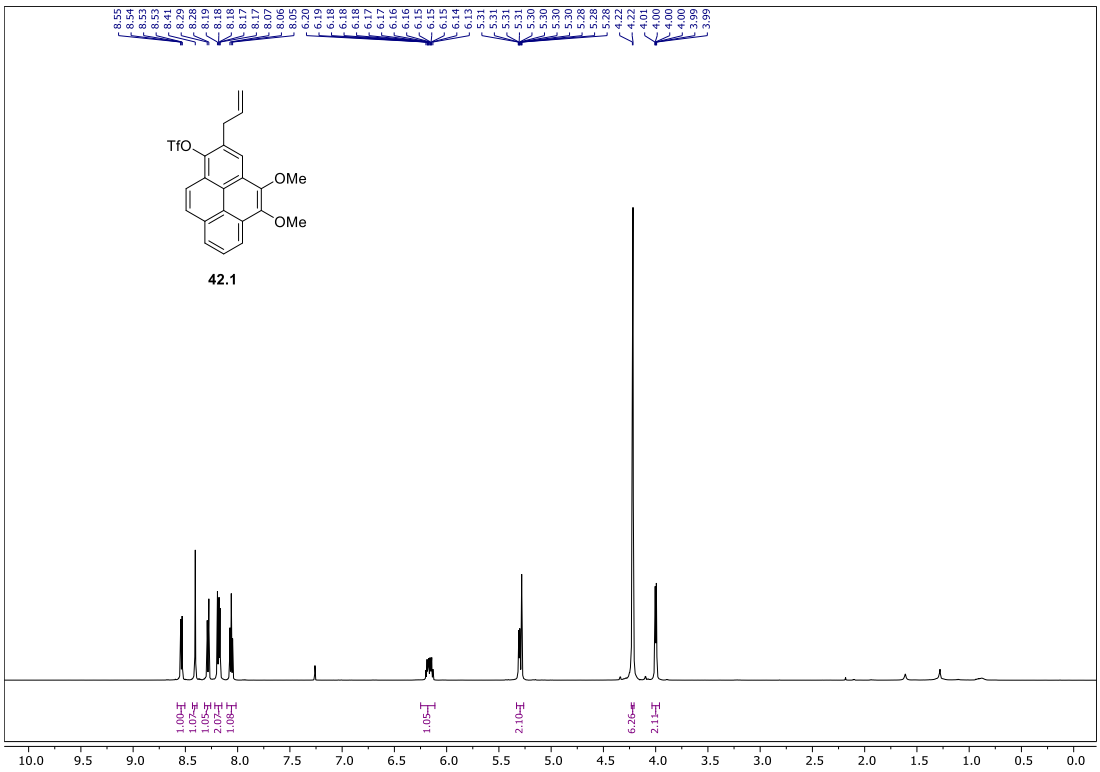
TfO
OMe
OMe
42.1

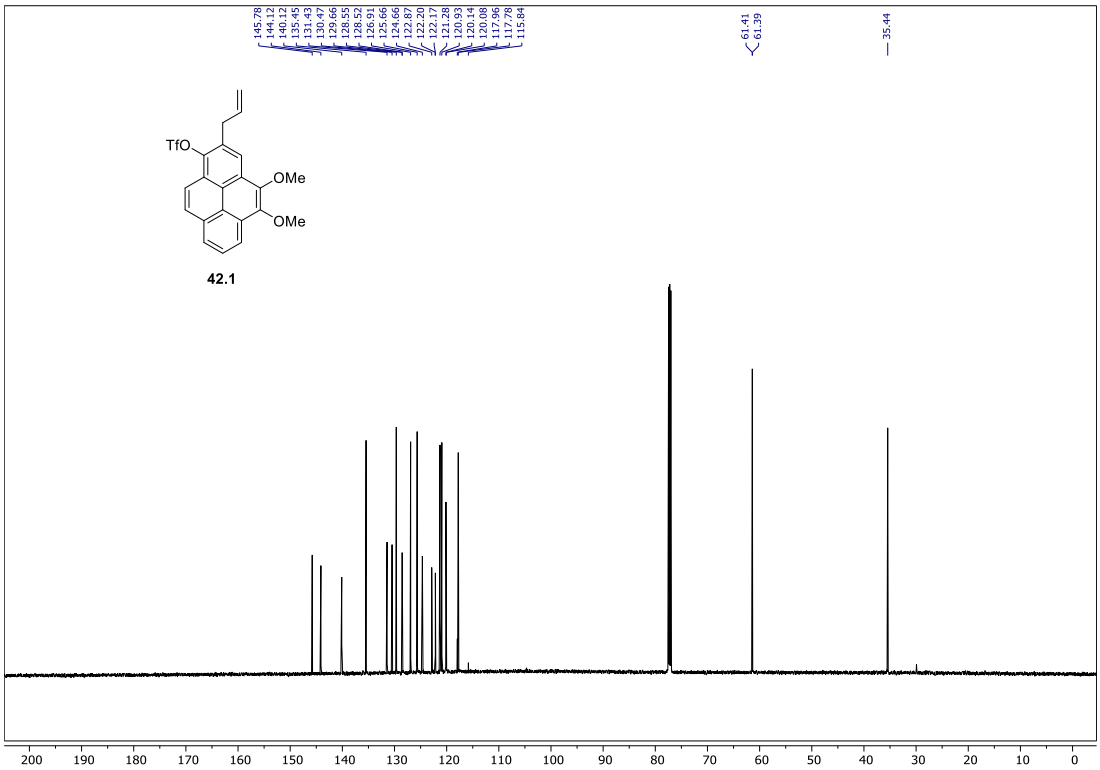
TfO
OMe
OMe
42.1

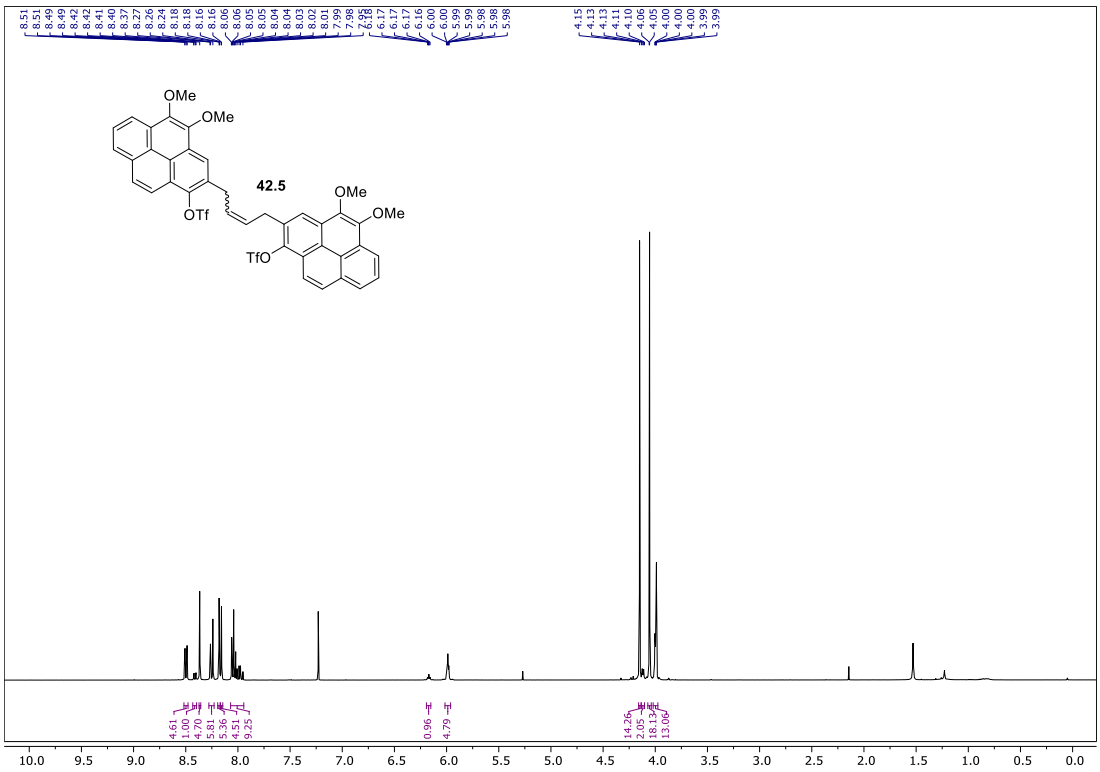
OMe
OMe
OTf
42.5
OMe
OMe
TfO

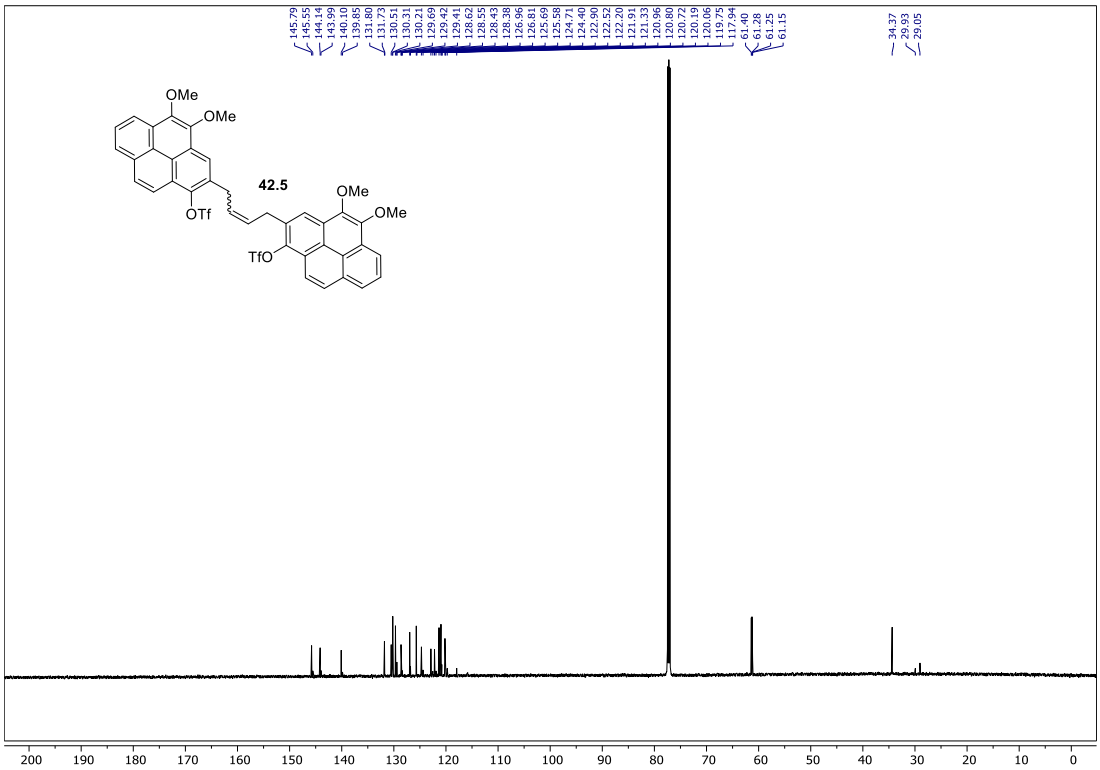
OMe
OMe
OTf
42.5
OMe
OMe
TfO

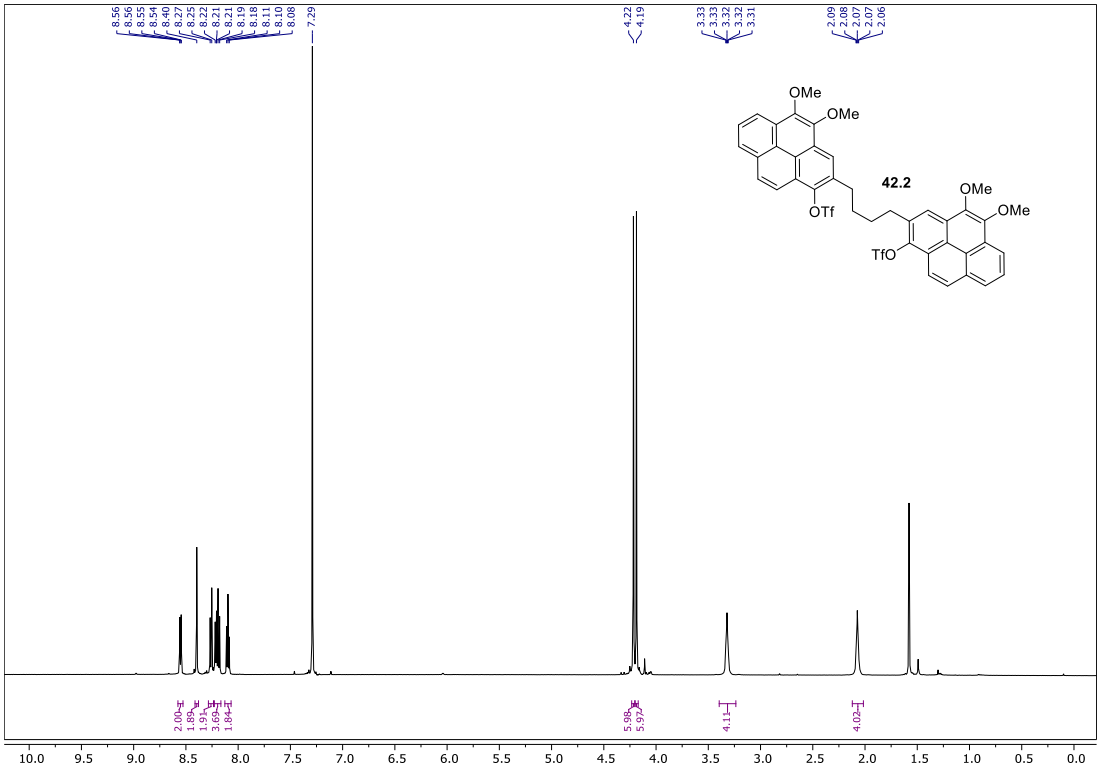
OMe
OMe
OTf
42.2
OMe
OMe
TfO

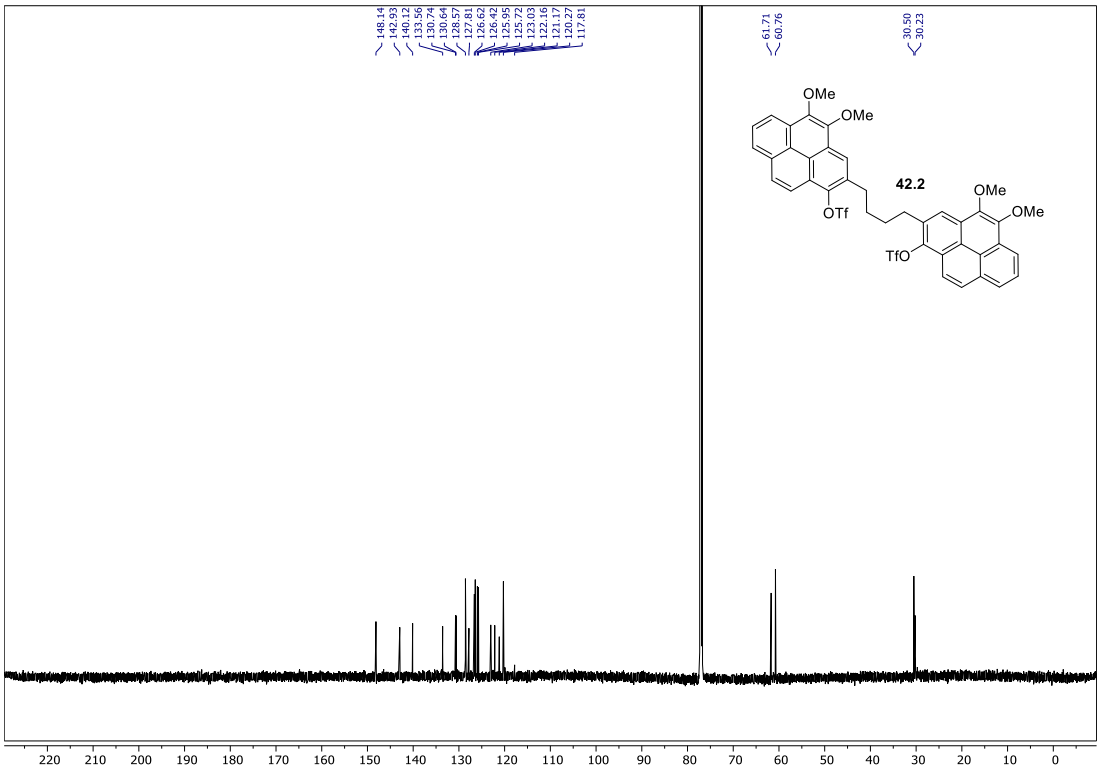
OMe
OMe
OTf
42.2
OMe
OMe
TfO

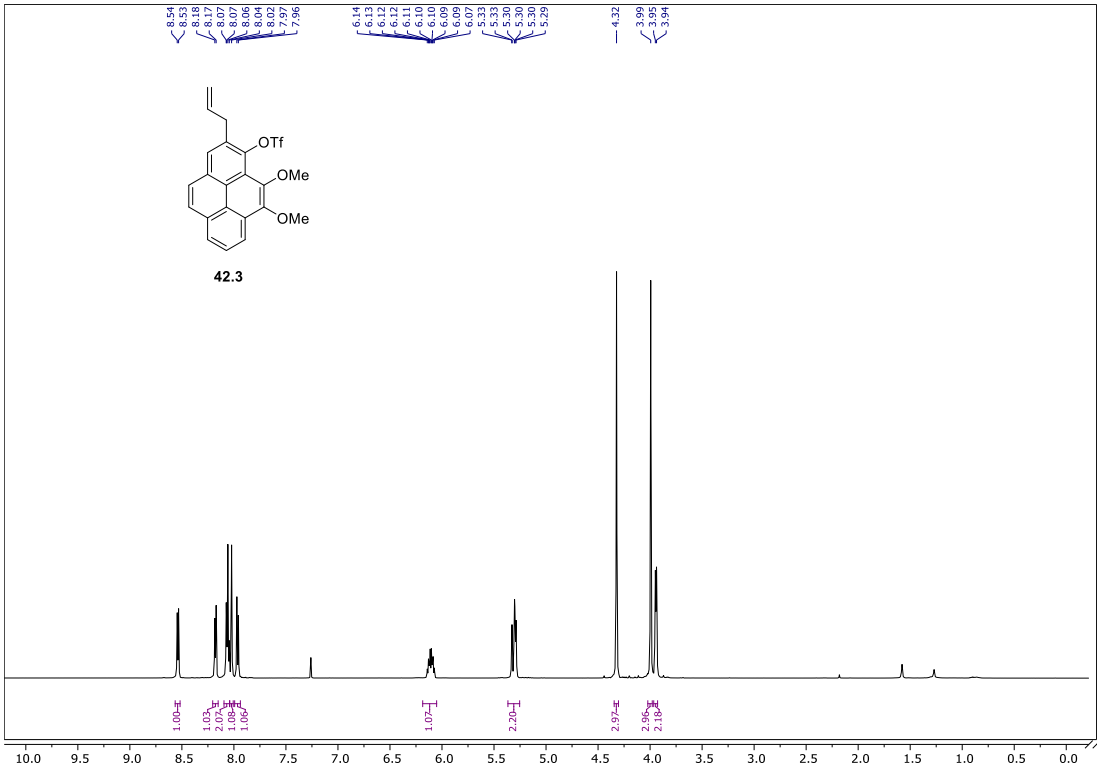
8.54
8.53
8.18
8.17
8.07
8.07
8.06
8.04
8.02
7.97
7.96
6.14
6.13
6.12
6.12
6.11
6.10
6.09
6.09
6.07
5.33
5.30
5.30
5.30
5.29
4.32
3.99
3.95
3.94
OTf
OMe
OMe
42.3
1.00
1.03
1.02
1.08
1.06
1.07
2.20
2.97
2.96
2.18
10.0 9.5 9.0 8.5 8.0 7.5 7.0 6.5 6.0 5.5 5.0 4.5 4.0 3.5 3.0 2.5 2.0 1.5 1.0 0.5 0.0

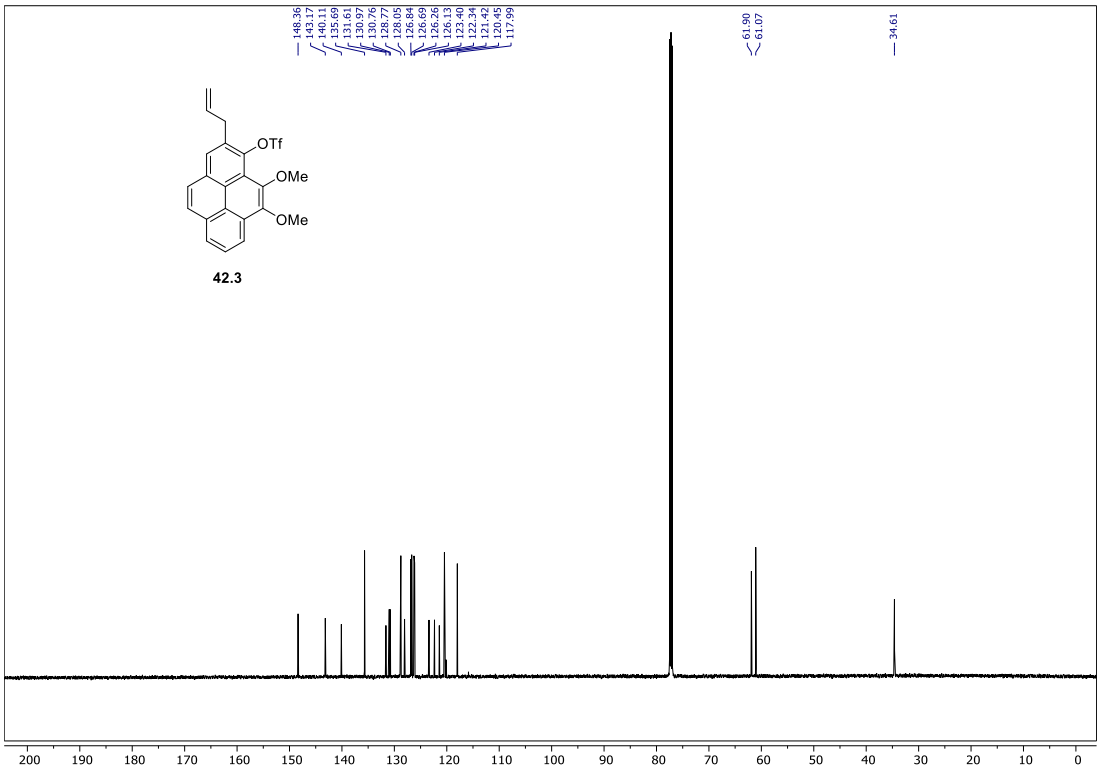
148.36
143.17
140.11
135.69
131.61
130.97
130.76
128.77
128.05
126.84
126.69
126.26
126.13
123.40
122.34
121.42
120.45
117.99
61.90
61.07
34.61
OTf
OMe
OMe
42.3
200 190 180 170 160 150 140 130 120 110 100 90 80 70 60 50 40 30 20 10 0

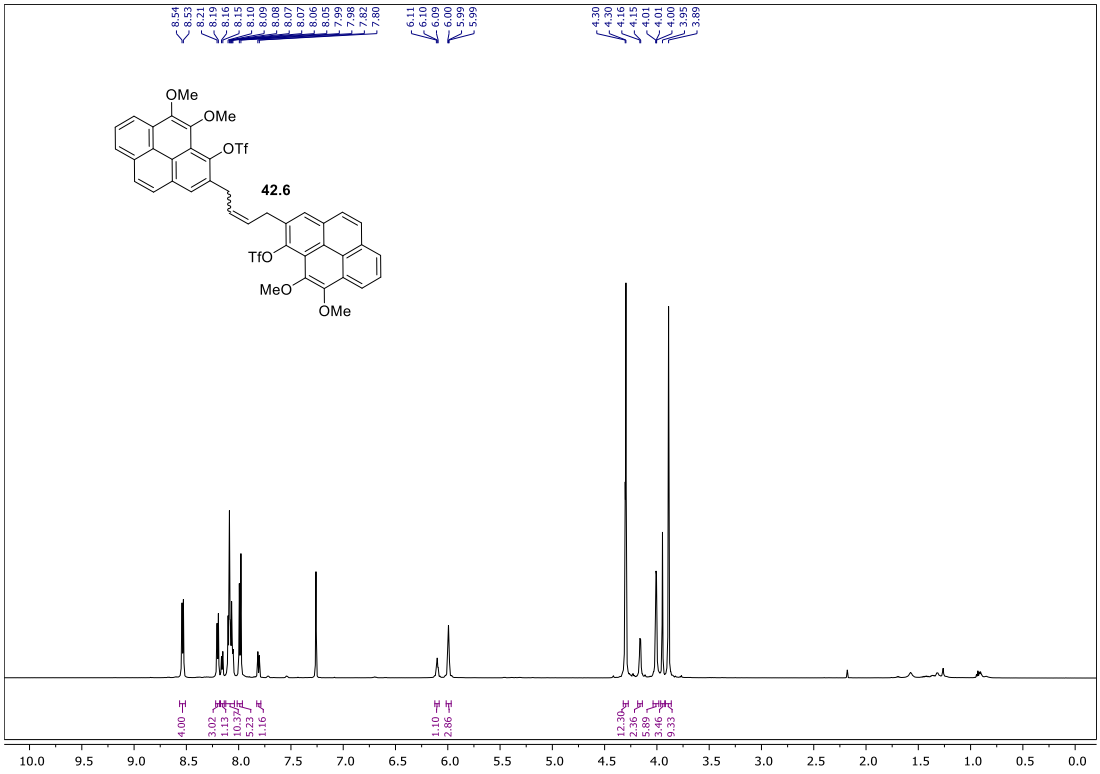
OMe
OMe
OTf
42.6
TfO
MeO
OMe

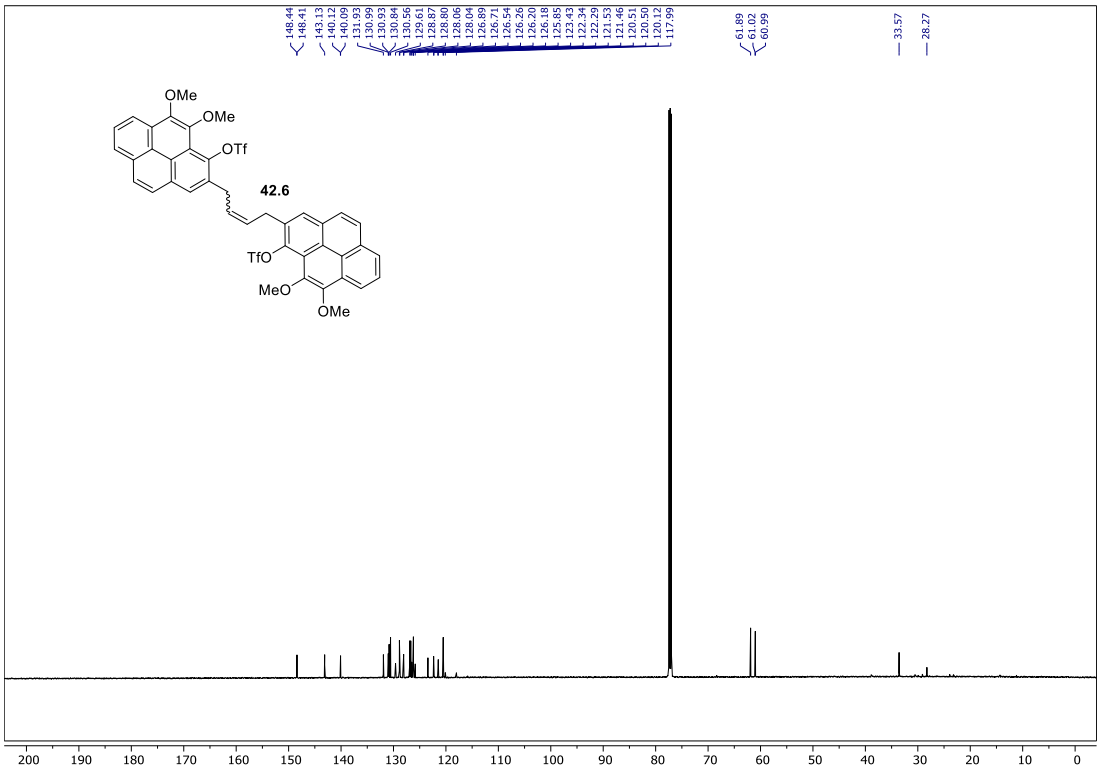
OMe
OMe
OTf
42.6
TfO
MeO
OMe

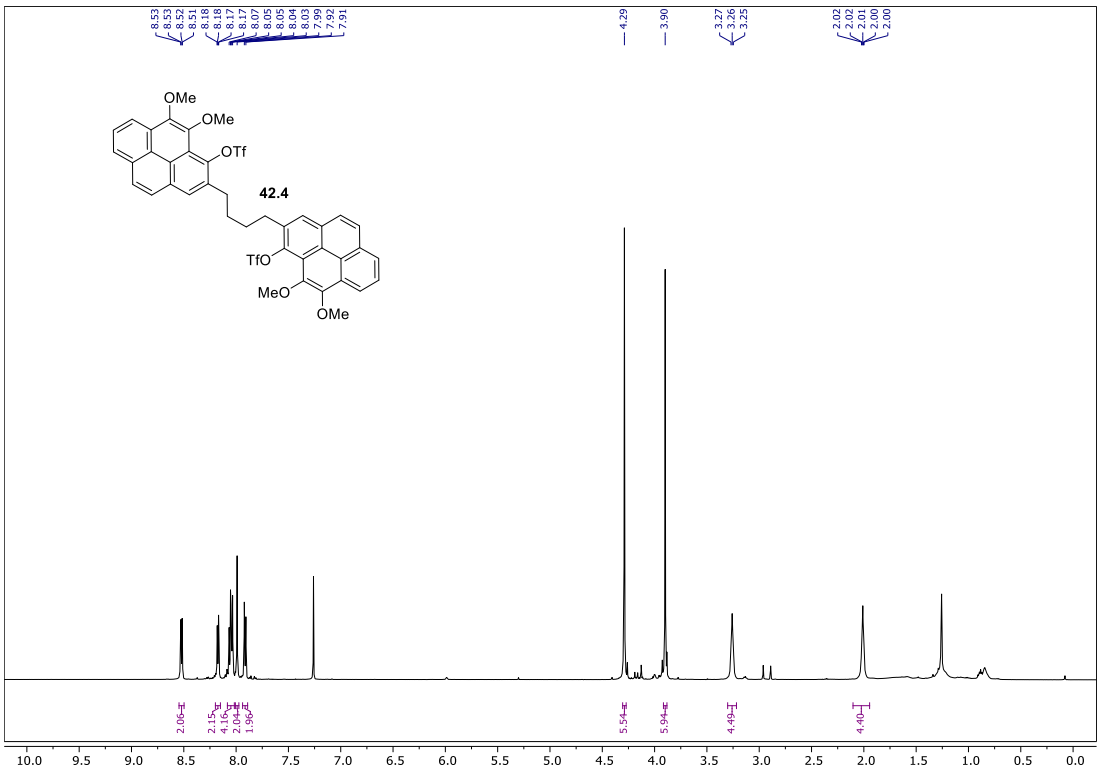
OMe
OMe
OTf
42.4
TfO
MeO
OMe

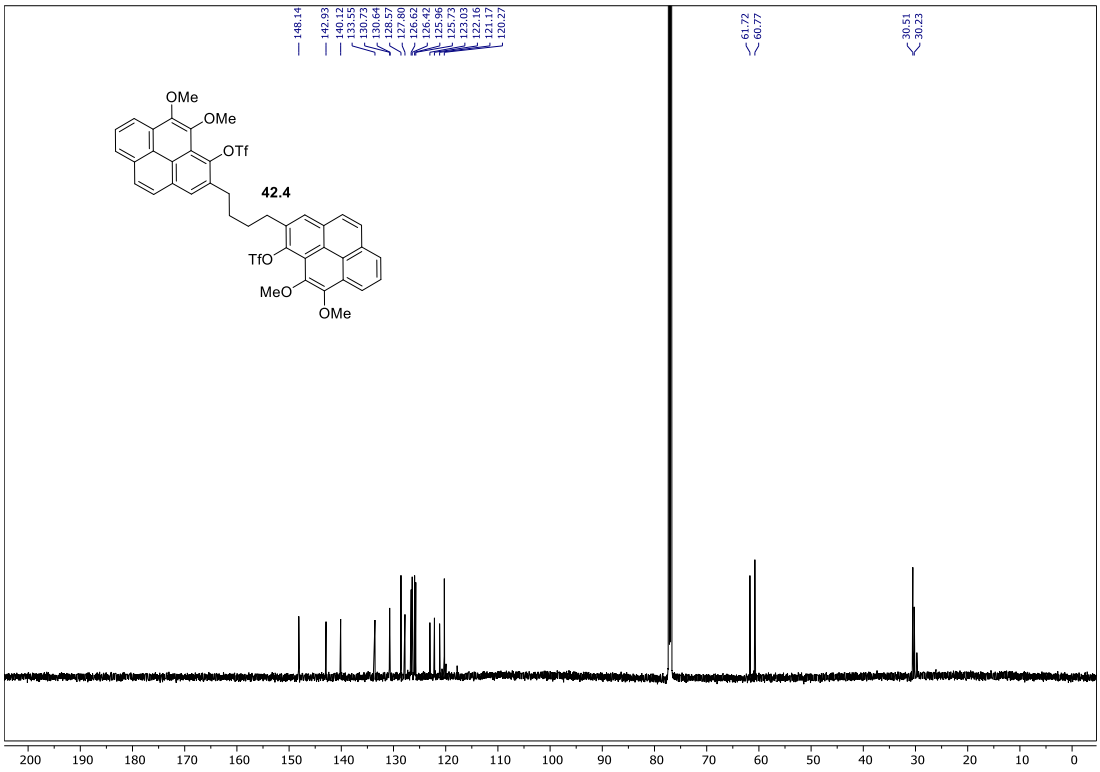
OMe
OMe
OTf
42.4
TfO
MeO
OMe

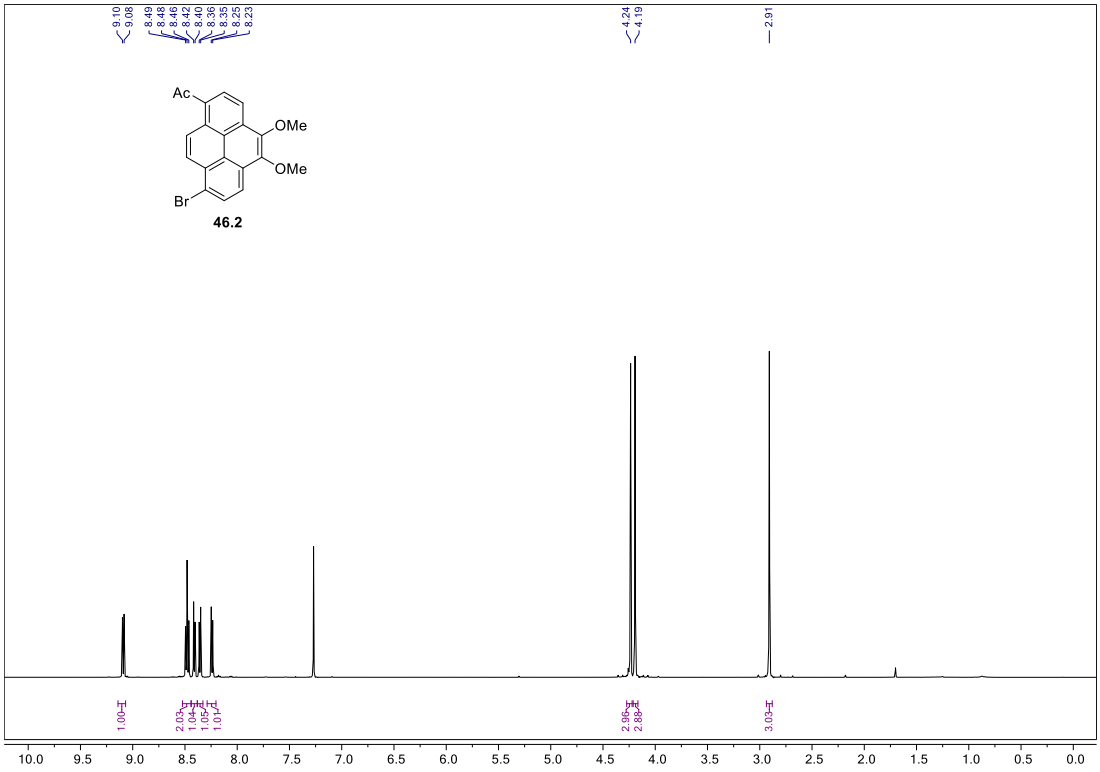
9.10
9.08
8.49
8.48
8.46
8.42
8.40
8.36
8.35
8.25
8.23
4.24
4.19
2.91
Ac
OMe
OMe
Br
46.2
1.00
2.03
1.04
1.05
1.01
2.06
2.88
3.03
10.0
9.5
9.0
8.5
8.0
7.5
7.0
6.5
6.0
5.5
5.0
4.5
4.0
3.5
3.0
2.5
2.0
1.5
1.0
0.5
0.0

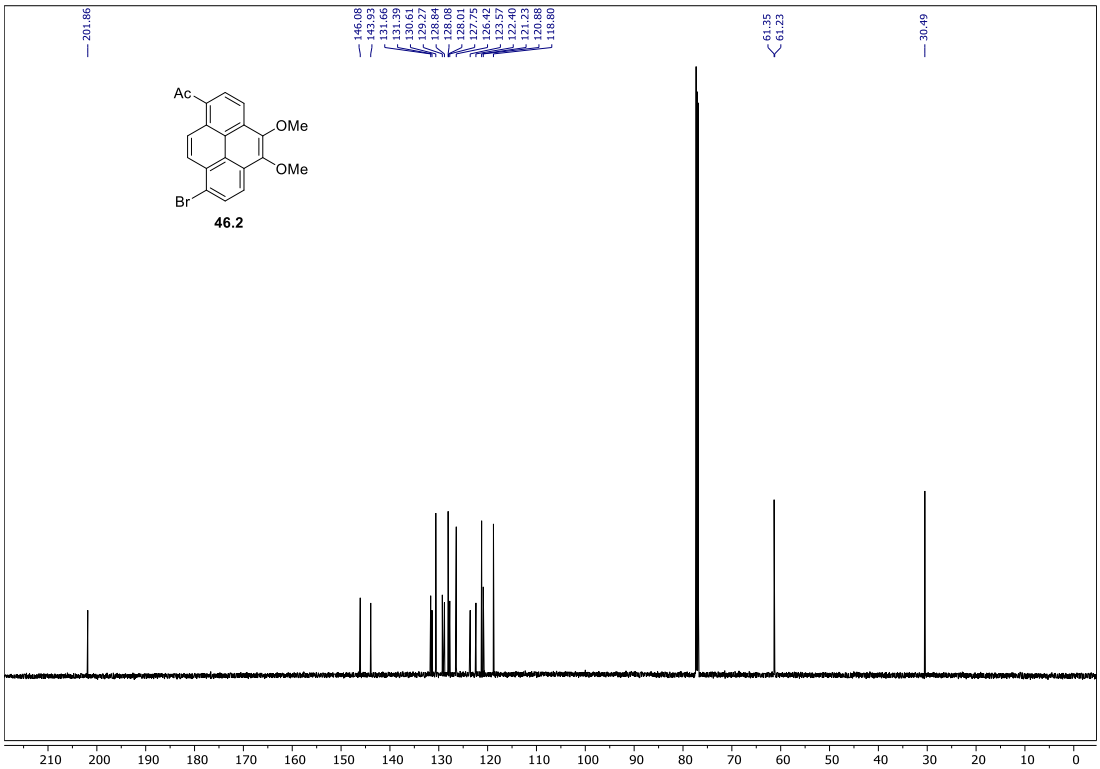
201.86
146.08
143.93
131.66
131.39
130.61
129.27
128.84
128.08
128.01
127.75
126.42
125.57
122.40
121.23
120.88
118.80
61.35
61.23
30.49
Ac
OMe
OMe
Br
46.2
210
200
190
180
170
160
150
140
130
120
110
100
90
80
70
60
50
40
30
20
10
0

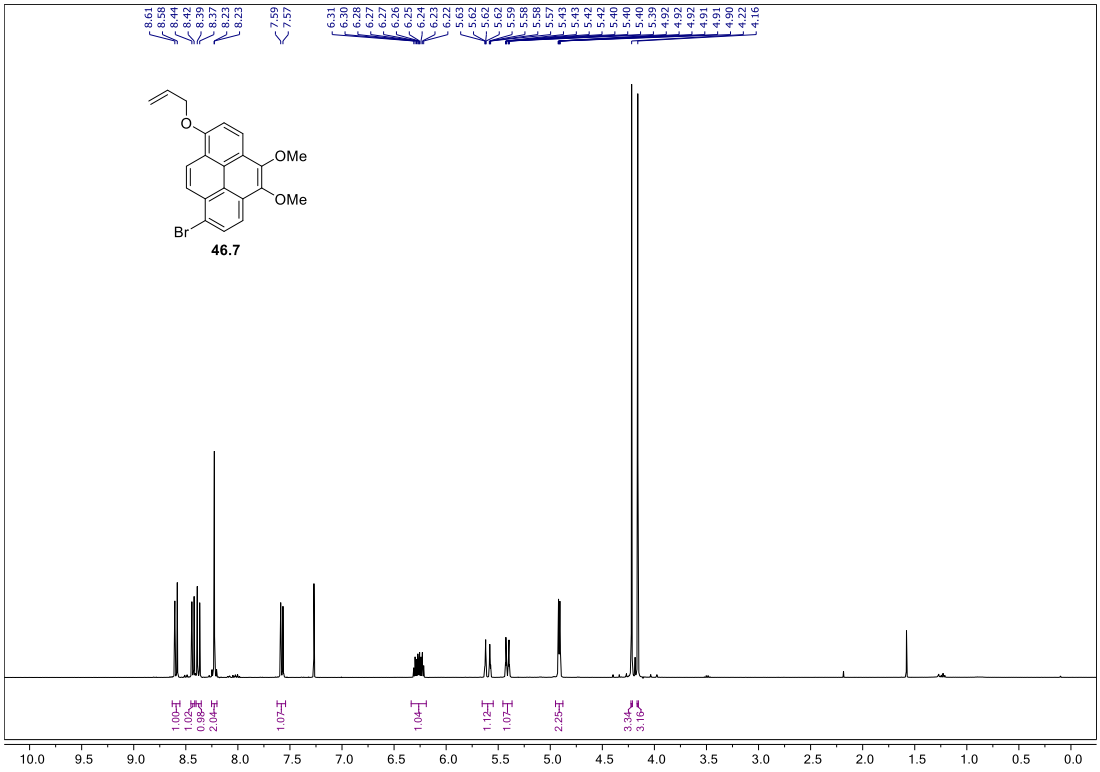
8.61
8.58
8.44
8.42
8.39
8.37
8.23
8.23
7.59
7.57
6.31
6.30
6.28
6.27
6.27
6.26
6.25
6.24
6.23
6.22
5.63
5.62
5.62
5.62
5.59
5.58
5.58
5.57
5.43
5.43
5.42
5.42
5.40
5.40
5.40
5.39
4.92
4.92
4.92
4.91
4.91
4.90
4.22
4.16
O
OMe
OMe
Br
46.7
1.00
1.02
0.98
2.04
1.07
1.04
1.12
1.07
2.25
3.34
3.16
10.0
9.5
9.0
8.5
8.0
7.5
7.0
6.5
6.0
5.5
5.0
4.5
4.0
3.5
3.0
2.5
2.0
1.5
1.0
0.5
0.0

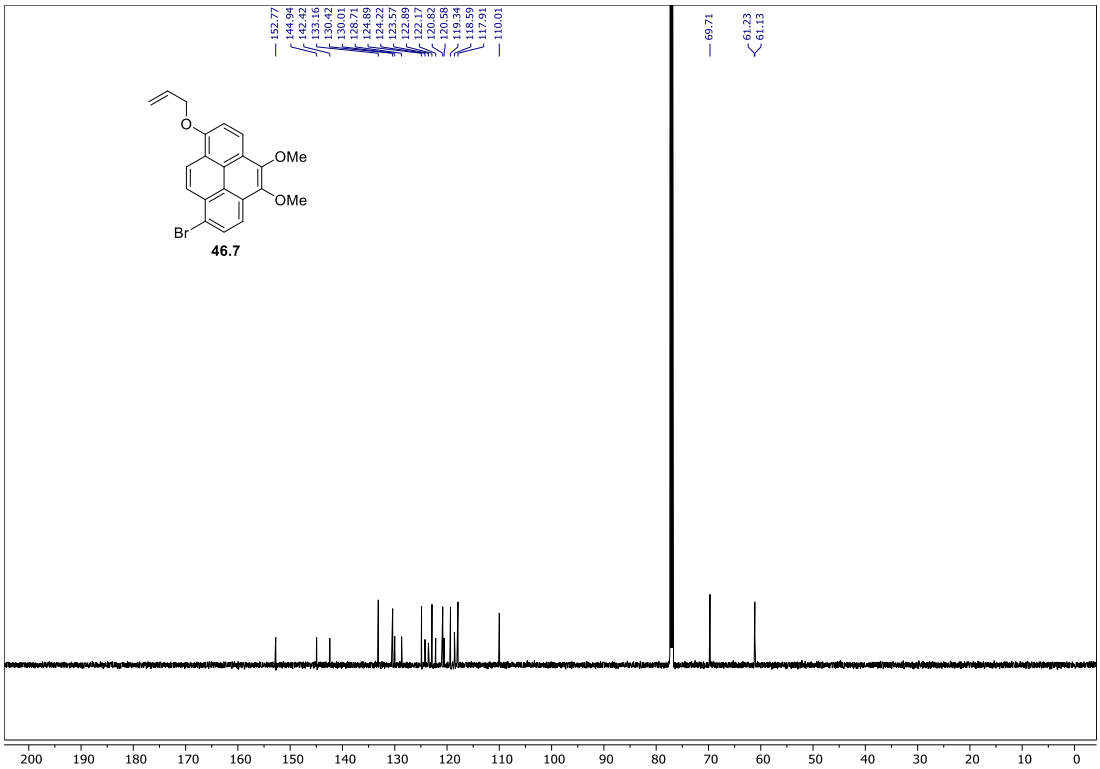
152.77
144.94
143.23
133.16
130.42
130.01
128.71
124.89
124.22
123.57
122.89
122.17
120.82
120.58
119.24
118.59
117.91
110.01
69.71
61.23
61.13
O
OMe
OMe
Br
46.7
200
190
180
170
160
150
140
130
120
110
100
90
80
70
60
50
40
30
20
10
0

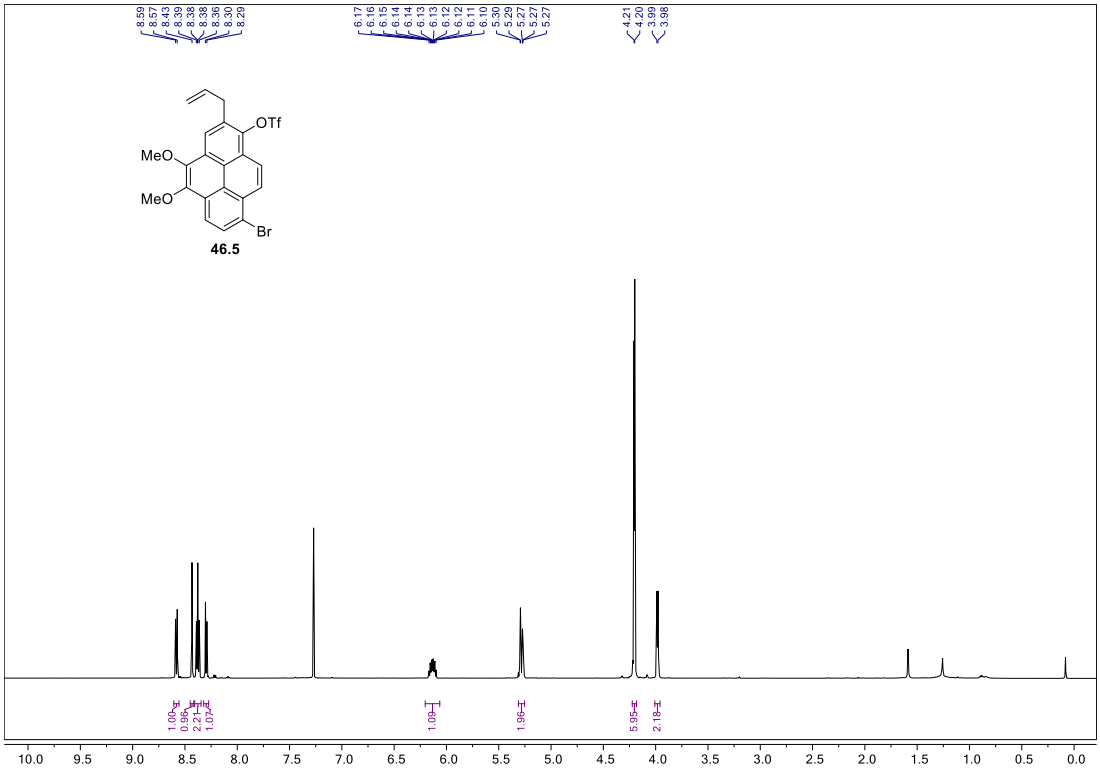
8.59
8.57
8.43
8.39
8.38
8.38
8.36
8.30
8.29
6.17
6.16
6.15
6.14
6.14
6.13
6.13
6.12
6.12
6.11
6.10
5.30
5.29
5.27
5.27
5.27
4.21
4.20
3.99
3.98
OTf
MeO
MeO
Br
46.5
1.00
0.96
2.21
1.07
1.09
1.98
5.95
2.18
10.0
9.5
9.0
8.5
8.0
7.5
7.0
6.5
6.0
5.5
5.0
4.5
4.0
3.5
3.0
2.5
2.0
1.5
1.0
0.5
0.0

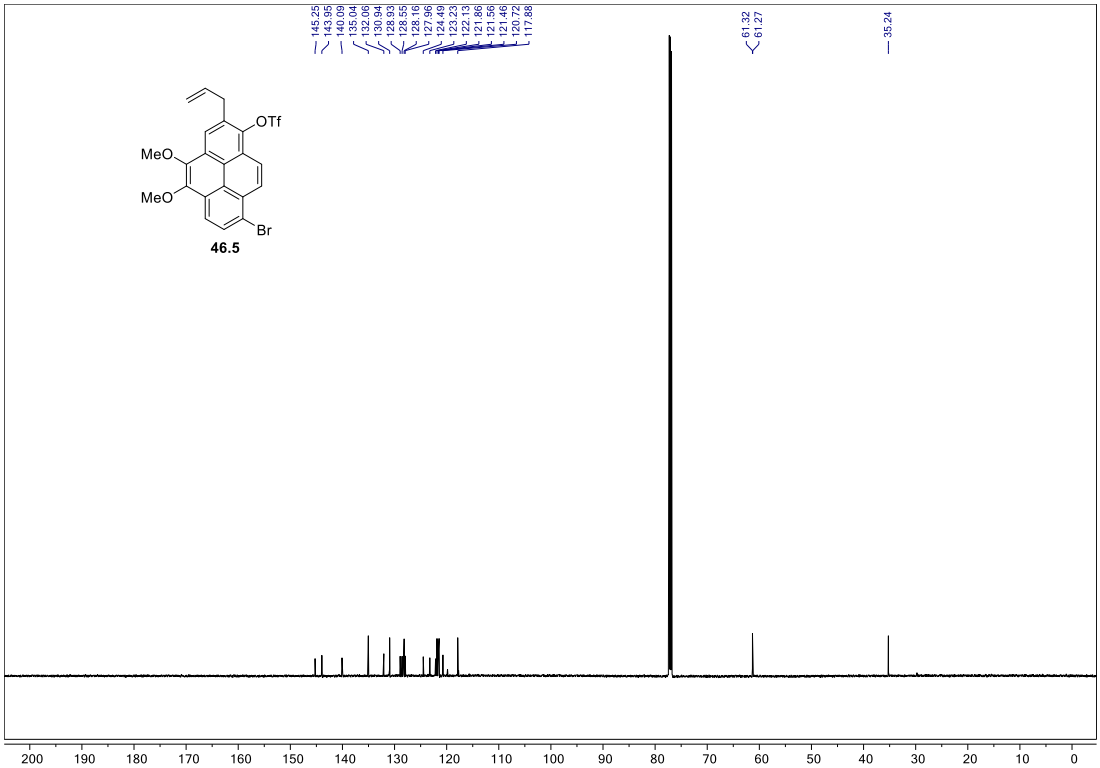
145.25
143.95
140.09
135.04
132.06
130.94
128.93
128.55
128.16
127.86
124.49
123.23
122.13
121.86
121.56
121.46
120.72
117.88
61.32
61.27
35.24
OTf
MeO
MeO
Br
46.5
200
190
180
170
160
150
140
130
120
110
100
90
80
70
60
50
40
30
20
10
0

X-ray Crystal Structure and Relevant Data for Compound 42.2

Figure 42: Crystal Data and Structure Refinement for Compound **42.2**

Identification code	Merner110714_0m
Empirical formula	$C_{21}H_{16}F_3O_5S$
Formula weight	437.42
Temperature/K	180.45
Crystal system	Triclinic
Space group	P-1
Unit cell dimensions	a = 8.7597(5) Å α = 94.022(2)°
	b = 10.6780(6) Å β = 98.197(2)°
	c = 11.1484(7) Å γ = 113.638(2)°
Volume	936.16(10) $Å^3$
Z	2
Density (calculated)	1.5516 cm^3
Absorption coefficient	0.235 mm^{-1}
F(000)	450.6
Crystal size	0.1 × 0.1 × 0.1 mm^3
Radiation	Mo Kα (λ = 0.71073)
Theta range for data collection/°	3.72 to 54.2
Index ranges	-11≤h≤11, -13≤k≤13, -14≤l≤14
Reflections collected	45973
Independent reflections	4128 [R(int) = 0.0364, R(sigma) = 0.0164]
Data/restraints/parameters	4128/0/272
Goodness-of-fit on F2	1.049
Final R indexes [I>=2σ (I)]	R1 = 0.0819, wR2 = 0.2095
Final R indexes [all data]	R1 = 0.0895, wR2 = 0.2170
Largest diff. peak and hole	1.10/-1.10

Table SI-1: Bond Lengths for (Merner110714_0m) Compound **10**

S1-C21	1.825(4)
S1-O3	1.583(2)
S1-O4	1.416(4)
S1-O5	1.396(3)
C16-C14	1.420(4)

C16-C15	1.404(4)
C16-C17	1.438(4)
C12-C18	1.441(4)
C12-C11	1.404(4)
C21-F1	1.296(5)
C21-F2	1.318(5)
C21-F3	1.301(5)
C4-C3	1.392(4)
C7-C8	1.441(4)
O3-C4	1.458(4)
C7-C6	1.355(4)
C1-C11	1.473(6)
C3-C15	1.398(4)
C1-C2	1.524(5)
C8-C9	1.401(4)
C2-C3	1.517(4)
C18-C17	1.362(5)
C5-C14	1.423(4)
C18-O2	1.378(4)
C5-C4	1.398(4)
C11-C10	1.392(5)
C5-C6	1.443(4)
C9-C10	1.387(5)
C13-C14	1.428(4)
C17-O1	1.382(4)
C13-C12	1.428(4)
C20-O2	1.432(5)
C13-C8	1.420(4)
C19-O1	1.427(4)

Table SI-1: Bond Angles for (Merner110714_0m) Compound **10**

O3-S1-C21	97.23(16)
C18-C12-C13	118.5(3)
O4-S1-C21	106.7(3)
C11-C12-C13	119.2(3)
O4-S1-O3	112.18(17)
C11-C12-C18	122.3(3)
O5-S1-C21	106.0(2)

C5-C4-O3 117.0(2)
O5-S1-O3 111.7(2)
C3-C4-O3 117.7(3)
O5-S1-O4 120.1(3)
C3-C4-C5 125.2(3)
F2-C21-S1 107.6(3)
C6-C7-C8 121.7(3)
F3-C21-S1 110.8(3)
C4-C3-C2 121.9(3)
F3-C21-F2 109.2(3)
C15-C3-C2 121.6(3)
F1-C21-S1 110.3(3)
C15-C3-C4 116.5(3)
F1-C21-F2 110.6(4)
C7-C8-C13 118.5(3)
F1-C21-F3 108.4(4)
C9-C8-C13 119.3(3)
C4-O3-S1 118.49(18)
C9-C8-C7 122.3(3)
C3-C2-C1 115.0(3)
C17-C18-C12 121.2(3)
C4-C5-C14 116.7(3)
O2-C18-C12 116.6(3)
C6-C5-C14 118.9(3)
O2-C18-C17 122.2(3)
C6-C5-C4 124.4(3)
C7-C6-C5 120.9(3)
C12-C13-C14 120.1(3)
C3-C15-C16 122.0(3)
C8-C13-C14 120.2(3)
C10-C11-C12 120.4(3)
C8-C13-C12 119.7(3)
C10-C9-C8 120.7(3)
C15-C16-C14 119.5(3)
C18-C17-C16 121.3(3)
C17-C16-C14 118.8(3)
O1-C17-C16 117.4(3)
C17-C16-C15 121.7(3)
O1-C17-C18 121.3(3)
C13-C14-C5 119.9(2)

C9-C10-C11	120.8(3)
C16-C14-C5	120.1(3)
C19-O1-C17	113.7(3)
C16-C14-C13	120.1(3)
C20-O2-C18	115.3(3)